Discovery and Development of Metal-Catalyzed Step-Growth Radical Polymerization

金属触媒による逐次ラジカル重合反応の発見と開発

Masato Mizutani

水谷　将人

2011

CONTENTS

General Introduction

Background

Chain-Growth and Step-Growth Polymerization. All synthetic polymers, such as acrylic polymers, polystyrenes, polyesters, and polyamides, heavily supporting our modern life, are produced by either a chain- or step-growth polymerization (Scheme 1). The former procedure is typically represented by addition polymerizations of vinyl monomers to produce C–C bond main-chain polymers, whereas the latter includes polycondensation for polyesters and polyaddition for polyurethane, mostly containing heteroatoms in the main chains.

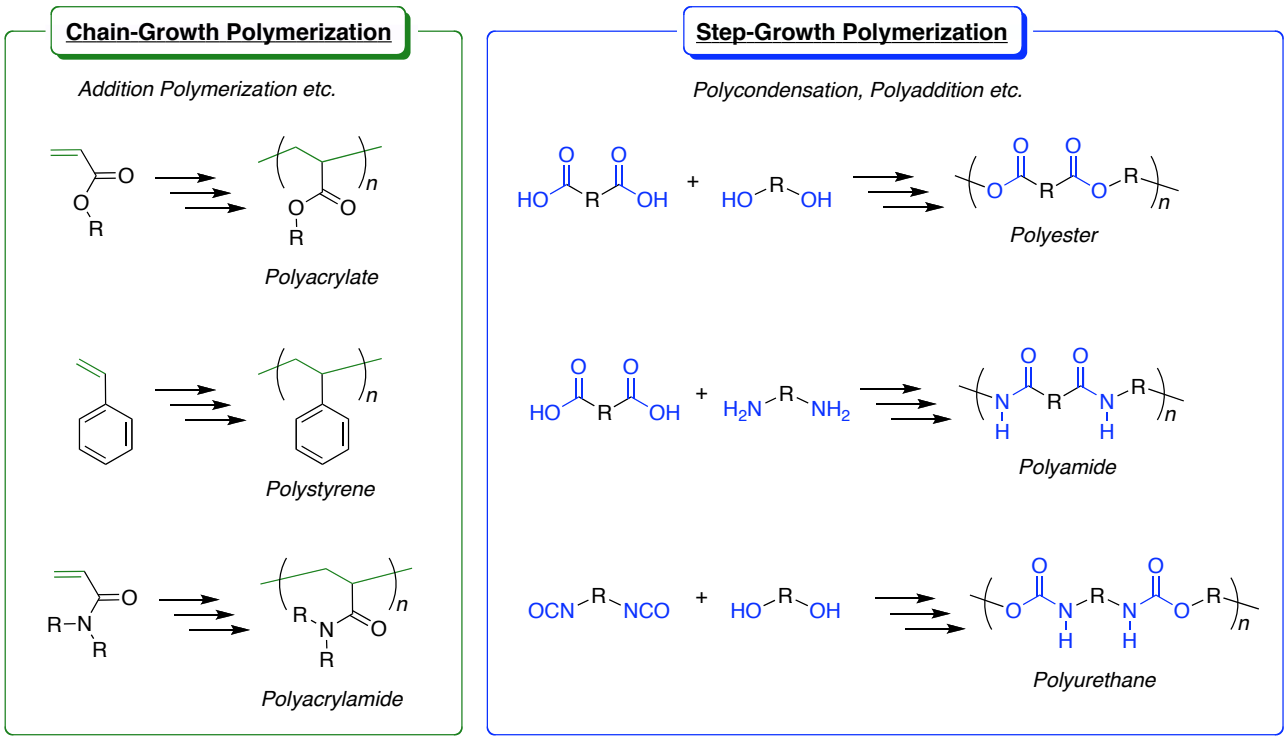

Scheme 1. Chain-Growth and Step-Growth Polymerization

The mechanisms of these two classes of polymerizations are completely different and each polymerization proceeds via the characteristic profile of the chain propagation to produce

polymers with the unique structures (Scheme 2).[1] In the chain-growth mechanism, the growing active species generated from initiators adds to monomers to grow the polymer chains. The molecular weights of the obtained polymers are constantly high throughout the polymerization, in which the rate of the propagation is much higher than that of the initiation. On the other hand, the step-growth propagation consumes most of monomers by the reactions of the functional groups between the monomers to form low molecular weight oligomers in the initial stage. After the complete consumption of the monomers, the molecular weight progressively increases to afford the polymers by the reactions between the oligomers.

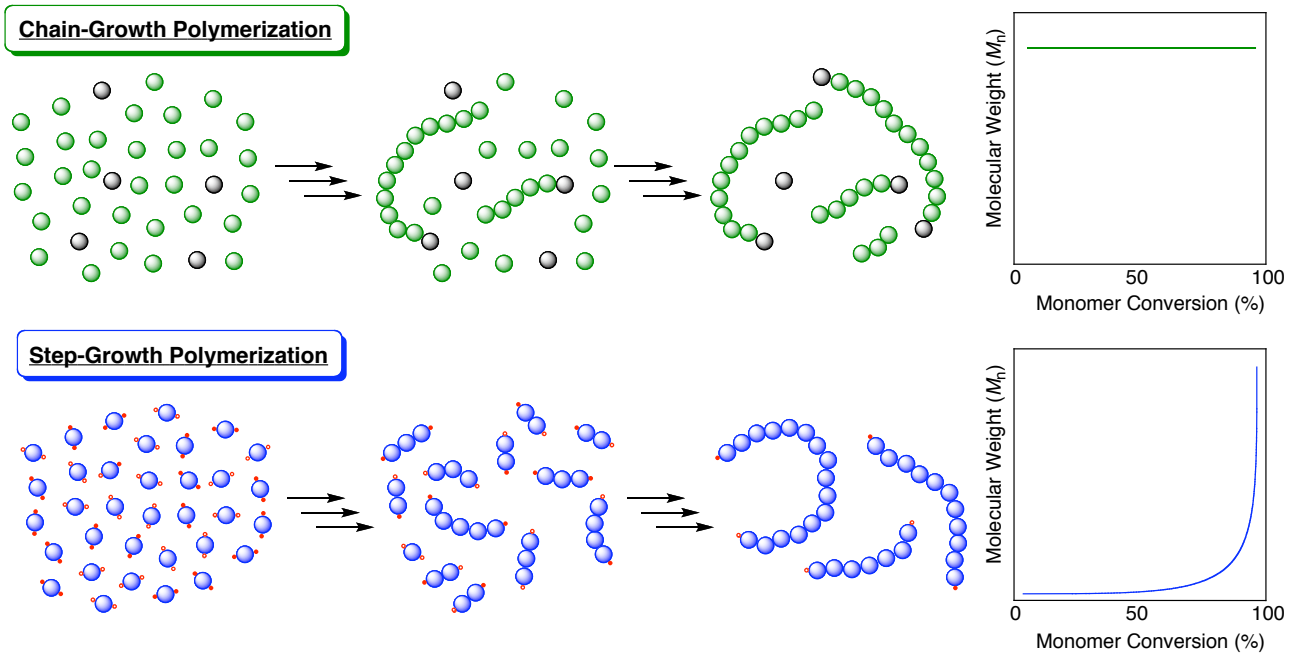

Scheme 2. Polymerization Mechanism of Chain-Growth and Step-Growth Polymerizations

Living Chain-Growth Polymerization. Living polymerization is defined as a chain-growth polymerization only with initiation and propagation, and enables the precise control of molecular weights and their distributions of the producing polymers (Scheme 3). Since the

groundbreaking discovery of living anionic polymerization by Szwarc in 1956,[2,3] a wide variety of well-defined (co)polymers have been synthesized using not only living anionic but also cationic and ring opening polymerization techniques.[4–6] On the other hand, radical polymerization is one of the most widespread methods for polymer synthesis in the chain-growth polymerization because of many advantages, such as wide variety of monomers, mild reaction conditions, and tolerance to polar groups. However, precise control of radical polymerization, or living radical polymerization, has been considered beyond one's reach since the highly reactive and electronically neutral growing radicals tend to undergo inevitable bimolecular terminations such as disproportionation and recombination.[7,8]

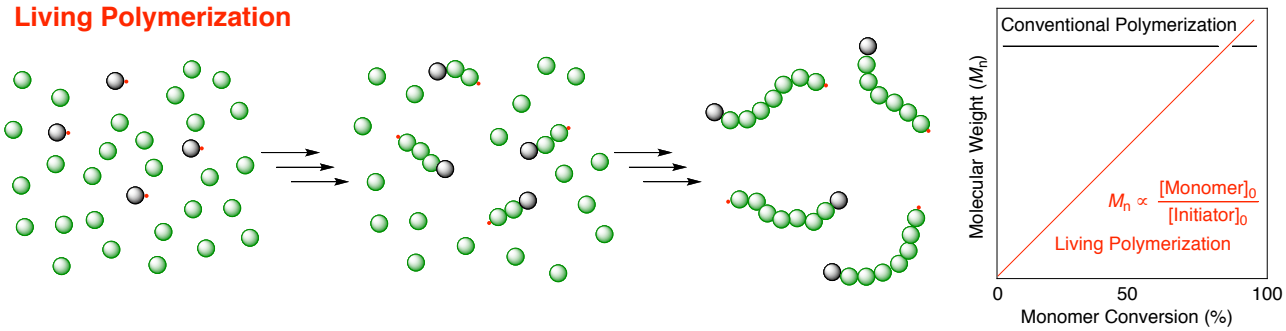

Scheme 3. Living Chain-Growth Polymerization

Evolution of Metal-Catalyzed Radical Addition into Living Chain-Growth Radical Polymerization. Starting with the pioneering work named "iniferter" by Otsu and co-workers in the 1980s,[9,10] a large variety of living chain-growth radical polymerization systems has been discovered from the mid 1990s. They all rely on a common concept, that is, to introduce the covalent dormant species at the chain end that can be reversibly converted into the growing radical species upon certain stimuli. Among them, the metal-catalyzed living radical polymerization or atom transfer radical polymerization (ATRP) is one of the most widely employed methods. In 1994,

Sawamoto et al. first reported the living radical polymerizations of methyl methacrylate using $RuCl_2(PPh_3)_3$ as the transition metal catalyst in conjunction with CCl_4 as the initiator.

This living radical polymerization has its origins in metal-catalyzed atom transfer radical addition (ATRA), sometimes called Kharasch addition. The radical addition between various vinyl compounds and organic halides is one of the most highly efficient and robust carbon-carbon (C–C) bond forming processes, and is utilized for the syntheses of small organic molecules via inter- and intramolecular additions.[11–19] In this reaction, the radical species is generated through the metal-assisted homolytic cleavage of the C–X bond, and adds to the carbon–carbon double (C=C) bond of the olefin to form the C–C bond followed by a new C–X bond formation upon retrieving the halogen from the oxidized metal catalyst and results in the 1:1 adduct (Scheme 4A).

This chemistry has thus been widely applied to chain-growth polymerizations as the metal-catalyzed living radical polymerization or ATRP, in which one polymer chain forms per molecule of organic halide as an initiator, while a catalytic amount of the metal complex serves as an activator to homolytically cleave the carbon-halogen terminal (Scheme 4B). The key for the controlled radical polymerization lies on iterative processes of the one-electron redox reaction during the entire polymerization reaction, i.e., the formation of the radical species from the C–X terminal catalyzed by the metal complex, addition to double bond of the monomers, and regeneration of the carbon–halogen terminal. The newly formed C–X bond between the carbon atom adjacent to the carbonyl or aryl group originating from the conjugated monomers and the halogen atom from the organic halide initiator is reactive for the appropriate metal catalyst to regenerate the growing radical species resulting in radical addition polymerization. During the process, the strategy for controlling radical polymerization is implemented, in which the instantaneous concentration of the growing radical species is kept low to avoid radical bimolecular

termination. The equilibrium between the dormant and active species can not only minimize the probability of the termination, but also give an equal opportunity of propagation to all dormant terminals via frequent interconversion. Therefore, the number-average molecular weight (M_n) of the resulting polymer increases in direct proportion to the monomer conversion and agrees with the calculated value on the assumption that one halide molecule (initiator) generates one polymer chain, as also shown in Scheme 3. Now that numerous metal-complexes and initiating systems have been developed for controlling the polymerization of various commercially available monomers, involving acrylates, styrene, and acrylamides, as well as the easy accessibility of stable carbon-halogen (C–X) bonds as the initiating sites,[20–33] the technique has been further used as a tool for the synthesis of the large variety of functional materials based on the controlled primary structures.

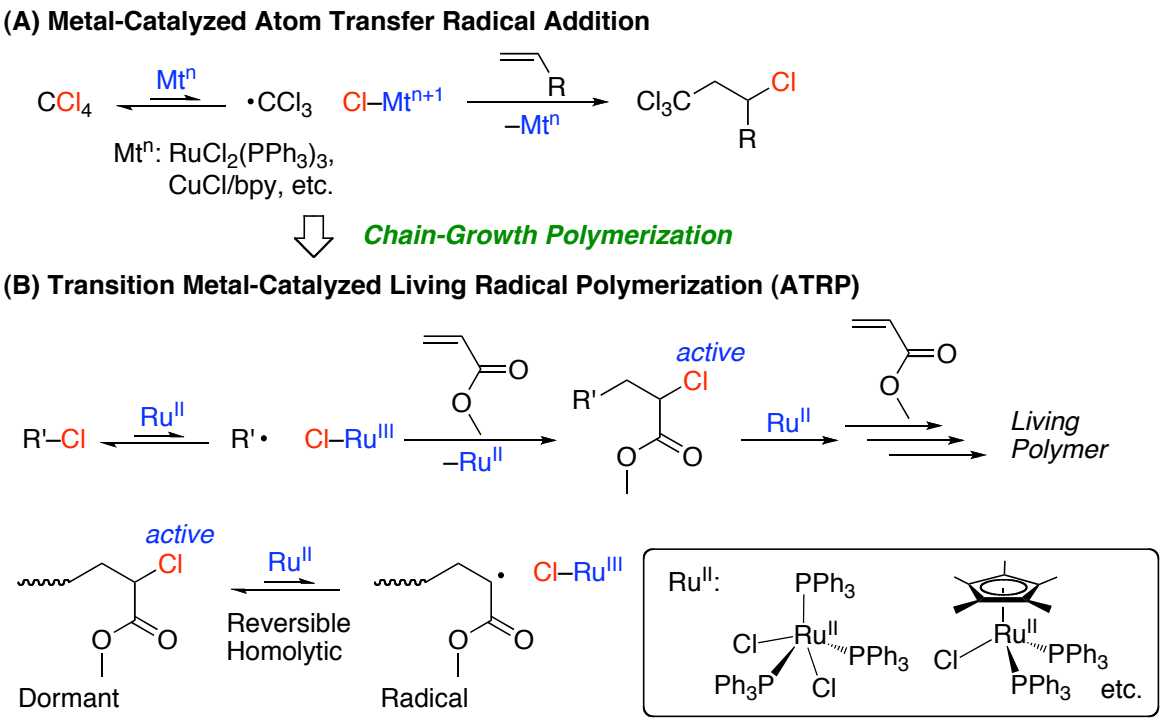

Scheme 4. (A) Metal-Catalyzed Atom Transfer Radical Addition and (B) Metal-Catalyzed Chain-Growth Living Radical Polymerization

Objectives

Considering these backgrounds, the author developed the radical addition reaction into step-growth polymerization, that is, metal-catalyzed radical polyaddition. In addition, using the same catalytic system, the simultaneous reaction of the chain-growth living radical polymerization and step-growth radical polyaddition was investigated. The two objectives are listed below.

(1) Metal-Catalyzed Step-Growth Radical Polyaddition

(2) Simultaneous Chain- and Step-Growth Radical Polymerization

(1) Metal-Catalyzed Step-Growth Radical Polyaddition. The first objective of this study was to evolve the metal-catalyzed radical addition into step-growth polymerization mechanism (Scheme 5). To achieve this new process, we designed a monomer possessing a reactive C–Cl bond, which can be activated by a metal catalyst to result in the carbon radical species, and an unconjugated C=C bond, to which the resulting carbon radical species can add to form a C–C bond along with an unreactive C–Cl pendant. In addition to the optimization of the reaction conditions for efficient polymerizations, the polymerization mechanism was analyzed in detail to establish the metal-catalyzed step-growth radical polyaddition.

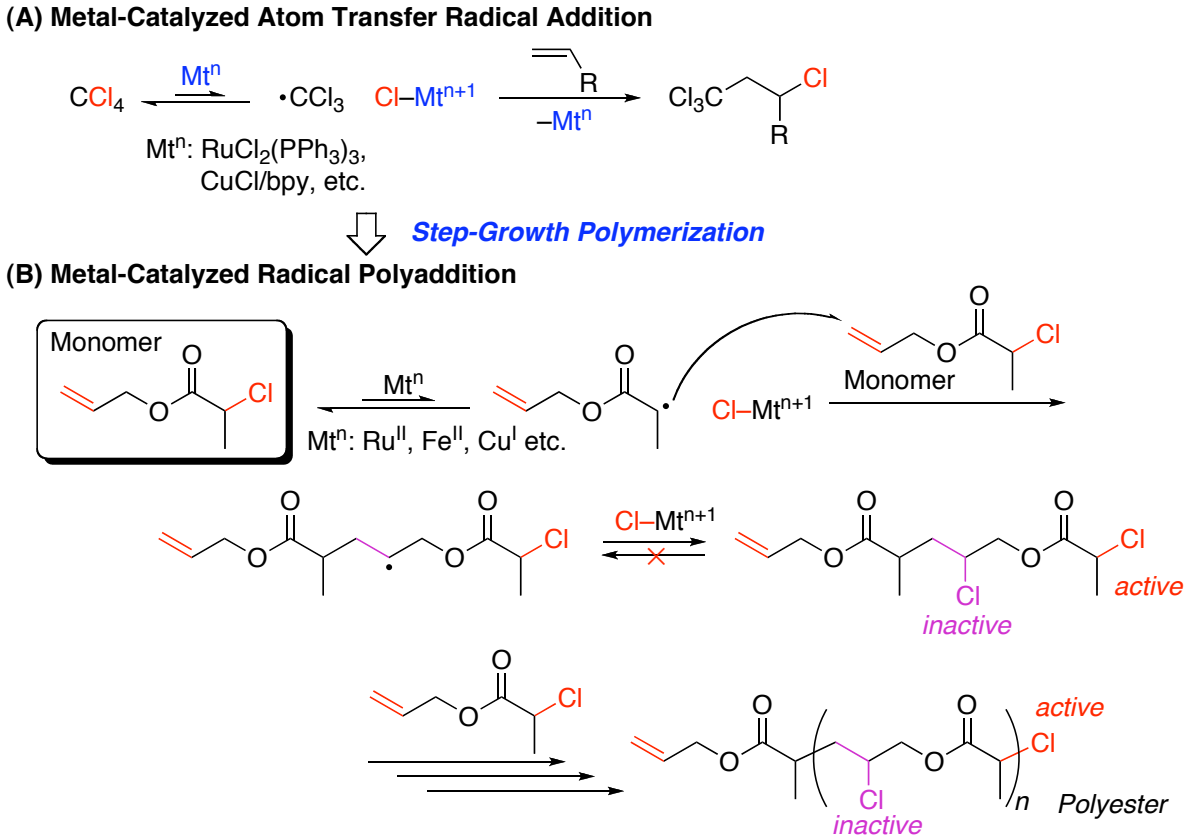

Scheme 5. (A) Metal-Catalyzed Atom Transfer Radical Addition and (B) Metal-Catalyzed Step-Growth Radical Polyaddition

(2) Simultaneous Chain- and Step-Growth Radical Polymerization. The second objective of this study was to develop the unprecedented simultaneous chain- and step-growth polymerizations (Scheme 6). Namely, the author investigated the simultaneous reaction of the chain-growth living radical polymerization and step-growth radical polyaddition by the same catalytic system. The simultaneous polymerizations were examined for common conjugated vinyl monomers and ester- or amide-linked monomers, in which various acrylates, acrylamides, or styrene were employed as the former for the chain-growth polymerization and the latter would afford polyester or polyamide unit via the step-growth polymerization, respectively. The author also applied this polymerization system to the synthesis of degradable functional vinyl polymers.

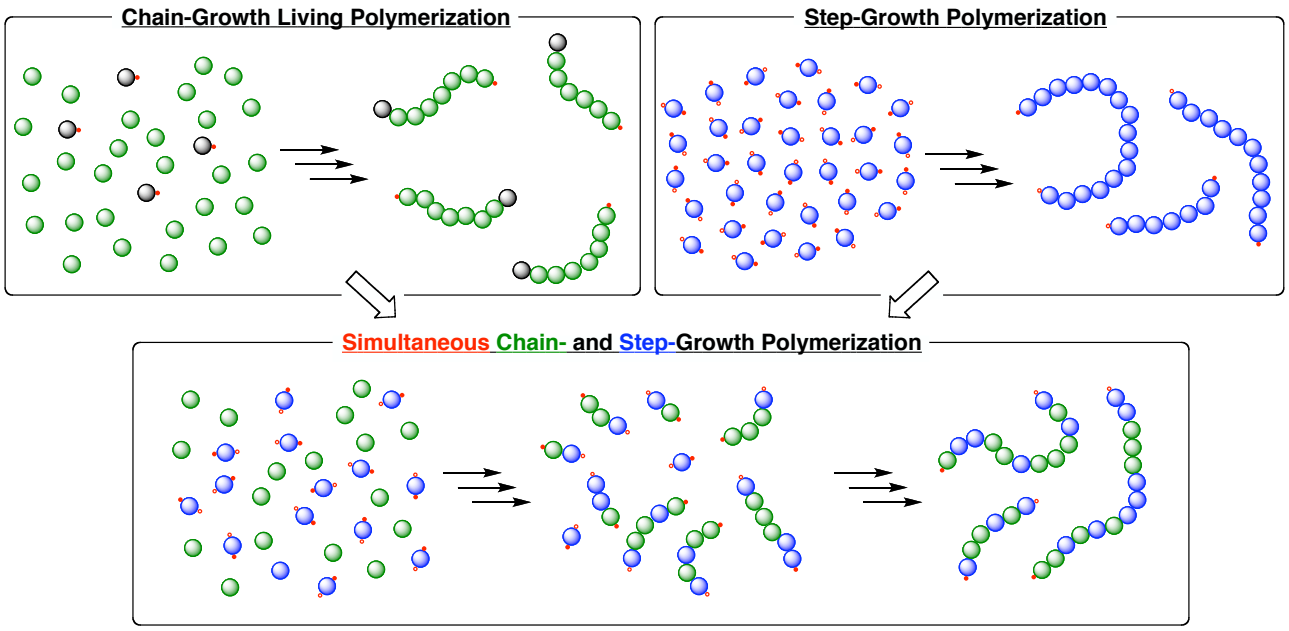

Scheme 6. Simultaneous Chain- and Step-Growth Polymerization

Outline of This Study

The present thesis consists of two parts: **Part I** (Chapter 1, 2) deals with the metal-catalyzed step-growth radical polyaddition of designed monomers that bear reactive C–Cl and unconjugated C=C double bonds. **Part II** (Chapter 3–6) presents the simultaneous polymerization of various conjugated vinyl monomers for the chain-growth polymerization and ester- or amide-linked monomers for the step-growth polymerization.

In Part I, ***Chapter 1*** describes metal-catalyzed C–C bond forming step-growth radical polyaddition; the monomers were designed to have a reactive C–Cl bond, which can be activated by the metal catalysts to generate a carbon radical species, along with a C=C double bond, to which the carbon radical generated from another molecule adds to form a C–C backbone polymer with an inactive C–Cl pendant (Scheme 7). The polyaddition reactions smoothly proceeded and the conversion reached over 99% with the $FeCl_2$/P*n*Bu_3 or

CuCl/*N*,*N*,*N'*,*N''*,*N''*-pentamethyldiethylenetriamine system to afford the polymers in high yield. In addition, alternating copolymer with vinyl chloride-methyl methacrylate sequence was obtained by polyaddition of designed monomer.

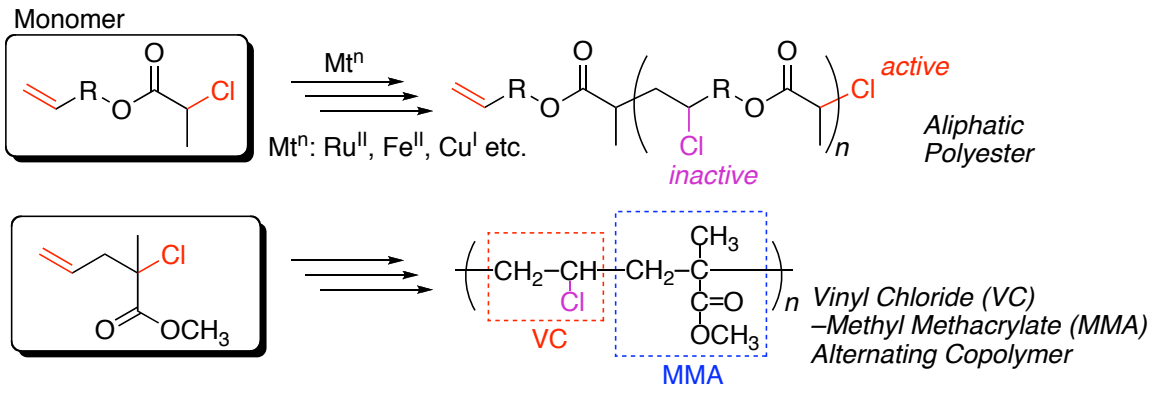

Scheme 7. Metal-Catalyzed Radical Polyaddition as a Novel Polymer Synthetic Route

Chapter 2 focuses on step-growth polymerization by using a series of designed monomers [CH_2=CH–R–OC(O)CH(CH_3)Cl] that bear a reactive C–Cl and an unconjugated C=C double bond via an ester linkage, and various metal catalysts to produce novel aliphatic polyesters (Scheme 8). The molecular weights progressively increased with the extent of reaction in the later stages and the molecular weight distributions were close to 2, indicating an ideal step-growth polymerization. The well-defined polymer structures were confirmed by ^{1}H-^{1}H correlation spectroscopy NMR analysis of the products along with the model 1:1 reactions between a halide and a vinyl compound. The polyester bearing an active C–Cl terminus obtained by the radical polyaddition was employed as a macroinitiator for the metal-catalyzed living radical polymerization of vinyl monomers such as styrene, methyl methacrylate, and methyl acrylate for block copolymers consisting of polyesters and vinyl polymers.

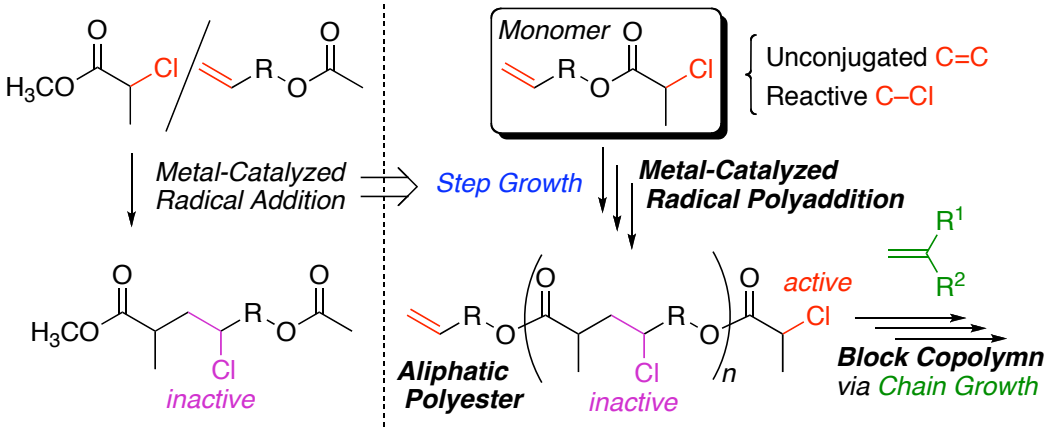

Scheme 8. Metal-Catalyzed Radical Polyaddition for Aliphatic Polyesters via Evolution of Atom Transfer Radical Addition into Step-Growth Polymerization

In Part II, ***Chapter 3*** discusses the simultaneous chain- and step-growth polymerization via the metal-catalyzed radical copolymerization of methyl acrylate (MA) for the chain-growth polymerization and 3-butenyl 2-chloropropionate (**1**) for the step-growth polymerization (Scheme 9). Especially, almost ideal linear random copolymers containing both vinyl polymer and polyester units in a single polymer chain were formed by the CuCl/1,1,4,7,10,10-hexamethyltriethylenetetramine- or $RuCp^*Cl(PPh_3)_2$-catalyzed copolymerization. In contrast, other transition metal catalysts, such as CuCl with tris[2-(dimethylamino)ethyl]amine or *N*,*N*,*N'*,*N''*,*N''*-pentamethyldiethylenetriamine and $FeCl_2$/P*n*Bu_3, resulted in branched structures via the concomitant chain-growth copolymerization of **1** with MA. The polymerization mechanism was studied in detail by NMR and MALDI-TOF-MS analyses of the polymerizations as well as the model reactions. Furthermore, a series of copolymers changing from random to multiblock polymer structures were obtained by varying the feed ratios of the two monomers. These copolymers can be easily degraded into lower molecular weight

oligomers or polymers via methanolysis of the ester-linkages in the main chain using sodium carbonate.

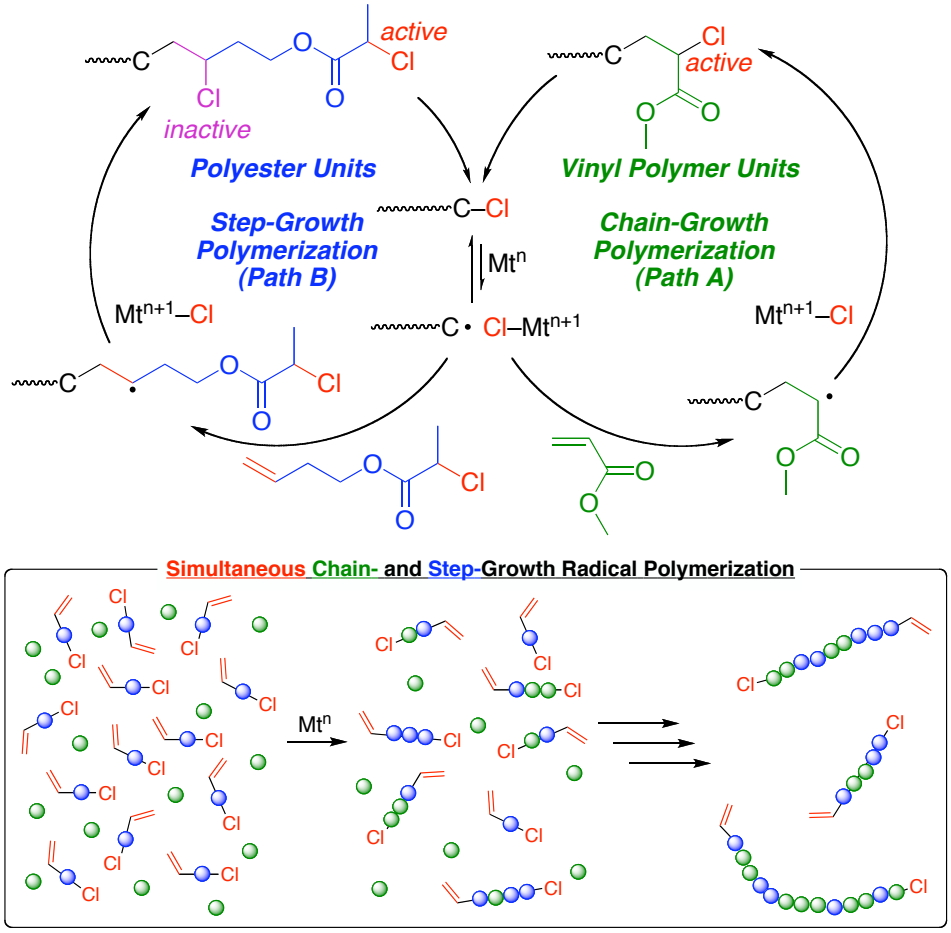

Scheme 9. Metal-Catalyzed Simultaneous Chain- and Step-Growth Radical Polymerization: Marriage of Vinyl Polymers and Polyesters

Chapter 4 illustrates the simultaneous chain- and step-growth radical polymerization for common conjugated vinyl monomers and designed ester- or amide-linked monomers bearing both an unconjugated carbon-carbon double bond and a reactive carbon-halogen bond in a single molecule. Herein, various alkyl and functional group-containing acrylates and styrene were employed as the former for the chain-growth polymerization, and the latter would afford polyester or polyamide unit via the step-growth polymerization (Scheme 10). In all cases, the simultaneous

polymerizations smoothly proceeded to afford the linear random copolymers containing both monomer units. Especially, for styrene as a vinyl monomer, the highly selective chain-growth living polymerization proceeded quantitatively before the step-growth polymerization took place between the living polystyrene chains. The molecular weights of the obtained copolymers progressively increased with monomer consumpstion and were close to the calculated values throughout the polymerization. The well-defined polymer structures were confirmed by ^{1}H NMR and MALDI-TOF-MS analysis of the products.

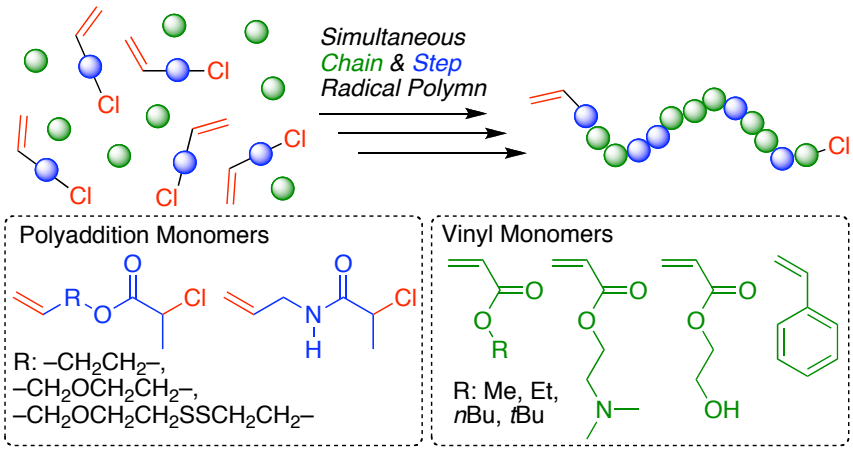

Scheme 10. Novel Copolymers by Metal-Catalyzed Simultaneous Chain- and Step-Growth Radical Polymerization of Various Monomers

Chapter 5 deals with the simultaneous chain- and step-growth radical polymerization of NIPAM for the dual control in degradability and thermoresponsivity of the product (Scheme 11). A very fast metal-catalyzed simultaneous chain- and step-growth radical polymerization of *N*-isopropylacrylamide (NIPAM) and ester- or amide-linked monomers was achieved at room temperature to afford the segmented poly(NIPAM) with controlled segment lengths connected by those linkages. The thermosensitivity of the polymer can be tuned from 24 to 40 °C by the

comonomer and feed ratios. Furthermore, upon hydrolysis of the ester linkages in the main chains, the phase-transition temperature of poly(NIPAM) dramatically increased to 38–81 °C.

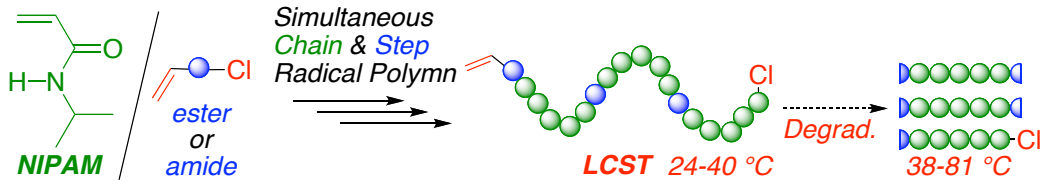

Scheme 11. Degradable Poly(*N*-Isopropylacrylamide) with Tunable Thermosensitivity by Simultaneous Chain- and Step-Growth Radical Polymerization

Chapter 6 is directed to the synthesis of self-degradable antimicrobial copolymers bearing cationic side chains and main-chain ester linkages were synthesized using the simultaneous chain- and step-growth radical polymerization of *t*-butyl acrylate and an ester linked monomer (3-butenyl 2-chloropropionate), followed by the transformation of *t*-butyl groups into primary ammonium salts (Scheme 12). The copolymers displayed antimicrobial activity against some bacteria depending on the side-chain structures and the molecular weights. The copolymers were degraded in aqueous solution to lower molecular weight products via the cleavage of the main-chain ester linkages attacked by the pendent primary amine groups. The degradation mechanism was studied in detail by the model reactions between amine compounds and precursor copolymers.

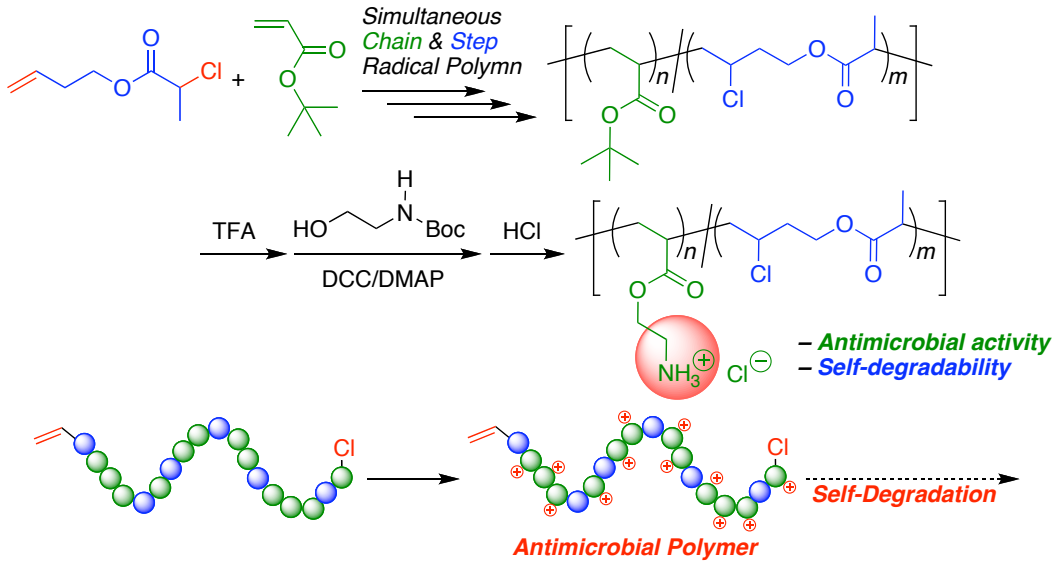

Scheme 12. Design and Synthesis of Self-Degradable Antimicrobial Polymers Consisting of Vinyl Polymer and Polyester Units by Simultaneous Chain- and Step-Growth Radical Copolymerization

NOTES AND REFERENCES

(1) Odian, G. *Principles of Polymerization, Fourth Edition*; John Wiley and Sons, Inc., New Jersey, 2004.

(2) Szwarc, M. *Nature (London)* **1956**, *178*, 1168–1169.

(3) Szwarc, M.; Levy, M.; Milkovich, R. J. *J. Am. Chem. Soc.* **1956**, *78*, 2656–2657.

(4) Morton, M. *Anionic Polymerization: Principles and Practice*; Academic Press: New York, 1983; pp 221–232.

(5) Kennedy, J. P.; Ivan, B. *Designed Polymers by Carbocationic Macromolecular Engineering: Theory and Practice*; Hanser Publishers: Munich, 1992; p 96.

(6) Sawamoto, M.; Kamigaito, M. In *New Methods of Polymer Synthesis*; Ebdon, J. R.; Eastmond, G. C., Eds.; Blackie: Glasqow, U. K., 1995; Vol. 2, pp 37–68.

(7) Moad, G.; Solomon, D. H. *The Chemistry of Radical Polymerization, 2nd Ed.*; Elsevier: Oxford, UK, 2006.

(8) Handbook of Radical polymerization; Matyjaszewski, K., Davis, T. P., Eds.; Wiley-Interscienece: New York, 2002.

(9) Otsu, T; Yoshida, M. *Chem. Rapid. Commun.* **1982**, *3*, 127–132.

(10) Otsu, T. *J. Polym. Sci., Part A: Polym. Chem.* **2000**, *38*, 2121–2136.

(11) Kharasch, M. S.; Jensen, E. V.; Urry, W. H. *Science* **1945**, *102*, 128–128.

(12) Kharasch, M. S.; Urry, W. H. *J. Am. Chem. Soc.* **1945**, *67*, 1626–1626.

(13) Minisci, F. *Acc. Chem. Res.* **1975**, 8, 165–171.

(14) Iqbal, J.; Bhatia, B.; Nayyar, N. K. *Chem. Rev.* **1994**, *94*, 519–564.

(15) Gossage, R. A.; van de Luil, L. A.; van Koten, G. *Acc. Chem. Res.* **1998**, *31*, 423–431.

(16) Nagashima, H. In *Ruthenium in Organic Synthesis*; Murahashi, S.-I. Ed.; Wiley-VCH,

Weinheim, 2004; pp. 333–343.

(17) Delaude, L.; Demonceau, A.; Noels, A. F. *Top. Organomet. Chem.* **2004**, *11*, 155–171.

(18) Pintauer, T.; Matyjaszewski, K. *Chem. Soc. Rev.* **2008**, *37*, 1087–1097.

(19) Fernández-Zúmel, M. A.; Thommes, K.; Kiefer, G.; Sienkiewicz, A.; Pierzchala, K.; Severin, K. *Chem. Eur. J.* **2009**, *15*, 11601–11607.

(20) Kato, M.; Kamigaito, M.; Sawamoto, M.; Higashimura, T. *Macromolecules* **1995**, *28*, 1721–1723.

(21) Wang, J.-S.; Matyjaszewski, K. *J. Am. Chem. Soc.* **1995**, *117*, 5614–5615.

(22) Percec, V.; Barboiu, B. *Macromolecules* **1995**, 28, 7970–7972.

(23) Patten, T. E.; Xia, J.; Abernathy, T.; Matyjaszewski, K. *Science* **1996**, *272*, 866–868.

(24) Granel, C.; Dubois, Ph.; Jérôme, R.; Teyssié, Ph. *Macromolecules* **1996**, *29*, 8576.

(25) Haddleton, D. M.; Jasieczek, C. B.; Hannon, M. J.; Shooter, A. J. *Macromolecules* **1997**, *30*, 2190.

(26) Matyjaszewski, K.; Xia, J. *Chem. Rev.* **2001**, *101*, 2921–2990.

(27) Kamigaito, M.; Ando, T.; Sawamoto, M. *Chem. Rev.* **2001**, *101*, 3689–3746.

(28) Kamigaito, M.; Ando, T.; Sawamoto, M. *Chem. Rec.* **2004**, *4*, 159–175.

(29) Tsarevsky, N. V. Matyjaszewski, K.; *Chem. Rev.* **2007**, *107*, 2270–2299.

(30) Braunecker, W. A.; Matyjaszewski, K. *Prog. Polym. Sci.* **2007**, *32*, 93–146.

(31) Matyjaszewski, K.; Tsarevsky, N. V. *Nat. Chem.* **2009**, *1*, 276–288.

(32) Ouchi, M.; Terashima, T.; Sawamoto, M. *Chem. Rev.*, **2009**, *109*, 4963–5050.

(33) Rosen, B. M.; Percec,V. *Chem. Rev.* **2009**, *109*, 5069–5119.

PART I

Metal-Catalyzed Step-Growth Radical Polyaddition

Chapter 1

Metal-Catalyzed Radical Polyaddition as a Novel Polymer Synthetic Route

ABSTRACT

A new class of polymerizations was developed via metal-catalyzed C–C bond forming radical polyaddition; the monomers were designed to have a reactive C–Cl bond, which can be activated by the metal catalysts to generate a carbon radical species, along with a C=C double bond, to which the carbon radical generated from another molecule adds to form a C–C backbone polymer with an inactive C–Cl pendant.

Introduction

The metal-catalyzed atom transfer radical addition (ATRA) is one of the highly efficient carbon–carbon bond forming radical reactions, in which the radical species is generated through the metal-catalyzed cleavage of a carbon–halogen (C–X) bond and adds to an olefin to form the 1 : 1 adduct of the halide and olefin.[1] This chemistry has been effectively and widely applied to radical addition polymerizations of vinyl monomers that developed into the metal-catalyzed living radical polymerization or atom transfer radical polymerization (ATRP) and to open a new era of precision polymer synthesis.[2–6] The radical addition polymerization proceeds via the metal-catalyzed reversible formation of the growing radical species from the dormant polymer terminal with a C–X bond, which originates from the halide initiator, and the addition of the growing radical species to the vinyl monomers.

In this chapter, novel radical polyaddition reactions are developed for a designed monomer that possesses an active C–X bond and an unconjugated carbon–carbon double bond via metal-catalyzed carbon–carbon bond forming radical reactions (Scheme 1). Namely, the active or dormant C–X bond in the monomer is activated by the metal catalysts to form a radical species, which adds to the C=C double bond of another monomer molecule to generate a C–C bond as the main chain, along with an inactive C–X bond as the pendant. The original C–X bond in the monomer or the resulting oligomer or polymer is active in the catalysis due to the adjacent carbonyl group while the resulting C–X bond is inactive due to the absence of the adjacent carbonyl moiety.[7] These conceptually new polyaddition reactions can provide new types of linear polymers, such as the equivalents for the sequence-regulated vinyl polymers, as shown below. While monomers with a C–X bond and a conjugated C=C double bond were used in the metal-catalyzed radical

addition polymerizations, the monomers served as an ‘‘ini-mer’’ to produce highly branched polymers via the activation of both the original and the resulting C–X bonds.[8]

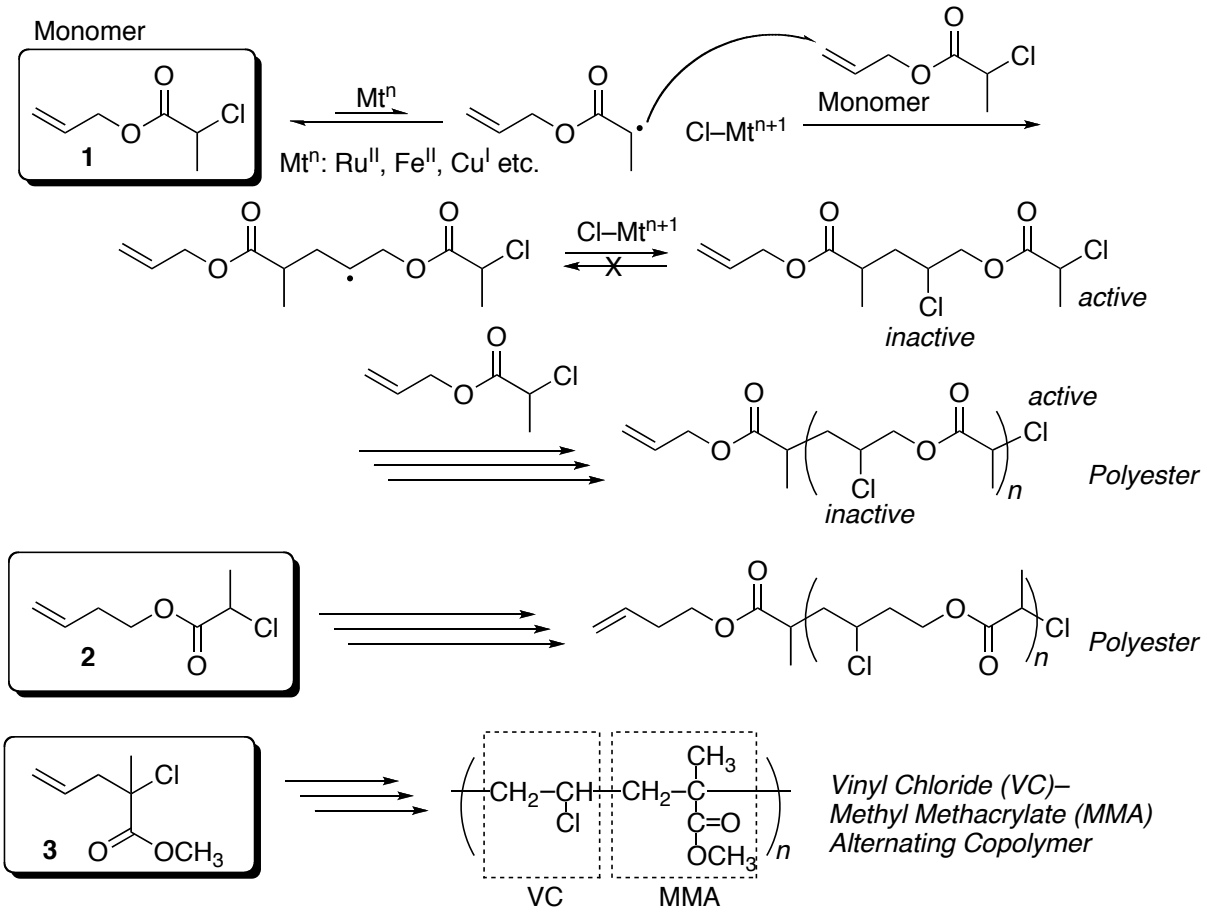

Scheme 1. Transition Metal-Catalyzed Radical Polyaddition

Results and Discussion

1. Polyaddition of Monomers (1–3) under Various Conditions. Herein, the author designed ester-linked monomers (**1** and **2**), which would afford aliphatic polyesters, and another monomer (**3**), which could apparently produce the equivalent structure of the alternating copolymer of vinyl chloride (VC) and methyl methacrylate (MMA). All these monomers were designed to have unconjugated double bonds, and the activated C–Cl bond adjacent to the carbonyl group.

For the first attempts to show the new radical polyaddition reactions, **1**, which can be easily obtained from allyl alcohol and 2-chloropropionyl chloride, was examined in conjunction with various transition metal complexes, such as Ru^{II}, Fe^{II}, and Cu^{I}, in toluene at 100 °C (Figure 1). The reactions were carried out by the appropriate combinations of the metals and the ligands, all of which are effective for the metal-catalyzed living radical polymerizations; i.e., the $RuCl_2(PPh_3)_3$ complex with an amine additive, $FeCl_2$ with 4 equiv. of P*n*Bu_3 or *N*,*N*,*N*',*N*'',*N*''-pentamethyldiethylenetriamine (PMDETA), and CuCl with 4 equiv. of PMDETA were used.[2,3,9–11] The monomer was smoothly consumed and the conversion reached over 90% to afford polymers in high yield with the $RuCl_2(PPh_3)_3$, $FeCl_2$/P*n*Bu_3, and CuCl/PMDETA systems.

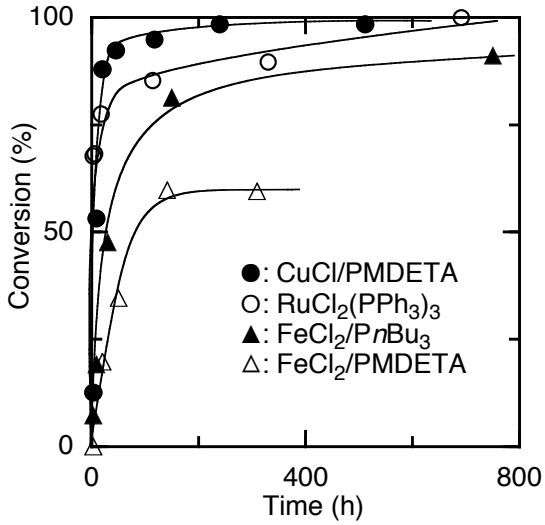

Figure 1. Time–conversion curves for the polyaddition of **1** with various metal complexes: $[\mathbf{1}]_0$ = 4.0 M; $[Metal]_0$ = 100 mM; $[PnBu_3]_0$ = 200 mM; $[PMDETA]_0$ = 400 mM in toluene at 100 °C. $[nBu_3N]_0$ = 400 mM (for Ru^{II}).

Figure 2 shows the size-exclusion chromatography (SEC) curves of the polymers obtained using $FeCl_2$/P*n*Bu_3 and CuCl/PMDETA. The peaks of the SEC curves shifted to a higher molecular weight and the peak areas of the lower molecular weight regions decreased as the

polymerization proceeded. Similar to the conventional step polymerizations, the molecular weight of the polymers increased exponentially at the later stage of the polymerizations. These results indicated that the step-growth polyaddition reactions effectively took place without unwanted ring-closing processes.[12]

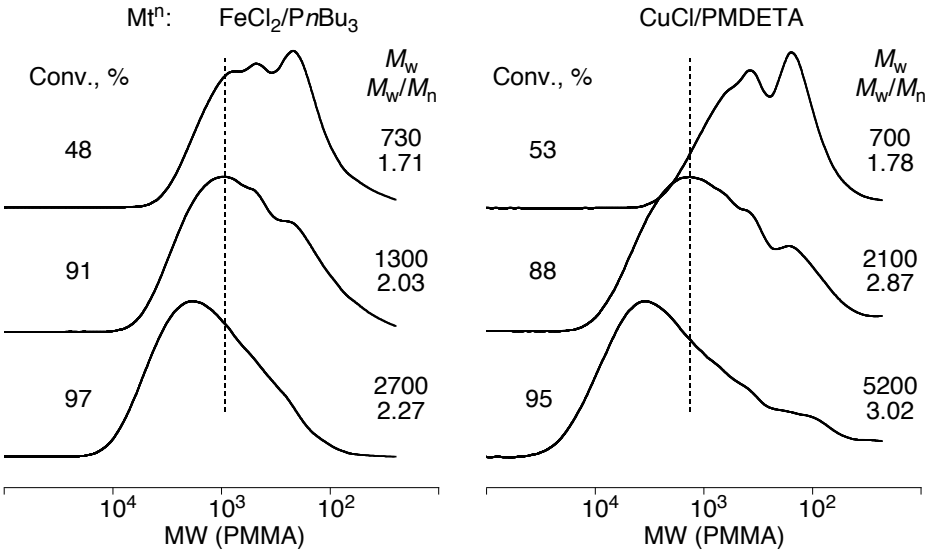

Figure 2. SEC curves of poly(**1**) obtained with the $FeCl_2$/P*n*Bu_3 and CuCl/PMDETA: $[\mathbf{1}]_0$ = 4.0 M; $[Metal]_0$ = 100 mM; $[PnBu_3]_0$ = 200 mM (for Fe); $[PMDETA]_0$ = 400 mM (for Cu) in toluene at 100 °C.

Table 1 summarizes the polymerizations of **1**–**3** with a series of the catalysts under various conditions. The reactions proceeded in all cases to produce the polymers, although the molecular weights of some polymers were relatively low. For **1** and **2**, the reaction rates and the molecular weights of the polymers were dramatically changed by a combination of the central metals and the ligands. Among them, higher molecular weights were attained with the $FeCl_2$/P*n*Bu_3 and CuCl/PMDETA systems that reached $M_w \sim 5 \times 10^3$. Furthermore, upon the addition of tin 2-ethylhexanoate [$Sn(EH)_2$], which recently proved effective as a reducing agent for

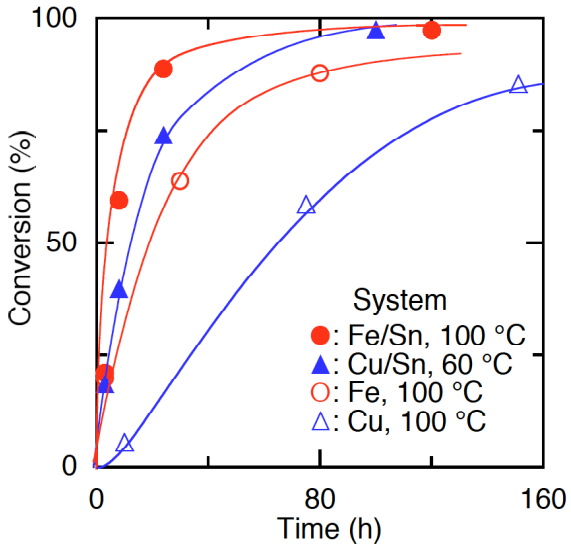

Figure 3. Effects of $Sn(EH)_2$ on the polyaddition of 3-butenyl 2-chloropropionate (**2**) with the $FeCl_2/PnBu_3$ or CuCl/PMDETA sytem: $[\mathbf{2}]_0 = 4.0$ M; $[Mt]_0 = 100$ mM; $[ligand]_0 = 200$ ($PnBu_3$) or 400 mM (PMDETA); $[Sn(EH)_2]_0 = 45$ mM (EH: 2-ethylhexanoate) in toluene.

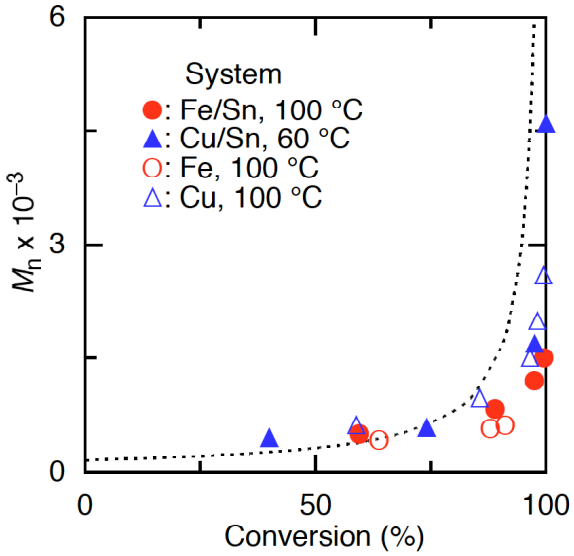

Figure 4. M_n, M_w/M_n, and MWD curves of poly(**2**) obtained in the same experiments as for Figure 3. The dotted line indicates the calculated M_n assuming the following equation: M_n = molecular weight of **2**/(1 - conversion).

Table 1 Transition metal catalyzed radical polyaddition of **1–3**[a]

Monomer	Metal	Ligand	$[Ligand]_0$	Additive	Temperature/°C	Time/h	Conversion (%)[e]	M_n[f]	M_w[f]	M_w/M_n[f]
1	$RuCl_2(PPh_3)_3$[b]	—	—	*n*-Bu_3N[c]	100	330	90	410	820	2.01
1	$FeCl_2$	P*n*-Bu_3	400 mM	None	100	1180	94	460	1000	2.28
1	$FeCl_2$	P*n*-Bu_3	200 mM	None	100	750	91	710	1800	2.51
1	$FeCl_2$	P*n*-Bu_3	200 mM	$Sn(EH)_2$[d]	100	750	87	630	1500	2.35
1	$FeCl_2$	PMDETA	400 mM	None	100	310	60	1100	4000	3.70
1	CuCl	PMDETA	400 mM	None	100	240	99	1300	5600	4.21
2	$FeCl_2$	P*n*-Bu_3	200 mM	None	100	250	91	620	1200	1.95
2	$FeCl_2$	PPh_3	400 mM	None	100	300	47	400	610	1.52
2	$FeCl_2$	P*n*-Bu_3	200 mM	$Sn(EH)_2$[d]	100	480	>99	1500	3500	2.32
2	CuCl	PMDETA	400 mM	None	100	460	97	1100	3000	2.74
2	CuCl	PMDETA	400 mM	None	80	240	97	1700	5500	3.30
2	CuCl	PMDETA	400 mM	None	60	1350	99	2600	11 000	4.12
2	CuCl	PMDETA	400 mM	$Sn(EH)_2$[d]	60	500	>99	4600	21 000	4.60
3	$RuCl_2(PPh_3)_3$[b]	—	—	*n*-Bu_3N[c]	100	700	92	540	910	1.68
3	$FeCl_2$	P*n*-Bu_3	200 mM	None	100	1500	75	470	660	1.42
3	$FeCl_2$	P*n*-Bu_3	400 mM	$Sn(EH)_2$[d]	100	480	79	490	770	1.57
3	CuCl	PMDETA	400 mM	None	100	540	62	570	980	1.73

[a] Polymerization conditions: $[M]_0$ = 4.0 M; $[Metal]_0$ = 100 mM in toluene. [b] $RuCl_2(PPh_3)_3$ was used as purchased. [c] $[n\text{-}Bu_3N]_0$ = 400 mM. [d] $[Sn(EH)_2]_0$ = 45 mM; EH: 2-ethylhexanoate. [e] Determined by gas chromatography. [f] The number-average and weight-average molecular weight (M_n and M_w, respectively) and polydispersity index (M_w/M_n) were determined by size-exclusion chromatography.

the oxidized catalyst in the Cu-mediated ATRP,[13] the reactions of **2** with the Cu and Fe systems were accelerated and the molecular weights of the polymers became the highest (Figure 3, 4). These indicate that the polyaddition proceeded via a one-electron redox reaction of the metal center and that this polyaddition reaction also suffered from the formation of small amounts of inactive catalysts during the metal-catalyzed radical reactions. For **3**, which possesses a C–Cl bond similar to that derived from methacrylate, the $RuCl_2(PPh_3)_3$ system was more effective, giving a higher monomer conversion than the others. These results are consistent with the fact that the Ru^{II}-based systems are more suitable for methacrylates in terms of the control of the polymerizations.[2,9] The addition of $Sn(EH)_2$ also accelerated the polyaddition of **3** with $FeCl_2$/P*n*Bu_3, though the effects on the polymer molecular weight increase were smaller than those for **2**.

2. Analysis of Polymers. The structures of the obtained polymers were then analyzed by ^{1}H NMR and matrix-assisted laser-desorption-ionization time-of-flight mass (MALDI-TOF-MS) spectroscopy. Figure 5 shows the ^{1}H NMR spectra of monomer **2** and typical samples of poly(**2**), which were obtained using $FeCl_2$/P*n*Bu_3 and CuCl/PMDETA and purified by preparative SEC to remove the residual monomer and the catalysts. In both spectra of the polymers, a series of sharp peaks (*1'–6'*) were observed, similar to those in the monomer (*1–6*), which indicates the presence of the double bond and the active C–Cl bonds at the chain ends of the polymers. In addition to these signals, broad and relatively large peaks (*a–f*) appeared, assignable to the main chain protons of the repeating units of the aliphatic polyester that should be generated via the expected polyaddition reactions. No unsaturated protons, possibly caused by chlorine elimination, were detected other than those of the original terminal C=C bond, further indicating that the effective polyaddition reactions proceeded without any significant side reactions under the appropriate conditions. The

molecular weights determined from the relative peak areas of the main-chain repeat units (*e*) to the end-group moiety (*1'* and *2'*) were close to those determined by SEC. These results show that the polymers were produced via the expected intermolecular polyaddition.

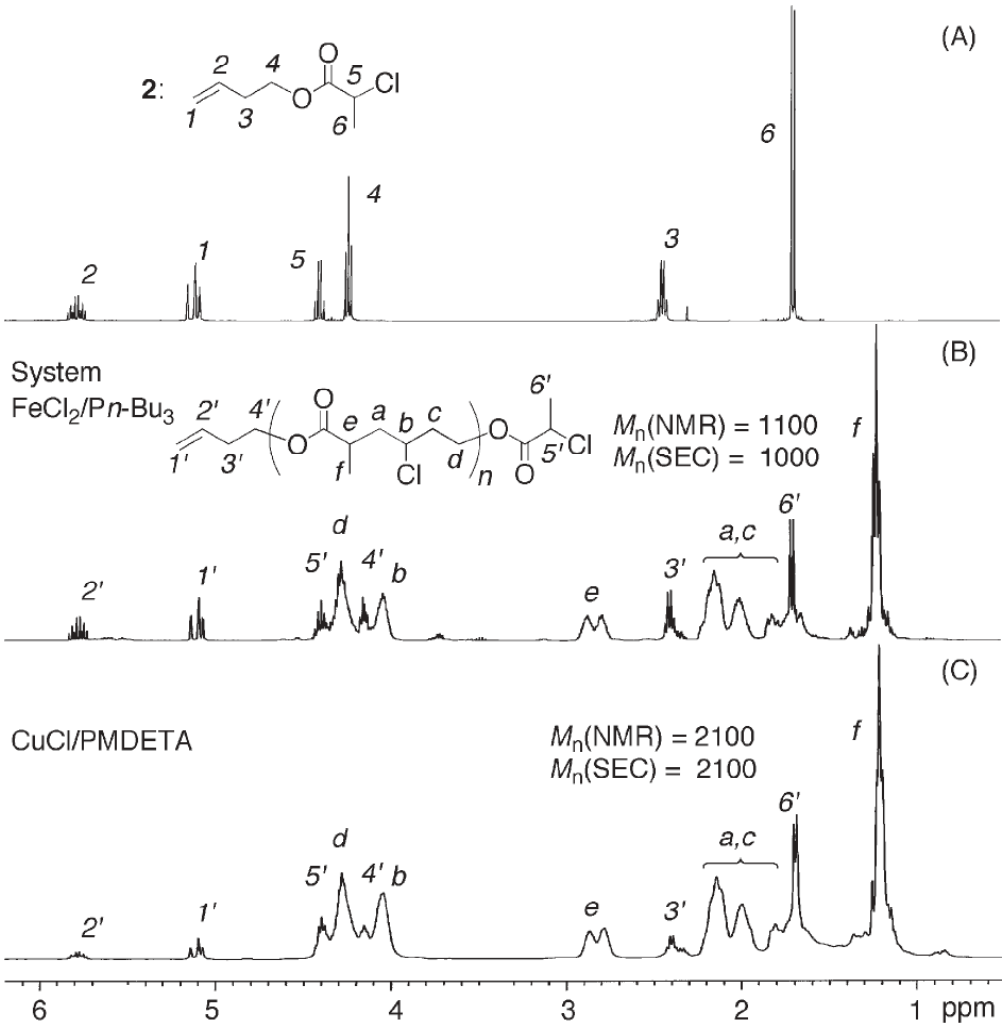

Figure 5. ^{1}H NMR spectra of (A) 3-butenyl 2-chloropropionate (**2**) and poly(**2**) obtained in toluene with (B) $FeCl_2/PnBu_3$ at 100 °C or (C) CuCl/PMDETA at 80 °C.

Figure 6 shows the MALDI-TOF-MS spectra of poly(**1**) and poly(**2**) obtained using the CuCl/PMDETA system. The spectra consist of a series of peaks each separated by 148.3 and 161.8 Da intervals, which correspond to the formula weight of monomers **1** and **2**, respectively.

The molecular weights of each individual peak were very close to the calculated values; *i.e.*, multiples of the formula weight of **1** or **2** plus the sodium ion from the salt for the MS analysis. This again indicates that the polymerizations proceed via intermolecular polyaddition. Both spectra exhibited a minor series of peaks, shifted by ca. 35 Da from the major series, which most probably suggests some loss of the reactive Cl atom at the chain end during the laser-induced ionization. Similar Cl-capped polymers synthesized via the living radical polymerization also lose the halogen at the *v*-end during the MS analysis.[14] In contrast, the resulting C–Cl bonds in the main chain are more stable even toward the laser ionization.

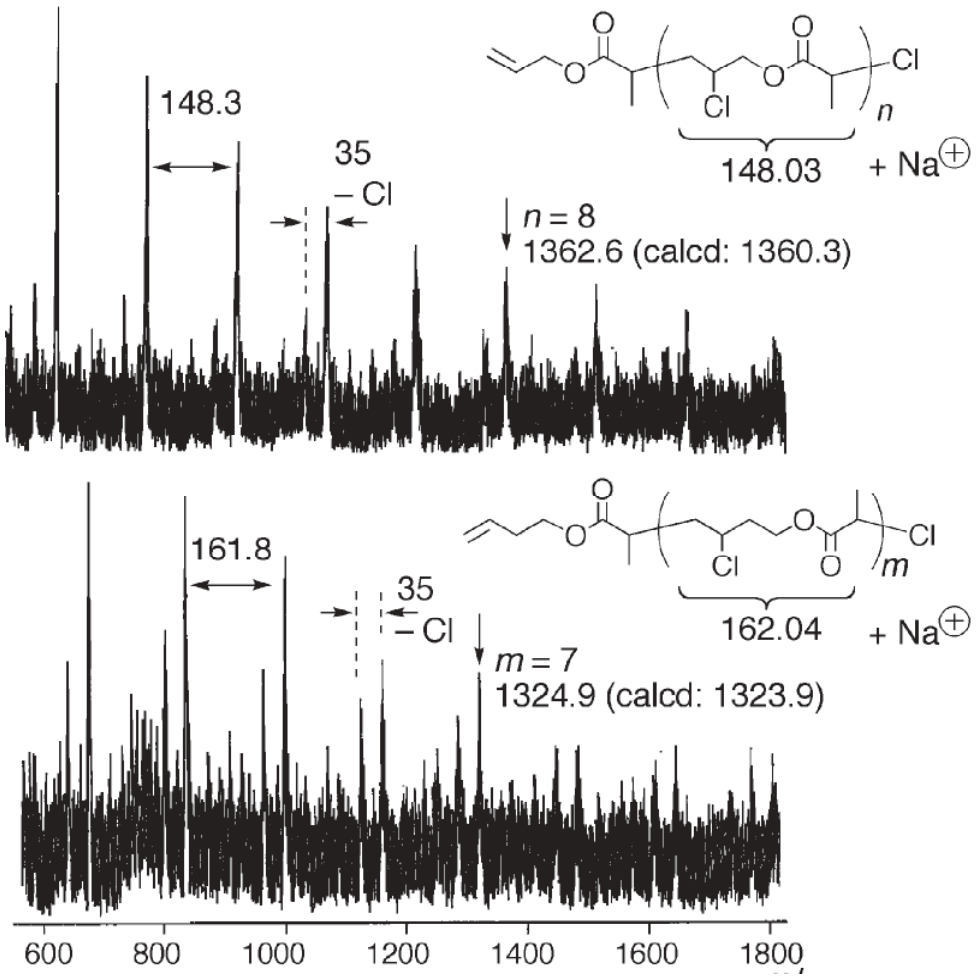

Figure 6. MALDI-TOF-MS spectra of poly(**1**) (M_n = 1600, M_w/M_n = 2.51) and poly(**2**) (M_n = 1300, M_w/M_n = 3.07) obtained using the CuCl/PMDETA: $[M]_0$ = 4.0 M; $[CuCl]_0$ = 100 mM; $[PMDETA]_0$ = 400 mM in toluene at 100 °C.

Conclusions

In conclusion, metal-catalyzed intermolecular radical polyadditions successfully proceeded for the designed monomers and proved a novel polymer synthetic method. Further studies are now in progress to explore the systems for designing the equivalents to the sequence-regulated vinyl polymers.

EXPERIMENTAL SECTION

Materials

$RuCl_2(PPh_3)_3$ (Wako), $FeCl_2$ (Aldrich; 99.99%), CuCl (Aldrich; 99.99%), and P*n*Bu_3 (KANTO ; > 98%) were used as received and handled in a glove-box (VAC Nexus) under a moisture- and oxygen-free argon atmosphere (O_2 < 1 ppm). PMDETA (Tokyo Kasei; > 98%) was distilled over calcium hydride before use. All other reagents were purified by usual methods.

Monomer Synthesis (1–3)

Allyl 2-chloropropanoate (**1**) and 3-butenyl 2-chloropropionate (**2**) were synthesized from 2-chloropropionyl chloride (Aldrich; 97%) and the corresponding alcohols; i.e. allyl alcohol (Tokyo Kasei; > 99%) and 3-buten-1-ol (Tokyo Kasei; > 98%) for **1** and **2**, respectively. CH_2=$CHCH_2C(CO_2Me)(Me)Cl$ (**3**) was prepared according to the litereture.[15] The reaction was carried out by the syringe technique under dry argon atmosphere in an oven-dried glass tube equipped with three-way stopcocks. A typical synthetic example for **2** is given below. 2-Chloropropionyl chloride (51.0 mL, 0.525 mol) was added dropwise with vigorous stirring to a solution of 3-buten-1-ol (42.4 mL, 0.50 mol) and triethylamine (76.7 mL, 0.55 mol) in dry THF

(80.0 mL) at 0 °C. The mixture kept stirred for 1 h at 0 °C, and then over 12 h at room temperature. After the dilution with diethyl ether, the mixture was washed with 10% aqueous solution of $NaHCO_3$ and then water and evaporated to remove the solvents. The monomer was distilled over calcium hydride under reduced pressure to give pure 3-butenyl 2-chloropropionate (**2**) (56.0 mL, 0.354 mol) (yield = 70.9%, purity > 99%). Figure 7 shows the ^{1}H NMR spectra of the monomers (**1**–**3**).

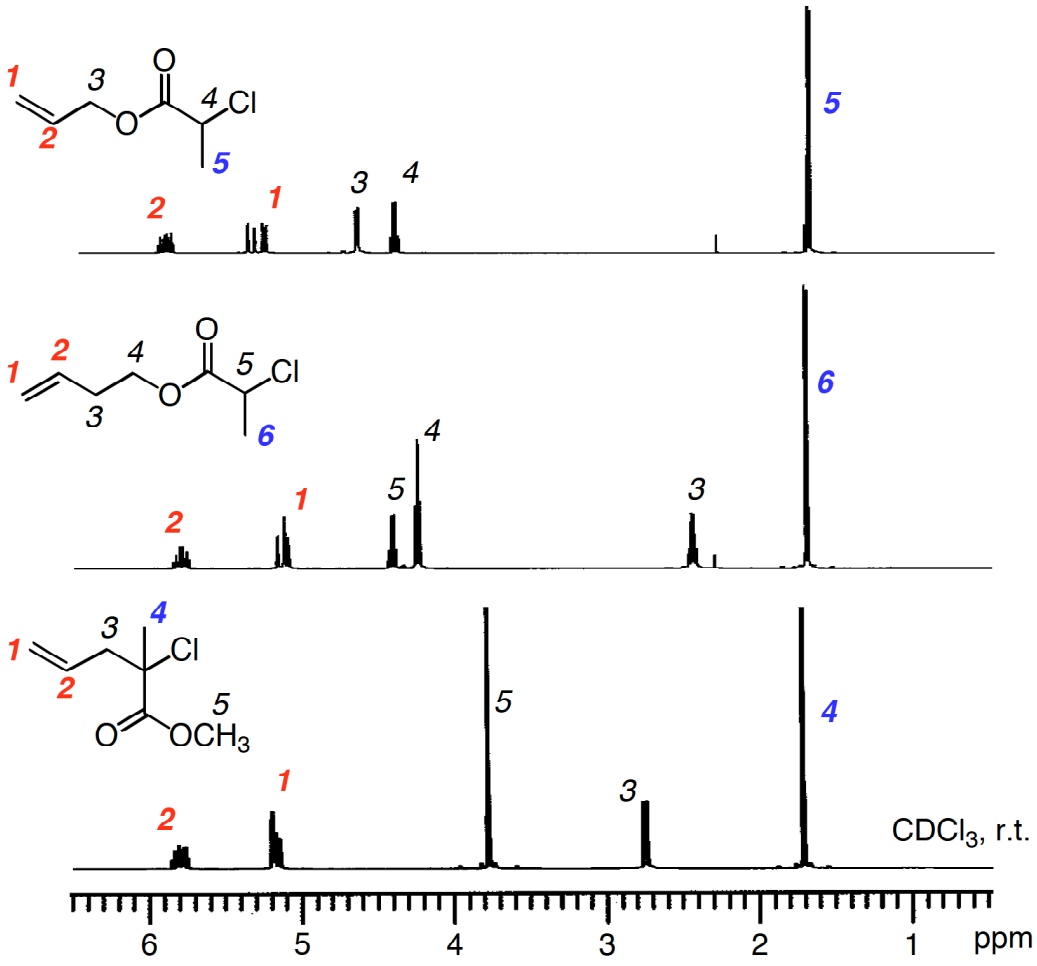

Figure 7. ^{1}H NMR spectra of **1**–**3**.

Polymerization

Polymerization was carried out under dry nitrogen in baked glass tubes equipped with a

three-way stopcock. A typical example for the polymerization procedure is given below. To a suspension of $FeCl_2$ (50.7 mg, 0.40 mmol) in toluene (1.27 mL) was added P*n*Bu_3 (0.20 mL, 0.80 mmol), and the mixture kept stirred for 24 h at 80 °C to give a homogeneous solution of the FeCl2(P*n*$Bu_3)_n$ complex. After the solution was cooled to the room temperature, 3-butenyl 2-chloropropionate (**2**) (2.53 mL, 16.0 mmol) was added. The solution was evenly charged in 8 glass tubes and the tubes were sealed by flame under nitrogen atmosphere. The tubes were immersed in thermostatic oil bath at 100 °C. In predetermined intervals, the polymerization was terminated by cooling the reaction mixtures to –78 °C. Monomer conversion was determined from the concentration of residual monomer measured by gas chromatography with toluene as an internal standard.

Measurements

Monomer conversion was determined from the concentration of residual monomer measured by gas chromatography [Shimadzu GC-8A equipped with a thermal conductivity detector and a 3.0 mm i.d. Å~ 2 m stainless steel column packed with SBS-200 (Shinwa Chemical Industries Ltd.) supported on Shimalite W; injection and detector temperature = 200 °C, column temperature = 160 °C] with toluene as an internal standard under He gas flow. ^{1}H NMR spectra were recorded in $CDCl_3$ at 25 °C on a Varian Gemini 2000 spectrometer, operating at 400 MHz. The number average molecular weight (M_n) and weight-average molecular weight (M_w) of the product polymers were determined by size-exclusion chromatography (SEC) in THF at 40 °C on two polystyrene gel columns [Shodex K-805L (pore size: 20–1000 Å; 8.0 mm i.d. Å~ 30 cm) Å~ 2; flow rate 1.0 mL/min] connected to Jasco PU-980 precision pump and a Jasco 930-RI detector. The columns were calibrated against 7 standard poly(MMA) samples (Shodex; M_p = 1990–1950000; M_w/M_n =

1.02–1.09). MALDI-TOF-MS spectra were measured on an Applied Biosystems Voyager-DE STR spectrometer (reflector mode) with dithranol (1,8,9-anthracenetriol) as the ionizing matrix and sodium trifluoroacetate as the ion source. The experiment was carried out at an accelerating potential of 22 kV, where 256 laser shots were accumulated.

NOTES AND REFERENCES

(1) (a) Kharasch, M. S.; Jensen, E. V.; Urry, W. H. *Science* **1945**, *102*, 128. (b) Minisci, F. *Acc. Chem. Res.* **1975**, *8*, 165–171. (c) Iqbal, J. P.; Bhatia B.; Nayyar, N. K. *Chem. Rev.* **1994**, *94*, 519–564. (d) Gossage, R. A.; van de Kuil, L. A.; van Koten, G. *Acc. Chem. Res.* **1998**, *31*, 423–431.

(2) (a) Kato, M.; Kamigaito, M.; Sawamoto, M.; Higashimura, T. *Macromolecules* **1995**, *28*, 1721–1723. (b) Kamigaito, M.; Ando, T.; Sawamoto, M. *Chem. Rev.* **2001**, *101*, 3689–3745. (c) Kamigaito, M.; Ando, T.; Sawamoto, M. *Chem. Rec.* **2004**, *4*, 159–175.

(3) (a) Wang, J.-S.; Matyjaszewski, K. *J. Am. Chem. Soc.* **1995**, *117*, 5614–5615. (b) Matyjaszewski, K.; Xia, J. *Chem. Rev.* **2001**, *101*, 2921–2990.

(4) Percec, V.; Barboiu, B. *Macromolecules* **1995**, *28*, 7970–7972.

(5) Granel, C.; Dubois, Ph.; Jérôme, R.; Teyssié, Ph. *Macromolecules* **1996**, *29*, 8576–8582.

(6) Haddleton, D. M.; Jasieczek, C. B.; Hannon, M. J.; Shooter, A. J. *Macromolecules* **1997**, 30, 2190–2193.

(7) Coessens, V.; Matyjaszewski, K. *Macromol. Rapid Commun.* **1999**, *20*, 127–134.

(8) (a) Fréchet, J. M. J.; Henmi, M.; Gitsov, I.; Aoshima, S.; Leduc, M. R.; Grubbs, R. B. *Science* **1995**, *269*, 1080–1083. (b) Matyjaszewski, K.; Gaynor, S. G.; Müller, A. H. E. *Macromolecules* **1997**, *30*, 7034–7041.

(9) Hamasaki, S.; Kamigaito, M.; Sawamoto, M. *Macromolecules* **2002**, *35*, 2934–2940.

(10) (a) Ando, T.; Kamigaito, M.; Sawamoto, M. *Macromolecules* **1997**, *30*, 4507–4510. (b) Matyjaszewski, K.; Wei, M.; Xia, J.; McDermott, N. E. *Macromolecules* **1997**, *30*, 8161–8164.

(11) Xia, J.; Matyjaszewski, K. *Macromolecules* **1997**, *30*, 7697–7700.

(12) De Campo, F.; Lastécouères, D.; Verlhac. J.-B. *J. Chem. Soc. Perkin Trans. 1* **2000**, *4*, 575–580.

(13) (a) Jakubowski, W.; Matyjaszewski, K. *Macromolecules* **2005**, *38*, 4139–4146. (b) Jakubowski, W.; Min, K.; Matyjaszewski, K. *Macromolecules* **2006**, *39*, 39–45.

(14) Nonaka, H.; Ouchi, M.; Kamigaito, M.; Sawamoto, M. *Macromolecules* **2001**, *34*, 2083–2088.

(15) Villiéras, J.; Payan, D.; Anguelova, Y.; Normant, J.-F. *J. Organomet. Chem.* **1972**, *42*, C5–C8.

Chapter 2

Metal-Catalyzed Radical Polyaddition for Aliphatic Polyesters via Evolution of Atom Transfer Radical Addition into Step-Growth Polymerization

ABSTRACT

The metal-catalyzed radical addition was evolved into a step-growth polymerization by using a series of designed monomers [CH_2=CH–R–OC(O)CH(CH_3)Cl] that bear a reactive C–Cl and an unconjugated C=C double bond via an ester linkage, and various metal catalysts to produce novel aliphatic polyesters by the metal-catalyzed radical polyaddition. The polyaddition reactions smoothly proceeded and the conversion reached over 99% with the $FeCl_2$/P*n*Bu_3 or CuCl/*N*,*N*,*N'*,*N''*,*N''*-pentamethyldiethylenetriamine system to afford the polymers in high yield. The molecular weights progressively increased with the extent of reaction in the later stages and the molecular weight distributions were close to 2, indicating an ideal step-growth polymerization. The well-defined polymer structures were confirmed by ^{1}H-^{1}H correlation spectroscopy NMR analysis of the products along with the model 1:1 reactions between a halide and a vinyl compound. The polyester bearing an active C–Cl terminus obtained by the radical polyaddition was employed as a macroinitiator for the metal-catalyzed living radical polymerization of vinyl monomers such as styrene, methyl methacrylate, and methyl acrylate for block copolymers consisting of polyesters and vinyl polymers.

Chapter 2

Introduction

Developing a conceptually novel polymerization reaction is important for generating a new family of polymers in terms of their structures, properties, and functions. Especially, a novel precision polymer synthetic method is required for constructing well-defined polymers that can exert their new or enhanced properties originating from the ordered structures. Upon developing an efficient polymerization reaction, one should design or choose a highly selective and robust organic reaction as a chain-constructing reaction and efficiently build up the reactions into the polymerization for the synthesis of high molecular weight polymers in high yield. In addition, a versatile and widely applicable polymerization is preferable for the prospective extension of the polymerization in terms of the variety of polymer structures and properties.

Metal-catalyzed atom transfer radical addition (ATRA)[1] is one of the most highly efficient and robust carbon-carbon bond forming processes between various vinyl compounds and organic halides and is utilized for the construction of small organic molecules via inter- and intramolecular additions. This reaction is triggered by the metal-assisted homolytic cleavage of the C–X bond followed by the formation of the carbon radical species, which then adds to the C=C double bond of the vinyl group to form the C–C bond followed by a new C–X bond formation upon retrieving the halogen from the oxidized metal catalyst and results in the 1:1 adduct. This radical addition reaction has quite successfully been extended to chain or chain-growth radical addition polymerizations of vinyl monomers to generate and build a new category of precision polymerizations, i.e.; metal-catalyzed living radical polymerization or atom transfer radical polymerization (ATRP)[2-6], which permits the precise control of the polymer molecular weights for various conjugated vinyl monomers such as (meth)acrylic and styrenic monomers, and enables the precision synthesis of well-defined polymers such as block,[2,3,5] end-functionalized,[2–4,7–9] graft,[3,10]

star,[2,3] and more complicated polymers.[11–17] The key for the controlled radical addition polymerization lies in the highly effective and selective reversible metal-catalyzed radical-forming reaction from the carbon–halogen terminal. The carbon–halogen terminal, between the carbon adjacent to the carbonyl or the aryl group originating from the conjugated monomers and the halogen stemming from the organic halide initiator, is reactive enough for the appropriate metal complex to result in a growing carbon radical species, which then induces radical addition polymerization. However, for unconjugated monomers such as vinyl acetate and vinyl chloride, one should use a highly active metal complex, which can activate the less reactive carbon–halogen terminal.[18,19] The judicious choice of the reaction conditions, including selections of the metal complex and the halide initiator, is thus important for the construction of a controlled/living radical addition polymerization.

The author evolved the metal-catalyzed radical addition reaction into another step or step-growth polymerization mechanism, i.e.; the metal-catalyzed radical polyaddition in Chapter 1.[20] To achieve this new process, we designed a monomer possessing a reactive C–Cl bond, which can be activated by a metal catalyst to result in the carbon radical species, and an unconjugated C=C bond, to which the resulting carbon radical can add to form a C–C bond along with an unreactive C–Cl pendant without cross-propagation via addition polymerization and polyaddition.[9] If the addition reaction can proceed intermolecularly between the monomers, it will generate a dimer with one reactive C–Cl and one C=C bond at its terminal, which can further be converted stepwise into oligomers and finally linear polymers via the step-growth mechanism, while the analogue with a conjugated C=C bond, “inimer”, has been polymerized into highly branched structures regenerating reactive C–Cl bonds for cross-propagation.[11–13,21] This conceptually new radical polyaddition reaction would provide a series of novel linear polymers via the C–C bond

forming reactions, in contrast to the well-known radical polyaddition with the formation of S–C bonds by thiol-ene reaction.[22] Although the author has reported very preliminary results on such a metal-catalyzed radical polyadditions of certain monomers, detailed studies of the effective catalysts, mechanism, polymer properties, and applications have not yet been done.

This study is thus directed to the developments and establishments of the metal-catalyzed radical polyadditions using various metal catalysts (Ru, Fe, and Cu) under different conditions for a series of monomers (**1**–**4**) possessing a C–Cl and a C=C bond linked through the ester linkage with different numbers of methylene or oxyethylene units (Scheme 1). In addition to the optimization of the reaction conditions for efficient polymerizations, the polymerization mechanisms and

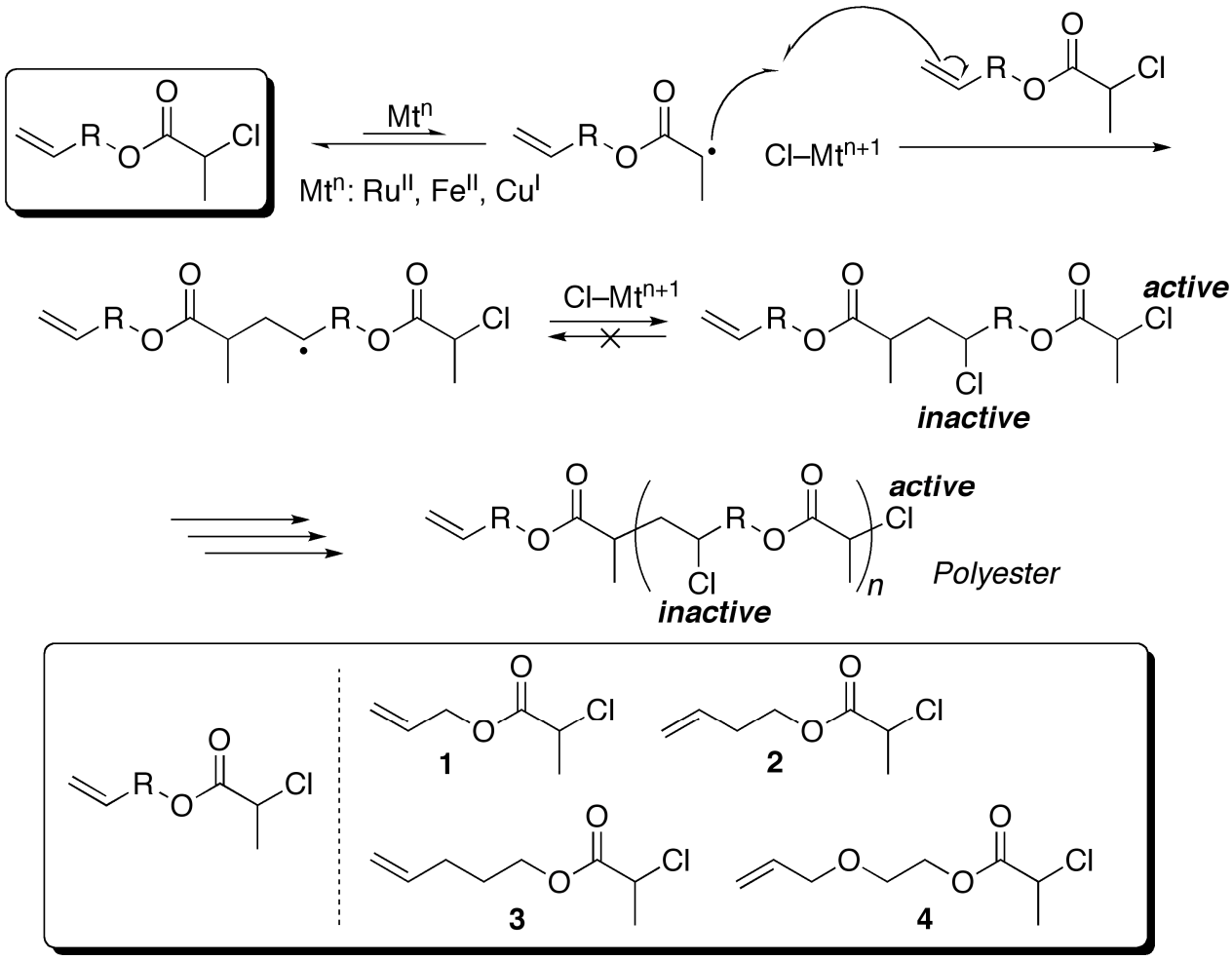

Scheme 1. Transition Metal-Catalyzed Radical Polyaddition of Ester-Linked Monomers.

products were analyzed in detail using the model 1:1 reactions between a chloride and a vinyl compound and the ^{1}H-^{1}H correlation spectroscopy (COSY) NMR analysis of the products. Further studies were devoted to the application of the radical polyaddition by a combination with the metal-catalyzed living radical addition polymerization through the block copolymerization of typical vinyl monomers such as styrene, methyl methacrylate (MMA), and methyl acrylate (MA) from the polyester-type macroinitiator obtained by the radical polyaddition.

Results and Discussion

1. Polyaddition of Ester-Linked Monomers under Various Conditions. A series of ester-linked monomers (**1**–**4**) with an unconjugated C=C and a reactive C–Cl bond were synthesized by a simple reaction between 2-chloropropionyl chloride and the ω-alkenyl alcohols in the presence of triethylamine. Figure 1 shows the ^{1}H NMR spectra of such prepared monomers, a series of

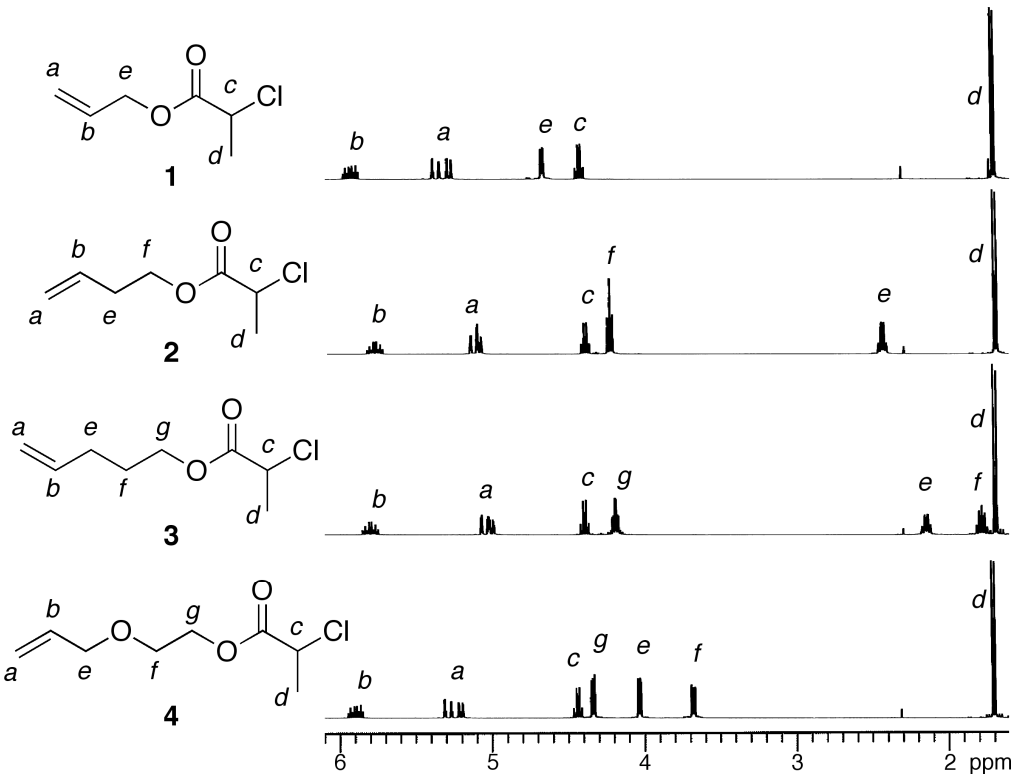

Figure 1. ^{1}H NMR spectra of the ester-linked monomers (**1**–**4**, see Scheme 1 for structure).

esters with α-(2-chloropropionyl) and ω-vinyl groups. Every spectrum showed a characteristic quartet at 4.4–4.5 ppm (*c*), assigned to the methine proton adjacent to the chlorine atom, and double doublets at 5.0–5.3 ppm (*a*) and a multiplet at 5.8–6.0 ppm (*b*) of the terminal vinyl group. All of these compounds possess the 2-chloropropionyl group, which can easily generate the acryloyl radical species via cleavage of the C–Cl bond upon activation with an appropriate metal complex, and an unconjugated vinyl group, to which the radical species can add to form a stable C–Cl bond upon receiving the halogen on the resulting unconjugated unstable radical species.

These ester-linked monomers were then treated with an iron catalyst ($FeCl_2$) in the presence of tri-*n*-butylphosphine (P*n*Bu_3) in toluene at 100 ˚C for the metal-catalyzed radical polyadditions. All of the monomers were smoothly consumed and the conversion reached over 90% (Figure 2A). The molecular weights of the obtained products progressively increased in the

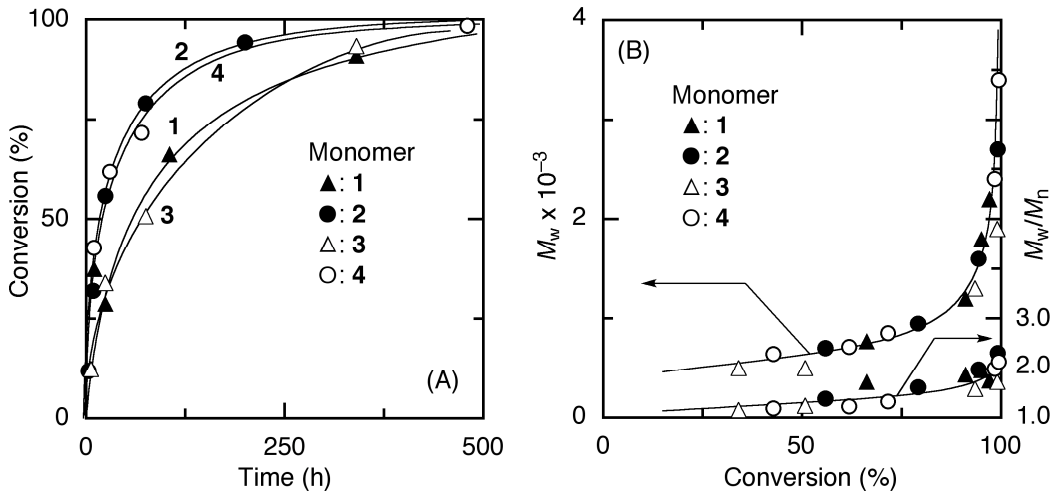

Figure 2. Time–conversion and conversion–weight-average molecular weight (M_w) curves for the polyaddition of **1**–**4** (Scheme 1) with $FeCl_2$/tri-*n*-butylphosphine (P*n*Bu_3): $[monomer]_0$ = 2.0 M; $[FeCl_2]_0$ = 100 mM; $[PnBu_3]_0$ = 200 mM in toluene at 100 °C. Monomer: **1** (▲), **2** (●), **3** (△), **4** (○).

later stages of the reactions, which suggests that the polymerization proceeds via the step-growth mechanism not via the chain-growth (Figure 2B). In addition, as the polymerization proceeded, the molecular weight distributions (M_w/M_n; M_w: weight-average molecular weight, M_n: number-average molecular weight) became broader and were approaching 2.0, the theoretical value for the products obtained by the step-growth polymerization. The ^{1}H NMR spectra also showed the characteristic signals of the polymers produced via the polyaddition mechanism (Figure 3).

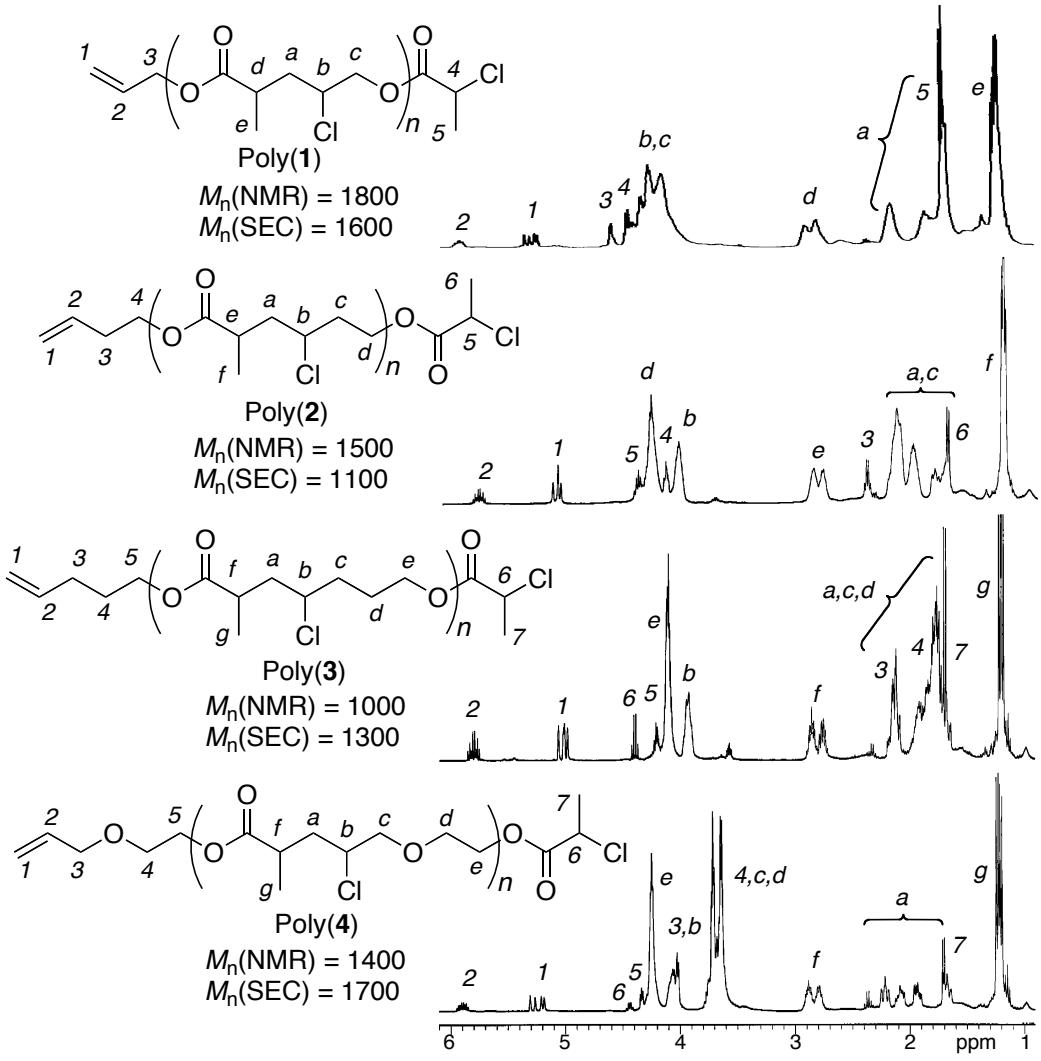

Figure 3. ^{1}H NMR spectra of the poly(**1**–**4**) obtained with $FeCl_2/PnBu_3$ in toluene at 100 ˚C ($CDCl_3$, r.t.).

These results indicate that the $FeCl_2$/P*n*Bu_3-catalyzed polymerization proceeded via an almost ideal step-growth propagation mechanism without significant intramolecular ring-closing processes. The key for the predominant intermolecular polyaddition reactions is due to the monomer structure and the relatively high monomer concentration because other α-chloro-ω-vinyl compounds undergo cyclization under diluted conditions.[23]

Figure 4 shows the size-exclusion chromatograms (SEC) of the products obtained from **1**–**4** using the $FeCl_2$/P*n*Bu_3 system. During the early stages of the reaction, the SEC curves consisted of only low molecular weight oligomers of which the highest peak was assumed to be the dimers (Figure 5). As the reaction proceeded, the curves shifted to the high molecular weight region especially after almost all of the monomers were consumed (>95%), also indicating that the polymers were produced via a metal-catalyzed step-growth polyaddition. However, the molecular weights of the final products were around several thousands in all cases. These might be due to the lower conversions of the C=C and C–Cl groups and/or the side reactions between the radical species, especially in the later stages of the reactions. The reaction conditions can be optimized by

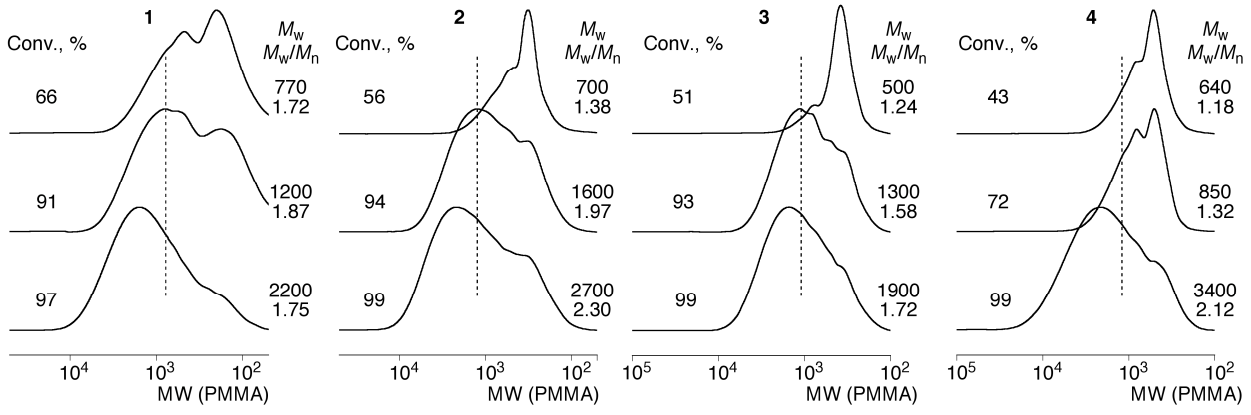

Figure 4. Size-exclusion chromatograms of the products in the polyaddition of **1**, **2**, **3**, and **4** (Scheme 1) with $FeCl_2$/tri-*n*-butylphosphine (P*n*Bu_3): $[monomer]_0$ = 2.0 M; $[FeCl_2]_0$ = 100 mM; $[PnBu_3]_0$ = 200 mM in toluene at 100 °C.

Table 1. Metal-Catalyzed Radical Polyaddition of 2 (See Scheme 1 for Structure)[a]

entry	metal catalyst	ligand[b]	$[ligand]_0$, mM	$[M]_0$, M	temp, °C	time, h	conv., %[c]	M_w[d]	M_w/M_n[d]
1	$RuCp^*Cl(PPh_3)_2$			2.0	100	530	49	960	1.93
2	$FeCl_2$	P*n*-Bu_3	100	4.0	100	1100	91	1200	1.83
3	$FeCl_2$	P*n*-Bu_3	200	4.0	100	250	91	1200	1.95
4	$FeCl_2$	P*n*-Bu_3	400	4.0	100	300	76	910	1.59
5	$FeCl_2$	P*n*-Bu_3	200	4.0	80	1700	97	1700	1.98
6	$FeCl_2$	P*n*-Bu_3	200	2.0	100	800	99	2700	2.30
7	$FeCl_2$	PCy_3	200	2.0	100	2200	95	1400	1.59
8	$FeCl_2$	PPh_3	200	2.0	100	2200	97	1700	2.05
9	$FeCl_2$	PMDETA	400	4.0	100	240	30	1300	1.85
10	CuCl	PMDETA	400	4.0	100	240	91	3600	3.51
11	CuCl	PMDETA	400	4.0	80	240	97	5500	3.30
12	CuCl	PMDETA	400	4.0	60	1400	99	11 000	4.12
13	CuCl	PMDETA	400	4.0	40	1400	99	9700	2.98
14	CuCl	PMDETA	200	4.0	60	350	58	830	1.66
15	CuCl	PMDETA	400	2.0	60	600	97	5400	2.14
16	CuCl	Me_6TREN	400	2.0	60	1200	90	1500	1.87
17	CuCl	HMTETA	400	2.0	60	1600	88	1800	1.74
18	CuCl	bpy	400	2.0	100	300	39	900	1.74
19[e]	$FeCl_2$	P*n*-Bu_3	200	4.0	100	480	>99	3500	2.32
20[e]	CuCl	PMDETA	400	4.0	60	490	>99	21 000	4.60

[a] $[metal\ catalyst]_0 = 100$ mM, in toluene. [b] Tri-*n*-butylphosphine (P*n*-Bu_3), tricyclohexylphosphine (PCy_3), triphenylphosphine (PPh_3), *N*,*N*,*N*′,*N*″,*N*″-pentamethyldiethylenetriamine (PMDETA), tris[2-(dimethylamino)ethyl]amine (Me_6TREN), 1,1,4,7,10,10-hexamethyltriethylenetetramine (HMTETA), 2,2′-bipyridine (bpy). [c] Determined by gas chromatography. [d] Weight-average molecular weight (M_w) and distribution (M_w/M_n) were determined by SEC. [e] Tin 2-ethylhexanoate [$Sn(EH)_2$] was added ($[Sn(EH)_2]_0 = 45$ mM).

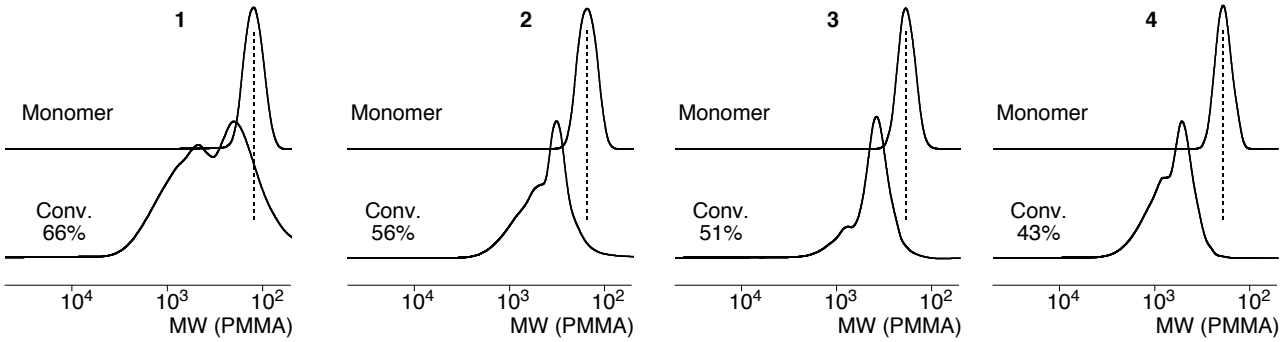

Figure 5. SEC curves of **1–4** and oligomer of **1–4**.

using other metal catalysts, changing the concentration of the monomer, catalysts, and ligands, or by changing the reaction temperatures for a higher molecular weight product.

A series of metal catalysts, which are effective for the metal-catalyzed living radical polymerization or ATRP, were then employed for the polyaddition reaction of **2**. Table 1 summarizes the monomer conversions, M_w, and M_w/M_n of the products obtained with RuCp*Cl(PPh_3)$_2$, $FeCl_2$/P*n*Bu_3, $FeCl_2$/PCy_3, $FeCl_2$/PPh_3, $FeCl_2$/PMDETA (PMDETA: *N*,*N*,*N'*,*N''*,*N''*-pentamethyldiethylenetriamine), CuCl/PMDETA, CuCl/bpy (bpy: 2,2'-bipyridine),

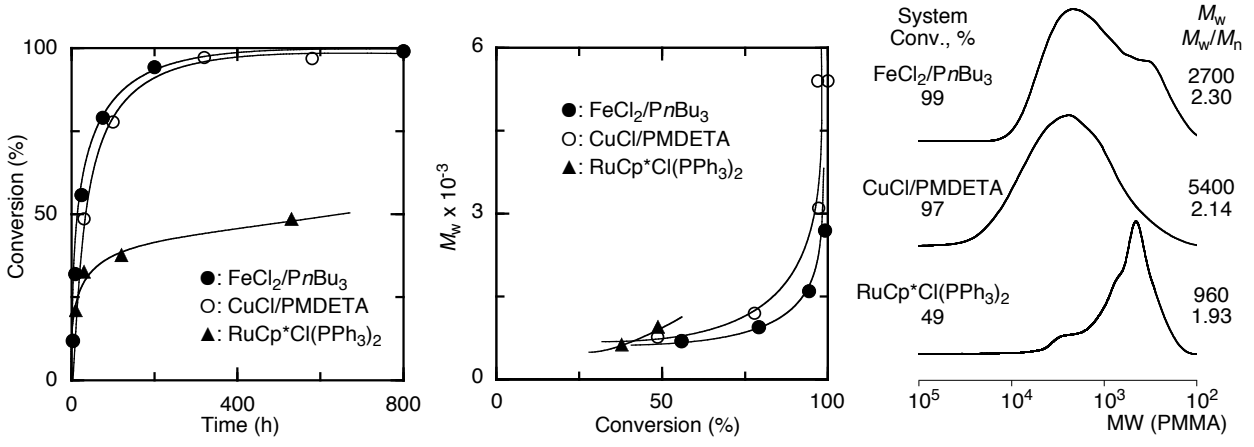

Figure 6. Time–conversion, conversion–M_w, and SEC curves for the polyaddition of **2** with various metal complex: $[\mathbf{2}]_0$ = 2.0 M; $[Metal]_0$ = 100 mM; $[PnBu_3]_0$ = 200 mM; $[PMDETA]_0$ = 400 mM in toluene at 100 [for Fe (●), Ru (▲)] and 60 °C [for Cu (○)].

CuCl/Me_6TREN (Me_6TREN: tris[2-(dimethylamino)ethyl]amine), and CuCl/HMTETA (HMTETA: 1,1,4,7,10,10-hexamethyltriethylenetetramine) as catalysts under various conditions.[2,3,24–27] More detailed data are plotted in Figures 6–8. Herein, the conversions in Table 1 and these figures are for the monomer molecule itself but not for the functional groups such as the C=C and C–Cl bonds in the monomer units. Although the reactions were all slow, they proceeded almost quantitatively (>90%) and gave the polymers under appropriate conditions, except for RuCp*Cl(PPh_3)$_2$ (entry 1), $FeCl_2$/PMDETA (entry 2), and CuCl/bpy (entry 18). Among them, the $FeCl_2$/P*n*Bu_3 and CuCl/PMDETA systems induced a quantitative monomer consumption (>99%) under appropriate conditions and produced polymers with relatively high molecular weights (M_w > 2500). Especially, with the $FeCl_2$/P*n*Bu_3 system, the M_w/M_n of the polymers was close to 2, which is a theoretical value for the ideal step-growth polymerizations, indicating that the $FeCl_2$/P*n*Bu_3 system is more suitable for the radical polyaddition of **2**.

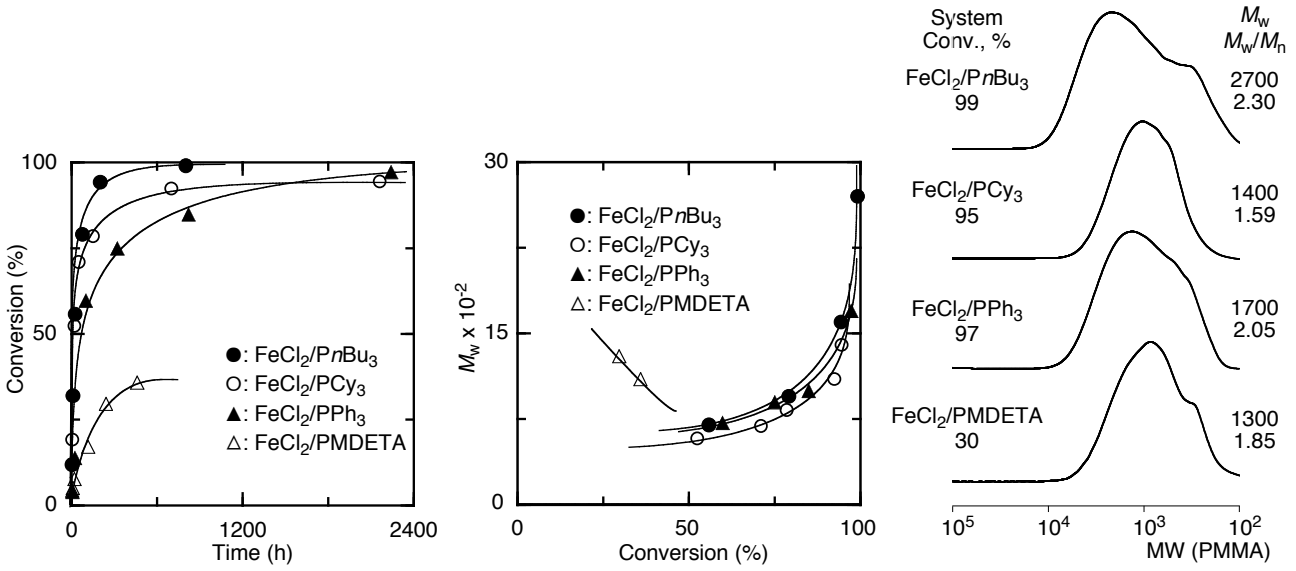

Figure 7. Time–conversion, conversion–M_w, and SEC curves for the polyaddition of **2** with iron complexes: $[\mathbf{2}]_0$ = 2.0 M (for P*n*Bu_3, PCy_3, and PPh_3), 4.0M (for PMDETA); $[FeCl_2]_0$ = 100 mM; $[Ligand]_0$ = 200 (for P*n*Bu_3, PCy_3, and PPh_3), 400 mM (for PMDETA) in toluene at 100 °C. Ligand: P*n*Bu_3 (●), PCy_3 (○), PPh_3 (▲), PMDETA (△).

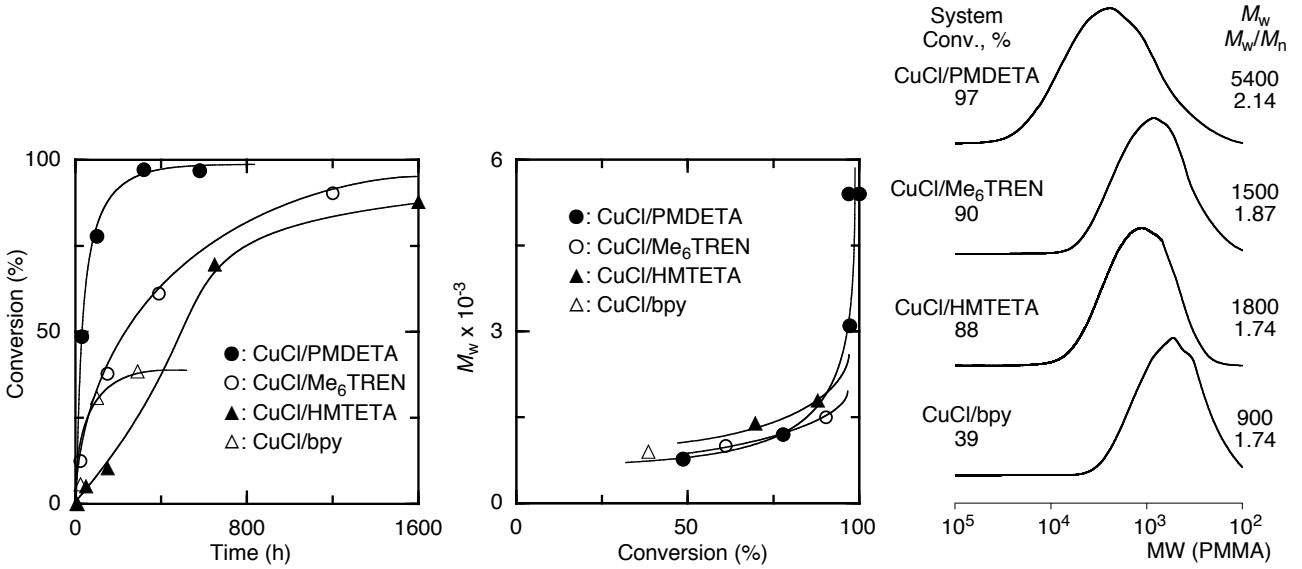

Figure 8. Time–conversion, conversion–M_w, and SEC curves for the polyaddition of **2** with copper complexes: $[\mathbf{2}]_0$ = 2.0 M; $[CuCl]_0$ = 100 mM; $[Ligand]_0$ = 400 mM in toluene at 60 °C(for PMDETA, Me_6TREN, HMTETA), 100 °C (for bpy). Ligand: PMDETA (●), Me_6TREN (○), HMTETA (▲), bpy (△)**.**

In the polyaddition of **2**, the effects of the monomer concentration, the $[ligand]_0/[metal]_0$ ratio, and the temperature were then examined with the $FeCl_2/PnBu_3$ (entries 2–5) and CuCl/PMDETA (entries 10–15) systems. More detailed results for a series of the reactions were also shown in Figures 9–13. Upon increasing $[ligand]_0/[metal]_0$ to 4.0 (entry 4), the reaction became slower because the excess phosphines decreased the activity of catalysts as in the metal-catalyzed radical addition and polymerization. Upon decreasing the ratio to 1.0 (entry 2), the reaction also became slower without affecting the final molecular weights, which suggests a decrease in the concentration of a soluble complex. The best ratio of $[PnBu_3]_0/[FeCl_2]_0$ was thus 2.0 (entry 3) in terms of the reaction rate and the molecular weight of the products, indicating that the effective catalyst would be the 1:2 complex of $FeCl_2(PnBu_3)_2$.[25] The lower temperature

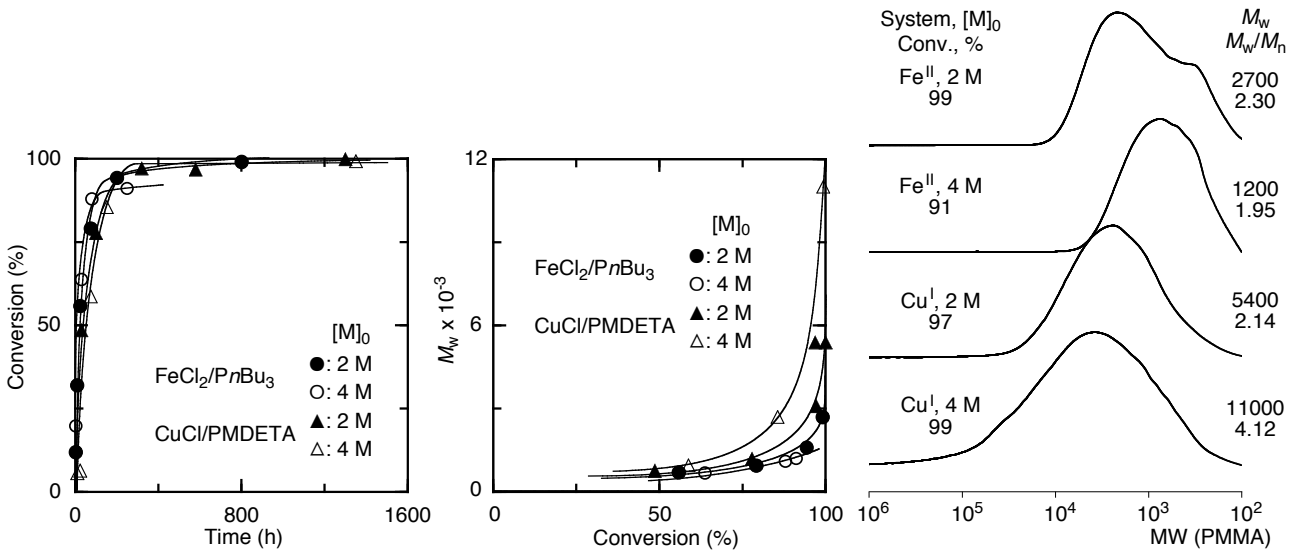

Figure 9. Time–conversion, conversion–M_w, and SEC curves for the polyaddition of **2** with $FeCl_2/PnBu_3$ or CuCl/PMDETA: $[\mathbf{2}]_0$ = 2.0, 4.0 M; $[MtX_n]_0$ = 100 mM; $[PnBu_3]_0$ = 200 mM; $[PMDETA]_0$ = 400 mM in toluene at 100 (for $FeCl_2/PnBu_3$), 60 °C (for CuCl/PMDETA): $[\mathbf{2}]_0$ = 2.0 M with $FeCl_2/PnBu_3$ (●), $[\mathbf{2}]_0$ = 4.0 M with $FeCl_2/PnBu_3$ (○), $[\mathbf{2}]_0$ = 2.0 M with CuCl/PMDETA (▲), $[\mathbf{2}]_0$ = 4.0 M with CuCl/PMDETA (△).

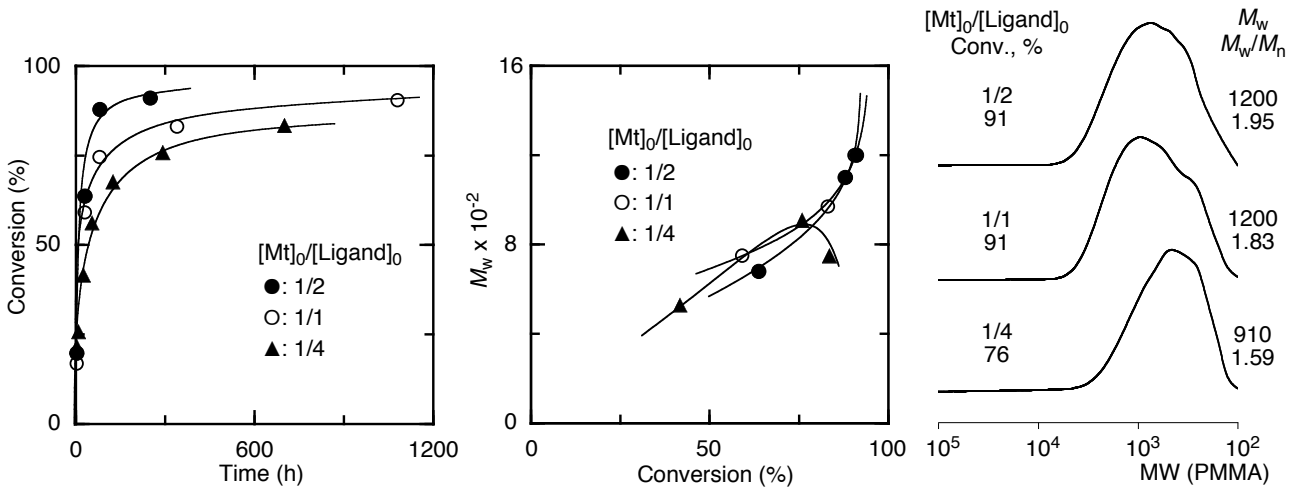

Figure 10. Time–conversion, conversion–M_w, and SEC curves for the polyaddition of **2** with $FeCl_2/PnBu_3$: $[\mathbf{2}]_0$ = 4.0 M; $[FeCl_2]_0$ = 100 mM; $[PnBu_3]_0$ = 100 (●), 200 (○), 400 (▲) mM in toluene at 100 °C.

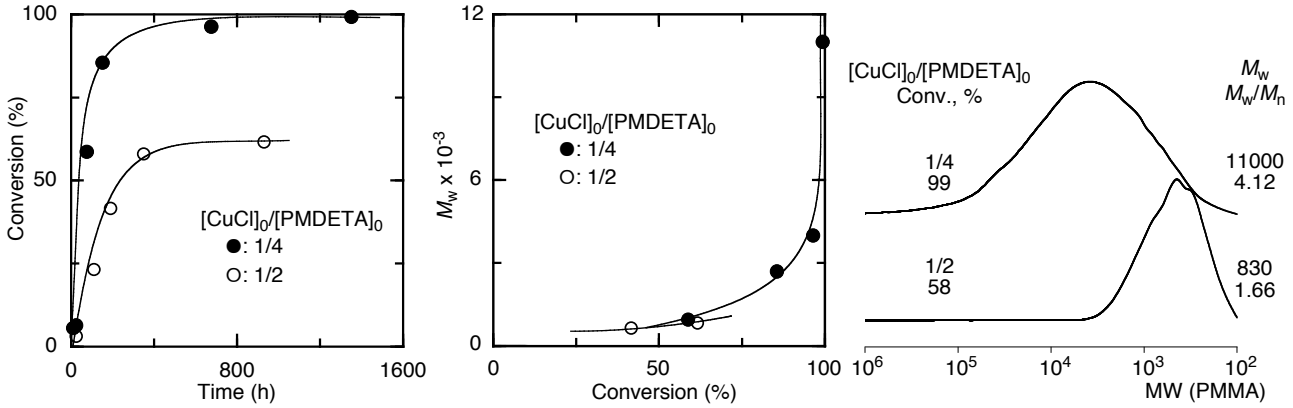

Figure 11. Time–conversion, conversion–M_w, and SEC curves for the polyaddition of **2** with CuCl/PMDETA: $[\mathbf{2}]_0$ = 4.0 M; $[CuCl]_0$ = 100 mM; $[PMDETA]_0$ = 200 (○), 400 (●) mM in toluene at 60 °C.

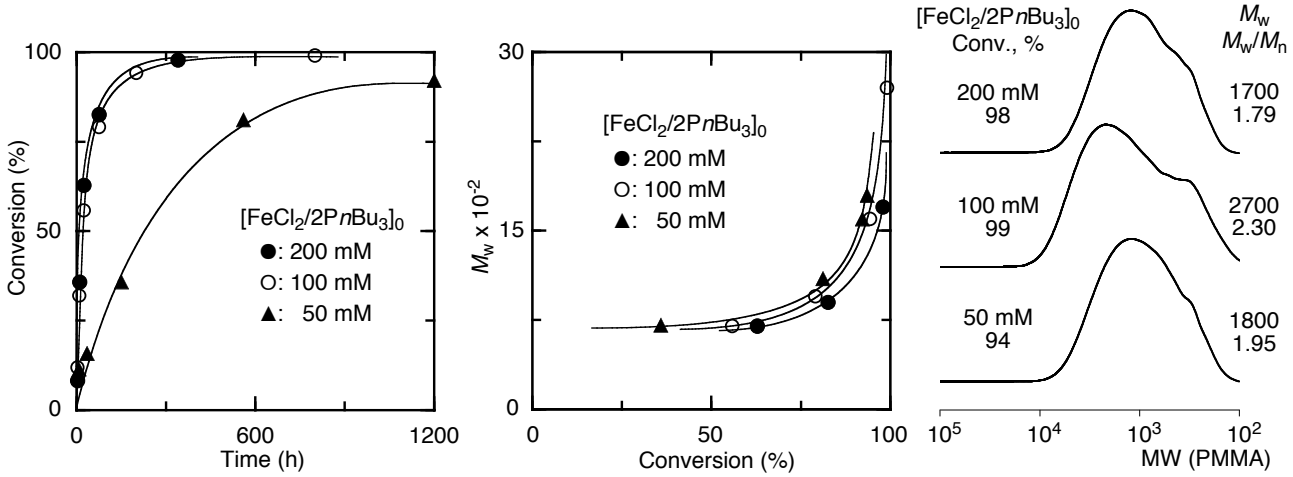

Figure 12. Time–conversion, conversion–M_w, and SEC curves for the polyaddition of **2** with $FeCl_2$/P*n*Bu_3: $[\mathbf{2}]_0$ = 2.0 M; $[FeCl_2]_0/[PnBu_3]_0$ = 200/400 (●), 100/200 (○), 50/100 (▲) mM in toluene at 100 °C.

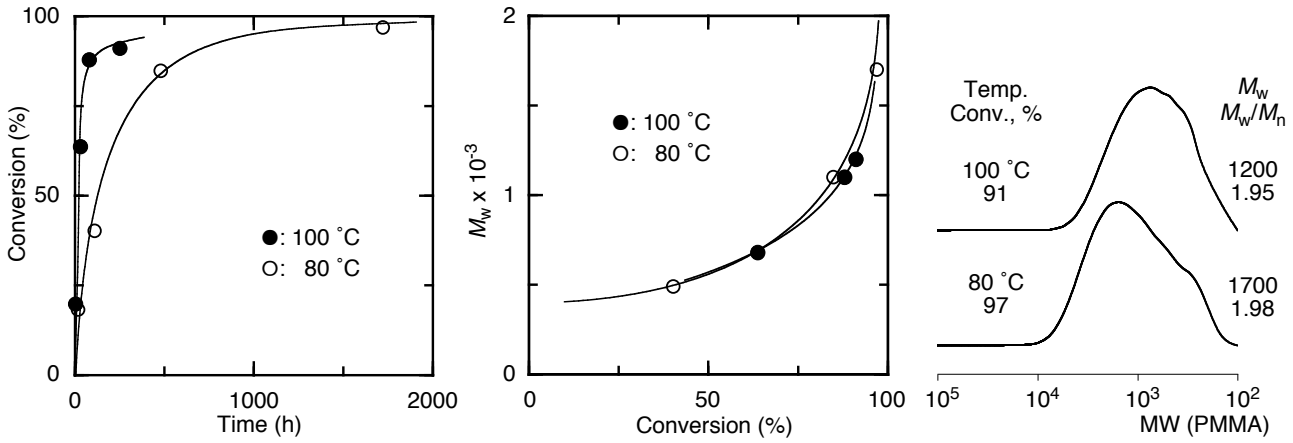

Figure 13. Time–conversion, conversion–M_w, and SEC curves for the polyaddition of **2** with $FeCl_2$/P*n*Bu_3: $[\mathbf{2}]_0$ = 4.0 M; $[FeCl_2]_0$ = 100 mM; $[PnBu_3]_0$ = 200 mM in toluene at 80 (○), 100 °C (●).

resulted in a slow polymerization, but was effective in producing a higher molecular weight polymer probably due to the suppression of the side reactions (entry 5). At a lower monomer concentration ($[M]_0$ = 2.0 M), the $FeCl_2$/P*n*Bu_3 system also led to an almost quantitative conversion (99%) to give the highest molecular weight of the products among the various conditions for the iron systems (entry 6), because the relative concentration of the catalyst ($FeCl_2$/P*n*Bu_3) to the monomer (C–Cl) increased by lowering the monomer concentration.

Similar effects of temperature were also observed for the CuCl/PMDETA system (entries 10–13 and Figure 14). With decreasing temperature, the reaction became slower and resulted in a higher molecular weight polymer. Especially, a quantitative monomer consumption (≥99%) was achieved below 60 °C to give the highest molecular weight polymers ($M_w > 10^4$). At 100 °C, however, the polymerization leveled off in the later stages of the reactions to result in the lower molecular weights probably due to the side reactions such as the termination between two radicals or the thermal decomposition of the catalyst. When the ratio of ligand to catalyst

($[PMDETA]_0/[CuCl]_0$) was decreased to 2.0, both the polymer yield and molecular weight decreased (entry 14).

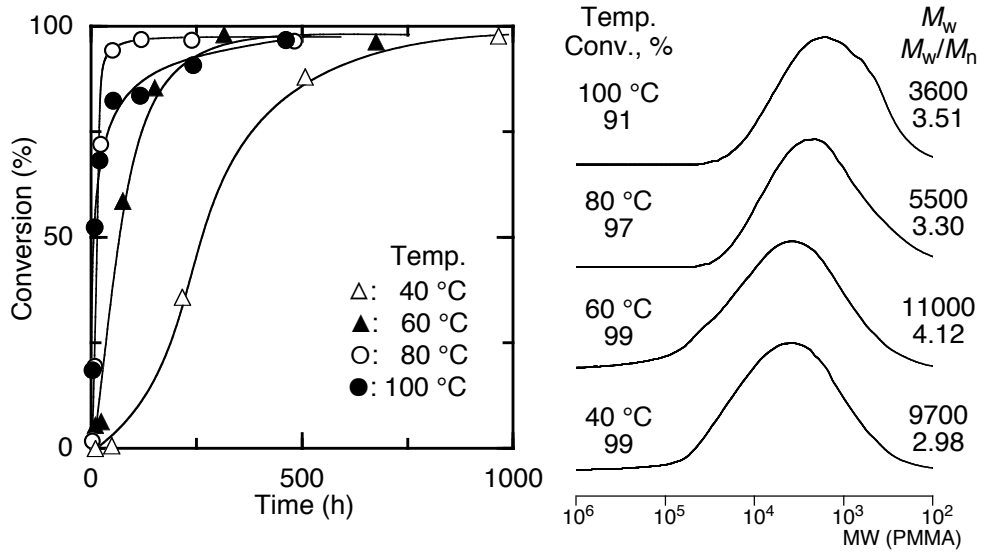

Figure 14. Time–conversion curves and size-exclusion chromatograms for the polyaddition of 3-butenyl 2-chloropropionate (**2**) with CuCl/ *N*,*N*,*N'*,*N''*,*N''*-pentamethyldiethylenetriamine (PMDETA) at various temperature: $[\mathbf{2}]_0$ = 4.0 M; $[CuCl]_0$ = 100 mM; $[PMDETA]_0$ = 400 mM in toluene at 40 (△), 60 (▲), 80 (○), or 100 °C (●).

The addition of tin 2-ethylhexanoate [$Sn(EH)_2$] was further investigated for the polymerization of **2** with the $FeCl_2/P\textit{n}Bu_3$ and CuCl/PMDETA systems for acceleration of the polymerization, in which the tin additive might work as a reducing agent for the accumulated oxidized Fe- and Cu-species.[28,29] As also shown in Table 1, $Sn(EH)_2$ increased the polymerization rate as well as the molecular weights in both the Fe- and Cu-catalyzed polyadditions (entry 19 vs 2 for Fe; entry 20 vs 12 for Cu). These suggest that a small amount of the metal catalysts was deactivated during the reactions and that the polymerizations can be enhanced by the addition of some reducing agents. However, the molecular weight distributions became broader than 2 upon

the addition of $Sn(EH)_2$, which suggests a deviation from the ideal step-growth polymerization especially with the CuCl/PMDETA/$Sn(EH)_2$ system (Figure 15).

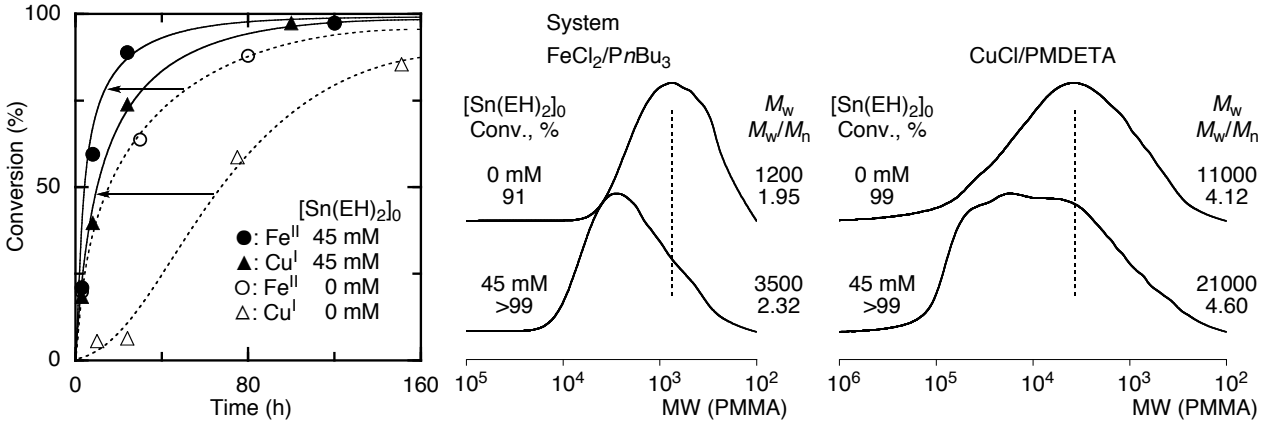

Figure 15. Time–conversion and SEC curves for the polyaddition of **2** with $FeCl_2/PnBu_3$ or CuCl/PMDETA in the presence of $Sn(EH)_2$: $[\mathbf{2}]_0 = 4.0$ M; $[MtX_n]_0 = 100$ mM; $[PnBu_3]_0 = 200$ mM; $[PMDETA]_0 = 400$ mM; $[Sn(EH)_2]_0 = 0$, 45 mM in toluene at 100 (for $FeCl_2/PnBu_3$), 60 °C (for CuCl/PMDETA): the presence of $Sn(EH)_2$ with $FeCl_2/PnBu_3$ (●), the absence of $Sn(EH)_2$ with $FeCl_2/PnBu_3$ (○), the presence of $Sn(EH)_2$ with CuCl/PMDETA (▲), the absence of $Sn(EH)_2$ with CuCl/PMDETA (△).

2. Analysis of the Mechanism of Radical Polyaddition Using Model Reactions. To confirm the polymerization mechanism and to clarify possible side reactions, the model reactions for the radical polyaddition were investigated between methyl 2-chloropropionate (**5**) and 3-butenyl acetate (**6**), which correspond to the model C–Cl and C=C parts for **2**, respectively, by using various

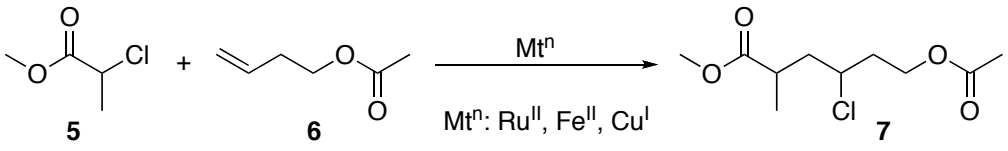

Scheme 2. Atom Transfer Radical Addition of Model Compounds.

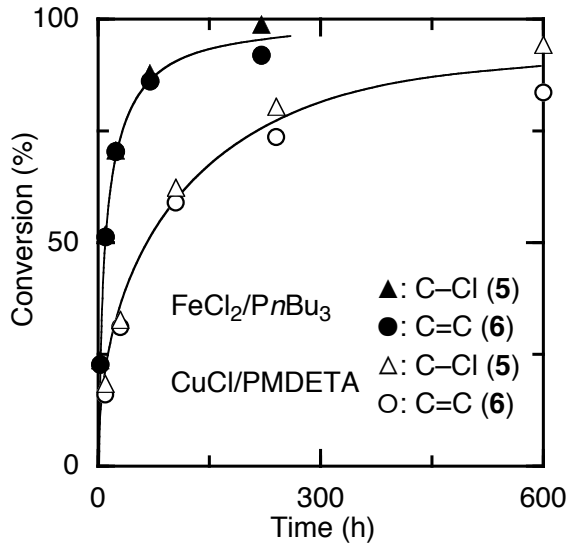

Figure 16. Time–conversion curves for the model Kharasch reactions between methyl 2-chloropropionate (**5**) and 3-butenyl acetate (**6**) with $FeCl_2$/tri-*n*-butylphosphine (P*n*Bu_3) (▲, ●) or CuCl/*N*,*N*,*N'*,*N''*,*N''*-pentamethyldiethylenetriamine (PMDETA) (△, ○): $[\mathbf{5}]_0 = [\mathbf{6}]_0 = 2.0$ M; $[MtX_n]_0 = 100$ mM; $[P\textit{n}Bu_3]_0 = 200$ mM; $[PMDETA]_0 = 400$ mM in toluene at 100 (for $FeCl_2$/P*n*Bu_3) or 60 °C (for CuCl/PMDETA).

transition metal complexes (Scheme 2). Figure 16 shows the consumptions of the chloride (**5**) and vinyl (**6**) compounds with $FeCl_2$/P*n*Bu_3 at 100 °C and CuCl/PMDETA at 60 °C. In both cases, the two compounds were smoothly and simultaneously consumed at the same rate to nearly quantitative conversions (>90%) to produce the 1:1 adduct (**7**) almost quantitatively as shown later. In the later stages of the reactions, however, the consumptions of C–Cl (**5**) became slightly faster than those of C=C (**6**), suggesting the existence of a small amount of side reactions.

Various metal complexes were also employed for the model reactions. Table 2 summarizes the conversions of **5** and **6** and the yields of the adduct (**7**) along with the contents of byproducts, methyl propionate (**8**) and dimethyl 2,3-dimethylsuccinate (**9**). The latter compound would be generated via combination of the radical species derived from **5** while the former via

disproportionation or hydrogen transfer from other compounds or solvents. Among them, the $FeCl_2/P\textit{n}Bu_3$ (entries 3 and 4) and CuCl/PMDETA (entries 7–9) systems induced the simultaneous consumptions of **5** and **6** at almost the same rate and gave the corresponding 1:1 adduct in good yields. Furthermore, the conversions of **6** were almost the same with the yields of the 1:1 adduct, indicating that no consecutive vinyl additions of **6** to the radical species took place. This also supports that the $FeCl_2/P\textit{n}Bu_3$ and CuCl/PMDETA systems polymerized **2** exclusively via polyaddition mechanism not via consecutive vinyl-addition chain-growth polymerization. The detailed analysis of the byproducts in the model reactions also gave useful information for understanding the polymerization. The negligible amount of combination products (**9**) means almost no significant coupling reactions between **2** and/or the oligomers/polymers, which might have led to a molecular weight increase via the polymer-polymer coupling as well as the formation of the polymers with vinyl groups at both ends. However, a minimal formation (< 2%) of **8** suggests a slight loss of the halogens at the polymer terminals, which would prevent the molecular weight increase especially in the later stages of the polymerization.

With the other metal catalyst systems, such as $RuCp^*(PPh_3)_2$ (entries 1and 2) and $FeCl_2$/PMDETA (entries 5 and 6), one of the components was consumed much faster than the other to result in a lower yield of the adduct and a higher content of the byproducts. These results indicate that one of the best catalytic systems for the model radical addition reaction is the $FeCl_2/P\textit{n}Bu_3$ or CuCl/PMDETA system, which is also the best for the radical polyaddition as shown above. Therefore, the search for a good catalyst for the corresponding model radical addition is helpful for the design of a good catalyst for the radical polyaddition.

Table 2. Model Reactions between methyl 2-chloropropionate (**5**) and 3-butenyl acetate (**6**) with Various Metal Catalysts[a]

entry	catalyst/ligand[b]	time, h	conv., %[c]		**7**, %[d]	**8**, %[e]	**9**, %[f]
			5	**6**			
1	$RuCp^*Cl(PPh_3)_2$	35	42	43	28 (66)	4 (13)	n.d.[g]
2	$RuCp^*Cl(PPh_3)_2$	150	63	46	37 (81)	3 (8)	<1
3	$FeCl_2/PnBu_3$	10	52	51	50 (98)	1 (2)	n.d.[g]
4	$FeCl_2/PnBu_3$	70	88	86	87 (>99)	2 (2)	<1
5	$FeCl_2$/PMDETA	35	39	0	0 (0)	3	n.d.[g]
6	$FeCl_2$/PMDETA	200	57	6	2 (4)	<1	n.d.[g]
7	CuCl/PMDETA	110	62	59	59 (>99)	n.d.	n.d.[g]
8	CuCl/PMDETA	240	80	74	73 (99)	2 (3)	n.d.[g]
9	CuCl/PMDETA	600	95	84	84 (>99)	5 (6)	n.d.[g]

[a]$[\mathbf{5}]_0$ = 2.0 M; $[\mathbf{6}]_0$ = 2.0 M; [b][metal catalyst]$_0$ = 100 mM; $[PnBu_3]_0$ = 200 mM; [PMDETA]$_0$ = 400 mM; in toluene at 100 °C (for Ru and Fe) or 60 °C (for Cu); tri-*n*-butylphosphine ($PnBu_3$), *N*,*N*,*N'*,*N''*,*N''*-pentamethyldiethylenetriamine (PMDETA). [c]Determined by gas chromatography. [d]The 1:1 adduct (**7,** see Scheme 2 for structure) yield was determined by ^{1}H NMR. The values in parentheses indicate the yields based on the consumptions of **6**. [e]The content of methyl propionate (**8**) was determined by gas chromatography. The values in parentheses indicate the relative ratio to **7**. [f]The content of dimethyl 2,3-dimethylsuccinate (**9**) was determined by gas chromatography. [g]Not being detected.

A more detailed mechanism of the radical polyaddition was investigated by measuring the total consumptions of the C=C and C–Cl groups that originated from **2** and the polymerized products by ^{1}H NMR while the consumption of the monomer **2** was measured by gas chromatography. As shown in Figure 17A, the consumptions of the C=C and C–Cl groups simultaneously occurred at the same rate, indicating the 1:1 reaction. The rates were close to those for the model reactions (Figure 16), suggesting the polyaddition via a similar radical addition reaction. Furthermore, the conversions of the functional groups (C=C and C–Cl) were consistently lower than those of the monomer. Especially, those of the functional groups (C=C and C–Cl) for the 49% monomer conversion were around 25%, almost half of the monomer conversion. These results indicate that most of the consumed monomers were converted into dimers without any significant intramolecular cyclization during the initial stages and then the reaction between the oligomers proceeded via an intermolecular polyaddition to result in the polymers.

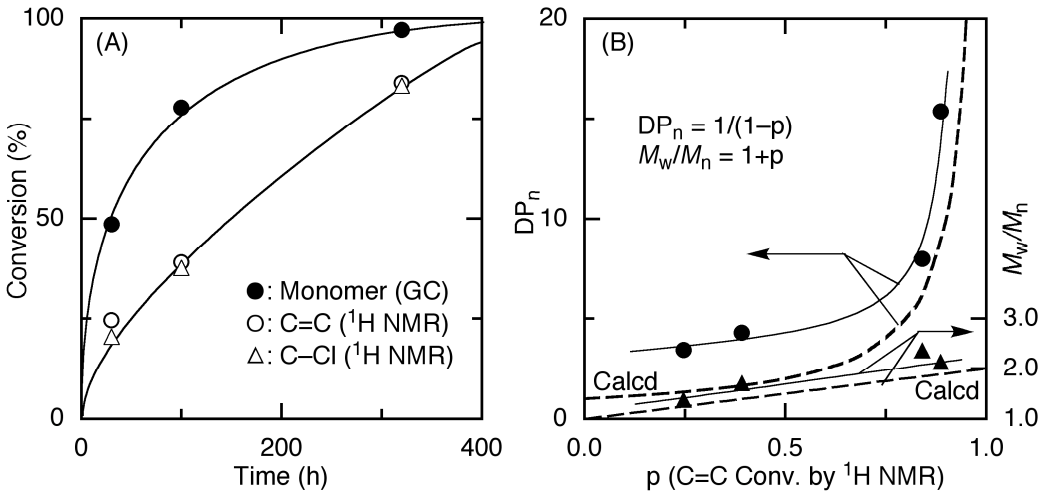

Figure 17. Time–conversion curves (A) and number-average polymerization degree (DP_n) and molecular weight distribution (M_w/M_n) as a function of C=C conversion (B) for the polyaddition of 3-butenyl 2-chloropropionate (**2**) with CuCl/*N*,*N*,*N'*,*N''*,*N''*-pentamethyldiethylenetriamine (PMDETA): $[\mathbf{2}]_0$ = 2.0 M; $[CuCl]_0$ = 100 mM; $[PMDETA]_0$ = 400 mM in toluene at 60 °C.

As shown in Figure 17B, the number-average polymerization degree (DP_n) of the products progressively increased and was close to the calculated line for the step-growth polymerization based on the assumption that the DP_n increases in inverse proportion to 1-p, where p means the consumption of the functional group or the extent of reaction. In addition, the molecular weight distribution increased with the conversion and was close to the calculated value of 2 ($M_w/M_n \sim 2$). All these relationships are typical for a step-growth polymerization and thus indicate that the polymers were produced via the expected intermolecular polyaddition based on the metal-catalyzed C–Cl activation followed by the radical addition to C=C.

Therefore, the polymerization with the optimized systems most probably proceeds via step-growth mechanism of successive ATRA, without the chain-growth reaction of the vinyl groups, because both C–Cl and C=C bonds are consumed at the same rate (Figure 16). However, the radical species derived from the C–Cl bond suffers from minimal side reactions similarly to the metal-catalyzed living polymerizations. A loss of the halogens at the polymer terminals would set a limit of the molecular weights and would decrease the reaction rate and the final conversion of the monomers due to the accumulation of the higher oxidation state metal species. However, we have recently found that iron(III) chloride ($FeCl_3$) can become active in the presence of P*n*Bu_3 without any added reducing agents to induce living radical polymerizations,[30] which may also support the highly effective $FeCl_2$/P*n*Bu_3 system in the polyaddition reactions. Thus, the conditions, such as the choice of both metal and ligand, concentrations of monomer and catalyst, and reaction temperature, are essential to the effective radical polyadditions by minimizing the side reactions such as vinyl chain-growth polymerization, radical termination, and intramolecular cyclization.

A further mechanism study was done by NMR analysis of the products obtained from the radical polyaddition of **2** and the model radical addition between **5** and **6**. Figure 18 shows the ^{1}H-^{1}H COSY NMR spectra of the model adduct (**7**) prepared from **5** and **6** and the polymer of **2** obtained by the CuCl/PMDETA system. In both 1D spectra, similar main peaks (*a'–f'* and *a–f*) were observed. A series of similar cross-peaks (*b–a*, *b–c*, *d–c*, *d–e*, *f–e*) were also observed in both of the 2D spectra. The peaks *a–f* can thus be assignable to the main chain protons of the aliphatic polyester with the C–Cl pendants. In addition to these main peaks, the polymer spectra exhibited small sharp peaks that originated from the protons neighboring to vinyl (*1* and *2*) and chlorine (*3* and *4*) groups at the α- and ω-ends, respectively. The DP_n of the polymers can be

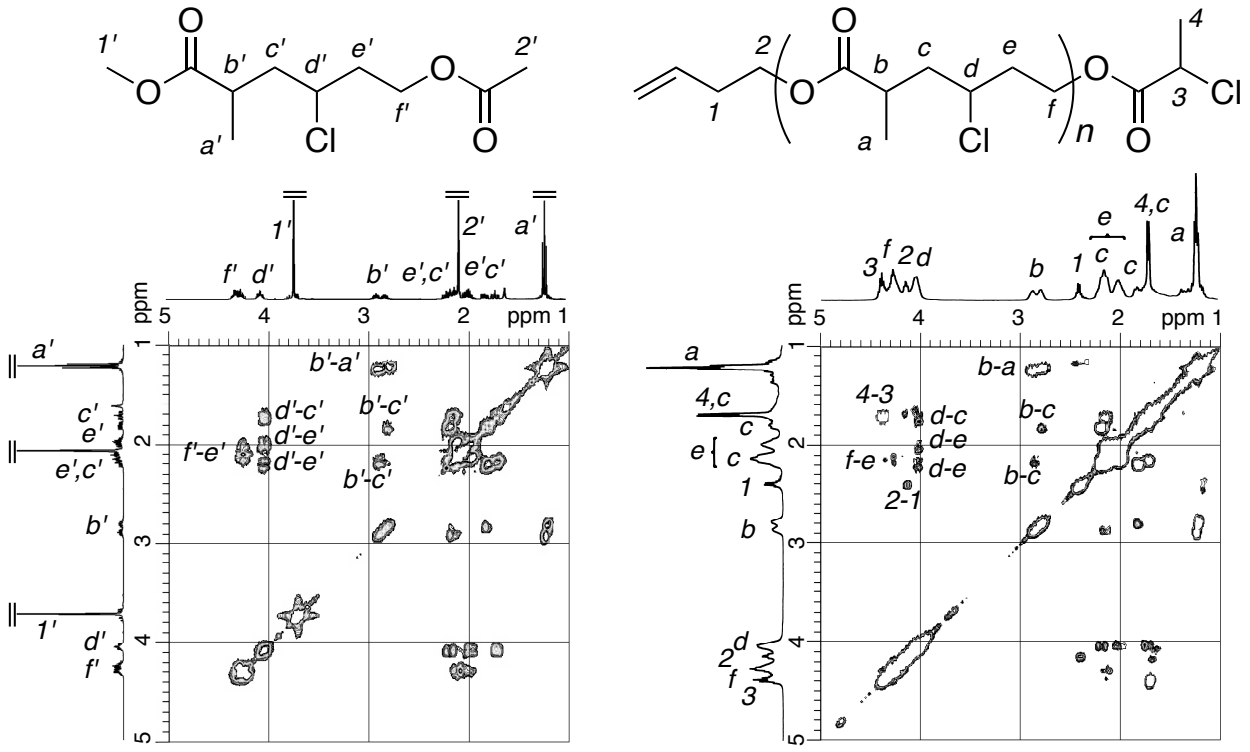

Figure 18. ^{1}H–^{1}H correlation spectra of the adduct (**7**) prepared from methyl 2-chloropropionate (**5**) and 3-butenyl acetate (**6**) (A) and the polymer of 3-butenyl 2-chloropropionate (**2**) (B), respectively, obtained with CuCl/*N,N,N',N'',N''*-pentamethyldiethylenetriamine (PMDETA) in toluene at 60 °C ($CDCl_3$, r.t.).

determined from the peak intensity ratio (*b*/*1*) of the methylene protons (*1*) adjacent to the terminal vinyl group to the methine (*b*) in the main chain unit of the polyester. The M_n(NMR) calculated from the DP_n and the formula weight of **2** was 850, which was lower than the molecular weight determined by SEC [M_n(SEC) = 1400], most probably due to the SEC standards of poly(methyl methacrylate). These NMR studies also support the fact that the metal-catalyzed radical polyaddition reactions mainly proceed via formation of the C–C linkage and the inactive C–Cl pendant to result in the polyester main chain predominantly with no visible formation of consecutive chain-growth vinyl-addition structures under the optimized conditions.

The thermal properties of the polyesters obtained from the metal-catalyzed polyaddition of **1** and **2** were also evaluated by differential scanning calorimetry (DSC) (Table 3 and Figure 19). The glass transition temperatures (T_g) were observed for all the polymers, which depended on the molecular weights of the polymers similar to general polymers. The DSC curves of the obtained polyesters with higher molecular weights exhibited endothermal peaks due to the melting

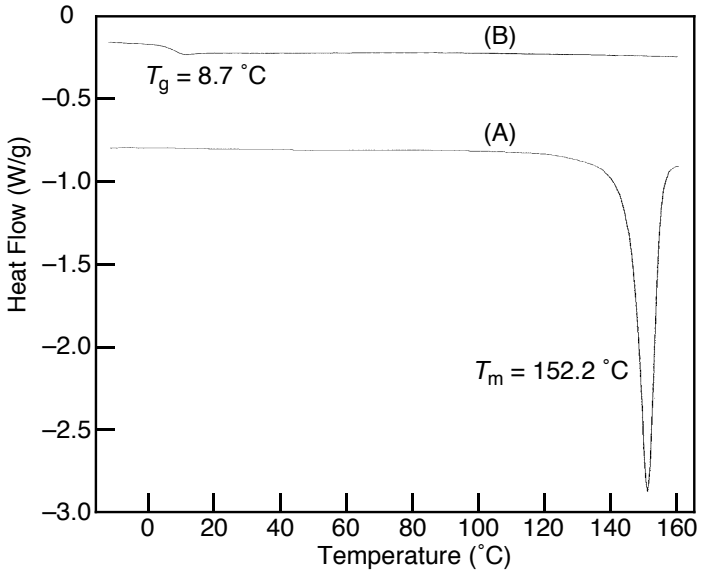

Figure 19. DSC traces of poly(**2**) (M_n = 4800, M_w/M_n = 2.66) obtained with CuCl/PMDETA/$Sn(EH)_2$ in toluene at 60 °C (A) after annealing at 100 °C for 10 min (B) second step.

temperatures (T_m). This indicates that the well-defined polyesters prepared by the metal-catalyzed radical polyaddition exhibit a crystalline domain like the usual aliphatic polyesters, whereas a similar brominated aliphatic polyester prepared by ring-opening polymerization was amorphous and showed no tendency to be crystalline even with a high molecular weight.[31]

Table 3. Thermal Analysis of Polyesters Obtained by Radical Polyaddition

entry	polymer	T_g, °C[d]	T_m, °C[d]	M_n(SEC)[e]	M_n(NMR)[f]
1	poly(**1**)[a]	–13.8	–	1700	1800
2	poly(**2**)[b]	–24.9	–	1600	2300
3	poly(**2**)[a]	8.5	151.9	5000	4100
4	poly(**2**)[c]	8.7	152.2	4800	3400

[a]Obtained with CuCl/*N*,*N*,*N'*,*N''*,*N''*-pentamethyldiethylenetriamine (PMDETA) in toluene at 60 °C; see Scheme 1 for structures. [b]Obtained with $FeCl_2$/tri-*n*-butylphosphine/tin 2-ethylhexanoate in toluene at 100 °C; see Scheme 1 for structures. [c]Obtained with CuCl/PMDETA/tin 2-ethylhexanoate in toluene at 60 °C. [d]The glass transition temperature (T_g) and melting temperature (T_m) were determined by differential scanning calorimetry. [e]The number-average molecular weight (M_n) determined by size-exclusion chromatography. [f]The M_n determined from the α-end functionalities by ^{1}H NMR, see Figure 18.

3. Combination with Metal-Catalyzed Living Radical Polymerization for Block Copolymerization. The polymers obtained by the metal-catalyzed radical polyaddition have a C–Cl bond at the ω-terminal, which can work as an initiating site for the living radical addition polymerization of vinyl monomers to form the block copolymers consisting of the polyesters and

the vinyl polymers. The polyester of **2** bearing an active C–Cl terminal obtained by the CuCl/PMDETA system was then employed as a macroinitiator for the ruthenium-catalyzed living radical polymerization of various vinyl monomers. The block copolymerizations of styrene,

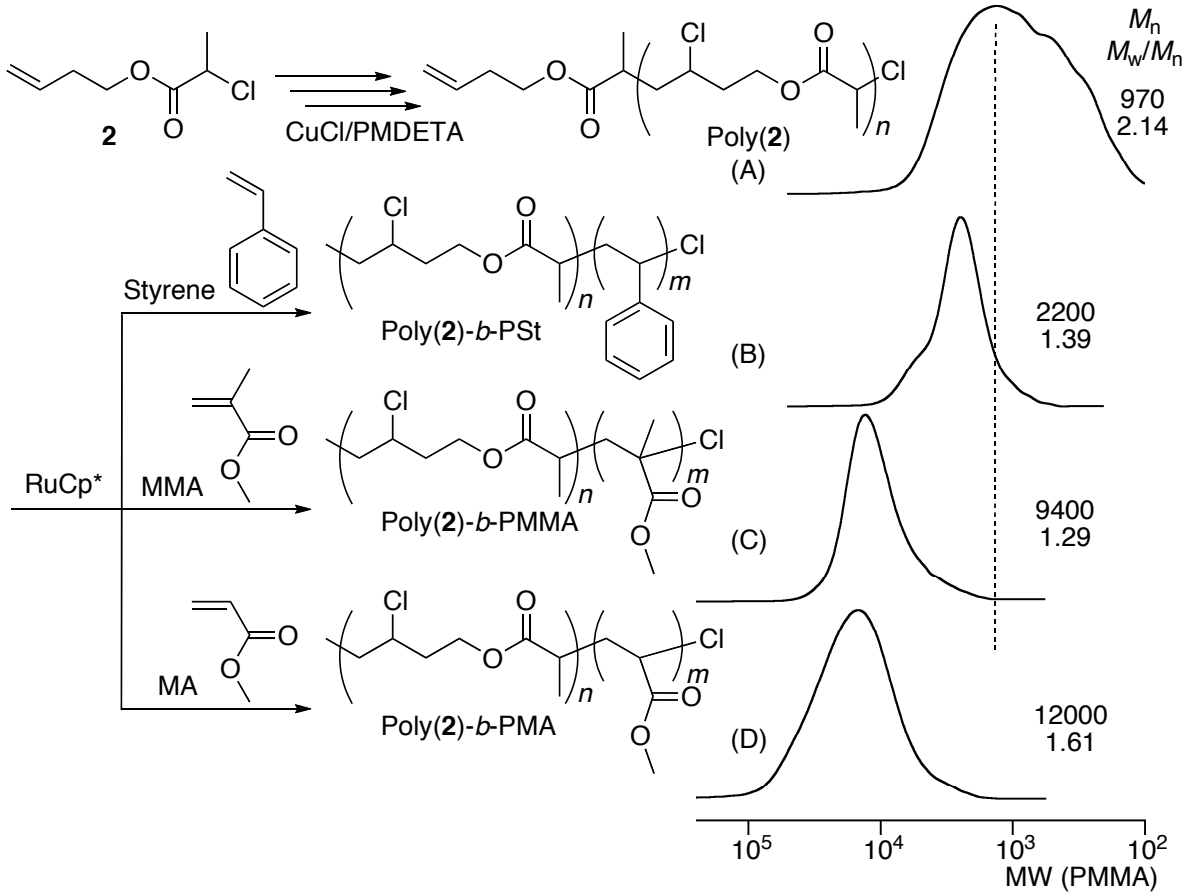

Figure 20. Size-exclusion chromatograms of the polymer of 3-butenyl 2-chloropropionate (**2**) (A), poly(**2**)-*b*-polystyrene (B), poly(**2**)-*b*-poly(methyl methacrylate) (C), and poly(**2**)-*b*-poly(methyl acrylate) (D) copolymers obtained in the block copolymerization from the macroinitiator poly(**2**) with RuCp*Cl(PPh_3)$_2$: [styrene, methyl methacrylate, or methyl acrylate]$_0$ = 4.0 M, [poly(**2**)]$_0$ = 10 mM, [RuCp*Cl(PPh_3)$_2$]$_0$ = 4 mM, [tri-*n*-butylamine]$_0$ = 40 mM in toluene at 80 °C. Monomer conversion: 5% for styrene (B); 7% for methyl methacrylate (C); 20% for methyl acrylate (D).

the intermolecular addition of a growing radical block polymer chain end to the C=C double bond terminal of another block polymer chain.

MMA, and MA from the macroinitiator were carried out with RuCp*Cl(PPh_3)$_2$ in toluene at 80 °C in the presence of tri-*n*-butylamine (*n*Bu_3N) as an additive (Figure 20).[24,32] All of the vinyl monomers were smoothly consumed to result in a higher molecular weight shift of the SEC curves with maintaining unimodal MWDs, which became narrower (M_w/M_n = 1.3–1.6) than the starting polyester. This suggests the formation of the block copolymers of **2** and the vinyl monomers. However, with consumption of the vinyl monomers, the MWDs became broader and bimodal due to

The structures of the obtained block copolymers were then analyzed by ^{1}H NMR. Figure 21 shows the ^{1}H NMR spectra of poly(**2**) and poly(**2**)-*b*-poly(MA) at a 20% MA conversion, which were purified by a chromatographic column packed with silica gel and preparative SEC to remove the residual monomer and catalyst for poly(**2**) and the block copolymer, respectively. The spectrum of the block copolymer exhibited typical changes, in which the signal of the methine proton (*5*) adjacent to the reactive chloride terminal in poly(**2**) completely disappeared, whereas the other peaks (*a–f*, *1–4*) were intact. In addition, large broad peaks (*g–i*), assignable to the protons of the repeating units in the poly(MA) part, appeared. The methoxy proton (*i'*) at the ω–terminal of the MA unit, which is adjacent to the chlorine, also appeared at 3.8 ppm. The DP_n of **2** and the MA units in the block copolymers can be determined from the peak intensity ratios (3*e*/*i'* and *i*/*i'*) of the methyl protons (*i'*) adjacent to the terminal chlorine group to the methine protons (*e*) of the polyester unit and the methyl protons (*i*) of the poly(MA) unit, respectively [DP_n(**2**) = 6.4; DP_n(MA) = 163]. The M_n(NMR, ω-end) calculated from each DP_n was 15100, which was close to the molecular weight determined by SEC [M_n(SEC) = 14800]. These results also indicate that the block copolymerization successfully proceeded using the polyester obtained from the metal-catalyzed polyaddition as a macroinitiator in conjunction with the metal-catalyzed living radical polymerization of vinyl monomers.

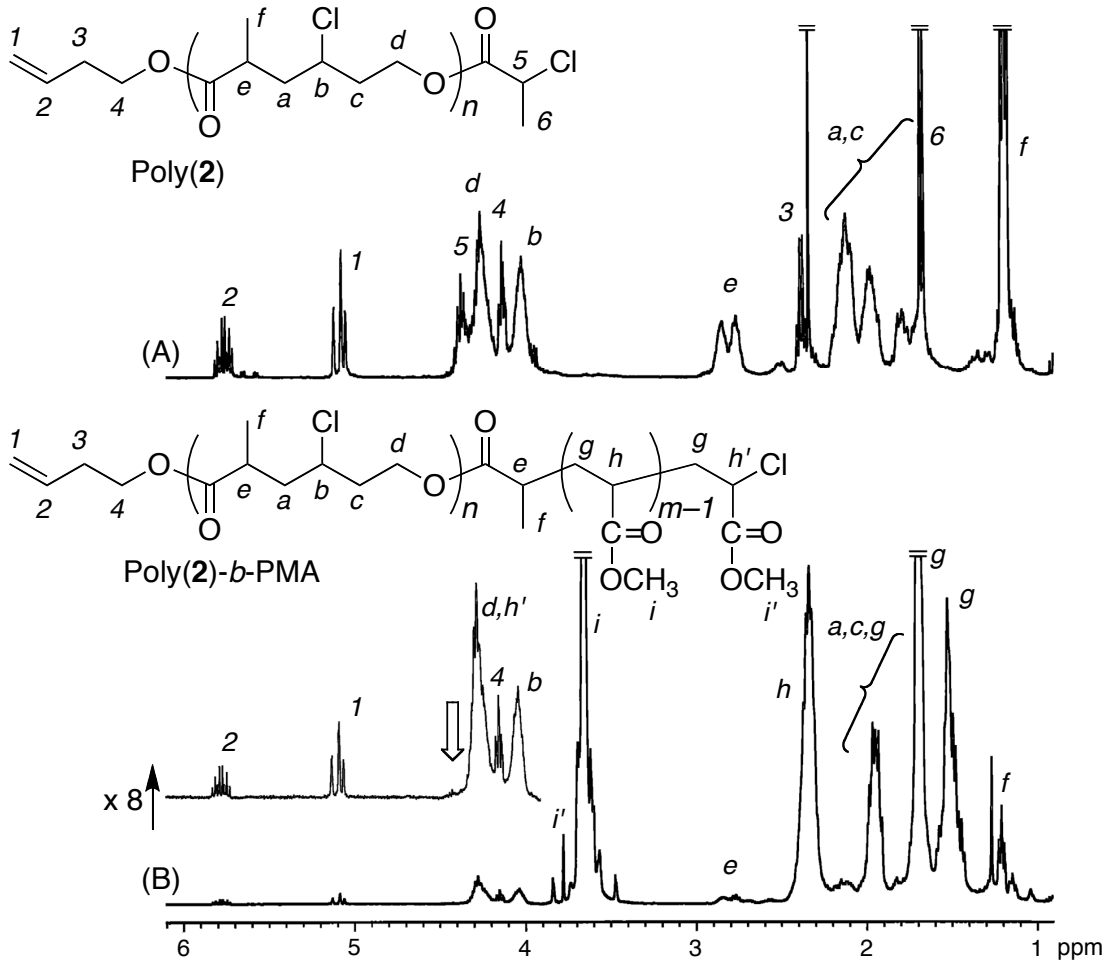

Figure 21. ^{1}H NMR spectra of the polymer of 3-butenyl 2-chloropropionate (**2**) [the number-average molecular weight (M_n) = 970, the molecular weight distribution (M_w/M_n) = 2.14] (A) and poly(**2**)-*b*- poly(methyl acrylate) (M_n =14800, M_w/M_n = 1.45) (B) obtained as in the same experiment for Figure 20 ($CDCl_3$, 55 °C).

Conclusions

The metal-catalyzed atom transfer radical addition was successfully converted into the metal-catalyzed radical polyaddition using the ester-linked monomers, which bear both a C–Cl bond and a C=C double bond in a single molecule, to produce the polyesters under various conditions via a step-growth mechanism. The obtained polyester had a precisely controlled structure of repeating main-chain ester units with the unreactive C–Cl pendants in addition to a

reactive C–Cl and unconjugated C=C double bond terminals. The terminal chlorine can also be activated again by the metal catalyst to initiate the living radical polymerization of the vinyl monomers forming novel block copolymers consisting of polyesters and vinyl polymers. The author believe sthat this radical polyaddition will provide new strategies not only in exploring novel polymerization mechanisms, but also in designing novel polymer structures.

EXPERIMENTAL SECTION

Materials

MMA (Tokyo Kasei, >98%), MA (Tokyo Kasei, >99%), styrene (Wako Chemicals, >98%), allyl acetate (Aldrich, 99%) and methyl 2-chloropropionate (TCI, >95%) were distilled from calcium hydride under reduced pressure before use. $RuCl_2(PPh_3)_3$ (Aldrich, 97%), $FeCl_2$ (Aldrich, 99.99%), CuCl (Aldrich, 99.99%), and $RuCp^*Cl(PPh_3)_2$ (provided from Wako Chemicals) were used as received. All metal compounds were handled in a glove box (VAC Nexus) under a moisture- and oxygen-free argon atmosphere (O_2, <1 ppm). Toluene was distilled over sodium benzophenone ketyl and bubbled with dry nitrogen over 15 minutes just before use. P*n*Bu_3 (KANTO, >98%), PCy_3 (KANTO, >97%), PPh_3 (KANTO, >98%), bpy (Kishida, >99%), and $Sn(EH)_2$ (Aldrich, ~95%) were used as received. *n*Bu_3N, PMDETA, Me_6TREN, HMTETA, and 3-butenyl acetate were distilled from calcium hydride before use.

Monomer Synthesis (1–4)

Allyl 2-chloropropionate (**1**), 3-butenyl 2-chloropropionate (**2**), 4-pentenyl 2-chloropropionate (**3**), and 2-(allyloxy)ethyl 2-chloropropionate (**4**) were synthesized from 2-chloropropionyl chloride (TCI, >95%) and the corresponding alcohols; i.e. allyl alcohol (KANTO,

>99%), 3-buten-1-ol (TCI, >98%), 4-penten-1-ol (TCI, >98%) and 2-allyloxyethanol (TCI, >98%) for **1**–**4**, respectively. The reaction was carried out with the use of a syringe technique under dry argon atmosphere in an oven-dried glass tube equipped with three-way stopcocks. A typical synthetic example for **2** is given below. 2-Chloropropionyl chloride (51.0 mL, 0.525 mol) was added dropwise with vigorous stirring to a solution of 3-buten-1-ol (42.4 mL, 0.500 mol) and triethylamine (76.7 mL, 0.550 mol) in dry THF (79.9 mL) at 0 ˚C. The mixture was kept stirring for 1 h at 0 ˚C, and then over 12 h at room temperature. After the dilution with diethyl ether, the mixture was washed with the aqueous solution of $NaHCO_3$ and then NaCl and evaporated to remove the solvents. The monomer was distilled over calcium hydride under reduced pressure to give pure 3-butenyl 2-chloropropionate (**2**) [56.0 mL, 0.354 mol; yield = 70.9%, purity >99%; see Figure 1 for the ^{1}H NMR spectra of the monomers (**1**–**4**)]. Monomer (**1**): ^{1}H NMR ($CDCl_3$) δ/ppm: 1.70–1.72 (d, 3H, CH–C*H*$_3$, *J* = 7.0 Hz), 4.40–4.46 (q, 1H, C*H*–CH_3, *J* = 7.0 Hz), 4.66–4.69 (dq, 2H, C*H*$_2$OCO, *J* = 5.7 Hz, 1.2 Hz), 5.27–5.40 (dq, dq, 2H, C*H*$_2$=CH, *J* = 10.4 Hz, 1.3 Hz, *J* = 17.2 Hz, 1.5 Hz), 5.88–5.98 (ddt, 1H, CH_2=C*H*, *J* = 17.2 Hz, 10.4 Hz, 5.7 Hz). Monomer (**2**): ^{1}H NMR ($CDCl_3$) δ/ppm: 1.68–1.69 (d, 3H, CH–C*H*$_3$, *J* = 7.0 Hz), 2.40–2.46 (qt, 2H, CH_2=CH–C*H*$_2$, *J* = 6.7 Hz, 1.3 Hz), 4.22–4.25 (t, 2H, C*H*$_2$OCO, *J* = 6.8 Hz), 4.37–4.42 (q, 1H, C*H*–CH_3, *J* = 6.9 Hz), 5.08–5.16 (dq, dq, 2H, C*H*$_2$=CH, *J* = 10.3 Hz, 1.3 Hz, *J* = 17.4 Hz, 1.7 Hz), 5.73–5.84 (ddt, 1H, CH_2=C*H*, *J* = 17.2 Hz, 10.3 Hz, 6.8 Hz). Monomer (**3**): ^{1}H NMR ($CDCl_3$) δ/ppm: 1.68–1.70 (d, 3H, CH–C*H*$_3$, *J* = 6.9 Hz), 1.75–1.82 (m, 2H, C*H*$_2$–CH_2OCO), 2.12–2.18 (m, 2H, CH_2=CH–C*H*$_2$), 4.17–4.21 (td, 2H, C*H*$_2$OCO, *J* = 6.6 Hz, 2.6 Hz), 4.37–4.42 (q, 1H, C*H*–CH_3, *J* = 6.9 Hz), 4.99–5.08 (ddt, dq, 2H, C*H*$_2$=CH, *J* = 10.2 Hz, 1.9 Hz, 1.2 Hz, *J* = 17.0 Hz, 1.7 Hz), 5.75–5.85 (dt, 1H, CH_2=C*H*, *J* = 17.0 Hz, 10.3 Hz, 6.6 Hz). Monomer (**4**): ^{1}H NMR ($CDCl_3$) δ/ppm: 1.70–1.71 (d, 3H, CH–C*H*$_3$, *J* = 7.0 Hz), 3.67–3.69 (m, 2H, C*H*$_2$–CH_2OCO), 4.02–4.05 (dt, 2H, CH_2=CH–C*H*$_2$,

J = 5.7 Hz, 1.3 Hz), 4.33–4.35 (m, 2H, C*H*$_2$OCO), 4.41–4.46 (q, 1H, C*H*–CH$_3$, *J* = 6.9 Hz), 5.19–5.32 (dq, dq, 2H, C*H*$_2$=CH, *J* = 10.3 Hz, 1.4 Hz, *J* = 17.2 Hz, 1.6 Hz), 5.85–5.95 (ddt, 1H, CH$_2$=C*H*, *J* = 17.2 Hz, 10.4 Hz, 5.7 Hz).

Polymerization

Polymerization was carried out under dry nitrogen in baked glass tubes equipped with a three-way stopcock. Typically, a mixture of $FeCl_2$ (50.7 mg, 0.40 mmol) and P*n*Bu$_3$ (0.20 mL, 0.80 mmol) in toluene (2.54 mL) was stirred for 24 h at 80 ˚C to give a homogeneous solution of $FeCl_2$(P*n*-Bu$_3$)$_2$ complex. After the solution was cooled to room temperature, 3-butenyl 2-chloropropionate (**2**) (1.26 mL, 8.0 mmol) was added. The solution was evenly charged in seven glass tubes, and the tubes were sealed by flame under a nitrogen atmosphere. The tubes were immersed in thermostatic oil bath at 100 ˚C. In predetermined intervals, the polymerization was terminated by cooling the reaction mixtures to –78 ˚C. Monomer conversion was determined from the concentration of residual monomer measured by gas chromatography with toluene as an internal standard (800 h, 99% conversion). The quenched reaction mixture was diluted with ethyl acetate (30 mL), washed with dilute citric acid and water to remove complex residues, evaporated to dryness under reduced pressure, and vacuum-dried to give the product polymers (0.14 g, 87 % yield; M_n = 1200, M_w = 2700, M_w/M_n = 2.30), including a small amount of remaining catalyst residues.

Model Radical Addition

Radical addition reaction was carried out under dry nitrogen in baked glass tubes equipped with a three-way stopcock. Typically, a mixture of $FeCl_2$ (50.7 mg, 0.40 mmol) and

P*n*Bu$_3$ (0.20 mL, 0.80 mmol) in toluene (1.88 mL) was stirred for 24 h at 80 ˚C to give a homogeneous solution of $FeCl_2(PnBu_3)_2$ complex. After the solution was cooled to room temperature, methyl 2-chloropropionate (**5**) (0.91 mL, 8.0 mmol) and 3-butenyl acetate (**6**) (1.01 mL, 8.0 mmol) was added. The solution was evenly charged in seven glass tubes, and the tubes were sealed by flame under a nitrogen atmosphere. The tubes were immersed in thermostatic oil bath at 100 ˚C. In predetermined intervals, the reaction was terminated by cooling the reaction mixtures to –78 ˚C. The conversions of the functional groups (C=C and C–Cl) and the yields of the adducts were determined from the concentration of **5**, **6**, and **7** measured by ^{1}H NMR spectroscopy with toluene as an internal standard (88% and 86% conversions and 87% yield, respectively, in 70 h). The contents of the byproducts, methyl propionate (**8**) and dimethyl 2,3-dimethylsuccinate (**9**), were measured by gas chromatography with methyl 2-chloropropionate as an internal standard (2% and <1%, respectively in 70 h). The quenched reaction mixture was diluted with toluene (30 mL), washed with dilute citric acid and water to remove complex residues, evaporated to dryness under reduced pressure, and vacuum-dried. The residue was purified by column chromatography eluted with diethyl ether to give the 1:1 adduct (**7**) as a mixture of diastereomers due to two asymmetric carbons, i.e. two pairs of enantiomers: (2*R*,4*R*)- and (2*S*,4*S*)-, or (2*R*,4*S*)- and (2*S*,4*R*)-isomers (ratio of diastereomers = 51:49). Yield: 0.16 g (68%). ^{1}H NMR ($CDCl_3$) δ/ppm: 1.21 (dd, 3H, CH–C*H*$_3$), 1.67–1.75, 1.76–1.85, 2.08–2.22 (m, 2H, CH–C*H*$_2$–CHCl), 1.93–2.04, 2.08–2.22 (m, 2H, CHCl–C*H*$_2$–CH$_2$O), 2.06 (d, 3H, OCOC*H*$_3$), 2.75–2.92 (m, 1H, OCOC*H*), 3.70 (d, 3H, C*H*$_3$OCO), 3.99–4.07 (m, 1H, C*H*Cl), 4.15–4.32 (m, 2H, C*H*$_2$OCO). ^{13}C NMR ($CDCl_3$) δ/ppm: 16.23, 18.28 (CH–*C*H$_3$), 20.97, 20.99 (OCO*C*H$_3$), 36.71, 36.78 (OCO*C*H), 37.43, 37.69 (CHCl–*C*H$_2$–CH$_2$O), 41.58, 42.45 (CH–*C*H$_2$–CHCl), 51.78, 51.84 (*C*H$_3$OCO), 57.16, 58.15 (*C*HCl), 61.26, 61.29 (*C*H$_2$OCO), 170.66, 170.69 (O*C*OCH$_3$), 176.06, 176.15 (CH$_3$O*C*O).

Measurements

Monomer conversion was determined from the concentration of residual monomer measured by gas chromatography [Shimadzu GC-8A equipped with a thermal conductivity detector and a 3.0 mm i.d. × 2 m stainless steel column packed with SBS-200 (Shinwa Chemical Industries Ltd.) supported on Shimalite W; injection and detector temperature = 200 ˚C, column temperature = 160 ˚C] with toluene as an internal standard under He gas flow. ^{1}H NMR and COSY spectra were recorded in $CDCl_3$ at room temperature on a Varian Gemini 2000 spectrometer, operating at 400 MHz. The number-average molecular weight (M_n), the weight-average molecular weight (M_w) and the molecular weight distribution (M_w/M_n) of the product polymers were determined by SEC in THF at 40 ˚C on two polystyrene gel columns [Shodex K-805L (pore size: 20–1000 Å; 8.0 mm i.d. × 30 cm) × 2; flow rate 1.0 mL/min] connected to a Jasco PU-980 precision pump and a Jasco 930-RI refractive index detector. The columns were calibrated against eight standard poly(MMA) samples (Shodex; M_p = 202–1,950,000; M_w/M_n = 1.02–1.09). Glass transition temperature (T_g: midpoint of the transition) and melting temperature (T_m: endothermic maximum) of the polymers were recorded on SSC-5200 differential scanning calorimetry (Seiko Instruments Inc.). Certified indium and tin were used for temperature and heat flow calibration. Samples were first heated to 100 or 150 ˚C at 10 ˚C/min., equilibrated at this temperature for 0 or 10 min, and cooled to –100 ˚C at 10 ˚C/min. After being held at this temperature for 20 min, the samples were then reheated to 200 ˚C at 10 ˚C/min. All T_g and T_m values were obtained from the second scan, after removing the thermal history.

NOTES AND REFERENCES

(1) (a) Kharasch, M. S.; Jensen, E. V.; Urry, W. H. *Science* **1945**, *102*, 128. (b) Minisci, F, *Acc. Chem. Res.* **1975**, *8*, 165–171. (c) Iqbal, J.; Bhatia, B.; Nayyar, N. K. *Chem. Rev.* **1994**, *94*, 519–564. (d) Gossage, R. A.; van de Kuil, L. A.; van Koten, G. *Acc. Chem. Res.* **1998**, *31*, 423–431.

(2) (a) Kato, M.; Kamigaito, M.; Sawamoto, M.; Higashimura, T. *Macromolecules* **1995**, *28*, 1721–1723. (b) Kamigaito, M.; Ando, T.; Sawamoto, M. *Chem. Rev.* **2001**, *101*, 3689–3745. (c) Kamigaito, M.; Ando, T.; Sawamoto, M. *Chem. Rec.* **2004**, *4*, 159–175.

(3) (a) Wang, J.-S.; Matyjaszewski, K. *J. Am. Chem. Soc.* **1995**, *117*, 5614–5615. (*b*) Matyjaszewski, K.; Xia, J. *Chem. Rev.* **2001**, *101*, 2921–2990. (c) Tsarevsky, N. V.; Matyjaszewski, K.; *Chem. Rev.* **2007**, *107*, 2270–2299.

(4) Percec, V.; Barboiu, B. *Macromolecules* **1995**, *28*, 7970–7972.

(5) Granel, C.; Dubois, Ph.; Jérôme, R.; Teyssié, Ph. *Macromolecules* **1996**, *29*, 8576–8582.

(6) Haddleton, D. M.; Jasieczek, C. B.; Hannon, M. J.; Shooter, A. J. *Macromolecules* **1997**, 30, 2190–2193.

(7) Baek, K.-Y.; Kamigaito, M.; Sawamoto, M. *J. Polym. Sci. Part A: Polym. Chem.* **2002**, *40*, 1937–1944.

(8) (a) Ando, T.; Kamigaito, M.; Sawamoto, M. *Macromolecules* **1998**, *31*, 6708–6711. (b) Bon, S. A. F.; Steward, A. G.; Haddleton, D. M. *J. Polym. Sci. Part A: Polym. Chem* **2000**, *38*, 2678–2686.

(9) (a) Coessens, V.; Matyjaszewski, K. *Macromol. Rapid Commun.* **1999**, *20*, 127–134. (b) Coessens, V.; Pyun, J.; Miller, P. J.; Gaynor, S. G.; Matyjaszewski, K. *Macromol. Rapid Commun.* **2000**, *21*, 103–109. (c) Coessens, V.; Pintauer, T.; Matyjaszewski, K. *Prog. Polym. Sci.* **2001**, *26*, 337–377. (d) Müller, A. H. E. *Macromol. Rapid Commun.* **2005**, *26*,

1893–1894.

(10) (a) Paik, H. J.; Gaynor, S. G.; Matyjaszewski, K. *Macromol. Rapid Commun.* **1998**, *19*, 47–52. (b) Matyjaszewski, K.; Teodorescu, M.; Miller, P. J.; Peterson, M. L. *J. Polym. Sci. Part A: Polym. Chem.* **2000**, *38*, 2440–2448.

(11) (a) Gaynor, S. G.; Edelman, S.; Matyjaszewski, K. *Macromolecules* **1996**, *29*, 1079–1081. (b) Matyjaszewski, K.; Gaynor, S. G.; Kulfan, A.; Podwika, M. *Macromolecules* **1997**, *30*, 5192–5194. (c) Matyjaszewski, K.; Gaynor, S. G.; Müller, A. H. E. *Macromolecules* **1997**, *30*, 7034–7041. (d) Matyjaszewski, K.; Gaynor, S. G. *Macromolecules* **1997**, *30*, 7042–7049. (e) Matyjaszewski, K.; Pyun, J.; Gaynor, S. G. *Macromol. Rapid Commun.* **1998**, *19*, 665–670.

(12) Weimer, M. W.; Fréchet, J. M. J.; Gitsov, I. *J. Polym. Sci. Part A: Polym. Chem.* **1998**, *36*, 955–970.

(13) (a) Mori, H.; Böker, A.; Krausch, G.; Müller, A. H. E. *Macromolecules* **2001**, *34*, 6871–6882. (b) Hong, C.-Y.; Pan, C.-Y. *Polymer* **2001**, *42*, 9385–9391. (c) Bibiao, J.; Yang, Y.; Jian, D.; Shiyang, F.; Rongqi, Z.; Jianjun, H.; Wenyun, W. *J. Appl. Polym. Sci.* **2002**, *83*, 2114–2123. (d) Mori, H.; Seng, D. C.; Zhang, M.; Müller, A. H. E. *Langmuir* **2002**, *18*, 3682–3693. (e) Powell, K. T.; Cheng, C.; Wooley, K. L. *Macromolecules* **2007**, *40*, 4509–4515.

(14) (a) Matyjaszewski, K.; Ziegler, M. J.; Arehart, S. V.; Greszta, D.; Pakula, T. *J. Phys. Org. Chem.* **2000**, *13*, 775–786. (b) Borner, H. G.; Duran, D.; Matyjaszewski, K.; da Silva, M.; Sheiko, S. S. *Macromolecules* **2002**, *35*, 3387–3394.

(15) Miura, Y.; Shibata, T.; Satoh, K.; Kamigaito, M.; Okamoto, Y. *J. Am. Chem. Soc.* **2006**, *128*, 16026–16027.

(16) Percec, V.; Barboiu, B.; Grigoras, C.; Bera, T. K. *J. Am. Chem. Soc.* **2003**, *125*, 6503–6516.

(17) (a) Miura, Y.; Kaneko, T.; Satoh, K.; Kamigaito, M.; Jinnai, H. Okamoto, Y. *Chem. Asian J.*

2007, *2*, 662–672. (b) Miura, Y.; Satoh, K.; Kamigaito, M.; Okamoto, Y.; Kaneko, T.; Jinnai, H.; Kobukata, S. *Macromolecules* **2007**, *40*, 465–473.

(18) Wakioka, M.; Baek, K.-Y.; Ando, T.; Kamigaito, M.; Sawamoto, M. *Macromolecules* **2002**, *35*, 330–333.

(19) (a) Asandei, A. D.; Percec, V. *J. Polym. Sci. Part A: Polym. Chem.* **2001**, *39*, 3392–3418. (b) Percec, V.; Popov, A. V.; Ramirez-Castillo, E.; Monteiro, M.; Barboiu, B; Weichold, O; Asandei, A. D.; Mitchell, C. M. *J. Am. Chem. Soc.* **2002**, *124*, 4940–4941. (c) Percec, V.; Guliashvili, T.; Ladislaw, J. S.; Wistrand, A.; Stjerndahl, A.; Sienkowska, M. J.; Monteiro, M. J.; Sahoo, S. *J. Am. Chem. Soc.* **2006**, *128*, 14156–14165.

(20) Satoh, K.; Mizutani, M.; Kamigaito, M. *Chem. Commun.* **2007**, 1260–1262.

(21) (a) Fréchet, J. M. J.; Henmi, M.; Gitsov, I.; Aoshima, S.; Leduc, M. R.; Grubbs, R. B. *Science* **1995**, *269*, 1080–1083. (b) Hawker, C. J.; Fréchet, J. M. J.; Grubbs, R. B.; Dao, J. *J. Am. Chem. Soc.* **1995**, *117*, 10763–10764. (c) Simon, P. F. W.; Radke, W.; Müller, A. H. E. *Macromol. Rapid Commun.* **1997**, *18*, 865–873. (d) Müller, A. H. E.; Yan, D.; Wulkow, M. *Macromolecules* **1997**, *30*, 7015–7023. (e) Yan, D.; Müller, A. H. E.; Matyjaszewski, K. *Macromolecules* **1997**, *30*, 7024–7033. (f) Yan, D.; Zhou, Z.; Müller, A. H. E. *Macromolecules* **1999**, *32*, 245–250. (g) Gao, C.; Yan, D. *Prog. Polym. Sci.* **2004**, *29*, 183–275.

(22) (a) Marvel, C. S.; Chambers, R. R. *J. Am. Chem. Soc.* **1948**, *70*, 993–998. (b) Kobayashi, E.; Ohashi, T.; Furukawa, J. *Makromol. Chem.* **1986**, *187*, 2525–2533. (c) Kobayashi, E.; Obata, T.; Aoshima, S.; Furukawa, J. *Polymer Journal* **1990**, *22*, 803–813. (d) Klemm, E.; Sensfuβ, S.; Holfter, U.; Schütz, H. *Makromol. Chem.* **1990**, *191*, 2403–2411. (e) Sato, E.; Yokozawa, T.; Endo, T. *Macromolecules* **1993**, *26*, 5187–5191.

(23) (a) Nagashima, H.; Wakamatsu, H.; Itoh, K.; Tomo, Y.; Tsuji, J. *Tetrahedron Lett.* **1983**, 24, 2395–2398. (b) Iritani, K.; Yanagihara, N.; Utimoto, K. *J. Org. Chem.* **1986**, 51, 5501–5503. (c) Hayes, T. K. Villani, R. Weinreb, S. M. *J. Am. Chem. Soc.* **1988**, 110, 5533–5543. (d) Phelps, J. C.; Bergbreiter, D. E.; Lee, G. M.; Villani, R.; Weinreb, S M. *Tetrahedron Lett.* **1989**, 30, 3915–3918. (e) Nagashima, H.; Seki, K.; Ozaki, N.; Wakamatsu, H.; Itoh, K.; Tomo, Y.; Tsuji, J. *J. Org. Chem.* **1990**, 55, 985–990. (f) Pirrung, F. O. H.; Steeman, W. J. M.; Hiemstra, H.; Speckamp, W. N.; Kaptein, B.; Boesten, W. H. J.; Schoemaker, H. E.; Kamphuis, J. *Tetrahedron Lett.* **1992**, 33, 5141–5144. (g) De Campo, F.; Lastécouères, D.; Verlhac. J.-B. *Chem. Commun.* **1998**, 2117–2118. (h) De Campo, F.; Lastécouères, D.; Vincent, J.-M.; Verlhac. J.-B. *J. Org. Chem.* **1999**, *64*, 4969–4971. (i) De Campo, F.; Lastécouères, D.; Verlhac. J.-B. *J. Chem. Soc. Perkin Trans. 1* **2000**, *4*, 575–580. (j) Clark, A. J. *Chem. Soc. Rev.* **2002**, *31*, 1–11.

(24) (a) Ando, T.; Kamigaito, M.; Sawamoto, M. *Macromolecules* **2000**, *33*, 5825–5829. (b) Watanabe, Y.; Ando, T.; Kamigaito, M.; Sawamoto, M. *Macromolecules* **2001**, *34*, 4370–4374.

(25) (a) Ando, T.; Kamigaito, M.; Sawamoto, M. *Macromolecules* **1997**, *30*, 4507–4510. (b) Matyjaszewski, K.; Wei, M.; Xia, J.; McDermott, N. E. *Macromolecules* **1997**, *30*, 8161–8164. (c) Uchiike, C.; Terashima, T.; Ouchi, M.; Ando, T.; Kamigaito, M. Sawamoto, M. *Macromolecules* **2007**, *40*, 8658–8662.

(26) Xia, J.; Matyjaszewski, K. *Macromolecules* **1997**, *30*, 7697–7700.

(27) Queffelec, J.; Gaynor, S. G.; Matyjaszewski, K. *Macromolecules* **2000**, *33*, 8629–8639.

(28) Jakubowski, W.; Matyjaszewski, K. *Macromolecules* **2005**, *38*, 4139–4146.

(29) Jakubowski, W.; Min, K.; Matyjaszewski, K. *Macromolecules* **2006**, *39*, 39–45.

(30) Satoh, K.; Aoshima, H.; Kamigaito, M. *J. Polym. Sci.: Part A: Polym. Chem.*, **2008**, *46*,

6358–6363.

(31) (a) Detrembleur, C.; Mazza, M.; Halleux, O.; Lecomte, Ph.; Mecerreyes, D.; Hedrick J. L.; Jérôme, R. *Macromolecules* **2000**, *33*, 14–18. (b) Lenoir, S.; Riva, R.; Lou, X.; Detrembleur, Ch.; Jérôme, R.; Lecomte, Ph. *Macromolecules* **2004**, *37*, 4055–4061.

(32) Hamasaki, S.; Kamigaito, M.; Sawamoto, M. *Macromolecules* **2002**, *35*, 2934–2940.

PART II

Simultaneous Chain- and Step-Growth Radical Polymerization

Chapter 3–1

Metal-Catalyzed Living Radical Polymerization and Radical Polyaddition for Precision Polymer Synthesis

ABSTRACT

The metal-catalyzed radical addition reaction can be evolved into two different polymerization mechanisms, i.e.; chain- and step-growth polymerizations, while both the polymerizations are based on the same metal-catalyzed radical formation reaction. The former is a widely employed metal-catalyzed living radical polymerization or atom transfer radical polymerization of common vinyl monomers, and the latter is a novel metal-catalyzed radical polyaddition of designed monomer with an unconjugated C=C double bond and a reactive C–Cl bond in one molecule. The simultaneous ruthenium-catalyzed living radical polymerization of methyl acrylate and radical polyaddition of 3-butenyl 2-chloropropionate was achieved with $Ru(Cp^*)Cl(PPh_3)_2$ to afford the controlled polymers, in which the homopolymer segments with the controlled chain length were connected by the ester linkage.

Introduction

Recent remarkable progress in controlled/living radical polymerizations has enabled the precision polymer synthesis of a wide variety of well-defined polymers, such as end-functionalized, block, graft, and star polymers.[1–4] Among them, the metal-catalyzed living radical polymerization or atom transfer radical polymerization (ATRP) is one of the most efficient systems for various conjugated vinyl monomers, such as methacrylates, acrylates, acrylamides, and styrenes.[2,3] This polymerization was originally developed from the metal-catalyzed Kharasch or atom-transfer radical addition reaction (ATRA), in which the carbon radical species is generated through the metal-catalyzed cleavage of a carbon–halogen (C–X) bond and adds to an olefin to form the 1:1 adduct of the halide and olefin.[5,6] The metal-catalyzed living radical chain-growth polymerization proceeds via the metal-catalyzed reversible formation of the growing radical species from the dormant C–X polymer terminal, and the addition of the growing radical species to the vinyl monomers.[7]

In contrast, the author found a novel radical polyaddition reaction of a designed monomer that possesses an active C–X bond and unconjugated C=C double bond via the evolution of the metal-catalyzed ATRA into the step-growth polymerization in Chapter 1 and 2.[8,9] In this polymerization, the active or dormant C–X bond in the monomer is activated by the metal catalysts to form a radical species, which adds to the C=C double bond of another monomer molecule to generate a C–C bond as the main chain, along with an inactive C–X bond as the pendant. This radical polyaddition can be catalyzed by the same metal catalyst for the living radical polymerization.

This chapter will first describe the metal-catalyzed chain-growth living radical polymerization of methyl acrylate (MA) and then the metal-catalyzed step-growth radical

polyaddition of a designed monomer (**1**), in which the unconjugated C=C and reactive C–C bonds are linked via ester linkage. Finally, the simultaneous metal-catalyzed radical living

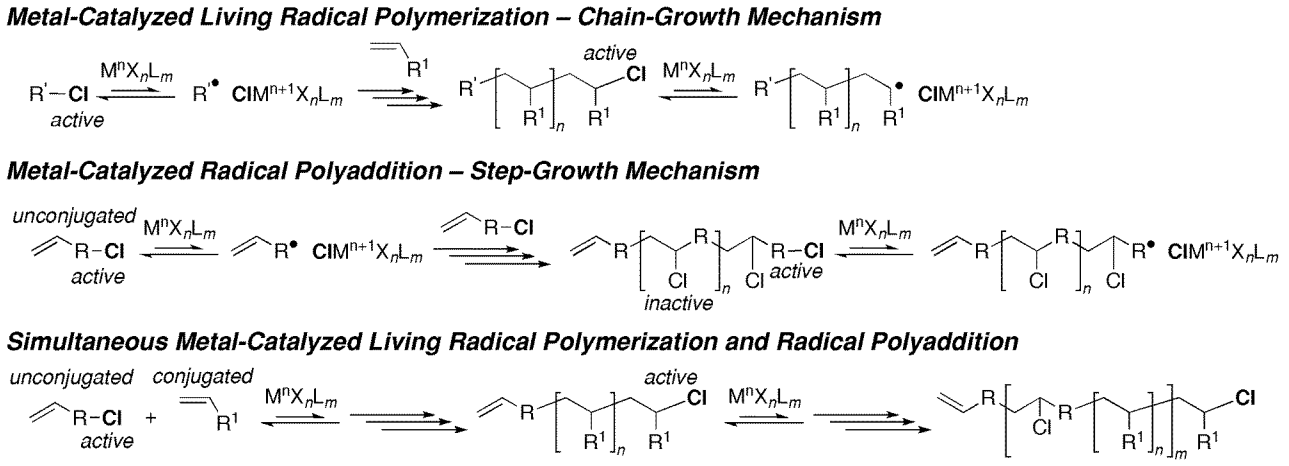

Scheme 1. Metal-catalyzed living radical polymerization and radical polyaddition

polymerization of MA and radical polyaddition of **1** was examined for novel precision polymer synthesis (Scheme 1).

Results and Discussion

1. Metal-catalyzed radical living polymerization of MA. First, the author investigated the ruthenium-catalyzed living radical polymerization of MA using $Ru(Cp^*)Cl(PPh_3)_2$ and methyl 2-chloropropionate (**2**), which has a similar secondary C–Cl bond to **1**, in the presence of nBu$_3$N in toluene at 80 °C. The polymerization occurred smoothly (Figure 1A) to give the polymers with relatively narrow MWDs (Figure 1C). However, the MWDs were slightly broader than those obtained with the methyl methacrylate dimer-type initiator [H–(MMA)$_2$–Cl], which has a more reactive C–Cl bond,[10] indicating a slower initiation from **2**. The M_n of the polymers increased in direct proportion to monomer conversion and agreed well with the calculated values, assuming that one molecule of **2** generates one living polymer chain (Figure 1B).

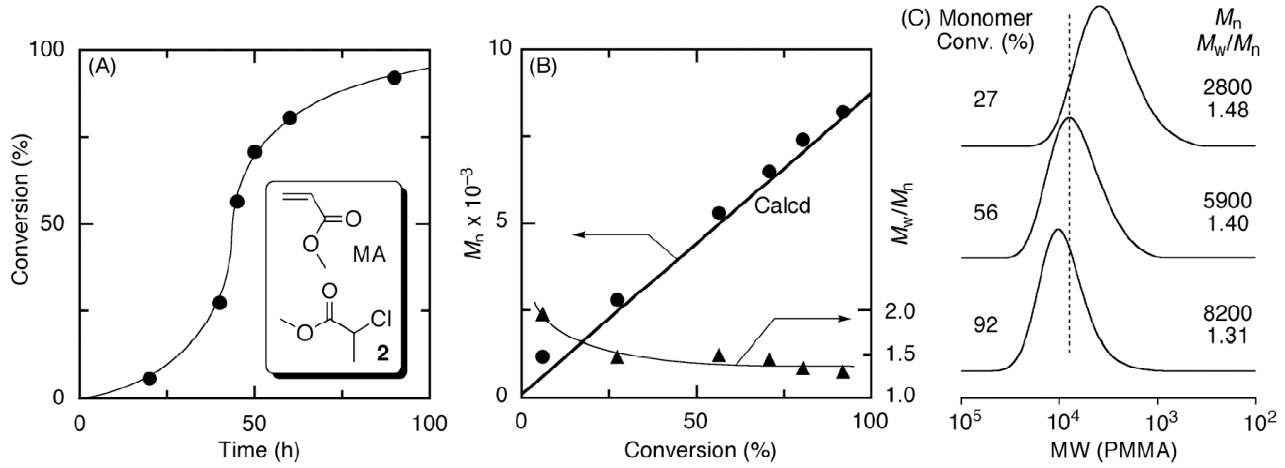

Figure 1. Metal-catalyzed living radical polyaddition of MA with **2**/Ru(Cp*)Cl(PPh_3)$_2$/$n$$Bu_3N$ in toluene at 80 °C: [MA]$_0$/[**2**]$_0$/[Ru(Cp*)Cl(PPh_3)$_2$]$_0$/[$n$$Bu_3N$]$_0$ = 4000/40/4/40 mM.

2. Metal-catalyzed radical polyaddition of 1. The metal-catalyzed radical polyaddition of **1** was conducted with CuCl/PMDETA in toluene at 60 °C.[11] The monomers were consumed smoothly and almost completely irrespective of the slow reaction (Figure 2A). The consumption of the two functional groups in **1**, C=C and C–Cl, occurred at the same rate and was slower than

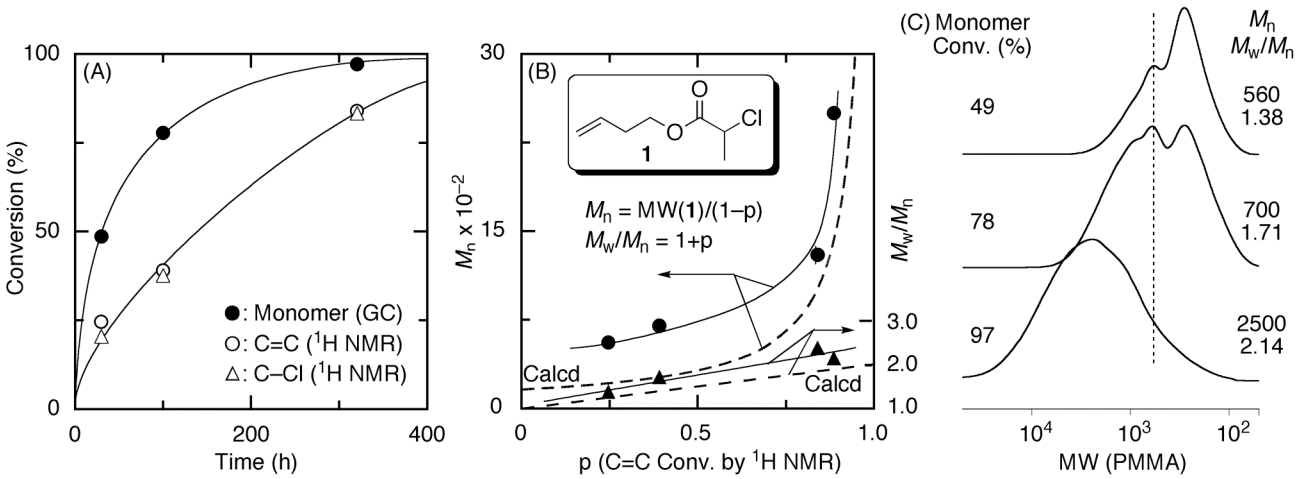

Figure 2. Metal-catalyzed radical polyaddition of **1** with CuCl/PMDETA in toluene at 60 °C: [**1**]$_0$/[CuCl]$_0$/[PMDETA]$_0$ = 2000/100/400 mM.

that of **1**, indicating the 1:1 intermolecular addition reaction. The SEC curves of the obtained polymers shifted to high molecular weights as the polymerization proceeded (Figure 2C). The M_n of the products progressively increased and was close to the calculated line for the step-growth polymerization, assuming that M_n increases in inverse proportion to 1-p, where p and MW(**1**) mean the consumption of the functional group and the molecular weight of the monomer (**1**) (Figure 2B).[9] The MWD increased with conversion and was also close to the calculated value of 2 for step-growth polymerization.

3. Simultaneous metal-catalyzed radical living polymerization of MA and polyaddition of 1. The simultaneous metal-catalyzed living radical polymerization of MA and radical polyaddition of **1** ($[MA]_0/[\mathbf{1}]_0$ = 4000/40 mM) was then investigated by the ruthenium catalyst in toluene at 80 °C. As shown in Figure 3A, both the monomers were consumed simultaneously, where the consumption of **1** was faster than that of MA. During the early stage of the polymerization, the M_n of the obtained polymers increased in direct proportion to the conversion of MA and agreed well with the calculated value, assuming that one molecule of **1** generates one polymer chain (Figure 3B). Furthermore, the SEC curves were relatively narrow and shifted to high molecular weights along with the consumption of MA (Figure 3C). These results indicate that living radical polymerization of MA first proceeds via reversible activation of the C–Cl terminal derived from the C–Cl bond of **1** via the metal-catalyzed initiation. However, in the later stage, the molecular weight of the polymers drastically increased along with change of the unimodal SEC curves into multimodal, indicating that the polyaddition reaction occurred between the living polymer chains possessing C=C and C–Cl groups at the a- and w-chain ends, respectively, both of which originated from **1**. Due to the lower reactivity of the unconjugated double bond of **1**, the

polyaddition reaction was slower than the addition polymerization of MA and resulted in a progressive increase of the molecular weight in the later stage of the reaction.

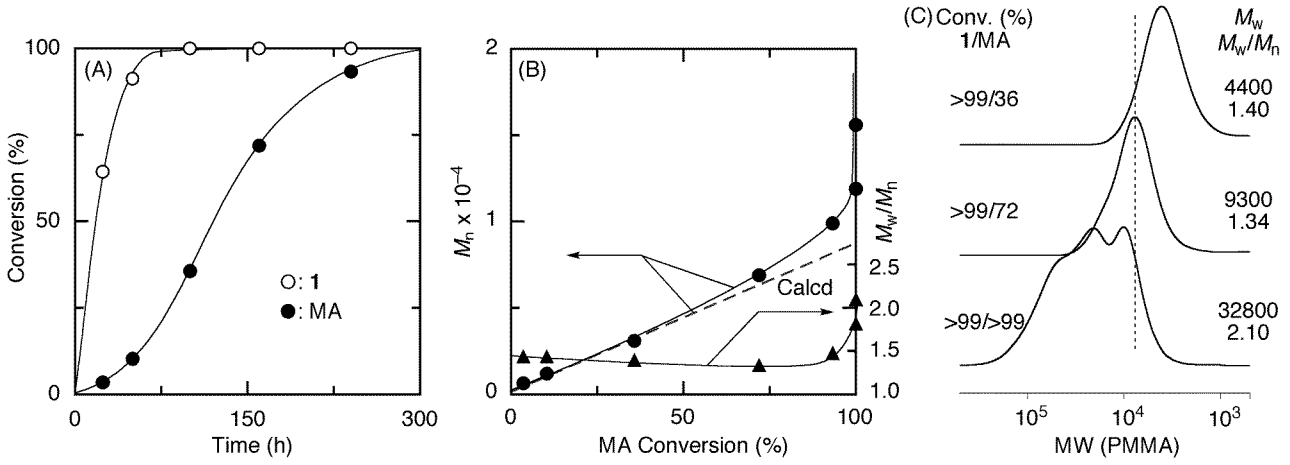

Figure 3. Simultaneous metal-catalyzed living radical polymerization of MA and radical polyaddition of **1** with $Ru(Cp^*)Cl(PPh_3)_2$/nBu_3N in toluene at 80 °C: $[MA]_0/[\mathbf{1}]_0/[Ru(Cp^*)Cl(PPh_3)_2]_0/[nBu_3N]_0$ = 4000/40/4/40 mM.

Conclusions

In conclusion, the simultaneous radical living polymerization and radical polyaddition occur via the same metal-catalyzed radical formation reaction to afford the controlled polymers, in which the homopolymer segments with the controlled chain length were connected by the ester linkage.

EXPERIMENTAL SECTION

Materials

$Ru(Cp^*)Cl(PPh_3)_2$ (provided from Wako) and CuCl (Aldrich, 99.99%) were used as received. All metal compounds were handled in a glovebox (VAC Nexus) under a moisture- and oxygen-free atmosphere (O_2, < 1 ppm). Toluene was distilled over sodium benzophenone ketyl and bubbled with dry nitrogen for 15 min just before use. Methyl acrylate (TCI, >99%), methyl 2-chloropropionate (TCI, >95%), *N*,*N*,*N'*,*N''*,*N''*-pentamethyldiethylenetriamine (PMDETA) (TCI, >98%), and nBu$_3$N (Wako, >98%) were distilled from calcium hydride under reduced pressure before use.

Monomer Synthesis (1–3)

3-Butenyl 2-chloropropionate (**1**) was synthesized from 2-chloropropionyl chloride (TCI, >95%) and 3-buten-1-ol (TCI, >98%).

Polymerization

Polymerization was carried out under dry nitrogen in baked glass tubes equipped with a three-way stopcock using syringe techniques.

Measurements

Monomer conversion was determined from the concentration of residual monomer measured by gas chromatography. Functional group (C=C and C–Cl) conversions were measured by 400 MHz ^{1}H NMR (Varian Gemini 2000). The number-average molecular weight (M_n), the weight-average molecular weight (M_w), and the molecular weight distribution (MWD) of the

polymers were determined by size-exclusion chromatography (SEC) in THF. The columns were calibrated against eight standard poly(methyl methacrylate) samples (Shodex; M_p = 202–1,950,000; M_w/M_n = 1.02–1.09).

NOTES AND REFERENCES

(1) Hawker, C. J.; Bosman, A. W.; Harth, E. *Chem. Rev.* **2001***, 101*, 3661–3688.

(2) Kamigaito, M.; Ando, T.; Sawamoto, M. *Chem. Rev.* **2001**, *101*, 3689–3745.

(3) Matyjaszewski, K.; Xia, J. *Chem. Rev.* **2001**, *101*, 2921–2990.

(4) Moad, G.; Rizzardo, E.; Thang, S. H. *Aust. J. Chem.* **2005**, *58*, 379–410.

(5) Kharasch, M. S.; Jensen, E. V.; Urry, W. H. *Science* **1945**, *102*, 128.

(6) Iqbal, J. P.; Bhatia B.; Nayyar, N. K. *Chem. Rev.* **1994**, *94*, 519–564.

(7) Kato, M.; Kamigaito, M.; Sawamoto, M.; Higashimura, T. *Macromolecules* **1995**, *28*, 1721–1723.

(8) Satoh, K.; Mizutani, M.; Kamigaito, M. *Chem. Commun.* **2007**, 1260–1262.

(9) Mizutani, M.; Satoh, K.; Kamigaito, M. *Macromolecules* **2009**, *42*, 472–480.

(10) Watanabe, Y.; Ando, T.; Kamigaito, M.; Sawamoto, M. *Macromolecules* **2001**, *34***,** 4370–4374.

(11) Xia, J.; Matyjaszewski, K. *Macromolecules* **1997**, *30*, 7697–7700.

Chapter 3–2

Metal-Catalyzed Simultaneous Chain- and Step-Growth Radical Polymerization: Marriage of Vinyl Polymers and Polyesters

ABSTRACT

All polymerization reactions are categorized into two large different families, chain- and step-growth polymerizations, which are typically incompatible. Here the author reports the simultaneous chain- and step-growth polymerization via the metal-catalyzed radical copolymerization of conjugated vinyl monomers and designed monomers possessing unconjugated C=C and active C–Cl bonds. Especially, almost ideal linear random copolymers containing both vinyl polymer and polyester units in a single polymer chain were formed by the CuCl/1,1,4,7,10,10-hexamethyltriethylenetetramine- or $RuCp^*Cl(PPh_3)_2$-catalyzed copolymerization of methyl acrylate (MA) for the chain-growth polymerization and 3-butenyl 2-chloropropionate (**1**) for the step-growth polymerization. In contrast, other transition metal catalysts, such as CuCl with tris[2-(dimethylamino)ethyl]amine or *N*,*N*,*N'*,*N''*,*N''*-pentamethyldiethylenetriamine and $FeCl_2$/P*n*Bu_3, resulted in branched structures via the concomitant chain-growth copolymerization of **1** with MA. The polymerization mechanism was studied in detail by NMR and MALDI-TOF-MS analyses of the polymerizations as well as the model reactions. Furthermore, a series of copolymers changing from random to multiblock polymer structures were obtained by varying the feed ratios of the two monomers. These copolymers can be easily degraded into lower molecular weight oligomers or polymers via methanolysis of the ester-linkages in the main chain using sodium carbonate.

Introduction

All synthetic polymers such as polystyrenes, acrylic polymers, polyesters, polyamides, etc., which heavily support our modern life, are obtained by either a chain- or step-growth polymerization. These two classes of polymerizations are mechanistically completely different and proceed via their characteristic profiles of polymer chain propagation to produce the polymers with their unique structures.[1] In the chain-growth mechanism, polymer chains grow via reactions of the growing chain end with monomers, while in the step-growth counterpart, the chain gradually propagates via reactions among the functional chain-end groups of the monomer, oligomers, and finally polymers. The former representatives are radical polymerizations of vinyl monomers, which produce C–C bond main-chain polymers, whereas the latter includes polycondensation for polyesters and polyaddition for polyurethane, mostly containing heteroatoms in the main chains. If one could simultaneously perform both the chain- and step-growth polymerizations, the accessible polymer structures and properties could be widely varied. However, these two polymerizations are generally incompatible, and no such systems have been reported.[2]

The metal-catalyzed atom transfer or Kharasch radical addition reaction[3,4] is one of the most highly efficient and robust carbon-carbon bond forming reactions between various vinyl compounds and organic halides.[5–11] This reaction has now quite successfully been developed into chain-growth radical polymerizations of mostly conjugated various vinyl monomers in the presence of an appropriate organic halide initiator to establish a new category of precision polymerizations; i.e., the metal-catalyzed living radical polymerization or atom transfer radical polymerization (ATRP).[12–25] In contrast, the author quite recently developed the radical addition reaction into step-growth polymerizations; i.e., the metal-catalyzed radical polyaddition of designed monomers (C=C–R–C–X) with active carbon–halogen and unconjugated C=C double bonds.[26–30] The

common process of both polymerizations lies in the metal-assisted formation of carbon-centered radical species from the active C–X bond followed by the addition to the C=C double bond and the formation of a new C–X bond. However, the differences in the reactivity[22] of the newly formed C–X bond determine the reaction pathway. In the metal-catalyzed living radical polymerizations, the C–X bond, which is adjacent to the conjugated carbonyl or aryl groups originating from the conjugated vinyl monomers, can be repeatedly activated by a metal catalyst with moderate activity to reversibly form the growing radical species and to induce the chain-growth propagation. In contrast, in the radical polyaddition, the newly formed C–X bond derived from the unconjugated C=C double bond is hardly activated by the usual metal catalyst, while the original active C–X bond at the monomer, oligomer, and polymer terminals is selectively activated to induce the step-growth radical polymerizations.

The author now reports the unprecedented simultaneous chain- and step-growth polymerizations, both of which proceed via the radical intermediate generated by the same metal catalyst, for the synthesis of novel polymer structures with varying random to multiblock copolymers consisting of vinyl and polyester monomer units (Scheme 1). A series of transition metal catalysts (Cu, Ru, and Fe) with various ligands, which are effective for the metal-catalyzed living radial polymerization or ATRP, were extensively tested under various conditions to achieve the ideal simultaneous polymerizations of methyl acrylate (MA) and 3-butenyl 2-chloropropionate [CH_2=$CHCH_2CH_2OC(O)CH(CH_3)Cl$: **1**]. One of the most important keys to the efficient simultaneous polymerizations resulting in the linear copolymers is to reduce any possible side reactions, such as the bimolecular radical termination and chain-growth copolymerization of **1** with MA. Detailed analyses of the polymerizations as well as the model reactions by NMR and MALDI-TOF-MS were thus done systematically to find the most efficient catalysts and to reveal

the polymerization mechanism. Among the various metal catalysts, CuCl/1,1,4,7,10,10-hexamethyltriethylenetetramine (HMTETA) and RuCp*Cl$(PPh_3)_2$ proved most effective for the ideal simultaneous chain- and step-growth radical polymerizations to yield the linear copolymers comprised of acrylate and polyester monomer units.

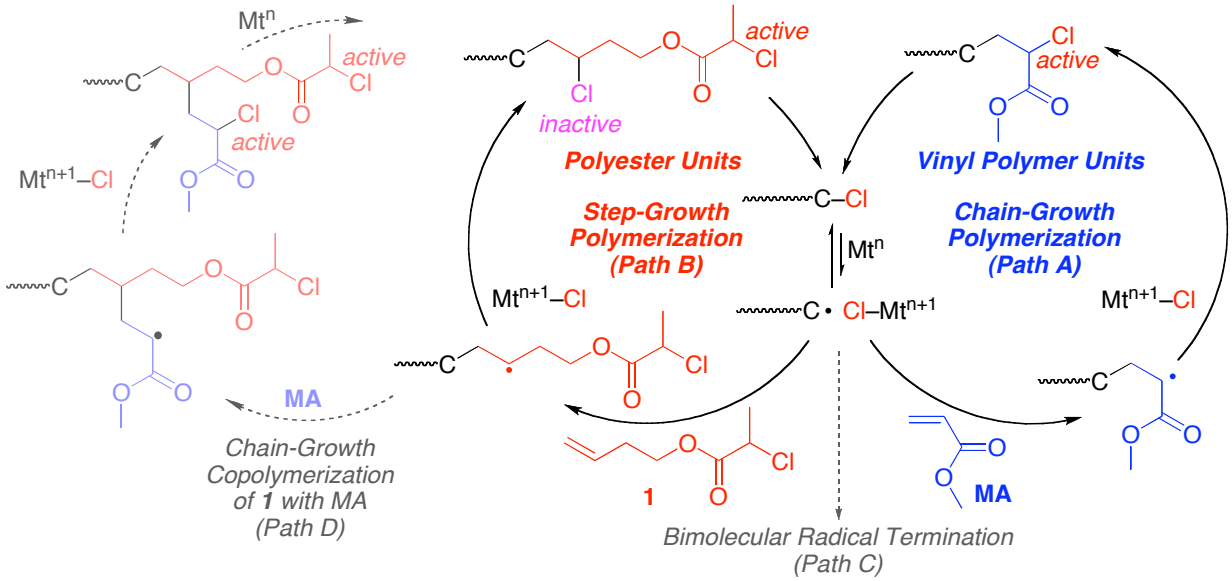

Scheme 1. Mechanism of Metal-Catalyzed Simultaneous Chain- and Step-Growth Radical Polymerization. Path A: Chain-Growth Radical Polymerization of MA. Path B: Step-Growth Radical Polymerization of **1**. Path C: Possible Bimolecular Radical Termination. Path D: Possible Chain-Growth Radical Copolymerization of **1** with MA.

Results and Discussion

1. Simultaneous Chain- and Step-Growth Radical Polymerization of MA and 1. An equimolar mixture of MA and **1** was copolymerized with CuCl/HMTETA in toluene at 80 °C. Both monomers were simultaneously and quantitatively consumed, in which the consumption of MA was slightly faster than that of **1** (Figure 1A). In addition to the gas-chromatographic analysis of the monomer conversions, the consumption of the original C–Cl and unconjugated C=C bonds

was measured by ^{1}H NMR analysis of the reaction mixture to clarify the polymerization mechanism. The original C–Cl bond (filled triangles in Figure 1A) was more rapidly consumed than the unconjugated C=C bond (open triangles), suggesting that the C–Cl bond was first activated by the copper catalyst to form the radical species followed by the addition of the C=C bonds of MA or **1**. The molecular weight of the copolymers was relatively low during the initial stage of the polymerizations and progressively increased in the later stage (filled black circles in Figure 1B).

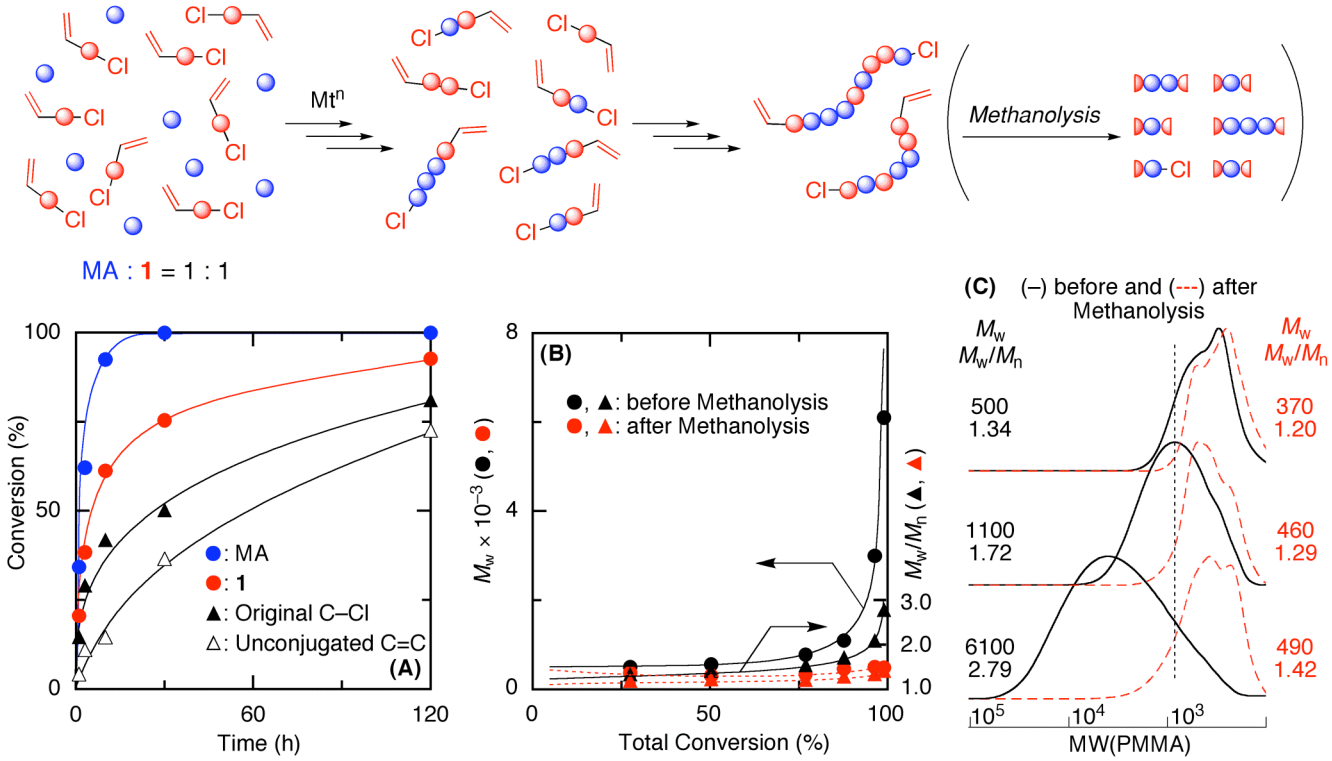

Figure 1. Simultaneous radical chain- and step-growth polymerization of MA and **1** with CuCl/HMTETA in toluene at 80 °C: $[MA]_0$ = 2.0 M; $[\mathbf{1}]_0$ = 2.0 M; $[CuCl]_0$ = 100 mM; $[HMTETA]_0$ = 100 mM. (A) Consumption of MA and **1** measured by gas chromatography and C–Cl and C=C bonds measured by ^{1}H NMR. (B) M_w and M_w/M_n values of the obtained copolymers vs total monomer conversion of MA and **1**. (C) Size-exclusion chromatograms of the obtained copolymers (solid lines) and the methanolyzed products (red dashed lines).

The size-exclusion chromatograms (SEC) of the obtained products drastically shifted to higher molecular weights especially in the later stage of the polymerization (bold black curves in Figure 1C), indicating contribution of the step-growth propagation to the product formation.[27]

As the author has already reported for the metal-catalyzed step-growth radical homopolymerization of **1** that one of the criteria for the ideal step-growth radical polymerization without side reactions is an equal consumption rate or equal remaining concentration of the active C–Cl and unconjugated C=C bonds during the polymerization.[27] Similarly, even for the ideal simultaneous polymerization of MA and **1**, the amount of the remaining unconjugated C=C bonds in the reaction mixture should be the same as the sum of the remaining original C–Cl bonds and another type of active C–Cl bonds formed via the MA addition. Thus the author further measured the concentration of the active C–Cl bonds derived from MA as well as those of the original C–Cl and unconjugated C=C bonds, which exist in the remaining monomer **1** or at the chain end of the reacted monomer **1** unit, by ^{1}H NMR analysis of the reaction mixture (Figure 2A). The methine proton of the active –CH–Cl (–MA–Cl) bond derived from MA can be distinguished from that of the original –CH–Cl of the **1** unit due to the different chemical shifts irrespective of very similar chemical structures (Figure 3). The concentrations of these C–Cl and unconjugated C=C groups were determined from the peak areas in comparison to the signals of toluene (solvent) as the internal standard, where their initial concentrations were set at 100%.

Along with a drastic decrease in the original C–Cl (open red triangles in Figure 2A) during the very early stage of the polymerization, the amount of the –MA–Cl abruptly increased (open blue triangles). This indicates that the radical species generated by the cleavage of the active C–Cl in **1** mainly added to the conjugated C=C double bond of MA to form the –MA–Cl terminal. Thus, radical addition to MA predominates in the very early stage. However, sooner or

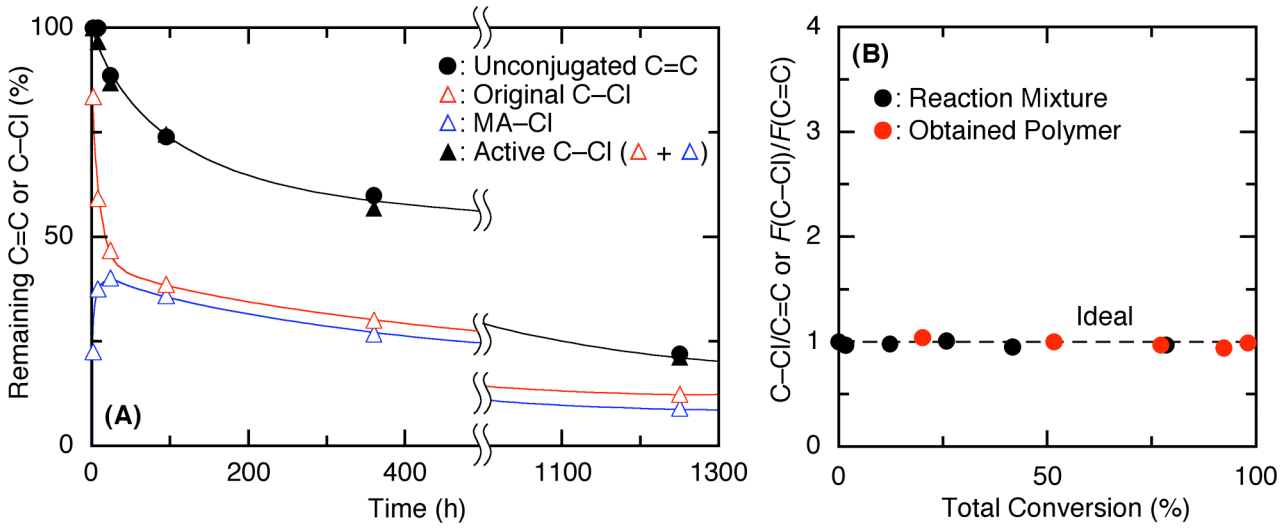

Figure 2. Simultaneous radical chain- and step-growth polymerization of MA and **1** with CuCl/HMTETA in toluene at 60 °C: $[MA]_0$ = 2.0 M; $[\mathbf{1}]_0$ = 2.0 M; $[CuCl]_0$ = 100 mM; $[HMTETA]_0$ = 100 mM. (A) Concentration of remaining unconjugated C=C, original C–Cl, MA–Cl, and sum of the active C–Cl (original C–Cl + MA–Cl) bonds in the reaction mixture measured by ^{1}H NMR. (B) Remaining C–Cl/C=C in the reaction mixture vs total conversion of active C–Cl and unconjugated C=C or *F*(C–Cl)/*F*(C=C) values of the obtained polymers after purification vs total monomer conversion of MA and **1**.

later, both concentrations of the original C–Cl and –MA–Cl simultaneously decreased at similar rates, suggesting that the reactivities of both C–Cl bonds are almost the same. Furthermore, the sum of the remaining concentrations of these active C–Cl bonds (filled black triangles) decreased at the same rate as that of the unconjugated C=C bonds (filled black circles). The ratios of the active C–Cl to the unconjugated C=C bonds (C–Cl/C=C) in the reaction mixture were plotted versus the total conversions of these functional groups (active C–Cl and unconjugated C=C) in Figure 2B (filled black circles) and proved nearly constant around 1.0, indicating the 1:1 reaction requirement for the ideal simultaneous radical polymerizations without side reactions.

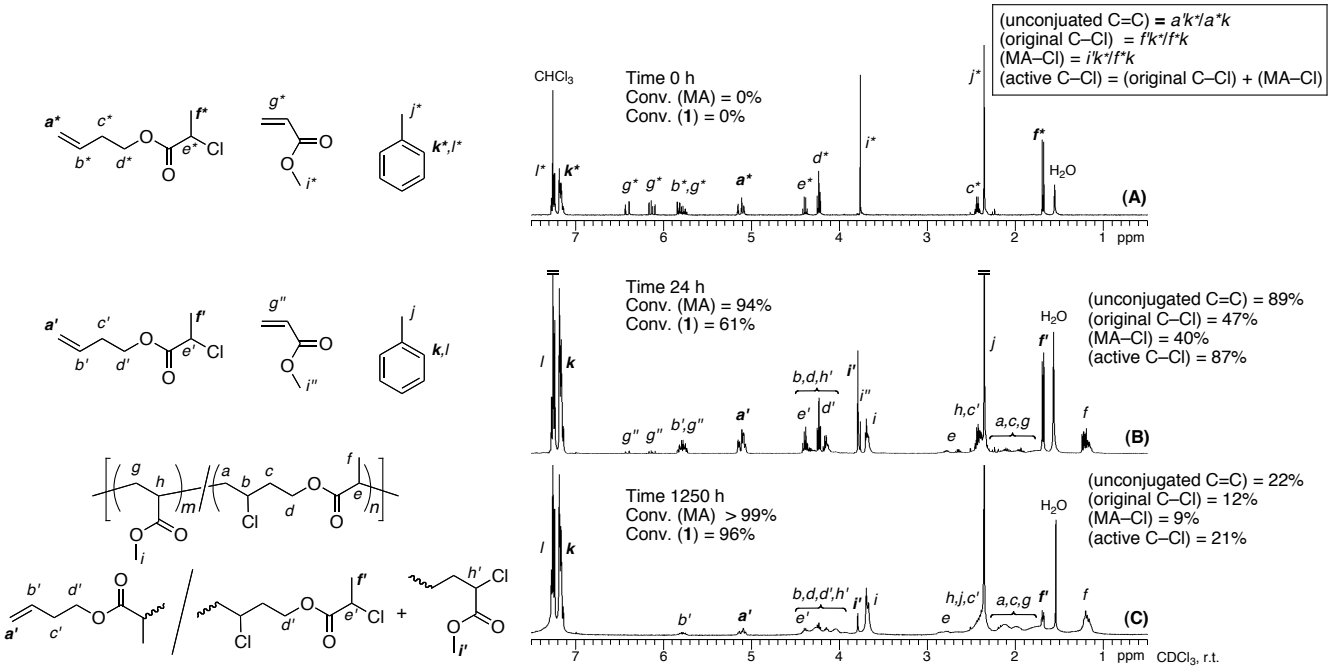

Figure 3. ^{1}H NMR spectra of the reaction mixture obtained with CuCl/HMTETA in toluene at 60 °C. (A) Before polymerization. (B) After polymerization for 24 h. (C) After polymerization for 1250 h.

The structure of the obtained copolymer was analyzed by ^{1}H and ^{13}C NMR after purification by preparative SEC to remove the residual monomers and catalysts. The ^{1}H and ^{13}C NMR spectra of the obtained products (Figures 4A and 4B, respectively) principally showed the combined signals of both the homopoly(MA) (Figures 4C and 4D) and homopoly(**1**) (Figures 4E and 4F).[27] However, the main-chain signals of each monomer unit (*b*, *d*, *e*, *f*, and *g* in ^{1}H NMR; *b*, *f*, and *g* in ^{13}C NMR) were relatively broad when compared to those of the homopolymers. This suggests that MA and **1** were randomly copolymerized via the chain- and step-growth mechanism, respectively. Furthermore, in the ^{1}H NMR spectrum of the products, almost the same amounts of the unconjugated C=C (*a'*) at the α-end and the active C–Cl (estimated from *i'* and *f'*) at the ω-end were observed [F(C–Cl)/F(C=C) = 0.99]. The number-average molecular weight (M_n) calculated

from the terminal to the main-chain protons [M_n(NMR) = 1500] was almost the same as that obtained by size-exclusion chromatography [M_n(SEC) = 1400].

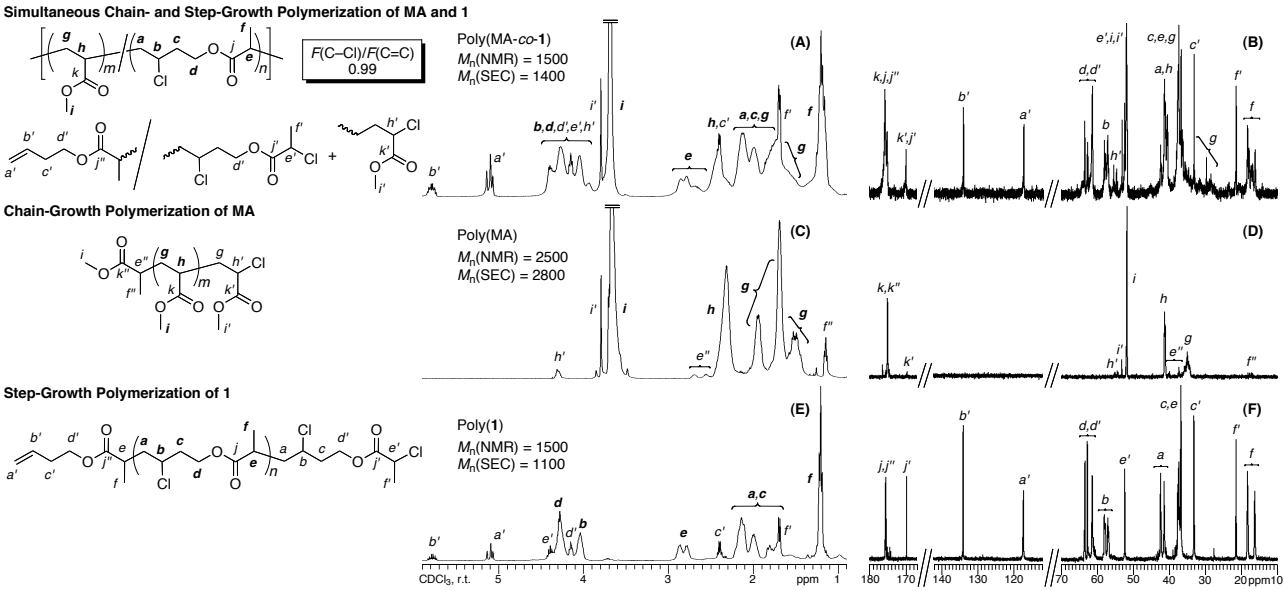

Figure 4. (A) ^{1}H and (B) ^{13}C NMR spectra of poly(MA-*co*-**1**) obtained with CuCl/HMTETA in toluene at 60 °C; (C) ^{1}H and (D) ^{13}C NMR spectra of poly(MA) obtained with RuCp*Cl$(PPh_3)_2$ in toluene at 80 °C; (E) ^{1}H and (F) ^{13}C NMR spectra of poly(**1**) obtained with $FeCl_2$/P*n*Bu_3 in toluene at 100 °C ($CDCl_3$, r.t.).

The ratios of the active C–Cl to the unconjugated C=C bonds at the polymer terminals for the copolymer samples obtained at different monomer conversions were also plotted versus the gas-chromatographic total monomer conversions in Figure 2B (filled red circles). The ratios were similarly close to unity during the entire course of the reactions. These results indicated that linear random copolymers of vinyl polymers [poly(MA)] and polyesters [poly(**1**)] without branching were obtained via almost ideal simultaneous metal-catalyzed chain- and step-growth polymerizations.

The sequence distribution of each monomer unit in the copolymers was analyzed by MALDI-TOF-MS. The polymers obtained at a 96% total monomer conversion showed a series of peaks, which were separated by the formula weights of each monomer unit (86.0 for MA and 162.0 for **1**) (Figure 5A). For example, a series of peaks of the 6-mers (m+n = 6; red circles) consist of the highest peak of 3-units of MA (m = 3) and the 3-units of **1** (n = 3) and lower populations of other combinations [(m,n) = (5,1), (4,2), (2,4), (1,5)], indicating that each monomer unit was randomly distributed in the main chains.

To further examine the random sequence, the copolymers obtained at various monomer conversions were methanolyzed by the cleavage of the main-chain ester linkage originating from **1** to generate the lower molecular weight oligomers as shown by the red dashed SEC curves in Figure 1C. All the molecular weights of the methanolyzed products were around 300–500 (Figure 1C and red filled circles in Figure 1B) and became slightly higher with the total monomer conversion, suggesting that the chain lengths of successive MA units sandwiched between the **1** units were nearly independent of the conversion.

The MALDI-TOF-MS spectrum of the methanolyzed products showed a series of low molecular weight oligomers of MA possessing the cleaved units (methyl propionate and 3-chlorobutyl alcohol units) of **1** at both terminals, in which the unimer and dimer (m = 1 and 2) of MA are predominant with lower amounts of higher mass oligomers (Figure 5B). A series of lower mass peaks (around 36) for each oligomer can be attributed to the loss of the pendent chlorine atom during the laser irradiation. These results indicate that the most probable number of the sequenced-MA units within the copolymers is around 1 to 2 and that MA sequences were randomly separated by the ester-linkages of **1** via the random copolymerizations. The random incorporation of **1** and MA units might seem strange when only considering the double-bond reactivity, which is

lower for the unconjugated C=C double bond of **1** than that of the conjugated counterpart of MA. However, it is a natural consequence because **1** is consumed faster as an initiator for the MA polymerization than as a monomer via activation of the C–Cl bond having a similar reactivity of the derived dormant MA terminal that results in short oligomers possessing the unconjugated C=C bond at the other terminal. The short oligomers can be copolymerized with the remaining MA or **1** or other oligomers to produce longer polymer chain, in which the two monomer units were randomly distributed.

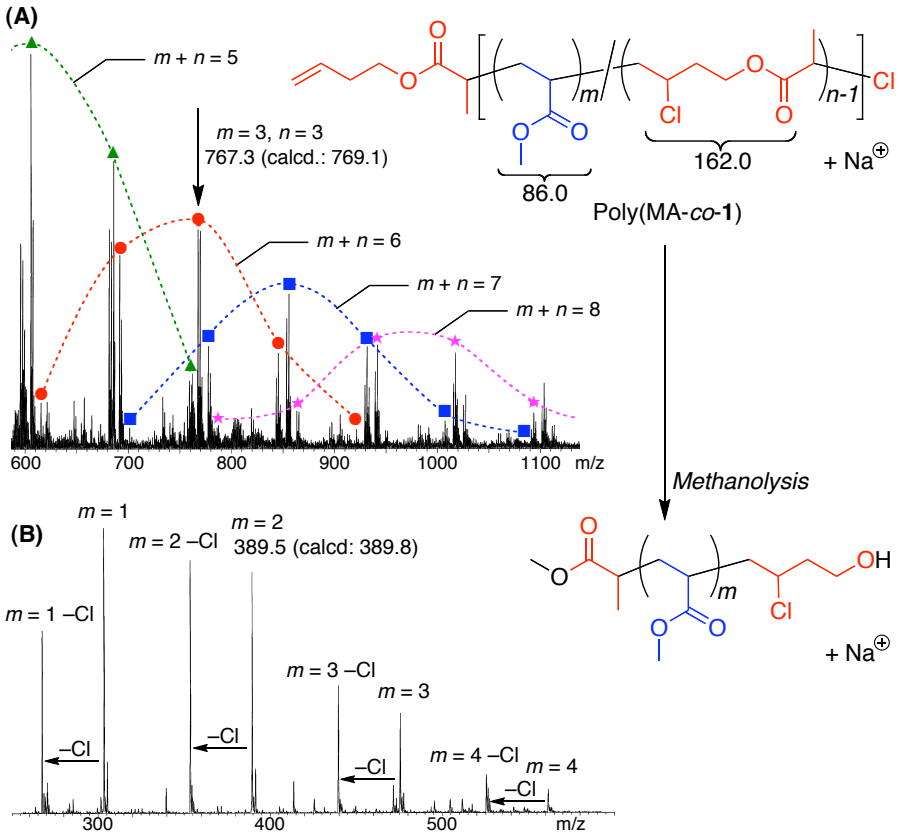

Figure 5. MALDI-TOF-MS spectra of (A) poly(MA-*co*-**1**) (M_n = 1200, M_w/M_n = 2.28) obtained with CuCl/HMTETA: $[MA]_0$ = 2.0 M; $[\mathbf{1}]_0$ = 2.0 M; $[CuCl]_0$ = 100 mM; $[HMTETA]_0$ = 100 mM in toluene at 80 °C and (B) the methanolyzed product (M_n = 340, M_w/M_n = 1.42).

The CuCl/HMTETA-catalyzed simultaneous chain- and step-growth polymerization is assumed to proceed by essentially the same secondary carbon-centered growing radical species adjacent to the carbonyl groups originating from MA or **1** as outlined in Scheme 1. The radical species is thus generated by the metal-catalyzed reversible activation of the reactive C–Cl bond adjacent to C=O and then adds to either of the C=C double bonds in MA or **1**. When the radical adds to MA (path A), the newly generated carbon radical species is similar to the original one and will generate a similarly active C–Cl bond adjacent to the carbonyl group via capping with the chlorine atom. The C–Cl bond can thus be activated again to induce chain-growth propagation. Meanwhile, the addition to **1** results in an unconjugated radical species (path B), which is then capped with chlorine to lead to the inactive C–Cl bond without adjacent carbonyl groups. In contrast, the C–Cl bond originating from the added **1** unit at the terminal can be activated to undergo step-growth propagation. The paths A and B give vinyl polymer and polyester structures, respectively, and thus the simultaneous copolymerizations lead to their random copolymers. The oligomers or polymers possessing the C=C terminals originating from **1** also react with the growing radical species via path B to induce a drastic molecular weight increase especially at the later stage of the polymerizations.

Although the results described above induced the almost ideal simultaneous radical polymerization under appropriate conditions, there are some possible side reactions, such as the bimolecular radical termination (path C) and chain-growth copolymerization of **1** with MA (path D) depending on the conditions. Before these possibilities with the CuCl/HMTETA system were examined in more detail by analyzing the model reactions (see the next section), other transition metal catalysts, which are effective for the living radical polymerization of acrylates, were used for

the copolymerization of MA and **1** at the 1:1 feed ratio under various conditions at different temperatures and with different catalyst concentrations.

All the catalytic systems we examined induced the simultaneous consumptions of MA and **1**, as summarized in Table 1 (entries 1–10) and Figures 6–9, while the activities, conversions, molecular weights, and composition ratios were dependent on the metals, ligands, and conditions. Among these, the $FeCl_2$/P*n*Bu_3 system (entry 8 and Figure 8) gave relatively high molecular weight polymers even at low monomer conversions, in which the consumption of MA was much faster than that of **1**, and resulted in decreased molecular weights with the increasing conversions. Furthermore, the content of the active C–Cl bond in the polymer was much higher than that of the C=C bond [F(C–Cl)/F(C=C) = 3.42] (entry 8 and Figure 10E). These results indicate that the chlorine-capping of the carbon radical species derived from **1** was not sufficiently fast using the iron catalyst. Thus, the radical species underwent the addition of MA before the Cl-capping to form the pendent active C–Cl groups originating from the unit **1** that was copolymerized not via the step- but via the chain-growth mechanism (path D in Scheme 1). A similar higher content of the active C–Cl bonds was obtained even with CuCl in the presence of different ligands, such as tris[2-(dimethylamino)ethyl]amine (Me_6TREN) [F(C–Cl)/F(C=C) = 1.95] (entry 5; Figures 6 and 10D) and *N*,*N*,*N'*,*N''*,*N''*-pentamethyldiethylenetriamine (PMDETA) [F(C–Cl)/F(C=C) = 1.43] (entry 6; Figures 7 and 10C), while the values were lower than that with $FeCl_2$/P*n*Bu_3. A higher oxidation metal species, such as $FeCl_3$ (entry 9) or $CuCl_2$ (entry 7), was also employed for the purpose of enhancing the capping reaction, but resulted in having almost no effect on lowering the F(C–Cl)/F(C=C) values. Even for the CuCl/HMTETA system, the F(C–Cl)/F(C=C) ratio slightly deviated from 1.0 upon increasing the temperature (entries 2 and 4). However, by lowering the metal-catalyst concentration, the value became close to unity even at the same temperature (entry 3).

Table 1. Metal-Catalyzed Simultaneous Chain- and Step-Growth Radical Polymerization of MA and **1**.

entry	metal catalyst[a]	[Monomer]$_0$, M		temp.,	time,	monomer conv., %[b]		M_w[c]	M_w/M_n[c]	MA/**1**[d]	F(C–Cl)/F(C=C)[d]
		MA	**1**	°C	h	MA	**1**				
1	CuCl/HMTETA	2.0	2.0	60	1250	>99	96	3300	2.17	49/51	0.99
2	CuCl/HMTETA	2.0	2.0	80	120	>99	93	3000	2.10	52/48	1.17
3	CuCl/HMTETA[g]	2.0	2.0	80	80	92	56	880	1.54	61/39	1.05
4	CuCl/HMTETA	2.0	2.0	100	25	>99	85	2100	2.26	56/44	1.43
5	CuCl/Me_6TREN	2.0	2.0	80	24	>99	50	1800	1.94	58/42	1.95
6	CuCl/PMDETA	2.0	2.0	80	600	>99	86	2100	1.99	56/44	1.43
7	CuCl/$CuCl_2$/PMDETA[e]	2.0	2.0	80	30	84	46	870	1.60	64/36	1.47
8	$FeCl_2$/PnBu$_3$	2.0	2.0	80	24	52	13	11000	2.67	81/19	3.42
9	$FeCl_3$/PnBu$_3$	2.0	2.0	80	30	69	14	9600	3.23	81/19	3.52
10	RuCp*Cl$(PPh_3)_2$[f]	2.0	2.0	80	1800	84	51	810	1.47	57/43	1.05
11	CuCl/HMTETA	3.0	1.0	80	30	98	87	1600	1.64	76/24	1.06
12	CuCl/HMTETA	3.5	0.5	80	30	95	95	2400	1.82	87/13	1.04
13	CuCl/HMTETA	3.8	0.2	80	200	>99	>99	5100	1.70	94/6	0.95
14	CuCl/HMTETA	3.9	0.1	80	100	91	>99	7100	1.60	97/3	1.06
15	CuCl/HMTETA	4.0	0.04	80	80	79	>99	10900	1.38	99/1	0.95
16	CuCl/HMTETA	10.0	0.1	80	10	97	>99	20700	1.68	99/1	1.05
17	RuCp*Cl$(PPh_3)_2$[f]	3.0	1.0	80	600	96	87	1500	1.82	79/21	1.01
18	RuCp*Cl$(PPh_3)_2$[f]	3.5	0.5	80	120	98	96	3000	1.81	85/15	0.93
19	RuCp*Cl$(PPh_3)_2$[f]	3.9	0.1	80	80	84	>99	6100	1.47	96/4	1.01
20	RuCp*Cl$(PPh_3)_2$[f]	4.0	0.04	80	200	98	>99	18200	1.86	99/1	1.09
21	RuCp*Cl$(PPh_3)_2$[f]	6.0	0.06	80	360	>99	>99	35700	2.01	99/1	1.05

[a][CuCl]$_0$ = 100 mM, [$FeCl_2$]$_0$ = 20 mM, [$FeCl_3$]$_0$ = 20 mM, [RuCp*Cl$(PPh_3)_2$]$_0$ = 4.0 mM, [1,1,4,7,10,10-hexamethyltriethylenetetramine (HMTETA)]$_0$ = 100 mM, [tris[2-(dimethylamino)ethyl]amine (Me_6TREN)]$_0$ = 100 mM, [*N*,*N*,*N*′,*N*″,*N*‴-pentamethyldiethylenetriamine (PMDETA)]$_0$ = 100 mM, [tri-*n*-butylphosphine (PnBu$_3$)]$_0$ = 40 mM, in toluene. [b]Determined by gas chromatography. [c]The weight-average molecular weight (M_w) and distribution (M_w/M_n) were determined by size-exclusion chromatography. [d]Determined by ^{1}H NMR. [e][CuCl]$_0$ = 50 mM, [$CuCl_2$]$_0$ = 50 mM. [f][nBu$_3$N]$_0$ = 40 mM. [g][CuCl]$_0$ = 20 mM, [HMTETA]$_0$ = 20 mM

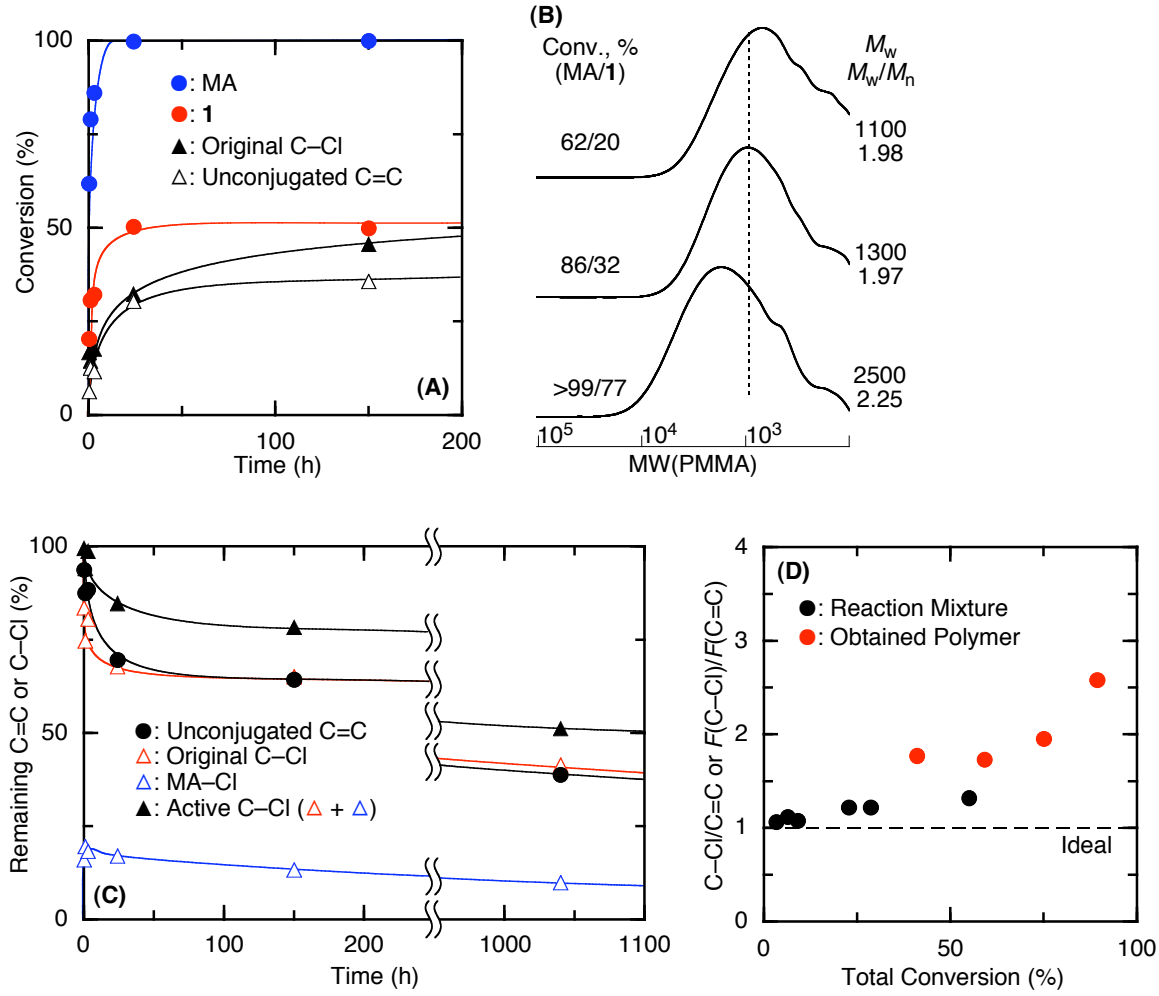

Figure 6. Simultaneous radical chain- and step-growth polymerization of MA and **1** with CuCl/Me_6TREN in toluene at 80 °C: $[MA]_0$ = 2.0 M; $[\mathbf{1}]_0$ = 2.0 M; $[CuCl]_0$ = 100 mM; $[Me_6TREN]_0$ = 100 mM. (A) Consumption of MA and **1** measured by gas chromatography and C–Cl and C=C bonds measured by ^{1}H NMR. (B) Size-exclusion chromatograms of the obtained copolymers. (C) Concentration of unconjugated C=C, original C–Cl, MA–Cl, and active C–Cl (original C–Cl + MA–Cl) bonds measured by ^{1}H NMR. (D) Remaining C–Cl/C=C in the reaction mixture vs total conversion of active C–Cl and unconjugated C=C or *F*(C–Cl)/*F*(C=C) values of the obtained polymers after purification vs total monomer conversion of MA and **1**.

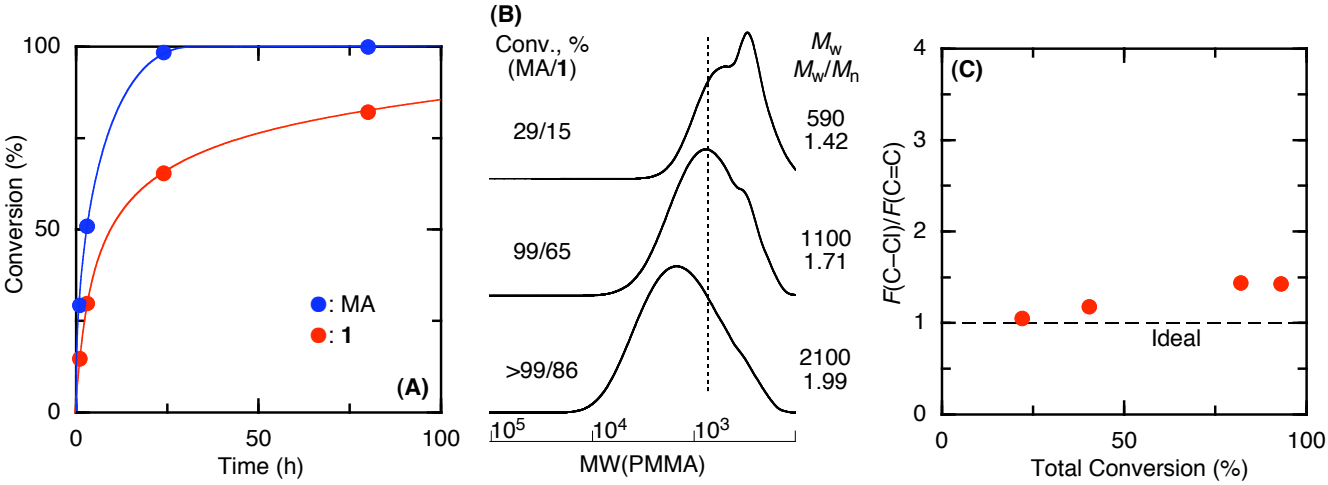

Figure 7 Simultaneous radical chain- and step-growth polymerization of MA and **1** with CuCl/PMDETA in toluene at 80 °C: $[MA]_0$ = 2.0 M; $[\mathbf{1}]_0$ = 2.0 M; $[CuCl]_0$ = 100 mM; $[PMDETA]_0$ = 100 mM. (A) Consumption of MA and **1** measured by gas chromatography. (B) Size-exclusion chromatograms of the obtained copolymers. (C) *F*(C–Cl)/*F*(C=C) values of the obtained polymers after purification vs total monomer conversion of MA and **1**.

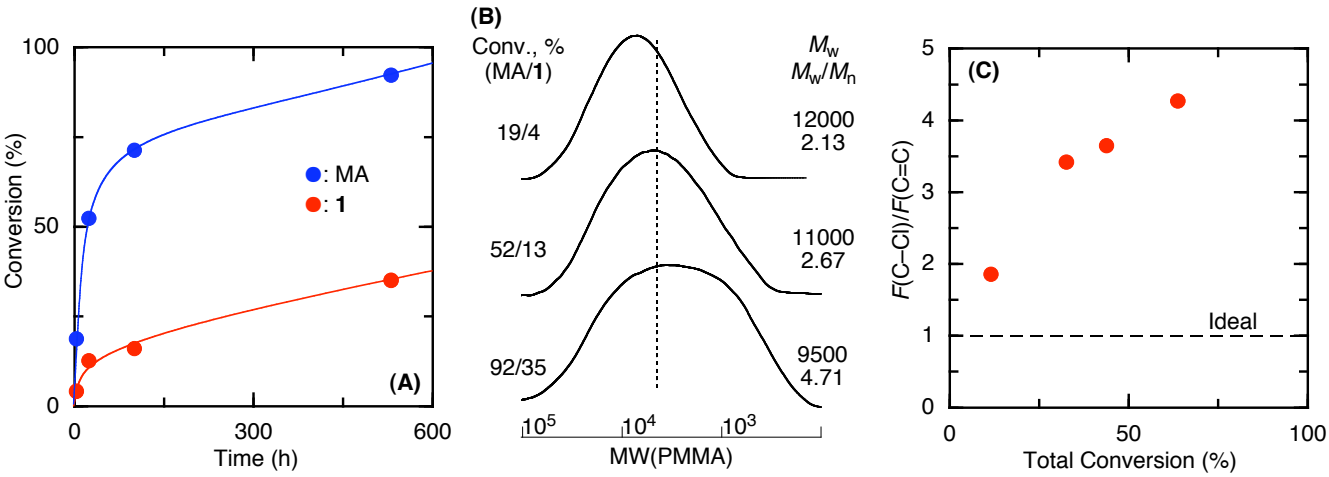

Figure 8. Simultaneous radical chain- and step-growth polymerization of MA and **1** with $FeCl_2$/P*n*Bu_3 in toluene at 80 °C: $[MA]_0$ = 2.0 M; $[\mathbf{1}]_0$ = 2.0 M; $[FeCl_2]_0$ = 20 mM; $[PnBu_3]_0$ = 40 mM. (A) Consumption of MA and **1** measured by gas chromatography. (B) Size-exclusion chromatograms of the obtained copolymers of MA and **1**. (C) *F*(C–Cl)/*F*(C=C) values of the obtained polymers after purification vs total monomer conversion of MA and **1**.

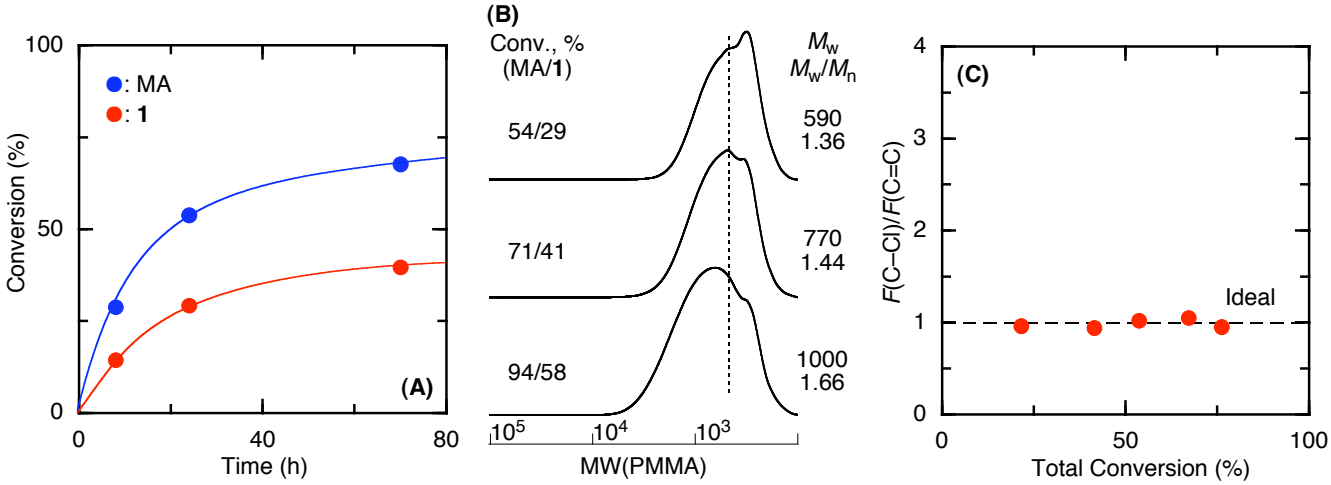

Figure 9. Simultaneous radical chain- and step-growth polymerization of MA and **1** in toluene at 80 °C with $RuCp^*Cl(PPh_3)_2$: $[MA]_0$ = 2.0 M; $[\mathbf{1}]_0$ = 2.0 M; $[RuCp^*Cl(PPh_3)_2]_0$ = 4.0 mM; $[n Bu_3N]_0$ = 40 mM. (A) Consumption of MA and **1** measured by gas chromatography. (B) Size-exclusion chromatograms of the obtained copolymers of MA and **1**. (C) *F*(C–Cl)/*F*(C=C) values of the obtained polymers after purification vs total monomer conversion of MA and **1**.

Another good metal catalyst candidate proved to be $RuCp^*Cl(PPh_3)_2$, which gave an almost equal content of the remaining active C–Cl and unconjugated C=C bonds in the copolymer (entry 10; Figure 10B), although the reaction was very slow to produce lower molecular weight oligomers (Figure 9). The author should now note how the *F*(C–Cl)/*F*(C=C) values reflect the obtained copolymer structures. For example, *F*(C–Cl)/*F*(C=C) = 1.10 means that 90% of the obtained copolymers are linear without any pendent or branching active C–Cl bonds and that the remaining 10% are copolymers with only one pendent C–Cl unit in the polymer chain on average. As another example, *F*(C–Cl)/*F*(C=C) = 2.0 means that the copolymers have one pendent or branching structure per chain on average. Therefore, most of the copolymers obtained using copper and ruthenium catalysts have nearly linear structures without significant branching.

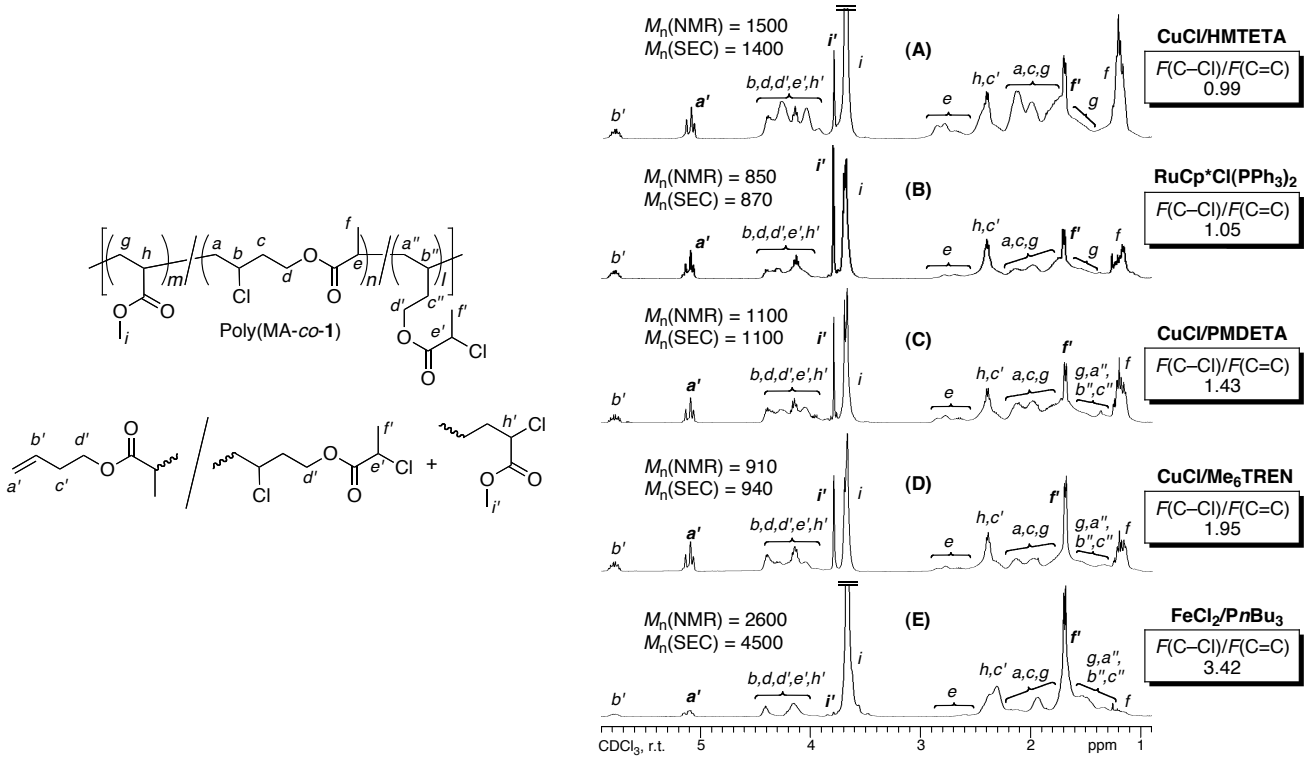

Figure 10. ^{1}H NMR spectra of poly(MA-*co*-**1**) obtained with (A) CuCl/HMTETA, (B) RuCp*Cl(PPh_3)$_2$, (C) CuCl/PMDETA, (D) CuCl/Me_6TREN, and (E) $FeCl_2$/P*n*Bu_3 after purification.

Thus, the choice of the catalyst as well as the reaction conditions is important for the ideal metal-catalyzed chain- and step-growth radical polymerizations so that the catalyst should induce a fast halogen capping for generating polyester structures from **1** as well as fast polymerization for giving higher molecular weight products. Among the various catalysts we investigated, the CuCl/HMTETA system proved most effective in giving the linear copolymers via almost ideal simultaneous chain- and step-growth radical polymerizations under the appropriate conditions (entries 1 and 3).

2. Model Reactions for Detailed Analysis of Simultaneous Radical Polymerization.

(a) Model Reaction for Estimating the Possible Bimolecular Radical Reactions (path C). To

reveal the effects of possible side reactions, especially the bimolecular termination between the radical species, the author first investigated the metal-catalyzed Kharasch radical addition or ATRA between methyl 2-chlroropropionate (**2**) and 3-butenyl acetate (**3**), which can be regarded as model compounds of the active C–Cl and unconjugated C=C bonds of **1**, respectively, by using various metal catalysts (Scheme 2).[27]

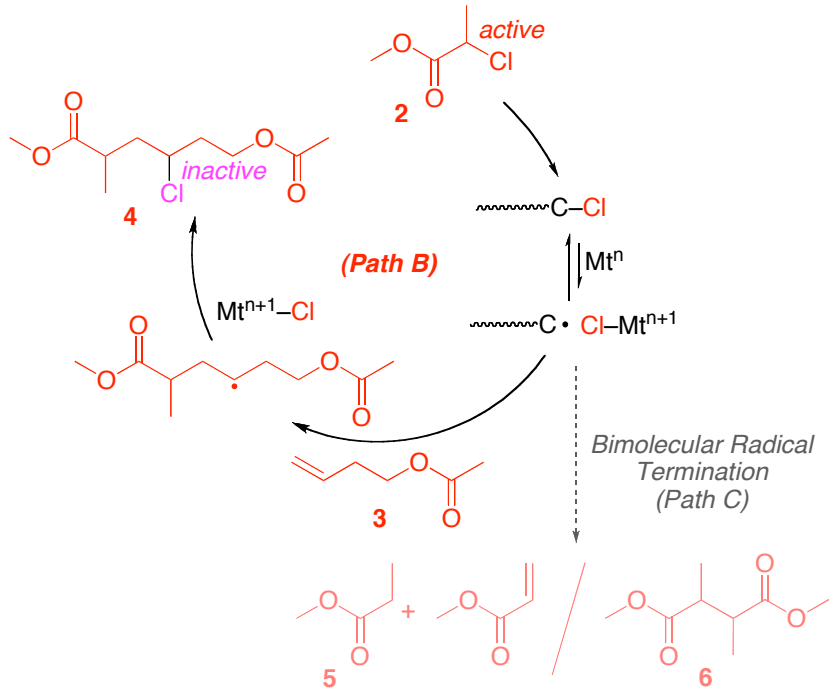

Scheme 2. Model Reaction between **2** (C–Cl Bond of **1**) and **3** (C=C Bond of **1**) in the Absence of MA.

Figure 11A shows the conversions of the chloride (**2**) and vinyl (**3**) compounds (filled red circles and triangles, respectively) in the CuCl/HMTETA-catalyzed radical addition at 80 °C. Both model compounds were simultaneously consumed at the same rate to almost quantitatively produce the adduct (**4**). Furthermore, the consumption rates were almost the same as those of the active C–Cl (open black circles) and the unconjugated C=C (open black triangles) for the

polymerization under the same conditions (cf. Figure 1A), suggesting a good model reaction for the simultaneous polymerization.

The ^{1}H NMR analysis of the reaction mixture also revealed that the yield of the adduct (**4**) was almost the same for the conversion of **2** or **3** and that more than 99% of the reacted **2** and **3** were thus converted into **4** without any significant formation of byproducts (entry 1 in Table 2). A further detailed gas-chromatographic analysis of the reaction mixture showed the minimal formation (1%) of methyl propionate (**5**), which formed via disproportionation of the radical species

Table 2. Model Reaction between **2** and **3** with Various Metal Catalysts[a]

entry	catalyst[b]	time, h	conv., %[c]		**4**, %[d]	**5**, %[e]	**6**, %[f]
			2	**3**			
1	CuCl/HMTETA	580	84	83	84 (>99)	1	n.d.[g]
2	CuCl/PMDETA	600	95	84	84 (>99)	5	n.d.[g]
3	CuCl/Me_6TREN	300	73	75	70 (93)	2	<1
4	RuCp*Cl(PPh_3)$_2$	35	42	43	28 (66)	4	n.d.[g]
5	$FeCl_2$/P*n*Bu_3	70	88	86	87 (>99)	2	<1

[a][**2**]$_0$ = 2.0 M; [**3**]$_0$ = 2.0 M; [b][metal catalyst]$_0$ = 100 mM; [HMTETA]$_0$ = 100 mM; [PMDETA]$_0$ = 400 mM; [Me_6TREN]$_0$ = 100 mM; [P*n*Bu_3]$_0$ = 200 mM; in toluene at 80 °C (for HMTETA and Me_6TREN), 100 °C (for Ru and Fe), or 60 °C (for PMDETA). [c]Determined by ^{1}H NMR. [d]The 1:1 adduct (**4,** see Scheme 2 for structure) yield was determined by ^{1}H NMR. The values in parentheses indicate the yields based on the consumption of **3**. [e]The content of methyl propionate (**5**) was determined by gas chromatography. [f]The content of dimethyl 2,3-dimethylsuccinate (**6**) was determined by gas chromatography. [g]Not being detected.

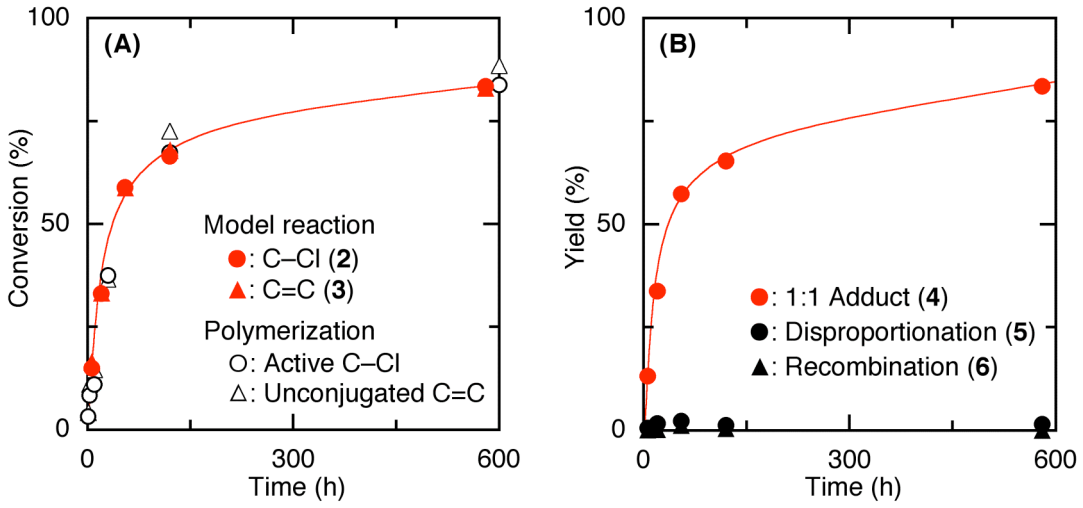

Figure 11. Model reaction of **2** and **3** with CuCl/HMTETA in the absence of MA in toluene at 80 °C: $[\mathbf{2}]_0$ = 2.0 M; $[\mathbf{3}]_0$ = 2.0 M; $[CuCl]_0$ = 100 mM; $[HMTETA]_0$ = 100 mM. (A) Consumption of **2** and **3** (solid lines) in the model reaction and active C–Cl and unconjugated C=C bonds in the polymerization of MA and **1** measured by ^{1}H NMR. (B) Yield of **4** measured by ^{1}H NMR and **5** and **6** measured by gas chromatography.

derived from **2**, and no coupling product [dimethyl 2,3-dimethyl succinate (**6**)] of the radical (Figure 11B and entry 1 in Table 2). In addition, the product obtained after purification by column chromatography followed by evaporation of the volatile compounds (**2**, **3**, **5**, and toluene) proved exclusively to be the adduct (**4**) without contamination by any byproducts, which might be formed via a bimolecular radical termination originating from the adduct radical. These results indicate that CuCl/HMTETA induced an almost ideal radical addition between **2** and **3** to give **4**. Similar results were obtained with CuCl/Me_6TREN or reported[27] with CuCl/PMDETA, RuCp*Cl$(PPh_3)_2$, and $FeCl_2$/P*n*Bu_3, in which a high yield of the adduct was attained without significant bimolecular radical termination, while the contents slightly depended on the catalytic systems (Table 2).

(b) Model Reactions for Estimating the Possible Chain-Growth Radical Copolymerization of 1 with MA (path D). To estimate the contribution of the possible chain-growth radical copolymerization of **1** with MA affording the pendent active C–Cl bonds in the copolymer chains, the author investigated the radical addition and/or possible polymerization of **3**, a model of the unconjugated C=C bond of **1**, and MA with **2**, a model of the active C–Cl bond of **1**, under the equimolar concentration ($[\mathbf{2}]_0 = [\mathbf{3}]_0 = [\mathrm{MA}]_0 = 2.0$ M) by using various catalysts in a way similar to the simultaneous polymerization. Under the conditions that **1** will undergo an ideal step-growth propagation during the simultaneous polymerization, the model compound, **3**, with the unconjugated C=C double bond, but without the active C–Cl bond, should not be incorporated into the main chain, but should be located at the chain end.

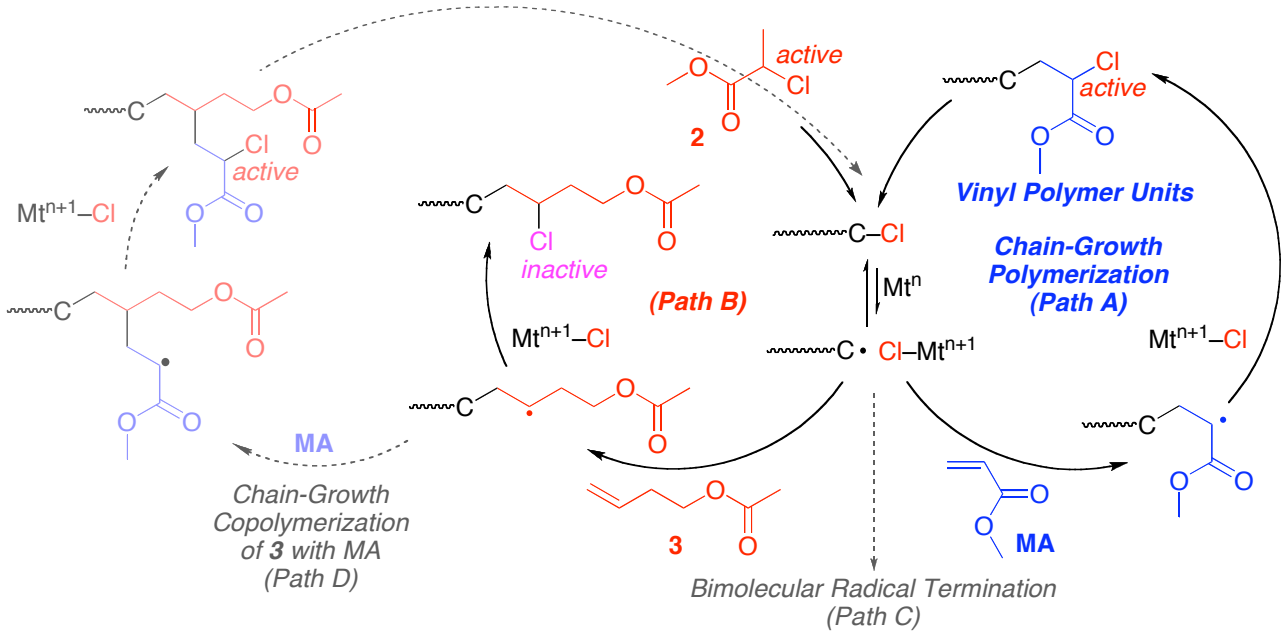

Scheme 3. Model Reaction between **2** (C–Cl Bond of **1**) and **3** (C=C Bond of **1**) in the Presence of MA.

Figure 12A shows the consumptions of MA (filled blue circles), **2** (filled red circles), and **3** (filled red triangles) in the model reaction with CuCl/HMTETA at 80 °C. The consumption rates of MA, **2**, and **3** for the model reaction indicated by the three solid curves were in good agreement with those of MA, the original C–Cl, and the unconjugated C=C bonds, respectively, for the simultaneous polymerization indicated by the three dashed curves. This also shows a good model reaction for the simultaneous polymerization.

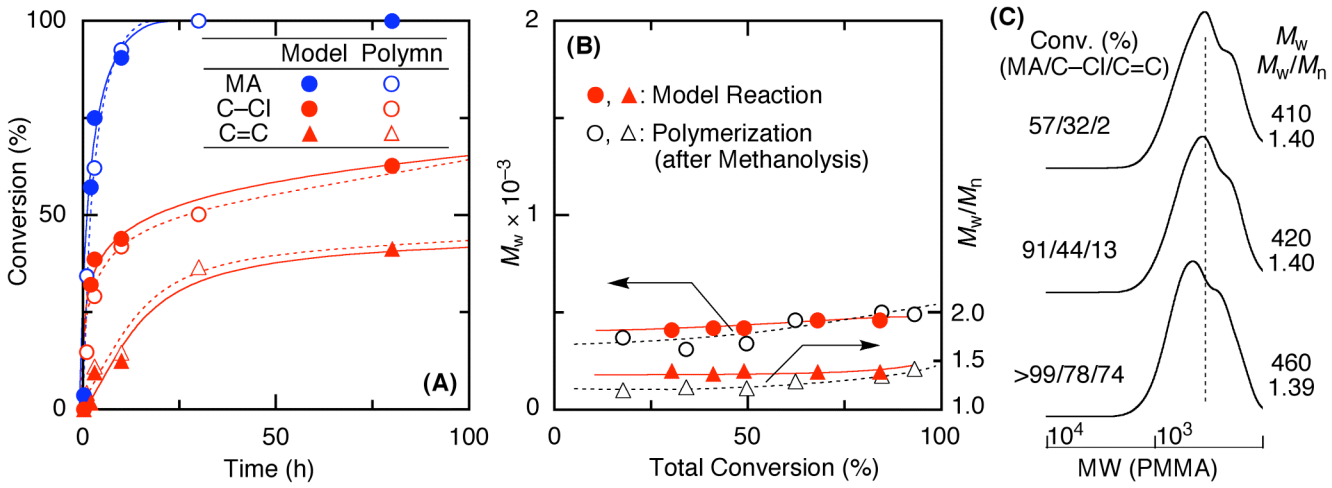

Figure 12. Model reaction of **2** and **3** with CuCl/HMTETA in the presence of MA in toluene at 80 °C: $[\mathbf{2}]_0$ = 2.0 M; $[\mathbf{3}]_0$ = 2.0 M; $[MA]_0$ = 2.0 M; $[CuCl]_0$ = 100 mM; $[HMTETA]_0$ = 100 mM. (A) Consumption of MA, **2**, and **3** (solid lines) in the model reaction and MA, original C–Cl, and unconjugated C=C bonds in the polymerization of MA and **1** (dotted lines) measured by ^{1}H NMR. (B) M_w and M_w/M_n values of the obtained oligomers in the model reaction vs total conversion of MA, **2**, and **3** (solid lines) and the methanolyzed products of the copolymers obtained in the polymerization of MA and **1** (dotted lines). (C) Size-exclusion chromatograms of the obtained oligomers in the model reaction.

The molecular weights of the obtained products were low (M_w ~ 400) and increased very slightly with the total conversion of these compounds (filled circles in Figure 12B). The molecular weights, molecular weight distributions (filled triangles), and SEC curves (Figure 12C) were quite similar to those of the products obtained by methanolysis of the copolymers in the simultaneous polymerization (open circles and triangles in Figure 12B; cf. Figures 1B and 1C). These results suggest that the model reaction induced oligomerization of MA via activation of the C–Cl bond of **2** with CuCl/HMTETA and the chain-propagation was irreversibly terminated sooner or later by the addition of the C=C bond of **3**.

Other metal catalysts, such as CuCl/Me_6TREN, CuCl/PMDETA, and RuCp*Cl(PPh_3)$_2$, induced the simultaneous consumption, in which the rates were dependent on the catalysts and principally resulted in similar oligomers in terms of what can be observed in the SEC analysis while the molecular weights were slightly higher than that with CuCl/HMTETA (Figures 13, 14, and 16). In contrast, the $FeCl_2$/P*n*Bu_3 system induced a much faster MA consumption than **2** and **3** to afford high molecular weight polymers (Figure 15) in a similar manner to the copolymerization of MA and **1** (Figure 8). Furthermore, the C=C model compound (**3**) was consumed faster than the C–Cl counterpart (**2**), suggesting that chain-growth copolymerization of **3** might occur in the $FeCl_2$/P*n*Bu_3 system.

The structures of the products obtained in the 1:1:1 model reactions of **2**, **3**, and MA with various metal catalysts were analyzed by ^{1}H NMR and MALDI-TOF-MS. The product obtained with CuCl/HMTETA (Figure 17B) showed several similar signals to those (*1*, *2*, *a–f* in Figure 17A) of the 1:1 adduct (**4**) of **2** and **3**. In addition to these, signals originating from the MA units (*g*, *h*, *i*, *h'*, and *i'*) were observed. These results suggests that the following consecutive reactions occurred: The radical addition or polymerization of MA was first initiated from **2** (α-end), and

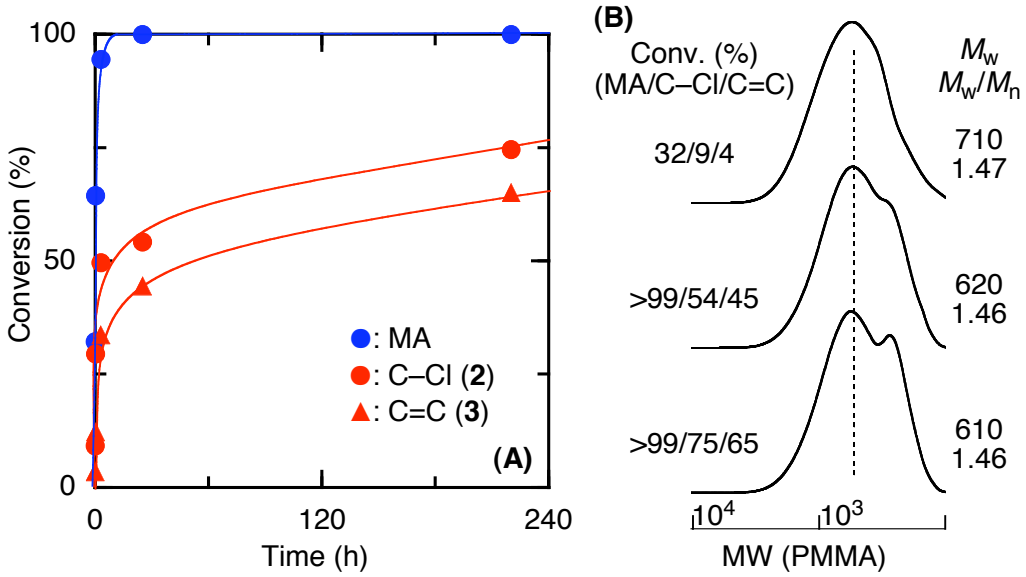

Figure 13. Model reaction of **2** and **3** with CuCl/Me_6TREN in the presence of MA in toluene at 80 °C: $[MA]_0$ = 2.0 M; $[\mathbf{2}]_0$ = 2.0 M; $[\mathbf{3}]_0$ = 2.0 M; $[CuCl]_0$ = 100 mM; $[Me_6TREN]_0$ = 100 mM. (A) Consumption of MA, **2**, and **3** measured by ^{1}H NMR. (B) Size-exclusion chromatograms of the obtained oligomers.

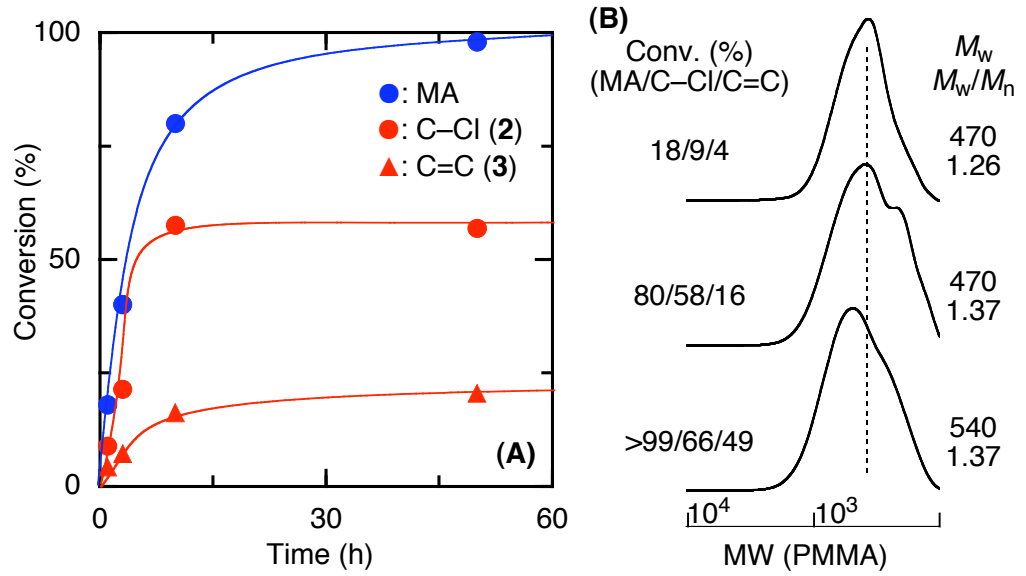

Figure 14. Model reaction of **2** and **3** with CuCl/PMDETA in the presence of MA in toluene at 80 °C: $[MA]_0$ = 2.0 M; $[\mathbf{2}]_0$ = 2.0 M; $[\mathbf{3}]_0$ = 2.0 M; $[CuCl]_0$ = 100 mM; $[PMDETA]_0$ = 100 mM. (A) Consumption of MA, **2**, and **3** measured by ^{1}H NMR. (B) Size-exclusion chromatograms of the obtained oligomers.

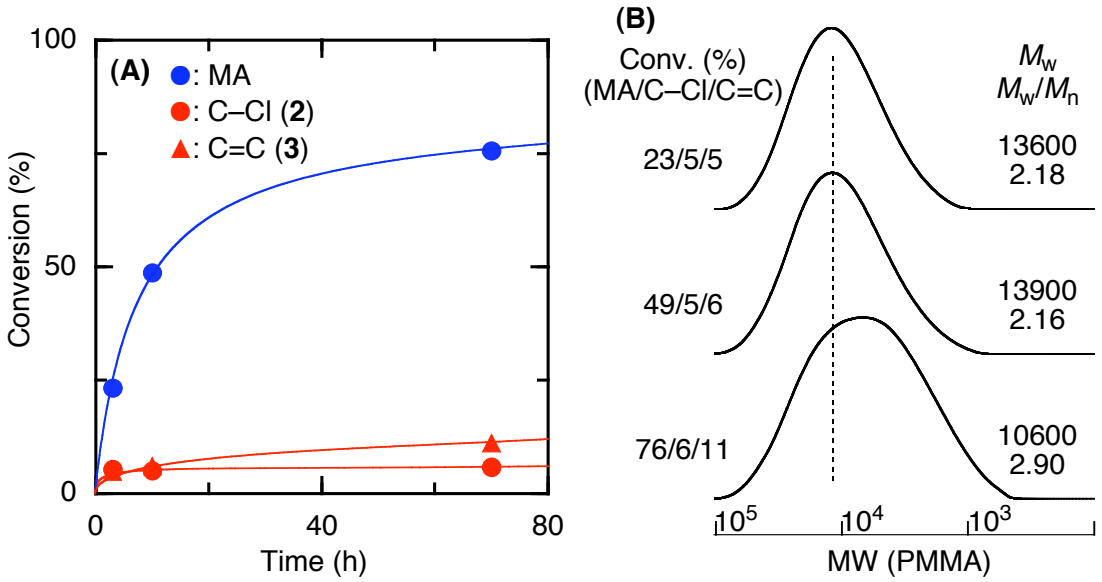

Figure 15. Model reaction of **2** and **3** with $FeCl_2/PnBu_3$ in the presence of MA in toluene at 80 °C: $[MA]_0$ = 2.0 M; $[\mathbf{2}]_0$ = 2.0 M; $[\mathbf{3}]_0$ = 2.0 M; $[FeCl_2]_0$ = 20 mM; $[PnBu_3]_0$ = 40 mM. (A) Consumption of MA, **2**, and **3** measured by ^{1}H NMR. (B) Size-exclusion chromatograms of the obtained oligomers.

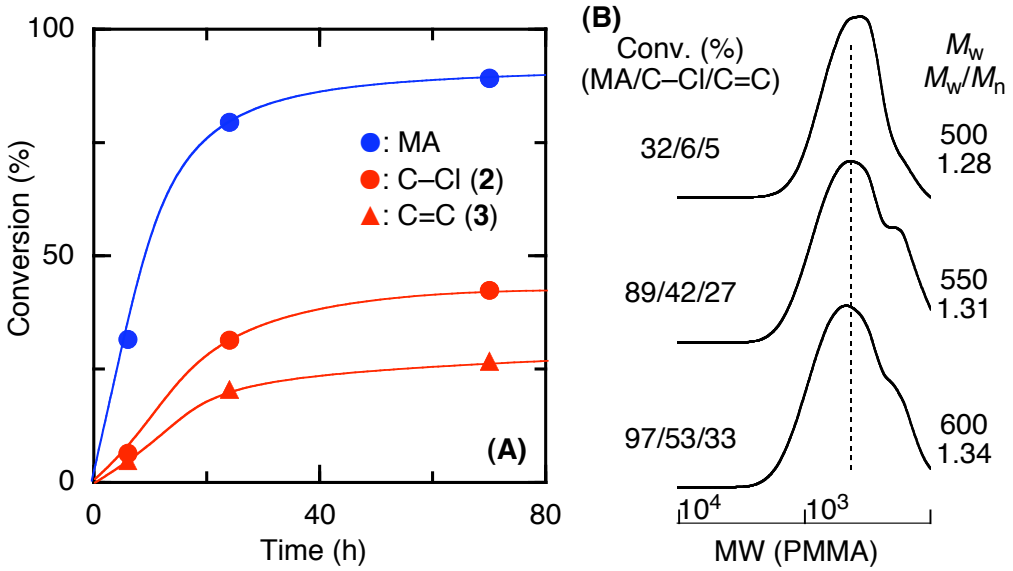

Figure 16. Model reaction of **2** and **3** with $RuCp^*Cl(PPh_3)_2$ in the presence of MA in toluene at 80 °C: $[MA]_0$ = 2.0 M; $[\mathbf{2}]_0$ = 2.0 M; $[\mathbf{3}]_0$ = 2.0 M; $[RuCp^*Cl(PPh_3)_2]_0$ = 4.0 mM; $[nBu_3N]_0$ = 40 mM. (A) Consumption of MA, **2**, and **3** measured by ^{1}H NMR. (B) Size-exclusion chromatograms of the obtained oligomers.

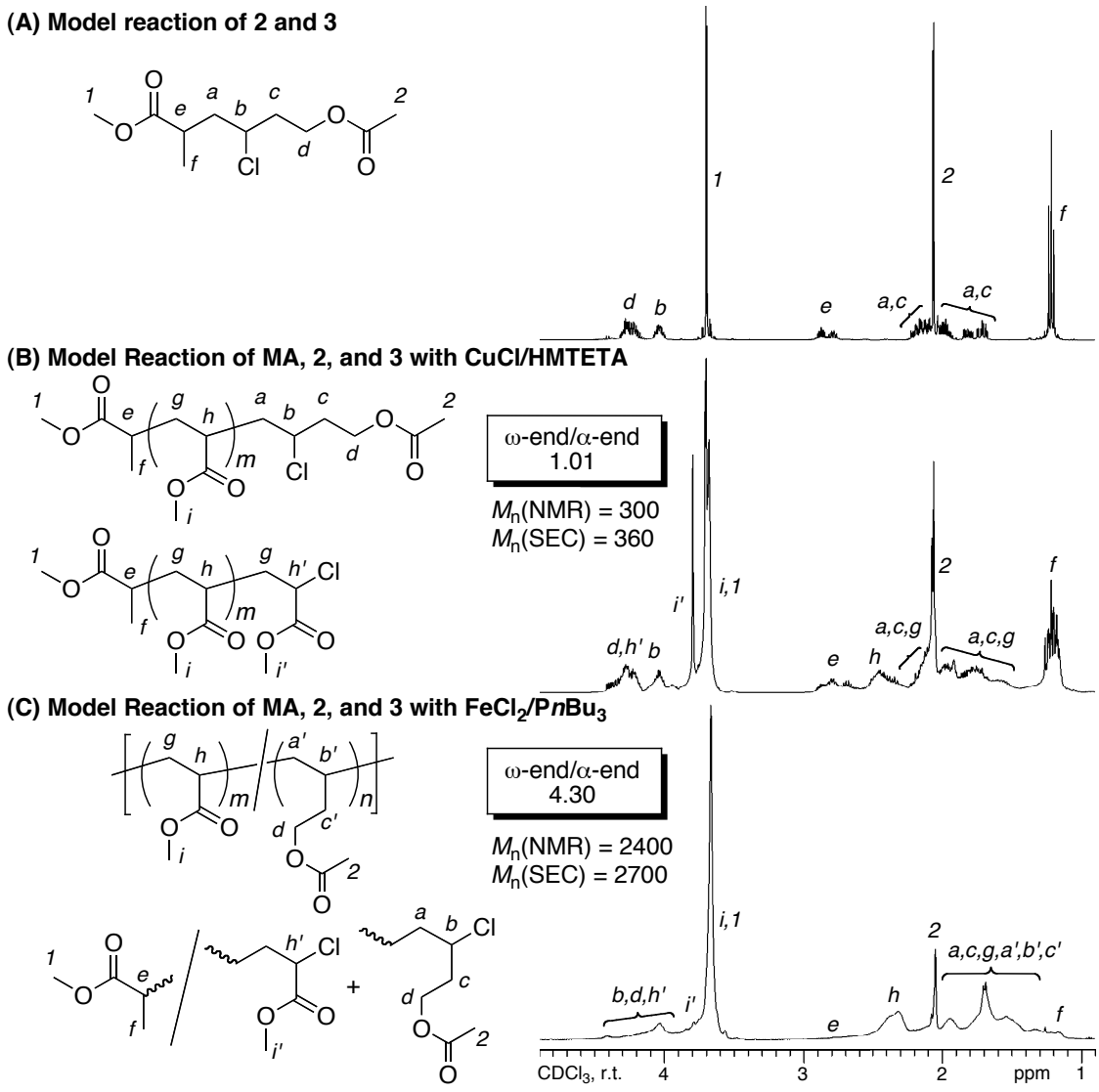

Figure 17. ^{1}H NMR spectra of (A) **4** and the oligomer obtained in the model reaction of **2**, **3**, and MA with (B) CuCl/HMTETA and (C) $FeCl_2$/P*n*Bu_3 in toluene at 80 °C ($CDCl_3$, r.t.).

some of the radical species were capped with **3** resulting in the inactive C–Cl terminal at the ω-end, while a part of the ω-ends was not capped with **3** and was still the active C–Cl terminal originating from MA. More importantly, **3** was not incorporated in the main chain, but located at the chain end, which was indicated by the fact that the ratio of the ω-end groups; i.e., sum of the acetyl signal (*2*) of **3** and the MA terminal (*i'*), to the α-end; i.e., the methyl group (*f*) of **2**, was close to unity (ω-end/α-end = 1.01). These results indicated that the chain-growth cross-propagation of the

radical species derived from **3** to MA is negligible with CuCl/HMTETA under the appropriate conditions. A similar result was also obtained with $RuCp^*Cl(PPh_3)_2$ (ω-end/α-end = 1.00; Figure 20).

On the other hand, $FeCl_2/PnBu_3$ gave a higher content of ω-ends than α-ends (ω-end/α-end = 4.30; Figure 17C), indicating that the chain-growth radical copolymerization of **3** with MA occurred to give the pendent acetyl moieties originating from **3** in the copolymers. A similar higher content of the ω-ends was observed with CuCl/PMDETA (ω-end/α-end = 1.27; Figure 20B) and CuCl/Me_6TREN (ω-end/α-end = 1.32; Figure 20C) while these values were lower than that with $FeCl_2/PnBu_3$. All these ω-end/α-end values in the model reactions were similar to

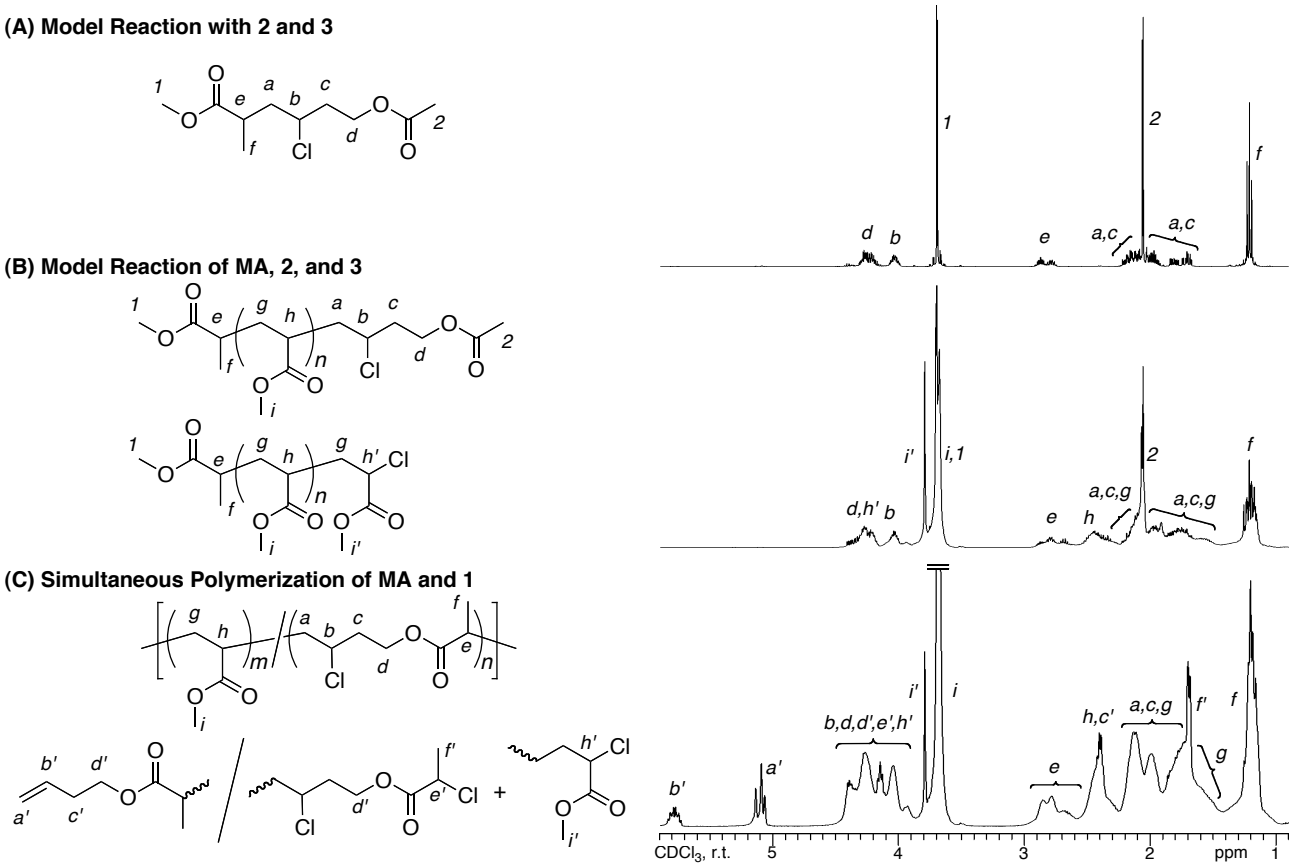

Figure 18. ^{1}H NMR spectra of (A) the adduct (**4**), (B) the oligomer obtained in the model reaction of **2**, **3**, and MA, and (C) the copolymer of MA and **1** obtained with CuCl/HMTETA ($CDCl_3$, r.t.).

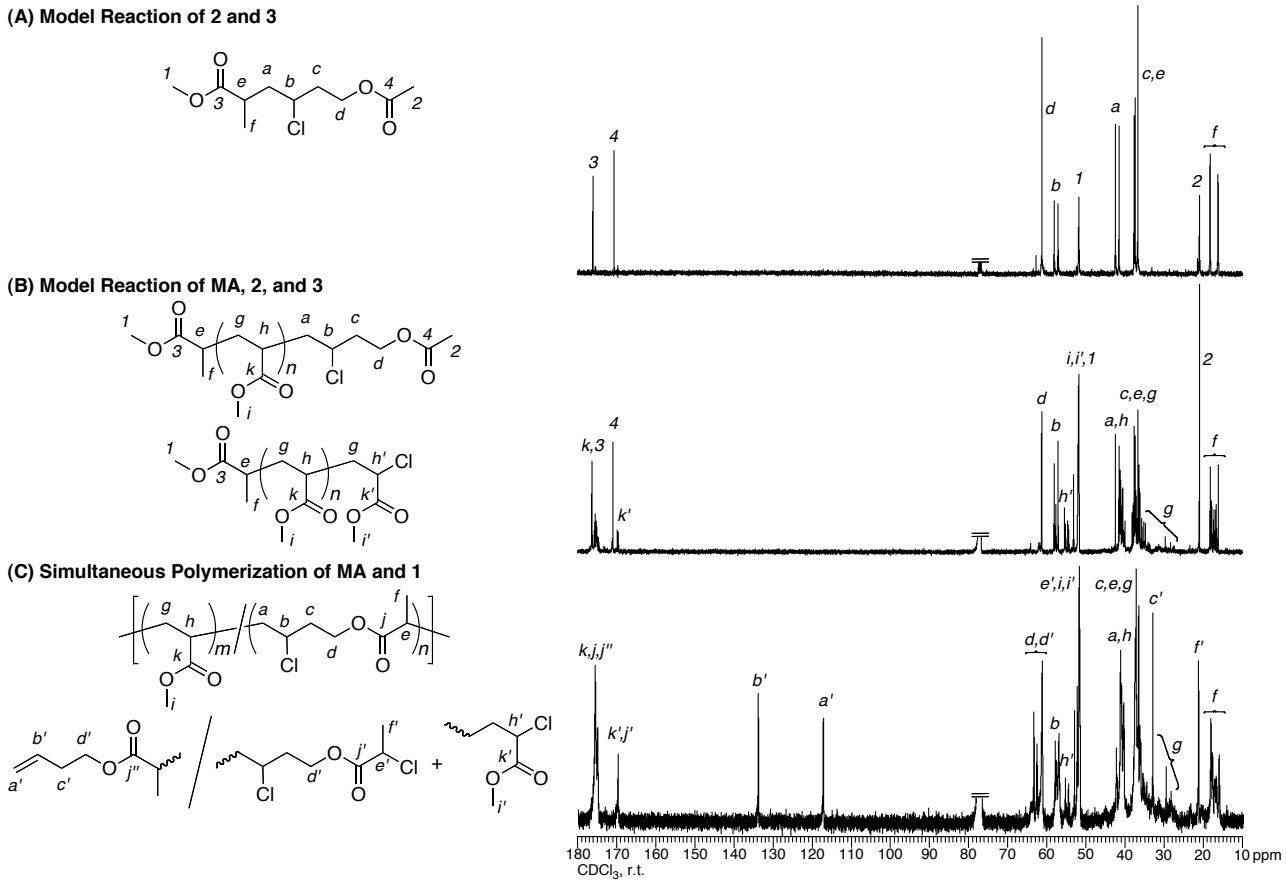

Figure 19. ^{13}C NMR spectra of (A) the adduct (**4**), (B) the oligomer obtained in the model reaction of **2**, **3**, and MA, and (C) the copolymer of MA and **1** obtained with CuCl/HMTETA ($CDCl_3$, r.t.).

those of *F*(C–Cl)/*F*(C=C) obtained during the simultaneous copolymerizations, indicating that these model reaction studies well reflect the copolymerizations.

The MALDI-TOF-MS analysis of the products obtained in the model reactions also gave useful information on the copolymerizations as shown in Figure 21. The MALDI-TOF-MS spectrum of the product obtained with CuCl/HMTETA (Figure 21A) shows a main series of peaks with one unit of **2**, a small number (*m*) of MA units, and one unit of **3** [(*m*,*n*) = (1,1), (2,1), (3,1)]. In addition to these peaks, a minor series of peaks appeared, assignable to the MA oligomers possessing **2** at the α-end and an active –MA–Cl bond at the ω-end [(*m*,*n*) = (2,0), (3,0), (4,0)]. In

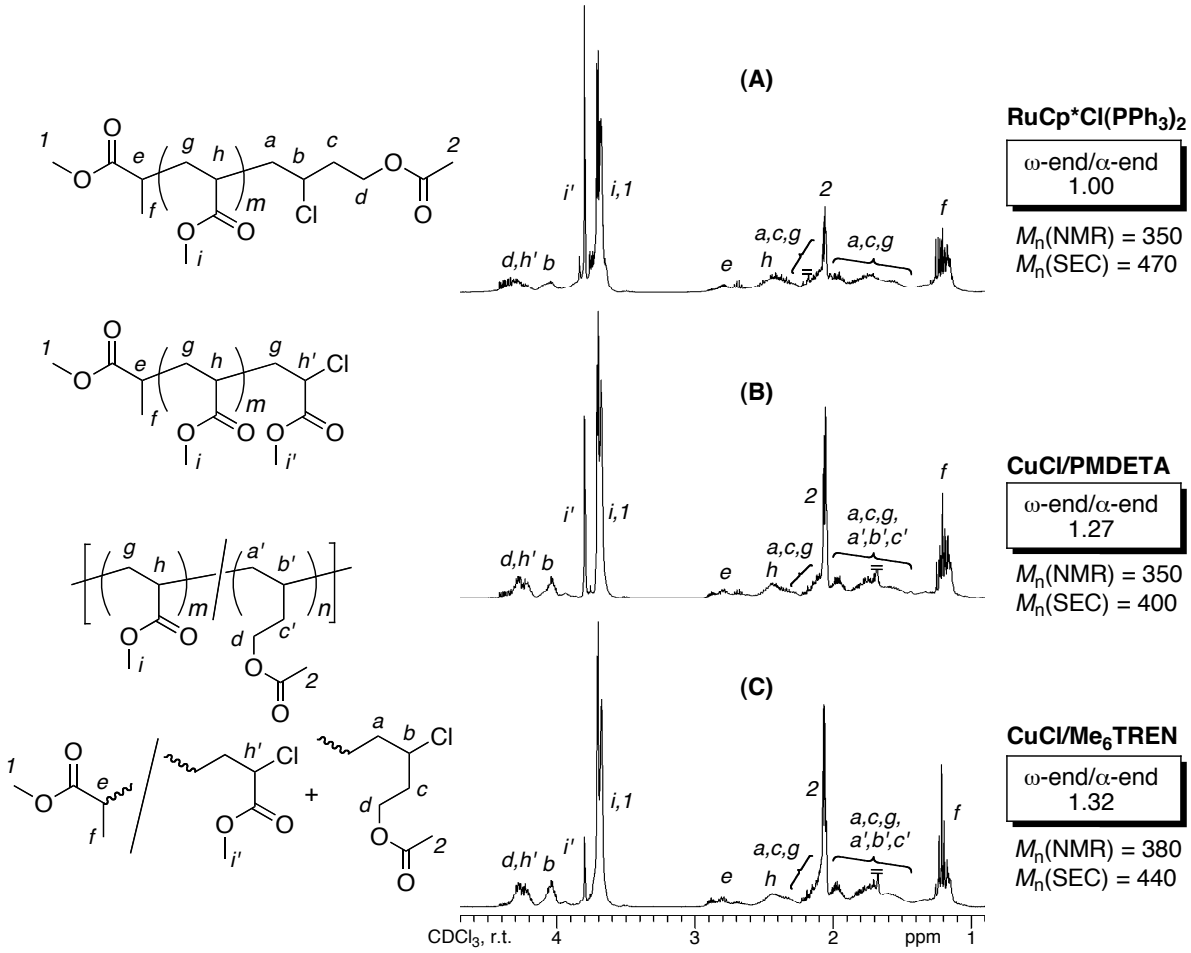

Figure 20. ^{1}H NMR spectra of the oligomer obtained in the model reaction of **2**, **3**, and MA with (A) RuCp*Cl(PPh_3)$_2$, (B) CuCl/PMDETA, and (C) CuCl/Me_6TREN ($CDCl_3$, r.t.).

contrast, another possible series of peaks with more than 2 units of **3**, such as (*m*,*n*) = (1,2), (2,2), was hardly observed. These results indicate again almost no contribution of the chain-growth radical copolymerization of **3** with MA. A similar MALDI-TOF-MS spectrum was also obtained with RuCp*Cl(PPh_3)$_2$ (Figure 22A).

In contrast, the products obtained with CuCl/Me_6TREN (Figure 21B) exhibited a series of peaks possessing 2 units of **3** [(*m*,*n*) = (1,2), (2,2)] in addition to two series of peaks with *n* = 1 and 0, suggesting that the chain-growth radical copolymerization of **3** with MA cannot be ruled out for this catalytic system. The CuCl/PMDETA system gave similar results (Figure 22B).

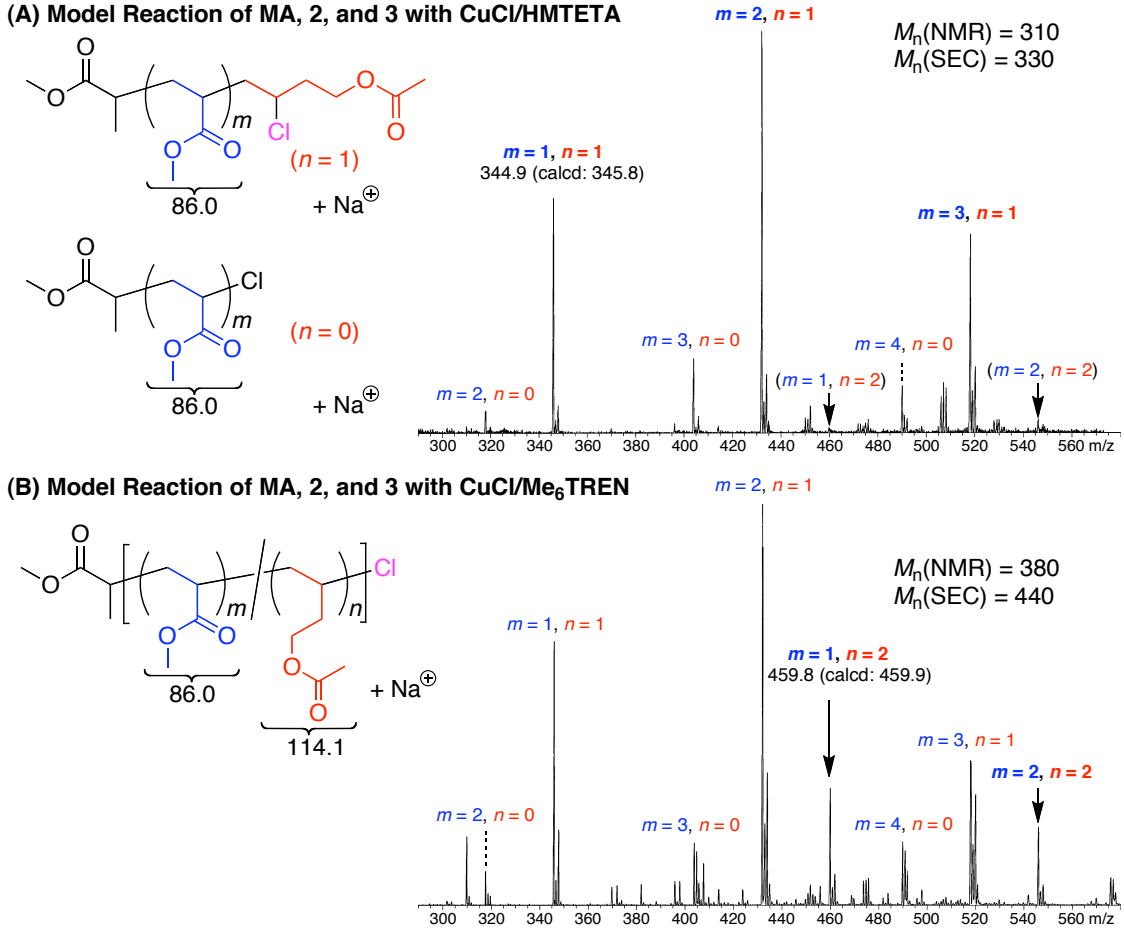

Figure 21. MALDI-TOF-MS spectra of the oligomer obtained in the model reaction of **2**, **3**, and MA with (A) CuCl/HMTETA (M_n = 330, M_w = 490, M_w/M_n = 1.48) and (B) CuCl/Me_6TREN in toluene at 80 °C (M_n = 440, M_w = 630, M_w/M_n = 1.43).

These detailed model studies support the fact that the metal-catalyzed simultaneous chain- and step-growth radical copolymerization of MA and **1** is achievable without any significant contribution of side reactions, such as the bimolecular radical termination and chain-growth propagation of **1**, by careful selection of the catalytic systems and the conditions. Among the various catalysts the author investigated, the best one proved to be CuCl/HMTETA or RuCp*Cl$(PPh_3)_2$, which afforded linear random copolymers of the vinyl monomer and polyester units.

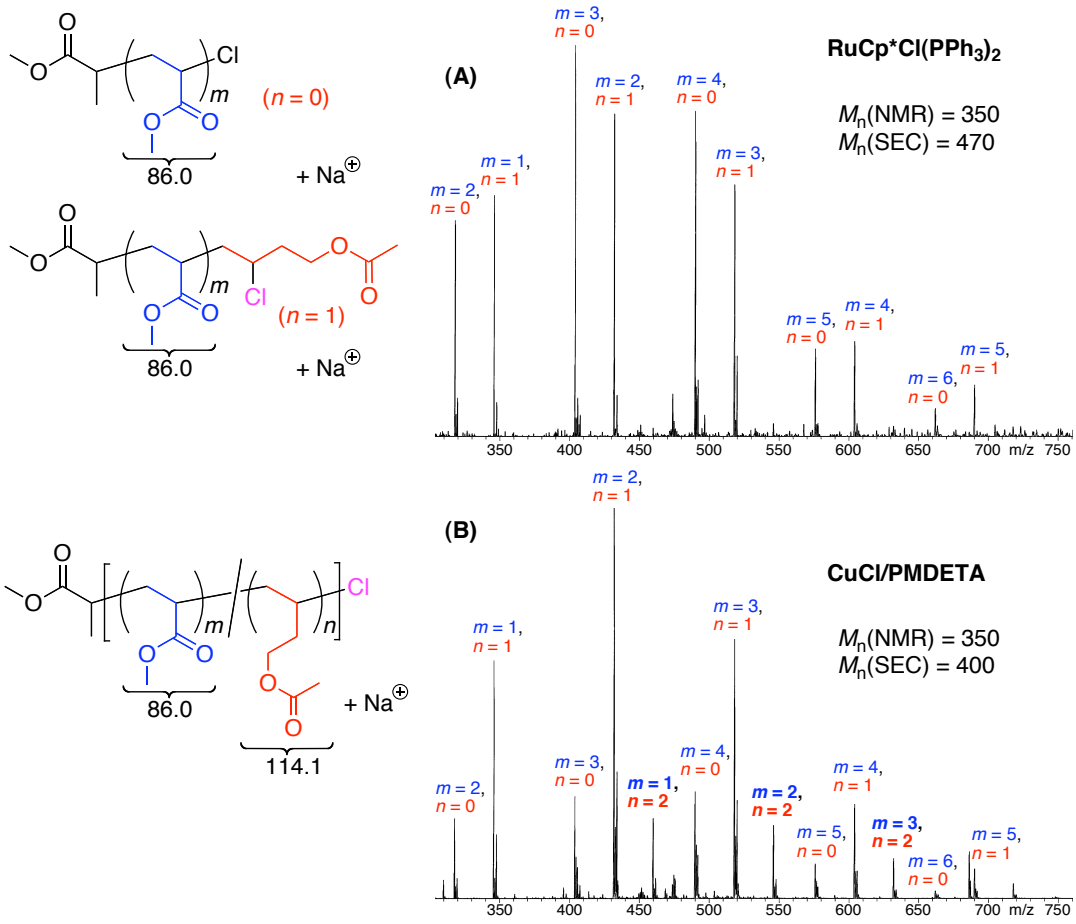

Figure 22. MALDI-TOF-MS spectra of the oligomer obtained in the model reaction of **2**, **3**, and MA with (A) RuCp*Cl(PPh_3)$_2$ and (B) CuCl/PMDETA.

In addition to these findings for the simultaneous polymerizations, the model reaction studies would provide useful information on the metal-catalyzed radical addition copolymerization of acrylate and unconjugated α-olefin, such as propylene and 1-hexene, because the model compound **3** possesses a similar C=C bond to these α-olefins. Based on the author's results in the model reactions, CuCl/HMTETA or RuCp*Cl(PPh_3)$_2$ may not be suitable for producing the high molecular weight copolymers while $FeCl_2$/P*n*Bu_3 can give relatively high molecular weight copolymers with a small amount of α-olefin units.

3. Synthesis of Various Composition Copolymers: From Multiblock to Random Copolymers. A series of copolymerizations of MA and **1** with different feed ratios ($[MA]_0/[\mathbf{1}]_0$ = 3/1, 7/1, 19/1, 39/1, and 100/1) was then carried out with CuCl/HMTETA or $RuCp^*Cl(PPh_3)_2$, which were effective for the simultaneous step- and chain-growth radical copolymerizations at the 1/1 monomer feed ratio, as summarized in Table 1 (entries 11–21). In all cases, both monomers were simultaneously consumed. More specifically, when the polymerization was carried out at the 100/1 feed ratio, the C–Cl bond of **1** was consumed faster than MA, as shown in Figure 23A. Furthermore, the consumption rate of the C–Cl bond of **1** was greater than that of the C=C double bond of **1**. These results suggest that most of **1** was consumed via the reaction of the C–Cl bond during the initial stage of the copolymerizations.

The M_n of the products (filled black circles in Figure 23B) increased in almost direct proportion to the total monomer conversion in the initial stage and agreed well with the calculated values assuming that one polymer chain is generated from one molecule of **1**. Furthermore, after the complete consumption of the monomers, the M_n values progressively increased and the SEC curves became multimodal (Figure 23C). These results indicated that the transition metal catalyst first activates the C–Cl bond of **1** to almost exclusively induce the chain-growth living radical polymerization of MA in the initial stage. The metal catalyst then gradually induces the step-growth propagation between the active C–Cl terminal of poly(MA), which was formed by the living chain-polymerization, and the unconjugated C=C double bond at the α-end originating from **1** to give the multiblock polymers consisting of poly(MA) segments connected by the ester linkage of **1**.

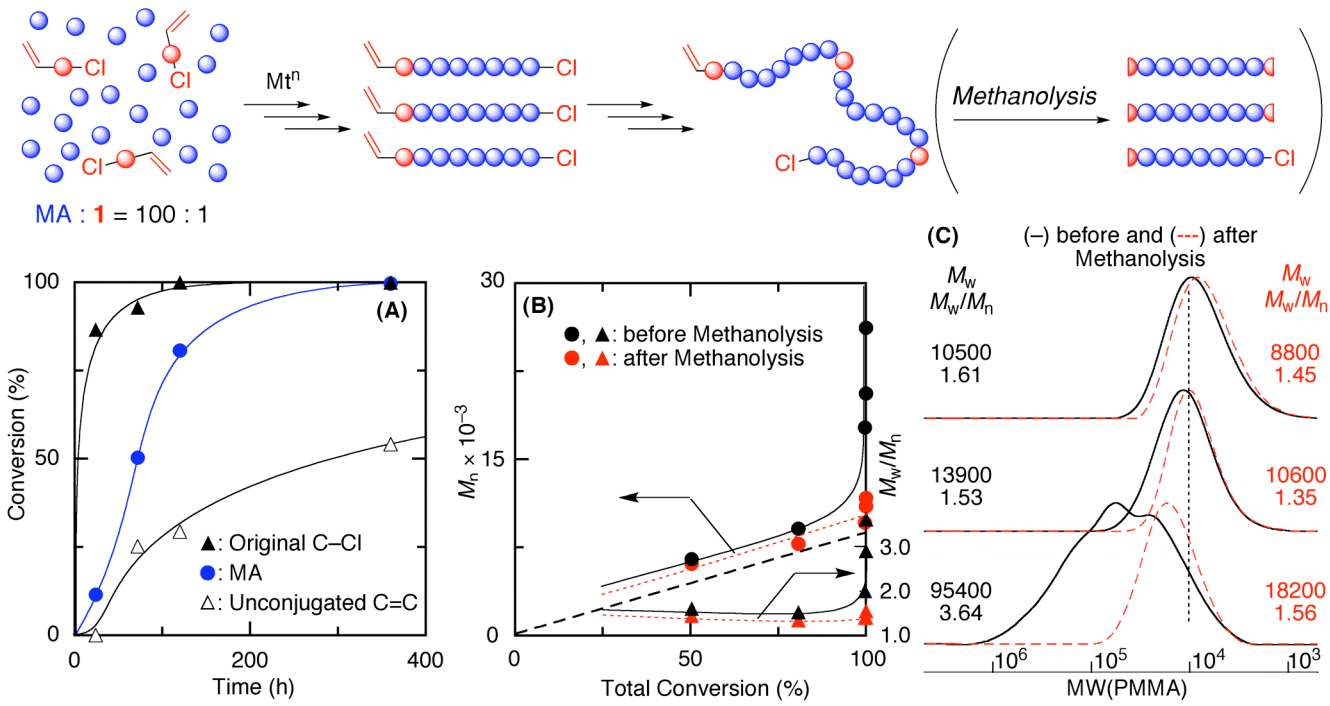

Figure 23. Simultaneous radical chain- and step-growth polymerization of MA and **1** with RuCp*Cl(PPh_3)$_2$ in toluene at 80 °C: [MA]$_0$ = 6.0 M; [**1**]$_0$ = 60 mM; [RuCp*Cl(PPh_3)$_2$]$_0$ = 4.0 mM; [*n*Bu_3N]$_0$ = 40 mM. (A) Consumption of MA measured by gas chromatography and original C–Cl and unconjugated C=C bonds measured by ^{1}H NMR. (B) M_n and M_w/M_n values of the obtained copolymers vs total monomer conversion of MA and **1**. The diagonal black dashed line indicates the calculated M_n assuming the formation of one living polymer of MA per one **1** molecule. (C) Size-exclusion chromatograms of the obtained copolymers (solid lines) and the methanolyzed products (red dashed lines).

These multiblock polymers were then methanolyzed by sodium carbonate which resulted in the unimodal SEC curves (red dashed curves in Figure 9C), and the M_n of which (filled red circles in Figure 23B) was very close to the calculated values for the formation of living polymers from **1**. Thus, the synthesis of a series of copolymers changing from random to multiblock polymer structures was attained by varying the monomer feed ratio of MA to **1** with the appropriate catalysts.

Conclusions

The author succeeded in inducing the simultaneous chain- and step-growth radical polymerizations of methyl acrylate and a designed monomer possessing unconjugated C=C and active C–Cl bonds via the same metal-catalyzed reaction to produce a series of novel linear copolymers consisting of vinyl polymer and polyester units. The choice of the catalysts and reaction conditions is crucial for the controlled synthesis of the linear random copolymers without branching structures originating from the unfavorable chain-growth propagation of the designed monomers. By varying the monomer feed ratios, the structures of the obtained copolymers were varied from random to multiblock copolymers having different segment lengths of vinyl monomer units chopped by the polyester units, which can be controlled by the monomer feed ratio. The copolymers thus possess ester linkages in the main chain, which can be degradable to lower molecular weight vinyl polymers or oligomers under the appropriate conditions. This will produce unique properties for the copolymers for certain applications. By using the advantage of the radical polymerization, the incorporation of functional groups between the C=C and C–Cl groups in the designed monomers as well as in the pendent groups of the vinyl monomer is promising for giving functions to the copolymers. The author is also expanding the scope to other linear random copolymers, such as those comprised of acrylamide and polyamide units in the main chain. The author believes that the simultaneous chain- and step-growth polymerization will provide new strategies for designing novel polymer syntheses.

EXPERIMENTAL SECTION

Materials

MA (TCI, >99%) was distilled from calcium hydride under reduced pressure before use. 3-Butenyl 2-chloropropionate (**1**) and 3-butenyl acetate were synthesized according to the literature.[1] CuCl (Aldrich, 99.99%), RuCp*Cl(PPh_3)$_2$ (provided from Wako), and $FeCl_2$ (Aldrich, 99.99%) were used as received. All metal compounds were handled in a glovebox (VAC Nexus) under a moisture- and oxygen-free argon atmosphere (O_2, < 1 ppm). Toluene was distilled over sodium benzophenone ketyl and bubbles with dry nitrogen for 15 min just before use. P*n*Bu_3 (KANTO, >98%) was used as received. HMTETA (Aldrich, 97%), PMDETA (TCI, >98%), *n*Bu_3N (Wako, >98%), and methyl 2-chloropropionate (TCI, >95%) were distilled from calcium hydride before use.

Polymerization

Polymerization was carried under dry nitrogen in baked glass tubes equipped with a three-way stopcock. A typical example for the polymerization procedure is given below. To a suspension of CuCl (39.6 mg, 0.40 mmol) in toluene (1.91 mL) was added HMTETA (0.11 mL, 0.40 mmol), and the mixture kept stirred for 12 h at 80 °C to give a heterogeneous solution of CuCl/HMTETA complex. After the solution was cooled to the room temperature, MA (0.72 mL, 8.0 mmol) and 3-butenyl 2-chloropropionate (**1**) (1.26 mL, 8.0 mmol) were added. The solution was evenly charged in 7 glass tubes and the tubes were sealed by flame under nitrogen atmosphere. The tubes were immersed in thermostatic oil bath at 80 °C. In predetermined intervals, the polymerization was terminated by cooling the reaction mixtures to –78 °C. Monomer conversion was determined from the concentration of residual monomer measured by gas chromatography with

toluene as an internal standard. The conversions of the functional groups (C=C and C–Cl) of **1** were determined from the concentration of C=C and C–Cl by ^{1}H NMR spectroscopy with toluene as an internal standard.

Model Reaction in the Absence of MA

Model reaction between **2** and **3** was carried under dry nitrogen in baked glass tubes equipped with a three-way stopcock similar to the polymerization. A typical example for the reaction procedure is given below. To a suspension of CuCl (50.9 mg, 0.51 mmol) in toluene (2.53 mL) was added HMTETA (0.14 mL, 0.51 mmol), and the mixture kept stirred for 12 h at 80 °C to give a heterogeneous solution of CuCl/HMTETA complex. After the solution was cooled to the room temperature, 3-butenyl acetate (**3**) (1.30 mL, 10.3 mmol), and methyl 2-chloropropionate (**2**) (1.17 mL, 10.3 mmol) were added. The solution was evenly charged in 14 glass tubes and the tubes were sealed by flame under nitrogen atmosphere. The tubes were immersed in thermostatic oil bath at 80 °C. In predetermined intervals, the reaction was terminated by cooling the reaction mixtures to –78 °C. The conversions of the functional groups (C–Cl and C=C) and the yields of the adducts were determined from the concentration of **2**, **3**, and **4** measured by ^{1}H NMR spectroscopy with toluene as an internal standard (for example in 580 h; 84%, 83%, and 84%, respectively). The contents of the byproducts, methyl propionate (**5**) and dimethyl 2,3-dimethylsuccinate (**6**), were measured by gas chromatography (1.3% and ~0%, respectively, in 580 h) with reference to the remaining methyl 2-chloropropionate, which can be measured by ^{1}H NMR analysis of the reaction mixture. The quenched reaction mixture was diluted with toluene (30 mL), washed with dilute citric acid and water to remove complex residues, evaporated to dryness under reduced pressure, and vacuum-dried. The residue was purified by column

chromatography eluted with diethyl ether to give the 1:1 adduct (**4**) as a mixture of diastereomers due to two asymmetric carbons, i.e. two pairs of enantiomers: (2*R*,4*R*)- and (2*S*,4*S*)-, or (2*R*,4*S*)- and (2*S*,4*R*)-isomers (ratio of diastereomers = 51:49).[1] Yield: 55 mg (39%).

Model Reaction in the Presence of MA

Model reaction among **2**, **3**, and MA was carried similarly under dry nitrogen in baked glass tubes equipped with a three-way stopcock. A typical example for the reaction procedure is given below. To a suspension of CuCl (72.8 mg, 0.74 mmol) in toluene (2.29 mL) was added HMTETA (0.20 mL, 0.74 mmol), and the mixture kept stirred for 12 h at 80 °C to give a heterogeneous solution of CuCl/HMTETA complex. After the solution was cooled to the room temperature, MA (1.32 mL, 14.7 mmol), 3-butenyl acetate (**3**) (1.86 mL, 14.7 mmol), and methyl 2-chloropropionate (**2**) (1.86 mL, 14.7 mmol) were added. The solution was evenly charged in 14 glass tubes and the tubes were sealed by flame under nitrogen atmosphere. The tubes were immersed in thermostatic oil bath at 80 °C. In predetermined intervals, the polymerization was terminated by cooling the reaction mixtures to –78 °C. The conversions of the functional groups (C–Cl and C=C) and MA were determined from the concentration of **2**, **3**, and MA measured by ^{1}H NMR spectroscopy with toluene as an internal standard (for example in 560 h; >99%, 78%, and 74% conversions, respectively). The quenched reaction mixture was diluted with toluene (30 mL) and rigorously shaken with an absorbent [Kyowaad-2000G-7 ($Mg_{0.7}Al_{0.3}O_{1.15}$); Kyowa chemical] (5 g) to remove the metal-containing residues. After the absorbent was separated by filtration, the filtrate was washed with dilute citric acid and water to remove metal-containing residues, evaporated to dryness under reduced pressure, and vacuum-dried to give the product oligomers (0.21 g, 66% yield; M_n = 340, M_w = 460, M_w/M_n = 1.39), including a small amount of remaining

catalyst residues.

Methanolysis

Methanolysis of the copolymers was carried under dry nitrogen in baked glass tubes equipped with a three-way stopcock. A portion of the obtained poly(MA-*co*-**1**) (30 mg) was dispersed in CH_3OH (30 mL) containing Na_2CO_3 (3.2 g) and the solution was refluxed for 48 h. After the dilution with toluene, the product was washed with distilled water and evaporated to remove the solvents to result in the mehanolyzed products (13 mg).[31]

Measurements

Monomer conversion was determined from the concentration of residual monomer measured by gas chromatography [Shimadzu GC-8A equipped with a thermal conductivity detector and a 3.0 mm i.d. × 2 m stainless-steel column packed with SBS-200 (Shinwa Chemical Industries Ltd.) supported on Shimalite W; injection and detector temperature = 200 °C, column temperature = 140 °C] with toluene as an internal standard under He gas flow. The conversions of the functional groups (C=C and C–Cl) of **1** were determined from the concentration of C=C and C–Cl by ^{1}H NMR spectroscopy with toluene as an internal standard. ^{1}H NMR spectra were recorded in $CDCl_3$ at 25 °C on a JEOL ECS–400 or a Varian Gemini 2000 spectrometer, operating at 400 MHz. The number-average molecular weight (M_n), weight-average molecular weight (M_w), and the molecular weight distribution (M_w/M_n) of the product polymers were determined by size-exclusion chromatography (SEC) in THF at 40 °C on two polystyrene gel columns [Shodex K-805L (pore size: 20–1000 Å; 8.0 mm i.d. × 30 cm); flow rate 1.0 mL/min] connected to Jasco PU-980 precision pump and a Jasco 930-RI refractive index detector. The columns were calibrated against 8

standard poly(MMA) samples (Shodex; M_p = 202–1950000; M_w/M_n = 1.02–1.09). MALDI-TOF-MS spectra were measured on a SHIMADZU AXIMA-CFR Plus mass spectrometer (reflector mode) with dithranol (1,8,9-anthracenetriol) as the ionizing matrix and sodium trifluoroacetate as the ion source.

NOTES AND REFERENCES

(1) Odian, G. *Principles of Polymerization, Fourth Edition*; John Wiley and Sons, Inc., New Jersey, 2004.

(2) Another approach at the interface between step and chain-growth polymerization was reported where polycondensation reaction was developed into chain-growth mechanism by design of the monomers: Yokozawa, T.; Yokoyama, A. *Chem. Rev.* **2009**, *109*, 5595–5619.

(3) Kharasch, M. S.; Jensen, E. V.; Urry, W. H. *Science* **1945**, *102*, 128–128.

(4) Kharasch, M. S.; Urry, W. H. *J. Am. Chem. Soc.* **1945**, *67*, 1626–1626.

(5) Minisci, F. *Acc. Chem. Res.* **1975**, 8, 165–171.

(6) Iqbal, J.; Bhatia, B.; Nayyar, N. K. *Chem. Rev.* **1994**, *94*, 519–564.

(7) Gossage, R. A.; van de Luil, L. A.; van Koten, G. *Acc. Chem. Res.* **1998**, *31*, 423–431.

(8) Nagashima, H. In *Ruthenium in Organic Synthesis*; Murahashi, S.-I. Ed.; Wiley-VCH, Weinheim, 2004; pp. 333–343.

(9) Delaude, L.; Demonceau, A.; Noels, A. F. *Top. Organomet. Chem.* **2004**, *11*, 155–171.

(10) Pintauer, T.; Matyjaszewski, K. *Chem. Soc. Rev.* **2008**, *37*, 1087–1097.

(11) Fernández-Zúmel, M. A.; Thommes, K.; Kiefer, G.; Sienkiewicz, A.; Pierzchala, K.; Severin, K. *Chem. Eur. J.* **2009**, *15*, 11601–11607.

(12) Kato, M.; Kamigaito, M.; Sawamoto, M.; Higashimura, T. *Macromolecules* **1995**, *28*,

1721–1723.

(13) Wang, J.-S.; Matyjaszewski, K. *J. Am. Chem. Soc.* **1995**, *117*, 5614–5615.

(14) Percec, V.; Barboiu, B. *Macromolecules* **1995**, 28, 7970–7972.

(15) Patten, T. E.; Xia, J.; Abernathy, T.; Matyjaszewski, K. *Science* **1996**, *272*, 866–868.

(16) Granel, C.; Dubois, Ph.; Jérôme, R.; Teyssié, Ph. *Macromolecules* **1996**, *29*, 8576.

(17) Haddleton, D. M.; Jasieczek, C. B.; Hannon, M. J.; Shooter, A. J. *Macromolecules* **1997**, *30*, 2190.

(18) Matyjaszewski, K.; Xia, J. *Chem. Rev.* **2001**, *101*, 2921–2990.

(19) Kamigaito, M.; Ando, T.; Sawamoto, M. *Chem. Rev.* **2001**, *101*, 3689–3746.

(20) Kamigaito, M.; Ando, T.; Sawamoto, M. *Chem. Rec.* **2004**, *4*, 159–175.

(21) Tsarevsky, N. V. Matyjaszewski, K.; *Chem. Rev.* **2007**, *107*, 2270–2299.

(22) Braunecker, W. A.; Matyjaszewski, K. *Prog. Polym. Sci.* **2007**, *32*, 93–146.

(23) Matyjaszewski, K.; Tsarevsky, N. V. *Nat. Chem.* **2009**, *1*, 276–288.

(24) Ouchi, M.; Terashima, T.; Sawamoto, M. *Chem. Rev.*, **2009**, *109*, 4963–5050.

(25) Rosen, B. M.; Percec,V. *Chem. Rev.* **2009**, *109*, 5069–5119.

(26) Satoh, K.; Mizutani, M.; Kamigaito, M. *Chem. Commun.* **2007**, 1260–1262.

(27) Mizutani, M., Satoh, K.; Kamigaito, M. *Macromolecules* **2009**, *42*, 472–480.

(28) Satoh, K.; Ozawa, S.; Mizutani, M.; Nagai, K.; Kamigaito, M. *Nat. Commun.* **2010**, *1*, 6.

(29) Monomers possessing a conjugated C=C and reactive C–X bonds, coined inimers, undergo self-condensing vinyl polymerization to result in hyperbranched polymers: (a) Fréchet, J. M. J.; Henmi, M.; Gitsov, I.; Aoshima, S.; Leduc, M. R.; Grubbs, R. B. *Science* **1995**, *269*, 1080–1083. (b) Litvinenko, G. I.; Simon, P. F. W.; Müller, A. H. E. *Macromolecules* **1999**, *32*, 2410–2419.

(30) Recently, the metal-catalyzed radical forming reaction from organic halides was evolved into step-growth polycondensation of dihalides via atom transfer radical coupling reactions: Durmaz, Y. Y.; Aydogan, B.; Cianga, I.; Yagci, Y. *ACS Symp. Ser.* **2009**, *1023*, 171–187.

(31) Corey, E. J.; Achiwa, K. J.; Katzenellenbogen, A. *J. Am. Chem. Soc.* **1969**, *91*, 4318–4320.

Chapter 4

Novel Copolymers by Metal-Catalyzed Simultaneous Chain- and Step-Growth Radical Polymerization of Various Monomers

ABSTRACT

The simultaneous chain- and step-growth radical polymerization was examined for common conjugated vinyl monomers and designed ester- or amide-linked monomers bearing both an unconjugated carbon-carbon double bond and a reactive carbon-halogen bond in a single molecule. Herein, various alkyl and functional group-containing acrylates and styrene were employed as the former for the chain-growth polymerization and the latter would afford polyester or polyamide unit via the step-growth polymerization. In all cases, the simultaneous polymerizations smoothly proceeded to afford the linear random copolymers containing both monomer units. Especially, for styrene as a vinyl monomer, the highly selective chain-growth living polymerization proceeded quantitatively before the step-growth polymerization took place between the living polystyrene chains. The molecular weights of the obtained copolymers progressively increased with monomer consumption and were close to the calculated values throughout the polymerization. The well-defined polymer structures were confirmed by ^{1}H NMR and MALDI-TOF-MS analysis of the products.

Introduction

The synthesis of well-defined polymers has long been of great interest in polymer chemistry. A versatile and widely applicable polymerization is preferable for the prospective extension of the polymerization in terms of the variety of polymer structures, functions, and properties. Radical polymerization is one of the most widespread methods in polymer synthesis because of many advantages, such as wide variety of monomers, tolerance to polar groups, and mild reaction conditions. Although the processes were industrially developed, the precision polymer synthesis in radical polymerizations has become important for new polymer materials of well-defined architectures. Recently, widespread efforts have been made for attaining well-controlled radical polymerizations and these new radical processes are now rapidly approaching the controllability in ionic polymerizations.[1–5]

Owing to the tremendous precedent researchers for controlling the primary structures such as chain length and chain-end, the synthetic polymer structure has now been controlled by living radical polymerizations, which have had a great impact on the developments of polymeric materials based on their controlled structures. Among them, the metal-catalyzed living radical polymerization or atom transfer radical polymerization (ATRP) is one of the most widely employed methods mainly because of the high controllability, a wide variety of available monomers such as acrylates, styrene, and acrylamides, and the stability and easy accessibility of the carbon-halogen (C–X) bonds as the initiating sites.[3,4,6–8] This living radical polymerization has been developed via evolution of metal-catalyzed atom transfer radical addition (ATRA), sometimes called Kharasch addition, into chain-growth propagation. This radical addition is one of the highly efficient and robust carbon-carbon (C–C) bond forming processes between various vinyl compounds and organic halides and is utilized for the construction of small organic molecules.[9] In this reaction, the radical

species is generated through the metal-assisted homolytic cleavage of the C–X bond and adds to the carbon–carbon double (C=C) bond of the olefin to form the C–C bond followed by a new C–X bond formation upon retrieving the halogen atom from the oxidized metal catalyst, which results in the 1:1 adduct of the halide and olefin. This reaction has successfully been extended to chain-growth radical addition polymerizations of vinyl monomers to open a new field of precision polymer synthesis. The key for the controlled radical polymerization lies on iterative processes of the one-electron redox reaction by the metal catalyst during the entire polymerization, that is, the formation of the radical species from the C–X terminal, addition to C=C double bond of the monomers, and regeneration of the C–X terminal. The newly C–X terminal is formed between the carbon atom adjacent to the carbonyl or the aryl group originating from the vinyl monomers and the halogen atom from the organic halide initiator and can be activated by the appropriate metal catalyst to regenerate the growing radical species resulting in the chain-growth addition polymerization. During the process, the strategy for controlling radical polymerization is implemented, in which the instantaneous concentration of the growing radical species is kept low to avoid radical bimolecular termination. The equilibrium between the dormant and radical species can not only minimize the probability of the termination, but also give an equal opportunity of propagation to all dormant via frequent interconversion. The precise control of the molecular weight was permitted for various conjugated vinyl monomers and it enables the precision synthesis of well-defined polymers such as block,[3,4,7,10] star,[3,4,11] graft,[4,12] end-functionalized,[3–5,13] and more complicated polymers.[14–24]

On the other hand, the author has found that the same metal catalysis as in the living radical polymerization can be evolved into the step-growth polymerization, that is the metal-catalyzed radical polyaddition of designed monomers possessing unconjugated C=C double and a reactive carbon-halogen (C–Cl) bonds in a single molecule.[25] In this step-growth radical

polyaddition, the C–Cl bond in the monomer is activated by the metal catalyst to form a radical species, which adds to the C=C double bond of another monomer molecule to generate a C–C bond as the main chain, along with an inactive C–Cl bond as the pendant. A series of linear aliphatic polyesters was synthesized by step-growth radical polyaddition of monomers, the C=C and C–Cl bonds of which are linked by an ester linkage. The newly formed $–CH_2–CHCl–$ unit is equivalent to the poly(vinyl chloride) repeating unit to construct sequence-regulated vinyl copolymers using step-growth polymerization of further designed monomers. The polyaddition of designed monomers prepared from common vinyl monomer building blocks leaded to structures equivalents to unprecedented ABC- or ABCC-sequence-regulated vinyl copolymers consisting of C–C-bond main chains.[26] Futhermore, the author succeeded in inducing the simultaneous chain- and step-growth radical polymerization of methyl acrylate (MA) and an ester-linked monomer with unconjugated C=C and active C–Cl bonds via the same metal-catalyzed reaction to produce a series of novel linear copolymers comprised of vinyl polymer and polyester units.[27] The obtained copolymers have various segment lengths of vinyl monomer units chopped by the polyester units, which can be controlled by the monomer feed ratio. Detailed analyses of the polymerization as well as the model reactions were done systematically to find the most efficient catalysts and to reveal the polymerization mechanism. The author also expanded the scope to other linear copolymers, such as those consisting of acrylamide and polyester or polyamide units in the main chain.[28] This provided a facile and practical approach to a tunable thermosensitivity and degradability of poly(*N*-isopropylacrylamide).

In this study, the author investigated the metal-catalyzed simultaneous radical polymerization of various common conjugated vinyl monomers for chain-growth polymerization and designed ester- or amide-linked monomers for step-growth polymerization. Acrylates with

various alkyl and functional groups in the side chain and styrene were used for the chain-growth polymerization, while ester- or amide-linked monomers containing functional groups such as ether and disulfide linkage were employed for step-growth polymerization. The structure of the obtained copolymers was analyzed in detail by ^{1}H NMR and MALDI-TOF-MS.

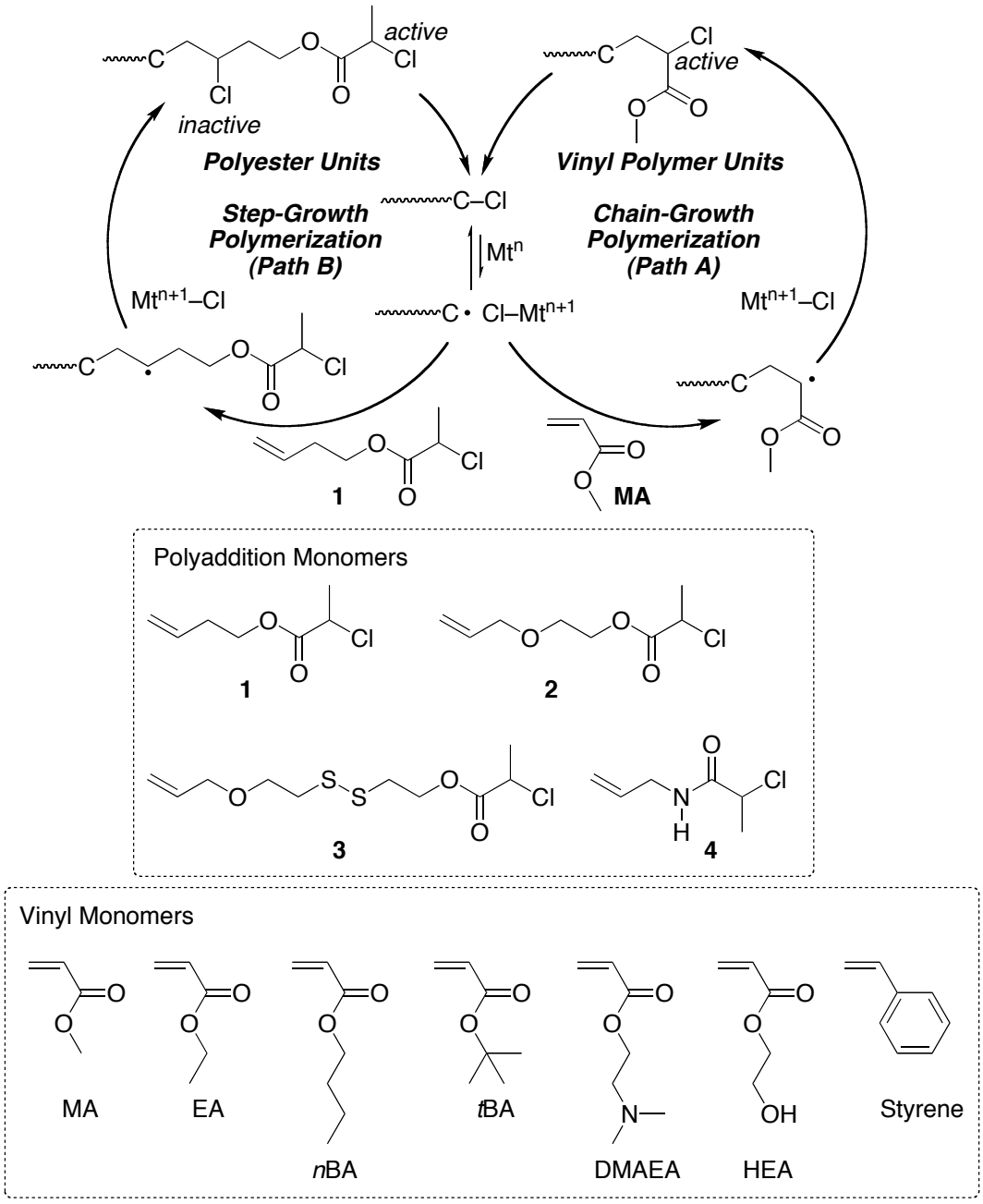

Scheme 1. Metal-Catalyzed Simultaneous Chain- and Step-Growth Radical Polymerization of Various Monomers.

Results and Discussion

1. Simultaneous Polymerization of MA and 1–4. First, the author examined the simultaneous chain- and step-growth radical polymerization of methyl acrylate (MA) and various functionalized ester-linked monomers with alkyl (**1**), ether (**2**), or disulfide (**3**) linkage between the C=C and C–Cl groups or amide-linked monomer (**4**) ($[MA]_0/[\mathbf{1}–\mathbf{4}]_0$ = 1/1). The reactions were carried out at 80 °C in toluene with CuCl/1,1,4,7,10,10-hexamethyltriethylenetetramine (HMTETA). Monomer conversion was determined by gas chromatography. All of the monomers were simultaneously consumed, although the polymerization of **1** or **2** with MA was faster than that of **3** or **4** (Figure 1). The total monomer conversions of MA and **1** or **2** reached over 97%, while **3** and

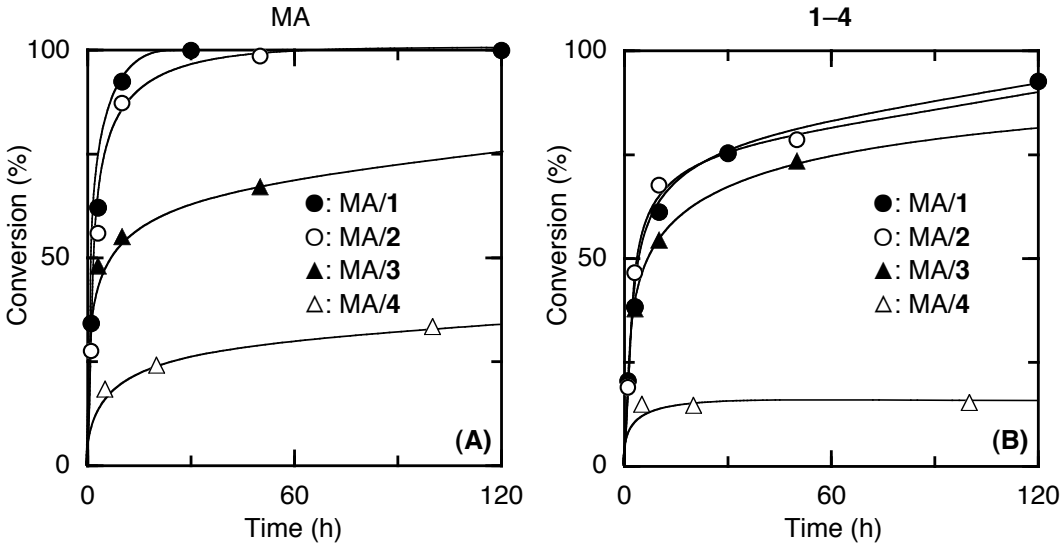

Figure 1. Simultaneous chain- and step-growth radical polymerization of MA and **1**–**4** with CuCl/HMTETA in toluene at 80 °C: $[MA]_0$ = 2.0 M; $[\mathbf{1}–\mathbf{4}]_0$ = 2.0 M; $[CuCl]_0$ = 100 mM; $[HMTETA]_0$ = 100 mM. (A) Consumption of MA measured by gas chromatography. (B) Consumption of **1**–**4** measured by gas chromatography. (C) Remaining C–Cl/C=C in the reaction mixture vs total monomer conversion of MA and **1**.

4 gave limited conversions. These results indicated that the simultaneous consumption of both monomers occurred in all cases, although the consumption rates depended on the structures of the step-growth monomers.

The conversion of the functional groups (original C–Cl and unconjugated C=C bonds) of step-growth monomers was measured by ^{1}H NMR analysis. The original C–Cl bonds were more rapidly consumed than the unconjugated C=C bonds, suggesting that the C–Cl bond was activated to form the radical species followed by the addition of the C=C bonds of MA or step-growth monomers (Figure 2–5). As the simultaneous polymerization proceeded, another type of active C–Cl bonds was formed via the addition of MA. For the ideal step-growth radical polymerization without side reactions such as consecutive vinyl additions of step-growth monomer to the radical

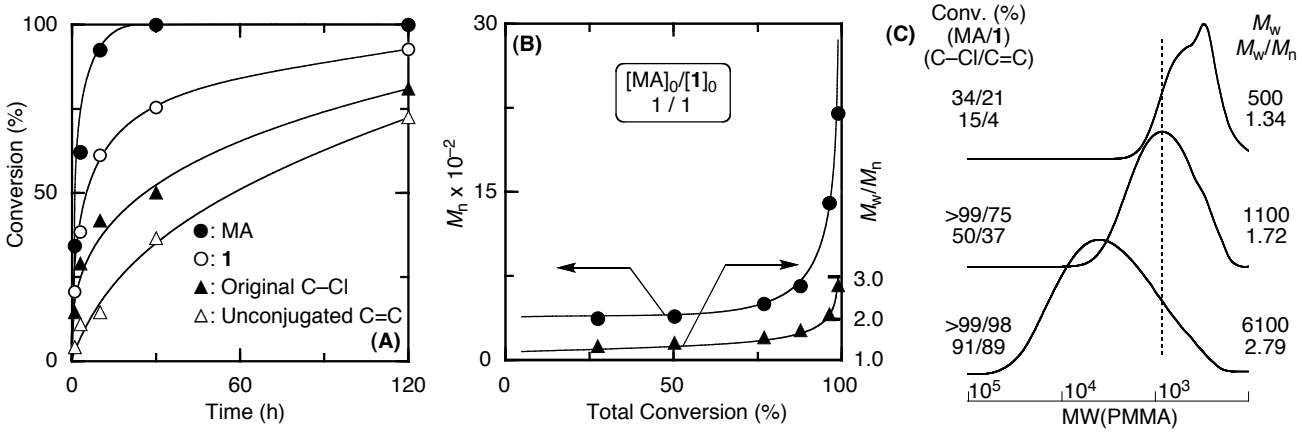

Figure 2. Simultaneous chain- and step-growth radical polymerization of MA and **1** in toluene at 80 °C: $[MA]_0$ = 2.0 M; $[\mathbf{1}]_0$ = 2.0 M; $[CuCl]_0$ = 100 mM; $[HMTETA]_0$ = 100 mM. (A) Consumption of MA and **1** measured by gas chromatography and original C–Cl and unconjugated C=C bonds measured by ^{1}H NMR. (B) M_n and M_w/M_n values of the obtained copolymers vs total monomer conversion of MA and **1**. (C) Size-exclusion chromatograms of the obtained copolymers of MA and **1**.

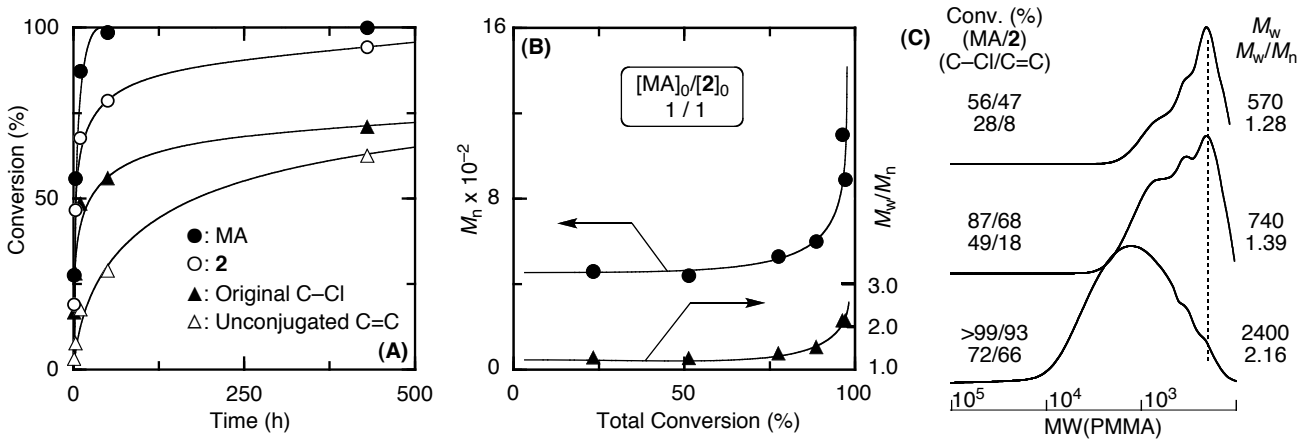

Figure 3. Simultaneous chain- and step-growth radical polymerization of MA and **2** in toluene at 80 °C: $[MA]_0$ = 2.0 M; $[\mathbf{2}]_0$ = 2.0 M; $[CuCl]_0$ = 100 mM; $[HMTETA]_0$ = 100 mM. (A) Consumption of MA and **2** measured by gas chromatography and original C–Cl and unconjugated C=C bonds measured by ^{1}H NMR. (B) M_n and M_w/M_n values of the obtained copolymers vs total monomer conversion of MA and **2**. (C) Size-exclusion chromatograms of the obtained copolymers of MA and **2**.

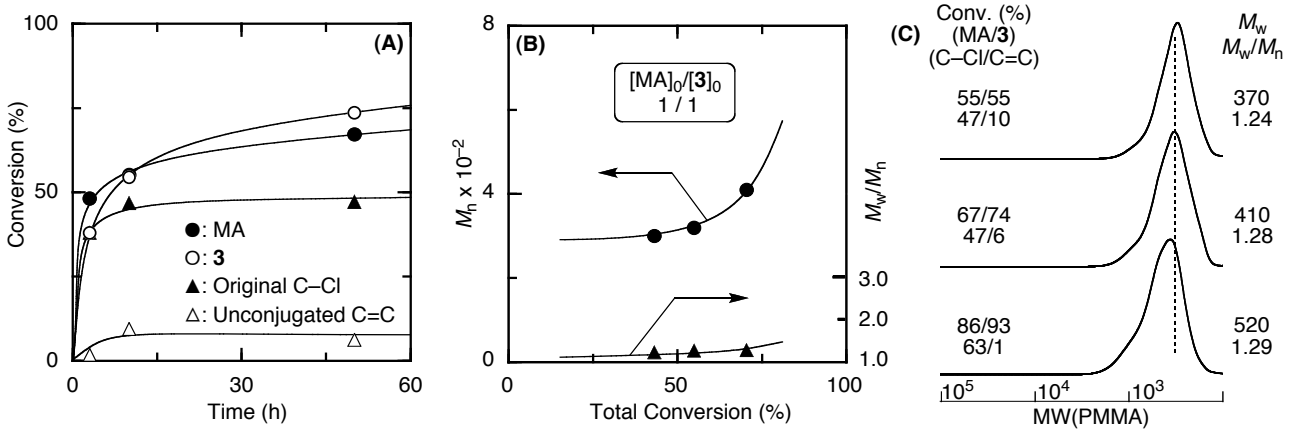

Figure 4. Simultaneous chain- and step-growth radical polymerization of MA and **3** in toluene at 80 °C: $[MA]_0$ = 2.0 M; $[\mathbf{3}]_0$ = 2.0 M; $[CuCl]_0$ = 100 mM; $[HMTETA]_0$ = 100 mM. (A) Consumption of MA and **3** measured by gas chromatography and original C–Cl and unconjugated C=C bonds measured by ^{1}H NMR. (B) M_n and M_w/M_n values of the obtained copolymers vs total monomer conversion of MA and **3**. (C) Size-exclusion chromatograms of the obtained copolymers of MA and **3**.

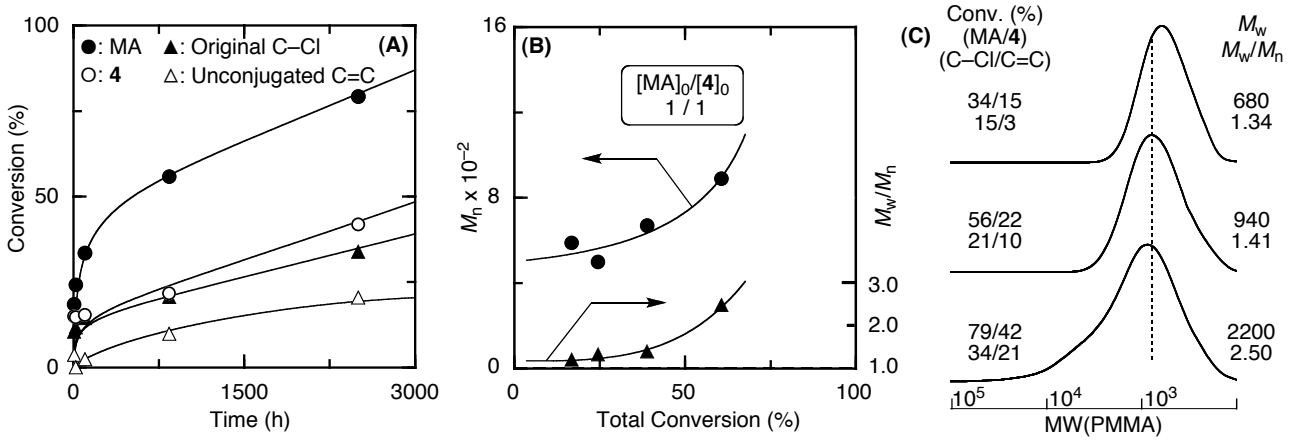

Figure 5. Simultaneous chain- and step-growth radical polymerization of MA and **4** in toluene at 80 °C: $[MA]_0$ = 2.0 M; $[\mathbf{4}]_0$ = 2.0 M; $[CuCl]_0$ = 100 mM; $[HMTETA]_0$ = 100 mM. (A) Consumption of MA and **4** measured by gas chromatography and original C–Cl and unconjugated C=C bonds measured by ^{1}H NMR. (B) M_n and M_w/M_n values of the obtained copolymers vs total monomer conversion of MA and **4**. (C) Size-exclusion chromatograms of the obtained copolymers of MA and **4**.

species or bimolecular termination between the radical species, one of the criteria is an equal consumption rate or equal remaining concentration of the unconjugated C=C and the active C–Cl bonds, even for the simultaneous polymerization. Thus, the concentration of the active C–Cl bonds derived from MA as well as those of the original C–Cl bonds were further measured by ^{1}H NMR analysis of the reaction mixture. In all of the polymerization, the sum of the remaining concentrations of these active C–Cl bonds decreased at the same rate as that of the unconjugated C=C bonds (Figure 6). The ratios of the active C–Cl to the unconjugated C=C bonds (C–Cl/C=C) were plotted versus the total monomer conversions and proved nearly constant around 1.0 (Figure 7). These results indicate that the ideal simultaneous polymerization proceeded for MA and designed step-growth monomers possessing functional groups between the C=C and C–Cl bonds

without side reactions such as chain-growth radical copolymerization of unconjugated C=C with MA or bimolecular radical termination.

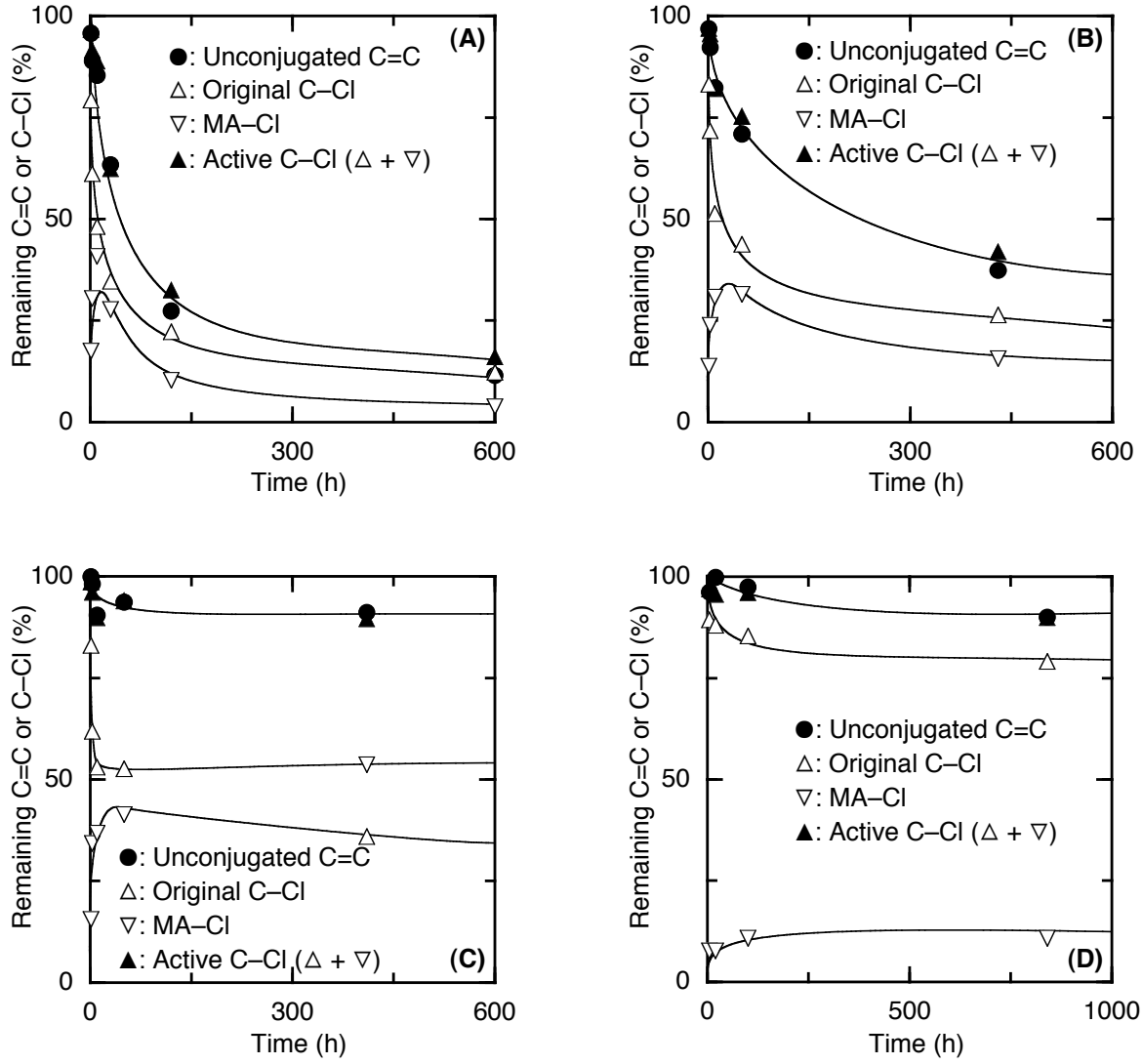

Figure 6. Simultaneous chain- and step-growth radical polymerization of MA and (A) **1**, (B) **2**, (C) **3**, or (D) **4** in toluene at 80 °C: $[MA]_0$ = 2.0 M; $[\mathbf{1}–\mathbf{4}]_0$ = 2.0 M; $[CuCl]_0$ = 100 mM; $[HMTETA]_0$ = 100 mM. Concentration of remaining unconjugated C=C, original C–Cl, MA–Cl, and sum of the active C–Cl (original C–Cl + MA–Cl) bonds in the reaction mixture measured by ^{1}H NMR.

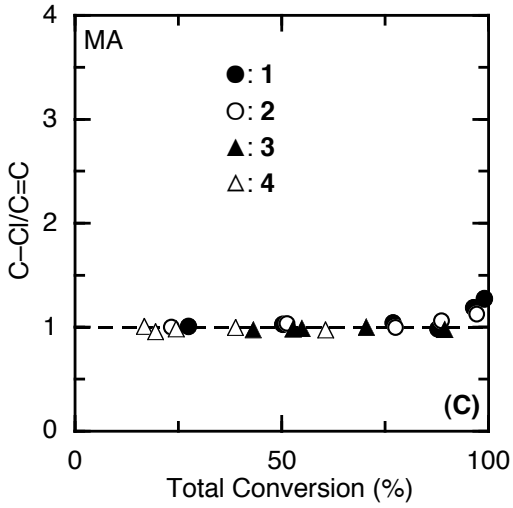

Figure 7. Remaining C–Cl/C=C in the reaction mixture vs total monomer conversion for the simultaneous chain- and step-growth radical polymerization of MA and (A) **1**, (B) **2**, (C) **3**, or (D) **4** in toluene at 80 °C: $[MA]_0$ = 2.0 M; $[\mathbf{1}–\mathbf{4}]_0$ = 2.0 M; $[CuCl]_0$ = 100 mM; $[HMTETA]_0$ = 100 mM.

Figure 8 shows the molecular weights and the size-exclusion chromatograms (SECs) of the products obtained from MA and **1**–**4**. The monomers afforded the copolymers in all cases, although the molecular weights were dependent on the monomer conversions (Figure 8C). The molecular weights of the obtained products were relatively low during the initial stage of the polymerizations. Especially for **1** and **2**, the molecular weights progressively increased in the later stage after quantitative monomer consumptions, indicating contribution of the step-growth propagation to the product formation (Figure 8A). On the other hand, the relatively low molecular weights products were obtained from **3** or **4** with MA because of low monomer conversions. Thus, the design of the step-growth monomers is important for the effective polymerization, leading to high molecular weights copolymers.

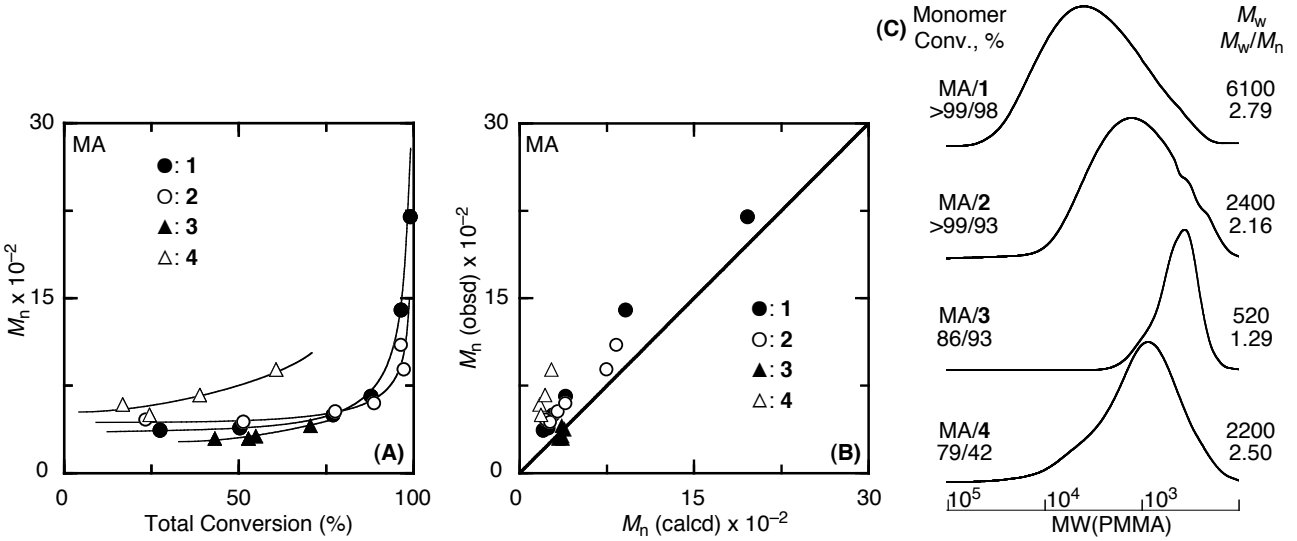

Figure 8. Simultaneous chain- and step-growth radical polymerization of MA and **1**–**4** with CuCl/HMTETA in toluene at 80 °C: (A) M_n and M_w/M_n values of the obtained copolymers vs total monomer conversion of MA and **1**–**4**. (B) M_n of the obtained copolymers vs. calculated M_n. (C) Size-exclusion chromatograms of the obtained copolymers.

The mechanism of the simultaneous polymerization was studied in detailed by the molecular weights calculated from the conversions. In the chain-growth living polymerization, the molecular weight of the obtained polymer depends on molecular weight of chain-growth monomer and initiator (MW_C, MW_I), monomer conversion (c), and initial charge ratio of monomer to initiator ($[M_C]_0/[I]_0$). The theoretical value of the molecular weight (M_n) is calculated by means of eq 1.

$$M_n = (MW_C) \times (c) \times ([M_C]_0/[I]_0) + (MW_I) \quad (1)$$

On the other hand, in the step-growth polymerization, the M_n depends on molecular weight of step-growth monomer (MW_C) and conversion of functional groups (p) and the degree of polymerization increases in inverse proportion to 1–p (eq 2).

$$M_n = (MW_S) / (1 - p) \quad (2)$$

Therefore the author determined the calculated values of the M_n for the simultaneous

polymerization by eq 3, where p means the consumption of the unconjugated C=C bond, the functional group in the step-growth monomer.

$$M_n = [(MW_C) \times (c) \times ([M_C]_0/[M_S]_0) + (MW_S)] / (1 - p) \quad (3)$$

Eq 4 must be used when initial charge ratio of two monomers is 1:1 ($[M_C]_0 = [M_S]_0$).

$$M_n = [(MW_C) \times (c) + (MW_S)] / (1 - p) \quad (4)$$

The M_ns of the obtained copolymers with a series of monomer combination increased in direct proportion to the monomer conversions and were relatively close to the calculated line throughout the polymerization (Figure 8B). The values of all the products were slightly higher than the calculated ones. This is probably because the calculated value contains the molecular weight of the unreacted step-growth monomers while the M_n of the obtained products excludes those of the residues monomers. These results support that the copolymers of MA and **1**–**4** were produced via the expected simultaneous polymerization via the chain- and step-growth mechanism.

2. Simultaneous Polymerization of Alkyl Acrylates and 1. A series of alkyl acrylates such as ethyl (EA), *n*-butyl (*n*BA), and *t*-butyl (*t*BA) acrylate with **1** was examined for the simultaneous polymerization with the same catalytic system ([EA, *n*BA, or *t*BA]$_0$/[**1**]$_0$ = 1/1). Similar to the polymerization of MA and **1**, the monomer conversion reached over 95% and the polymers were produced with relatively high molecular weights (M_w > 4000) (Figure 9–11). The molecular weights of the obtained products progressively increased as the monomers consumed and agreed well with the calculated values (Figure 12), indicating the formation of the copolymers by the ideal simultaneous chain- and step-growth polymerization. These results show that the simultaneous polymerization proceeded for various acrylates with **1**.

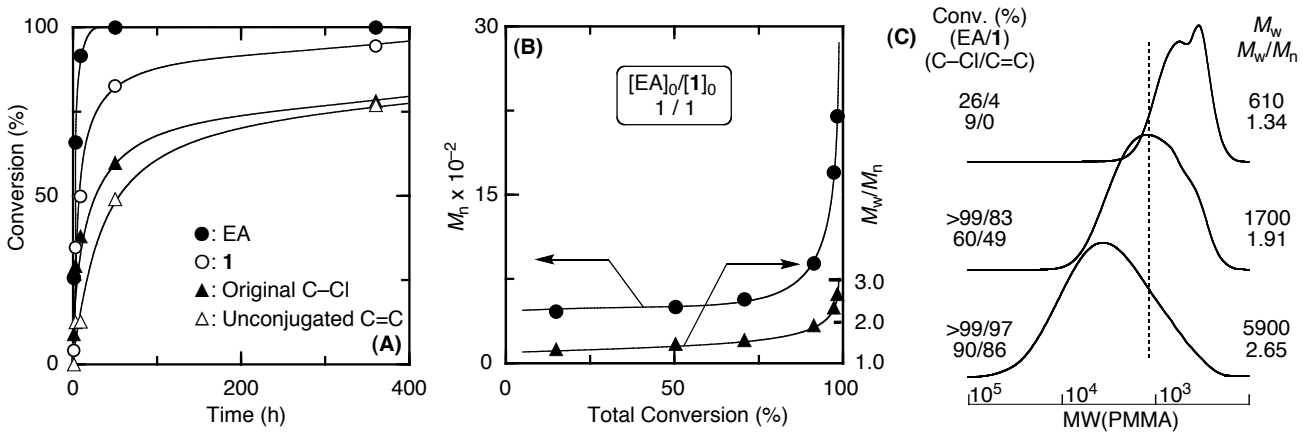

Figure 9. Simultaneous chain- and step-growth radical polymerization of EA and **1** in toluene at 80 °C: $[EA]_0$ = 2.0 M; $[\mathbf{1}]_0$ = 2.0 M; $[CuCl]_0$ = 100 mM; $[HMTETA]_0$ = 100 mM. (A) Consumption of EA and **1** measured by gas chromatography and original C–Cl and unconjugated C=C bonds measured by ^{1}H NMR. (B) M_n and M_w/M_n values of the obtained copolymers vs total monomer conversion of EA and **1**. (C) Size-exclusion chromatograms of the obtained copolymers of EA and **1**.

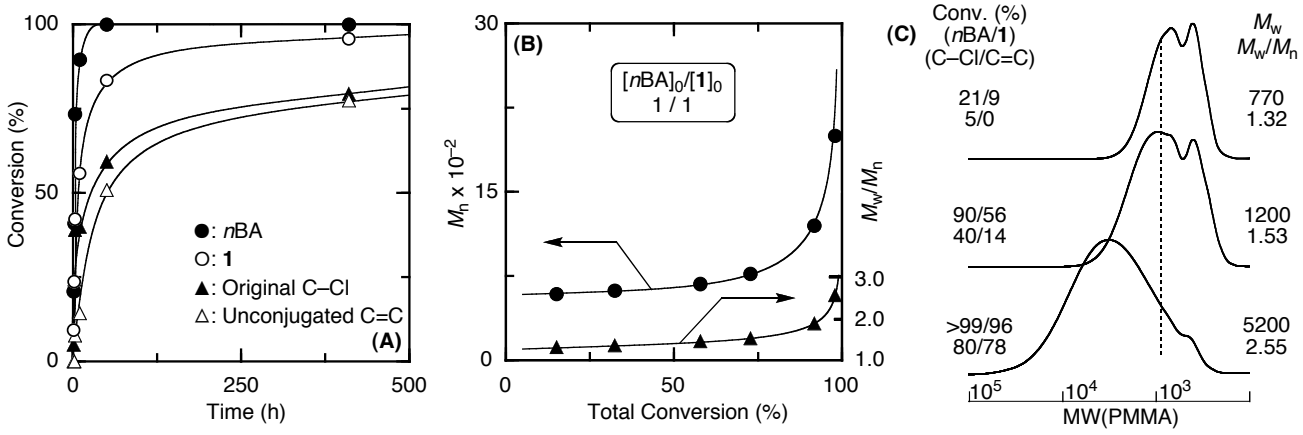

Figure 10. Simultaneous chain- and step-growth radical polymerization of *n*BA and **1** in toluene at 80 °C: $[n\text{BA}]_0$ = 2.0 M; $[\mathbf{1}]_0$ = 2.0 M; $[CuCl]_0$ = 100 mM; $[HMTETA]_0$ = 100 mM. (A) Consumption of *n*BA and **1** measured by gas chromatography and original C–Cl and unconjugated C=C bonds measured by ^{1}H NMR. (B) M_n and M_w/M_n values of the obtained copolymers vs total monomer conversion of *n*BA and **1**. (C) Size-exclusion chromatograms of the obtained copolymers of *n*BA and **1**.

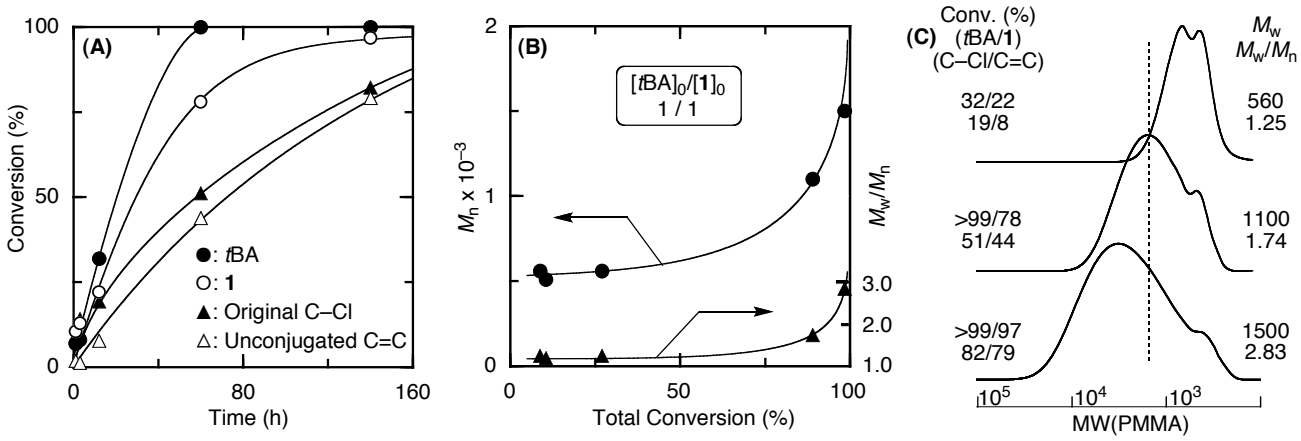

Figure 11. Simultaneous chain- and step-growth radical polymerization of *t*BA and **1** in toluene at 80 °C: $[t\text{BA}]_0$ = 2.0 M; $[\mathbf{1}]_0$ = 2.0 M; $[\text{CuCl}]_0$ = 100 mM; $[\text{HMTETA}]_0$ = 100 mM. (A) Consumption of *t*BA and **1** measured by gas chromatography and original C–Cl and unconjugated C=C bonds measured by ^{1}H NMR. (B) M_n and M_w/M_n values of the obtained copolymers vs total monomer conversion of *t*BA and **1**. (C) Size-exclusion chromatograms of the obtained copolymers of *t*BA and **1**.

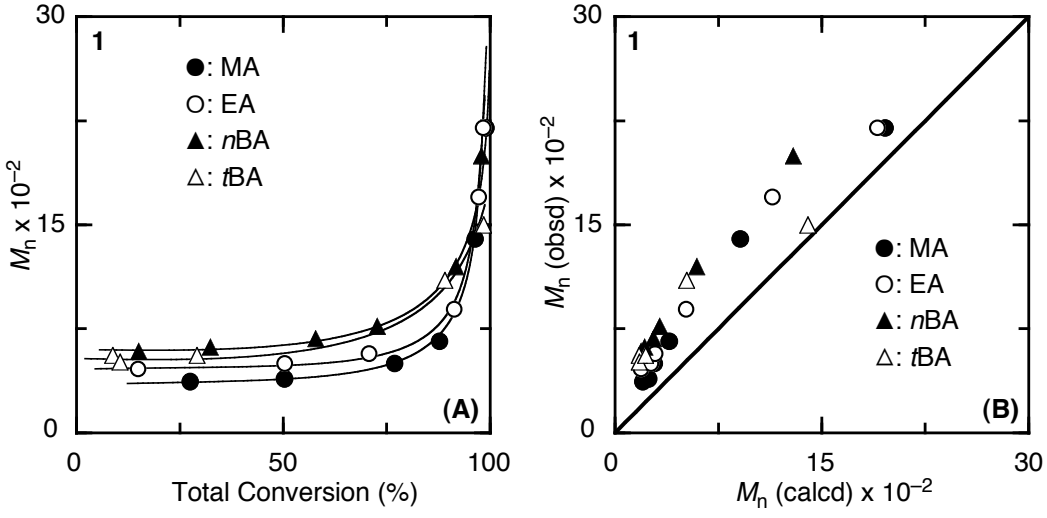

Figure 12. Simultaneous chain- and step-growth radical polymerization of MA, EA, *n*BA, or *t*BA and **1** with CuCl/HMTETA in toluene at 80 °C: (A) M_n and M_w/M_n values of the obtained copolymers vs total monomer conversion of MA, EA, *n*BA, or *t*BA and **1**. (B) M_n of the obtained copolymers vs. calculated M_n.

Figure 13 shows the SEC curves of the copolymers obtained from various alkyl acrylates and **1**. In the early stage of the polymerization, the SEC curves consisted of only low-molecular-weight oligomers, of which the highest peak was assumed to be that of the 1:1 adduct of acrylate and **1**. As the reactions proceeded, the curves shifted to higher molecular weights, especially after complete consumption of acrylates. In the SEC curves of the copolymers obtained from MA or EA with **1**, the peak in the low molecular weight region disappeared to afford the relatively high molecular weight polymers at the later stage of the polymerization. These results indicate that the simultaneous consumption of both monomers occurred to give oligomers mainly containing the 1:1 adduct of two monomers at the initial stage, and then step-growth propagation proceeded between the oligomers to afford the copolymers of acrylates and **1**.

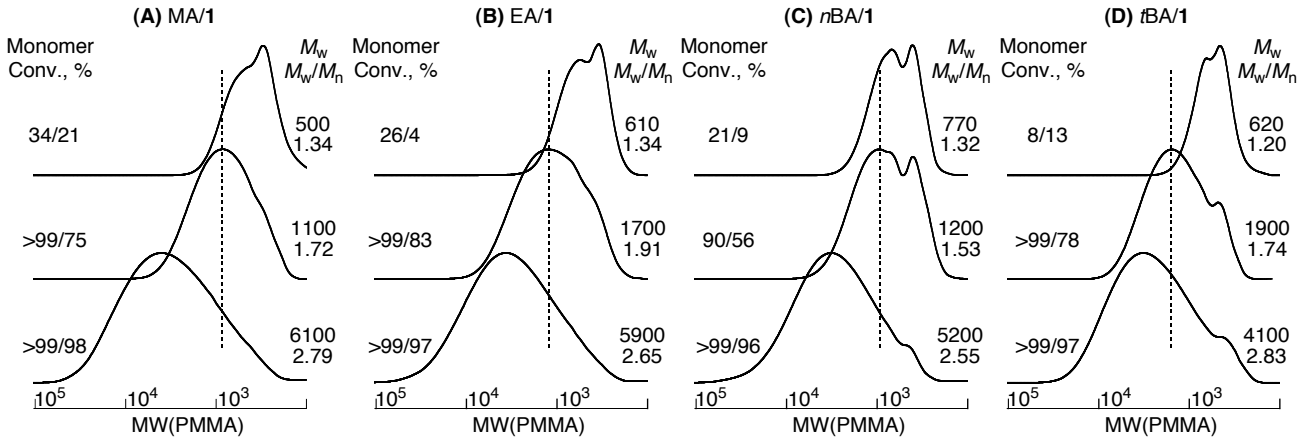

Figure 13. Size-exclusion chromatograms of the obtained copolymers in the simultaneous chain- and step-growth radical polymerization of (A) MA, (B) EA, (C) *n*BA, or (D) *t*BA and **1** with CuCl/HMTETA in toluene at 80 °C.

3. Copolymer Analysis. The structures of the obtained copolymers were analyzed by ^{1}H NMR and MALDI-TOF-MS. Figure 14 shows the ^{1}H NMR spectra of poly(MA-*co*-**1**), poly(MA-*co*-**2**), and poly(*n*BA-*co*-**1**), which were purified by preparative SEC to remove the residual monomers and catalysts. In all the spectra of the copolymers, broad and relatively large peaks (*a–g, h–m*) were observed, assignable to the main chain protons of the repeating units of the acrylates and the polyesters. In addition to these signals, the spectra showed a series of sharp peaks (*a'–j'*), which indicates the presence of the unconjugated C=C double and the active C–Cl bonds at the chain ends of the products. The M_ns calculated from the terminal (*a'*) to the main-chain protons (*f, j*) [M_n (NMR) = 1200, 1100, 2100] were almost the same as that obtained by SEC [M_n (SEC) = 1200, 1000, 2200]. These results indicate that ideal simultaneous chain- and step-growth polymerizations proceeded to give copolymers of polyacrylates and polyesters.

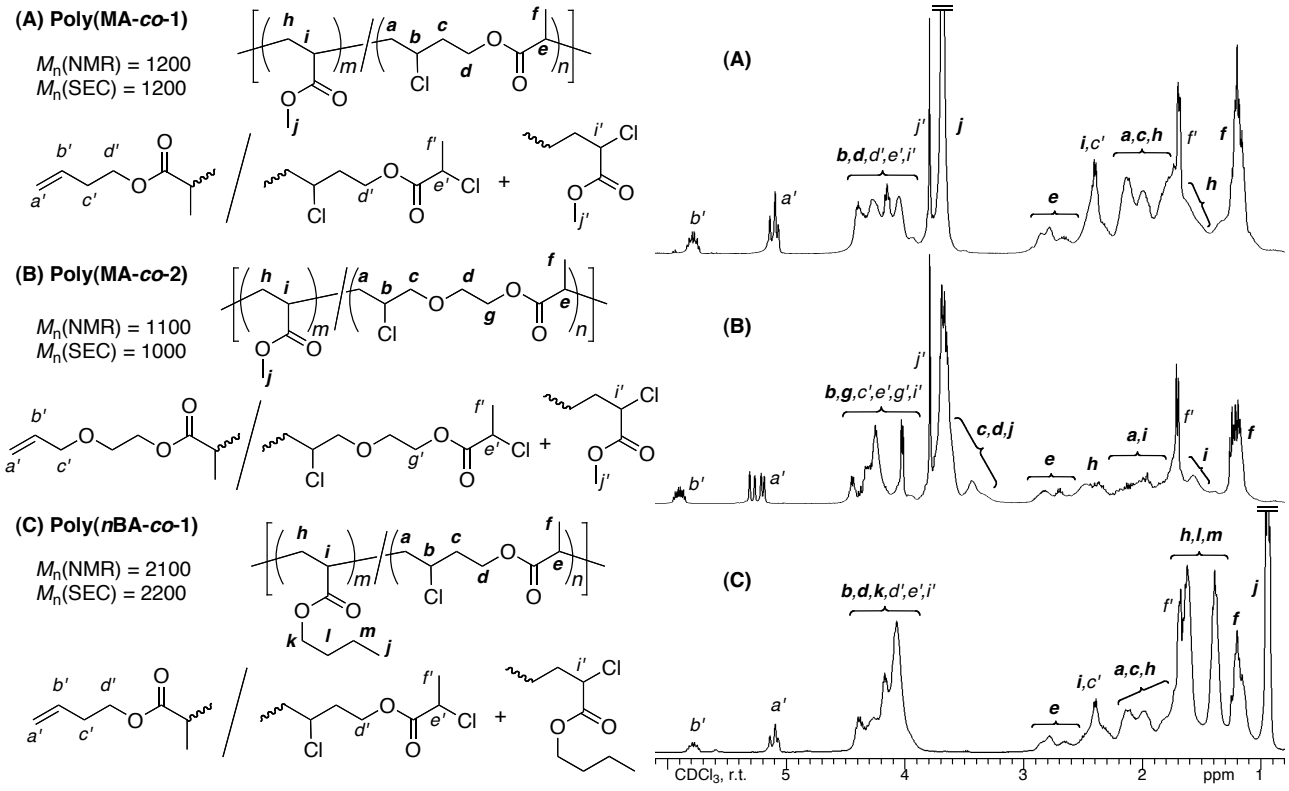

Figure 14. ^{1}H NMR spectra of (A) poly(MA-*co*-**1**), (B) poly(MA-*co*-**2**), and (C) poly(*n*BA-*co*-**1**) obtained with CuCl/HMTETA in toluene at 80 °C ($CDCl_3$, r.t.).

Figure 15 shows the MALDI-TOF-MS spectra of poly(MA-*co*-**1**), poly(MA-*co*-**2**), and poly(*n*BA-*co*-**1**). All the spectra show a series of peaks separated by the formula weight of each monomer unit. The molecular weights of each individual peak were very close to the calculated values; *i.e.*, multiples of the molecular weight of both monomers plus the sodium ion from the salt for the MS analysis. For example, in the spectrum of poly(MA-*co*-**1**), a series of 6-mers peaks ($m + n = 6$; circles) consists of the higher populations of 2-, 3-, or 4-units of MA and **1** [(m,n) = (2,4), (3,3), (4,2)] and lower peaks of other combinations [(m,n) = (1,5), (5,1)] (Figure 15A). This result supports that each monomer unit was randomly distributed in the main chain via the simultaneous polymerizations. A similar random sequence was also observed for poly(MA-*co*-**2**) (Figure 15B) and poly(*n*BA-*co*-**1**) (Figure 15C).

4. Simultaneous Polymerization of Various Monomers. *N*,*N*-dimethylaminoethyl (DMAEA) and 2-hydroxyethyl acrylate (HEA) are the one of the common functional acrylates. An equimolar mixture of DMAEA or HEA and **1** was copolymerized with the same catalytic system, as summarized in Table 1 (entries 15, 17). More detailed data are plotted in Figures 16 and 17. The polymerization of DMAEA with **1** proceeded slower than those of alkyl acrylates, in which the molecular weights of the obtained copolymer were relatively low ($M_w \sim 2000$). A similar retardation was reported for the chain-growth living polymerization of DMAEA.[29] For HEA, the monomers were smoothly consumed to afford the relatively high molecular weight polymers ($M_w \sim 9000$), although the molecular weights distributions became broad at high conversion ($M_w/M_n \sim 7.0$). Thus, this method proved effective for the synthesis of pendant-functionalized copolymers of polyacrylates and polyesters with amino or hydroxy groups derived from conjugated vinyl monomers.

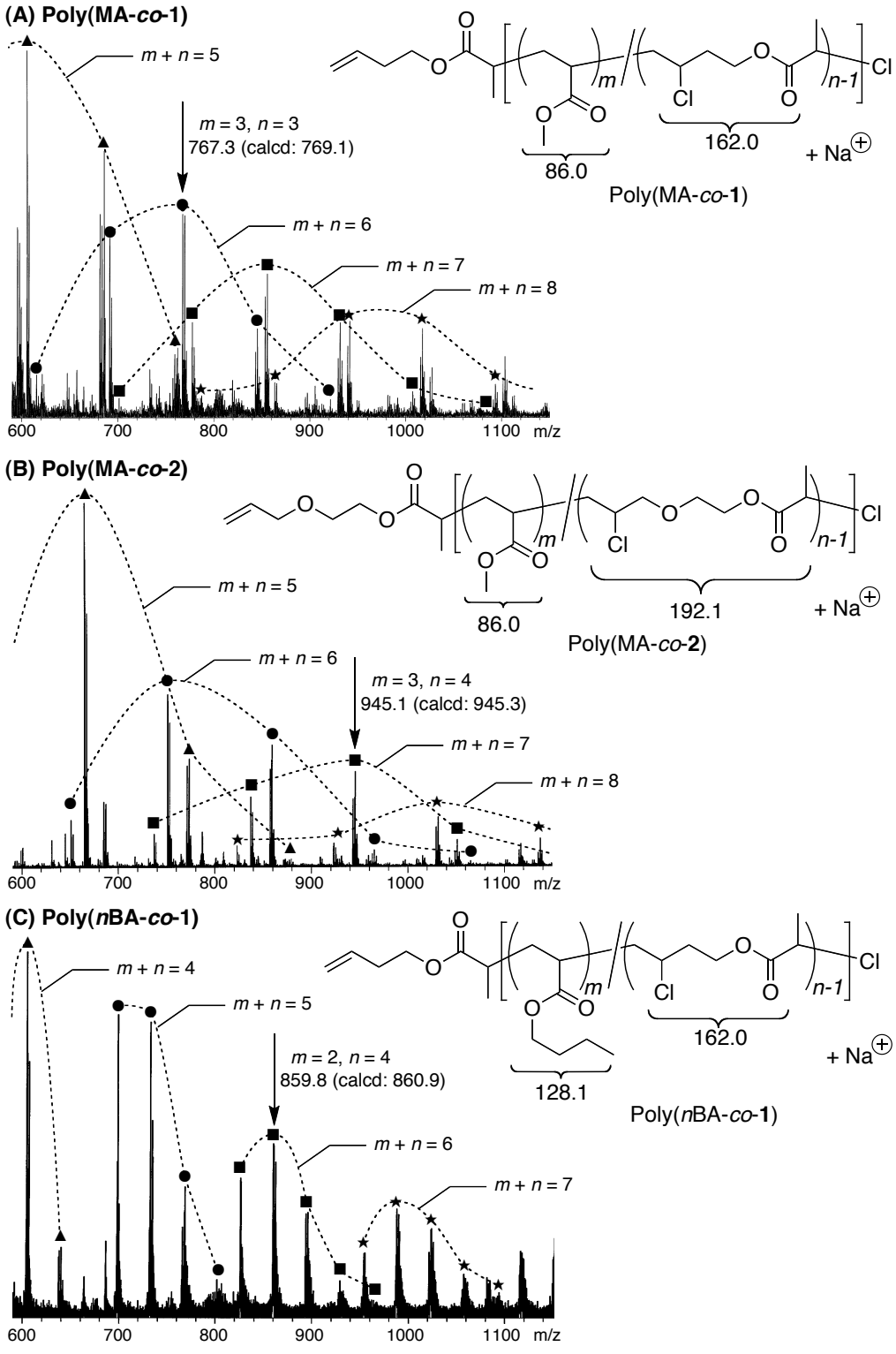

Figure 15. MALDI-TOF-MS spectra of (A) poly(MA-*co*-**1**) (M_n = 1200, M_w/M_n = 2.28) (B) poly(MA-*co*-**2**) (M_n = 1000, M_w/M_n = 2.18), and (C) poly(*n*BA-*co*-**1**) (M_n = 2200, M_w/M_n = 2.37) obtained with CuCl/HMTETA: [MA, EA, *n*BA, or *t*BA]$_0$ = 2.0 M; [**1**]$_0$ = 2.0 M; [CuCl]$_0$ = 100 mM; [HMTETA]$_0$ = 100 mM in toluene at 80 °C.

Table 1. Metal-Catalyzed Simultaneous Chain- and Step-Growth Radical Polymerization of Various Acrylates and **1**–**4**.

entry	Monomers	$[M]_0$, M	time, h	Conversion, %[b]	M_w[c]	M_w/M_n[c]
1[a]	MA/**1**	2.0/2.0 (1/1)	600	>99/98	6100	2.79
2[e]	MA/**1**	9.75/0.25 (39/1)	2000	>99/>99	36200	3.69
3[a]	EA/**1**	2.0/2.0 (1/1)	1200	>99/97	5900	2.65
4[f]	EA/**1**	7.8/0.20 (39/1)	220	>99/>99	41100	3.33
5[a]	MA/**2**	2.0/2.0 (1/1)	2500	>99/93	2400	2.16
6[f]	EA/**2**	7.8/0.20 (39/1)	320	>99/>99	28800	2.44
7[a]	MA/**3**	2.0/2.0 (1/1)	410	86/93	520	1.29
8[f]	EA/**3**	7.8/0.20 (39/1)	1400	>99/>99	16000	1.62
9[a]	MA/**4**	2.0/2.0 (1/1)	2500	79/42	2200	2.50
10[f]	EA/**4**	7.8/0.20 (39/1)	530	>99/>99	29300	1.85
11[a]	*n*BA/**1**	2.0/2.0 (1/1)	410	>99/96	5200	2.55
12[f]	*n*BA/**1**	6.24/0.16 (39/1)	1600	>99/>99	42100	2.69
13[a]	*t*BA/**1**	2.0/2.0 (1/1)	140	>99/97	4100	2.83
14[f]	*t*BA/**1**	6.24/0.16 (39/1)	1900	>99/>99	37100	2.37
15[a]	DMAEA/**1**	2.0/2.0 (1/1)	360	>99/82	2000	3.19
16[f]	DMAEA/**1**	5.85/0.15 (39/1)	360	>99/>99	14000	2.03
17[a]	HEA/**1**	2.0/2.0 (1/1)	50	>99/63	8900	6.80
18[f]	HEA/**1**	7.8/0.20 (39/1)	10	95/>99	109800	8.30

[a]$[CuCl]_0$ = 100 mM, [1,1,4,7,10,10-hexamethyltriethylenetetramine (HMTETA)]$_0$ = 100 mM, in toluene. [b]Determined by gas chromatography. [c]The weight-average molecular weight (M_w) and distribution (M_w/M_n) were determined by size-exclusion chromatography. [e]$[CuCl]_0$ = 10 mM, $[CuCl_2]_0$ = 10 mM. [f]$[CuCl]_0$ = 50 mM, $[CuCl_2]_0$ = 50 mM.

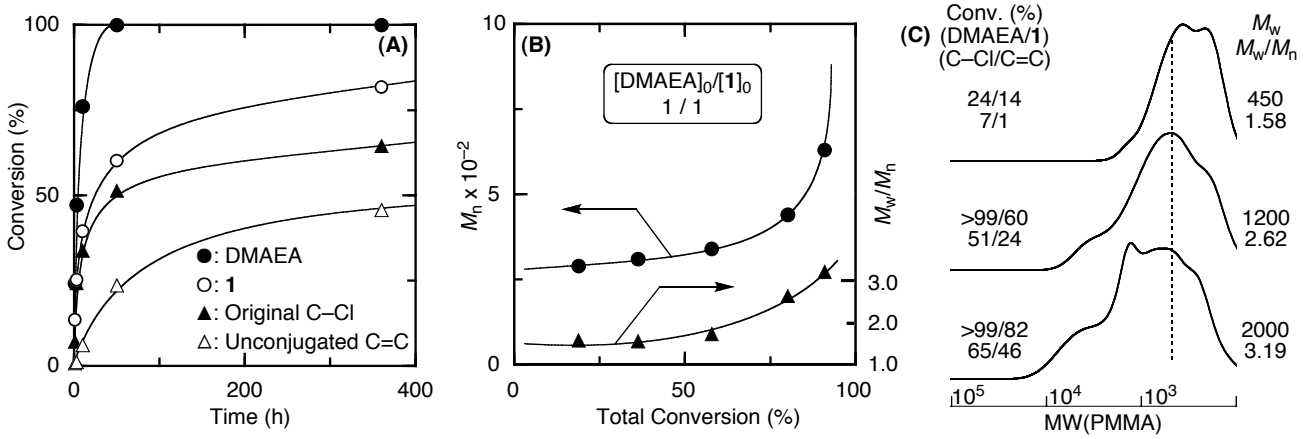

Figure 16. Simultaneous chain- and step-growth radical polymerization of DMAEA and **1** in toluene at 80 °C: $[DMAEA]_0$ = 2.0 M; $[\mathbf{1}]_0$ = 2.0 M; $[CuCl]_0$ = 100 mM; $[HMTETA]_0$ = 100 mM. (A) Consumption of DMAEA and **1** measured by gas chromatography and original C–Cl and unconjugated C=C bonds measured by ^{1}H NMR. (B) M_n and M_w/M_n values of the obtained copolymers vs total monomer conversion of DMAEA and **1**. (C) Size-exclusion chromatograms of the obtained copolymers of DMAEA and **1**.

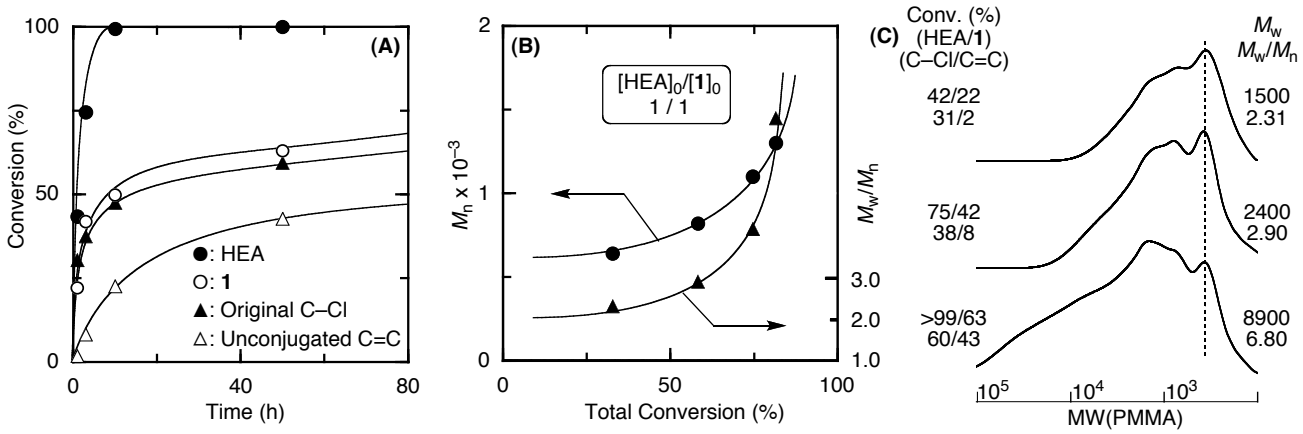

Figure 17. Simultaneous chain- and step-growth radical polymerization of HEA and **1** in toluene at 80 °C: $[HEA]_0$ = 2.0 M; $[\mathbf{1}]_0$ = 2.0 M; $[CuCl]_0$ = 100 mM; $[HMTETA]_0$ = 100 mM. (A) Consumption of HEA and **1** measured by gas chromatography and original C–Cl and unconjugated C=C bonds measured by ^{1}H NMR. (B) M_n and M_w/M_n values of the obtained copolymers vs total monomer conversion of HEA and **1**. (C) Size-exclusion chromatograms of the obtained copolymers of HEA and **1**.

A series of copolymerization of acrylates and ester- or amide-linked monomers with different monomer feed ratios was carried out with CuCl/HMTETA in bulk at 80 °C ($[\text{acrylate}]_0/[\mathbf{1}–\mathbf{4}]_0$ = 39/1), as summarized in Table 1 (entries 2, 4, 6, 8, 10, 12, 14, 16, 18 and Figure 18–26). In all cases, both of the monomers were simultaneously and quantitatively consumed. The molecular weights of the obtained copolymers were higher than those of the products obtained from an equimolar mixture of two monomers. These results indicate that the simultaneous polymerization enables the facile incorporation of a small amount of various functional groups into the C–C backbone of acrylate homopolymer to lead further application. For example, the obtained copolymers from EA and **3** could be easily degraded by the cleavage of the disulfide linkage as well as the ester linkage in the main-chain originating from **3** to afford the living homopolymer in the presence of reducing agents such as *n*-tributylphophine (P*n*Bu$_3$) and dithiothreitol (DTT)[30–32] or using Na_2CO_3 and methanol, respectively (Figure 27).

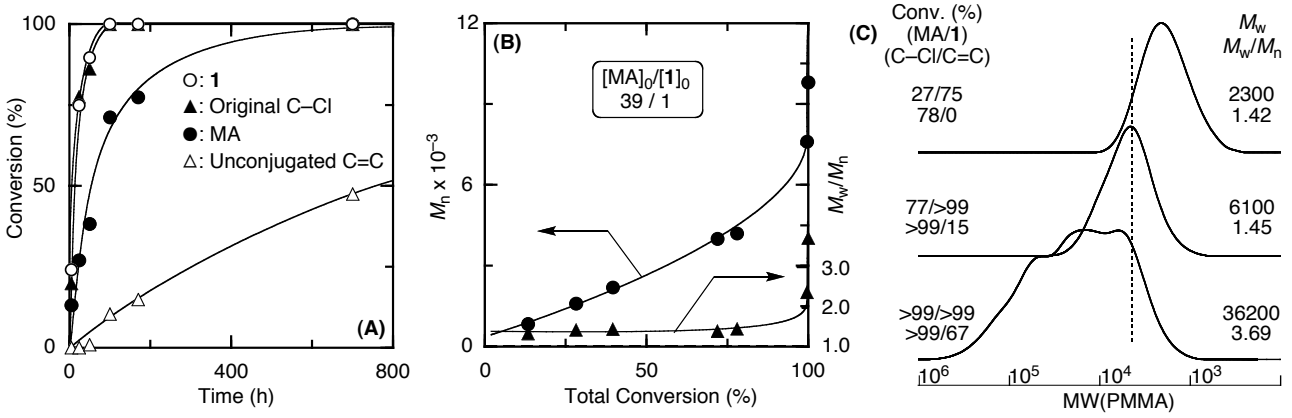

Figure 18. Simultaneous chain- and step-growth radical polymerization of MA and **1** in bulk at 80 °C: $[\text{MA}]_0$ = 9.75 M; $[\mathbf{1}]_0$ = 0.25 M; $[\text{CuCl}]_0$ = 10 mM; $[\text{CuCl}_2]_0$ = 10 mM; $[\text{HMTETA}]_0$ = 50 mM. (A) Consumption of MA and **1** measured by gas chromatography and original C–Cl and unconjugated C=C bonds measured by ^{1}H NMR. (B) M_n and M_w/M_n values of the obtained copolymers vs total monomer conversion of MA and **1**. (C) Size-exclusion chromatograms of the obtained copolymers of MA and **1**.

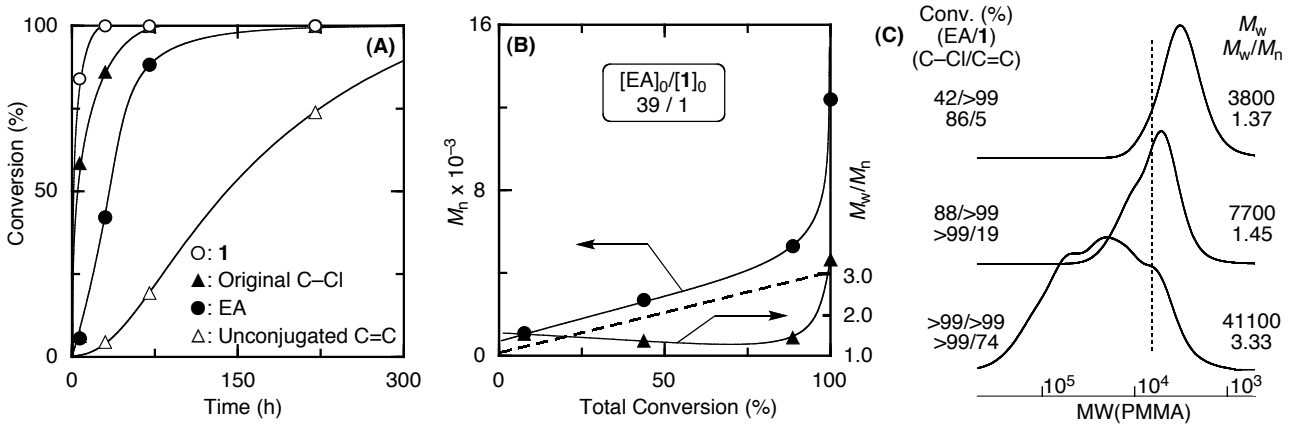

Figure 19. Simultaneous chain- and step-growth radical polymerization of EA and **1** in bulk at 80 °C: $[EA]_0$ = 7.8 M; $[\mathbf{1}]_0$ = 0.20 M; $[CuCl]_0$ = 50 mM; $[CuCl_2]_0$ = 50 mM; $[HMTETA]_0$ = 100 mM. (A) Consumption of EA and **1** measured by gas chromatography and original C–Cl and unconjugated C=C bonds measured by ^{1}H NMR. (B) M_n and M_w/M_n values of the obtained copolymers vs total monomer conversion of EA and **1**. (C) Size-exclusion chromatograms of the obtained copolymers of EA and **1**.

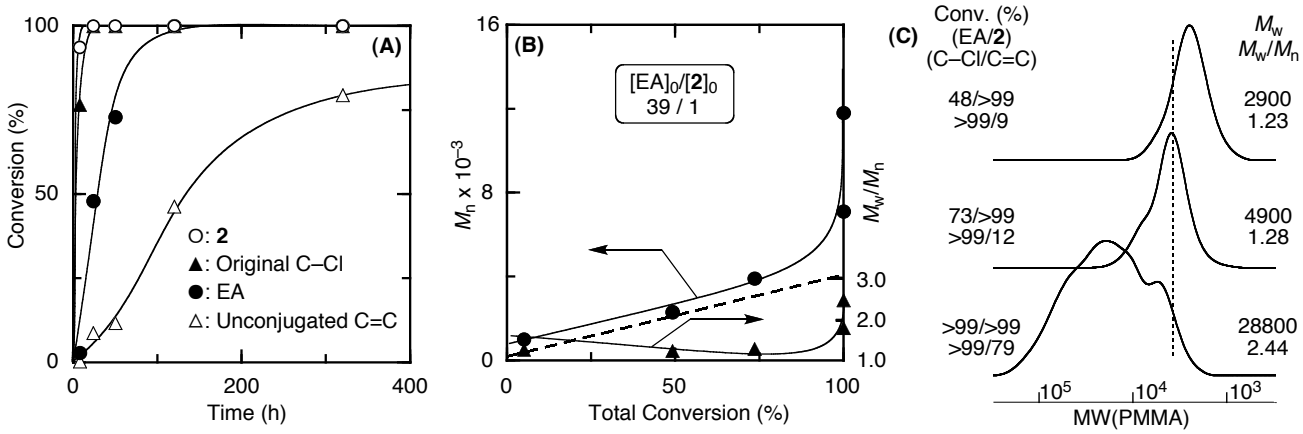

Figure 20. Simultaneous chain- and step-growth radical polymerization of EA and **1** in bulk at 80 °C: $[EA]_0$ = 7.8 M; $[\mathbf{2}]_0$ = 0.20 M; $[CuCl]_0$ = 50 mM; $[CuCl_2]_0$ = 50 mM; $[HMTETA]_0$ = 100 mM. (A) Consumption of EA and **2** measured by gas chromatography and original C–Cl and unconjugated C=C bonds measured by ^{1}H NMR. (B) M_n and M_w/M_n values of the obtained copolymers vs total monomer conversion of EA and **2**. (C) Size-exclusion chromatograms of the obtained copolymers of EA and **2**.

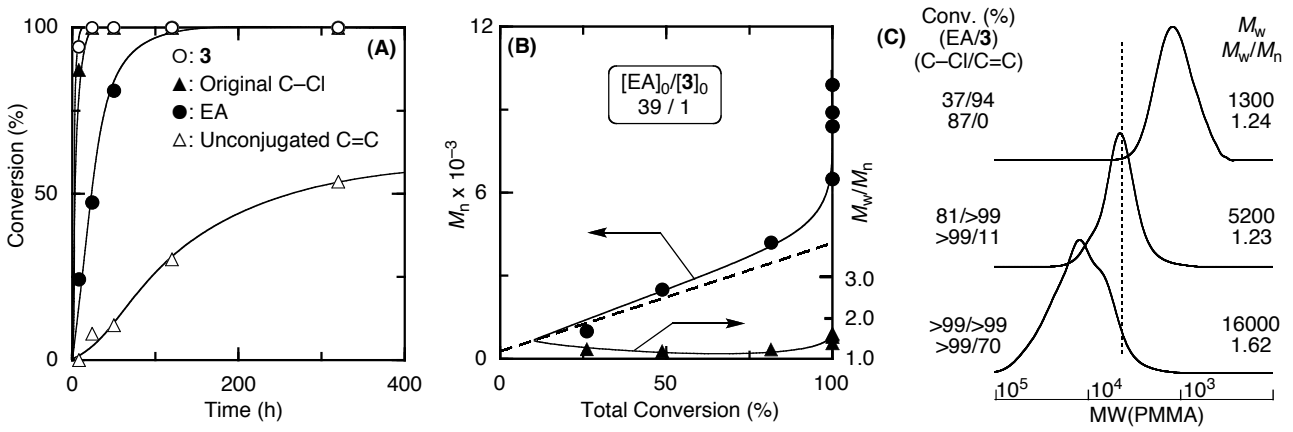

Figure 21. Simultaneous chain- and step-growth radical polymerization of EA and **3** in bulk at 80 °C: $[EA]_0$ = 7.8 M; $[\mathbf{3}]_0$ = 0.20 M; $[CuCl]_0$ = 50 mM; $[CuCl_2]_0$ = 50 mM; $[HMTETA]_0$ = 100 mM. (A) Consumption of EA and **3** measured by gas chromatography and original C–Cl and unconjugated C=C bonds measured by ^{1}H NMR. (B) M_n and M_w/M_n values of the obtained copolymers vs total monomer conversion of EA and **3**. (C) Size-exclusion chromatograms of the obtained copolymers of EA and **3**.

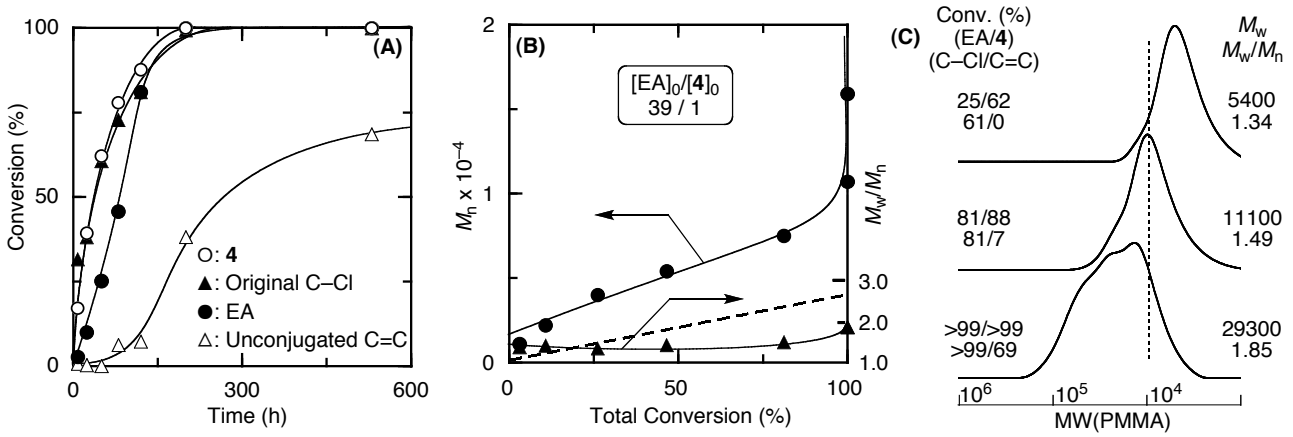

Figure 22. Simultaneous chain- and step-growth radical polymerization of EA and **4** in bulk at 80 °C: $[EA]_0$ = 7.8 M; $[\mathbf{4}]_0$ = 0.20 M; $[CuCl]_0$ = 50 mM; $[CuCl_2]_0$ = 50 mM; $[HMTETA]_0$ = 100 mM. (A) Consumption of EA and **4** measured by gas chromatography and original C–Cl and unconjugated C=C bonds measured by ^{1}H NMR. (B) M_n and M_w/M_n values of the obtained copolymers vs total monomer conversion of EA and **4**. (C) Size-exclusion chromatograms of the obtained copolymers of EA and **4**.

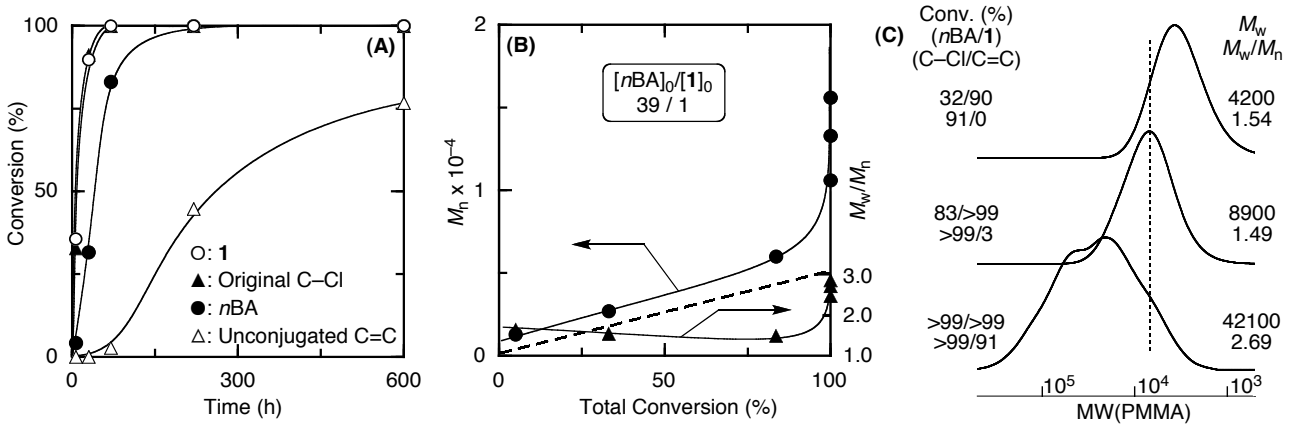

Figure 23. Simultaneous chain- and step-growth radical polymerization of *n*BA and **1** in bulk at 80 °C: $[n\text{BA}]_0$ = 6.24 M; $[\mathbf{1}]_0$ = 0.16 M; $[\text{CuCl}]_0$ = 50 mM; $[\text{CuCl}_2]_0$ = 50 mM; $[\text{HMTETA}]_0$ = 100 mM. (A) Consumption of *n*BA and **1** measured by gas chromatography and original C–Cl and unconjugated C=C bonds measured by ^{1}H NMR. (B) M_n and M_w/M_n values of the obtained copolymers vs total monomer conversion of *n*BA and **1**. (C) Size-exclusion chromatograms of the obtained copolymers of *n*BA and **1**.

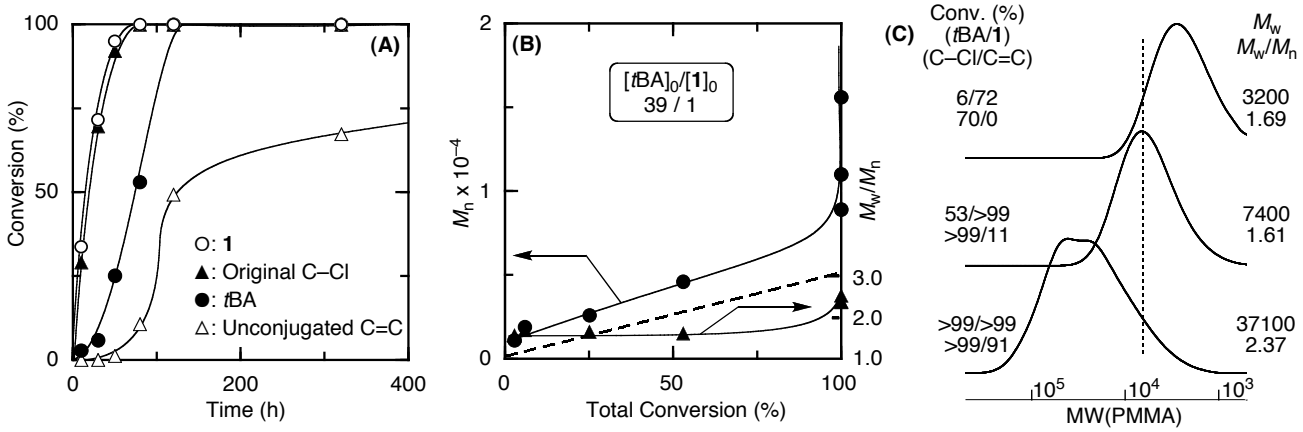

Figure 24. Simultaneous chain- and step-growth radical polymerization of *t*BA and **1** in bulk at 80 °C: $[t\text{BA}]_0$ = 6.24 M; $[\mathbf{1}]_0$ = 0.16 M; $[\text{CuCl}]_0$ = 50 mM; $[\text{CuCl}_2]_0$ = 50 mM; $[\text{HMTETA}]_0$ = 100 mM. (A) Consumption of *t*BA and **1** measured by gas chromatography and original C–Cl and unconjugated C=C bonds measured by ^{1}H NMR. (B) M_n and M_w/M_n values of the obtained copolymers vs total monomer conversion of *t*BA and **1**. (C) Size-exclusion chromatograms of the obtained copolymers of *t*BA and **1**.

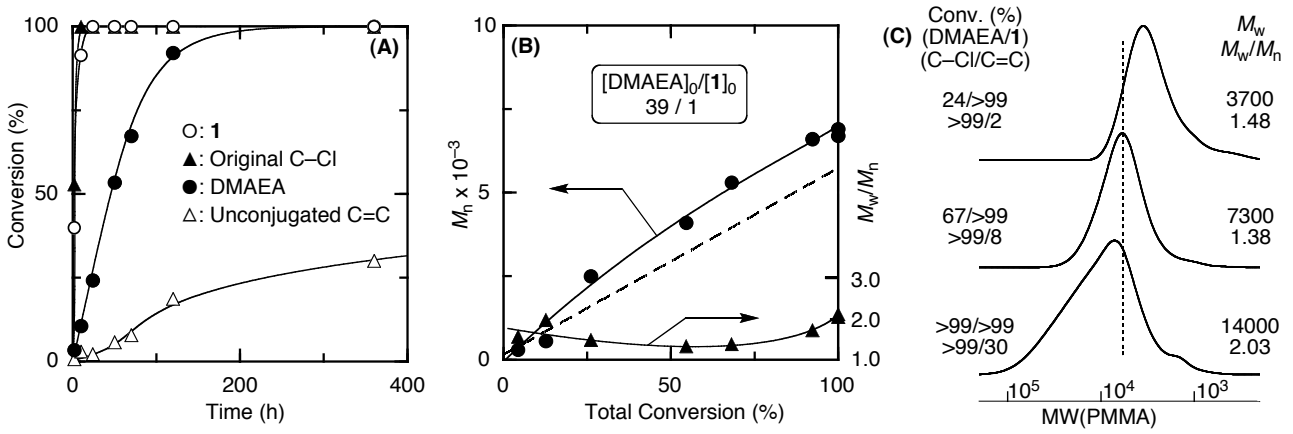

Figure 25. Simultaneous chain- and step-growth radical polymerization of DMAEA and **1** in bulk at 80 °C: $[DMAEA]_0$ = 5.85 M; $[\mathbf{1}]_0$ = 0.15 M; $[CuCl]_0$ = 50 mM; $[CuCl_2]_0$ = 50 mM; $[HMTETA]_0$ = 100 mM. (A) Consumption of DMAEA and **1** measured by gas chromatography and original C–Cl and unconjugated C=C bonds measured by ^{1}H NMR. (B) M_n and M_w/M_n values of the obtained copolymers vs total monomer conversion of DMAEA and **1**. (C) Size-exclusion chromatograms of the obtained copolymers of DMAEA and **1**.

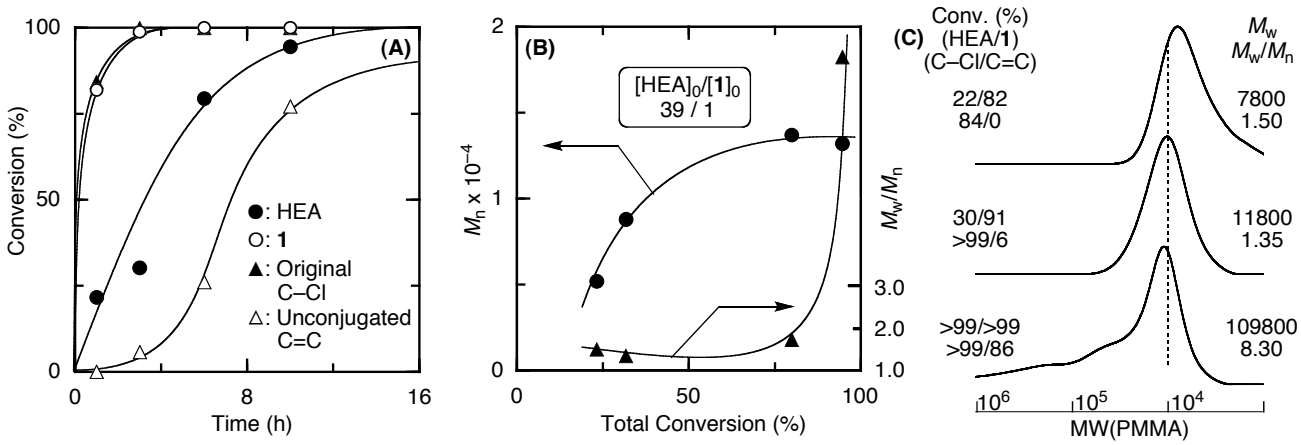

Figure 26. Simultaneous chain- and step-growth radical polymerization of HEA and **1** in bulk at 80 °C: $[HEA]_0$ = 5.85 M; $[\mathbf{1}]_0$ = 0.15 M; $[CuCl]_0$ = 50 mM; $[CuCl_2]_0$ = 50 mM; $[HMTETA]_0$ = 100 mM. (A) Consumption of HEA and **1** measured by gas chromatography and original C–Cl and unconjugated C=C bonds measured by ^{1}H NMR. (B) M_n and M_w/M_n values of the obtained copolymers vs total monomer conversion of HEA and **1**. (C) Size-exclusion chromatograms of the obtained copolymers of HEA and **1**.

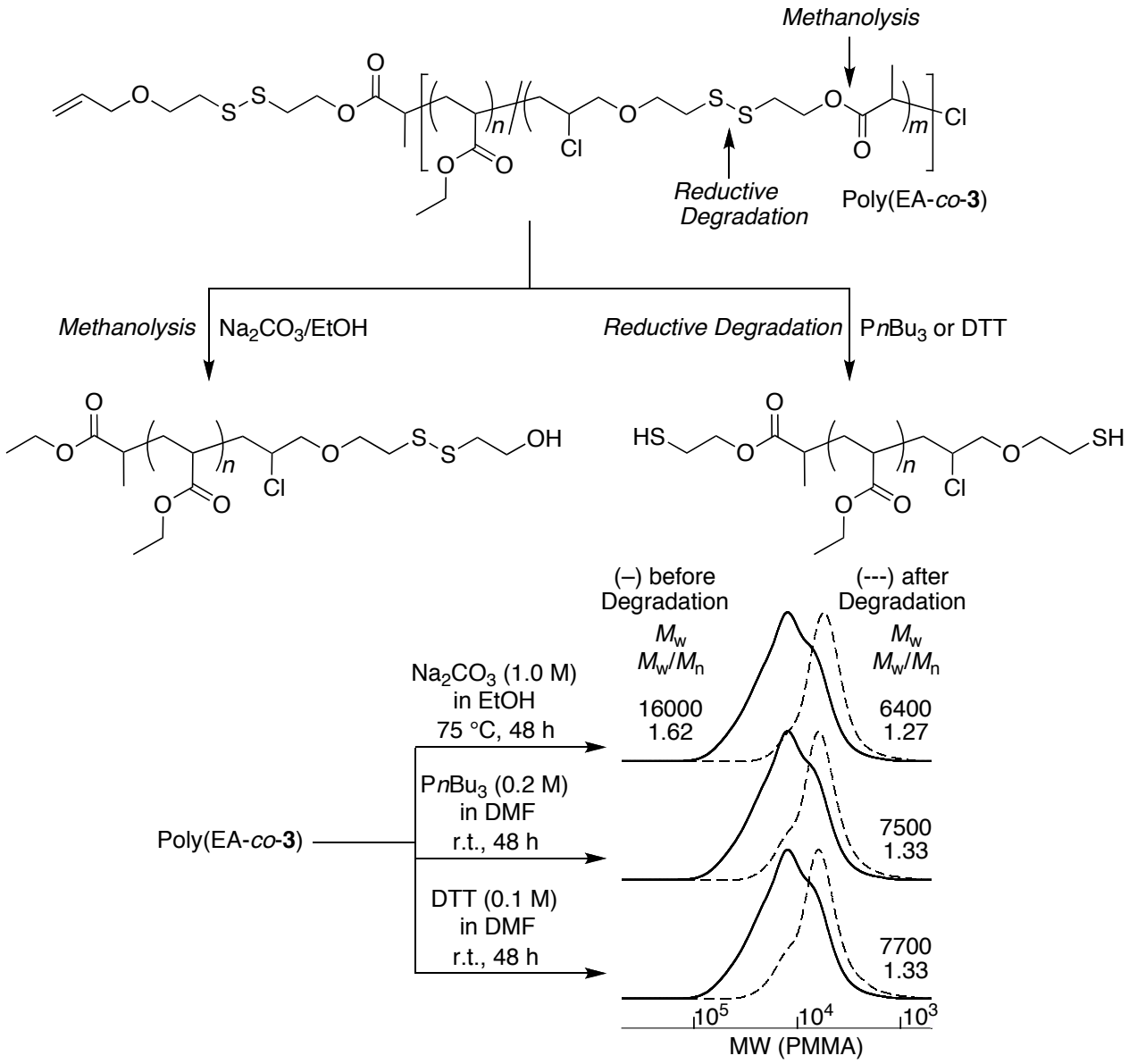

Figure 27. Size-exclusion chromatograms of poly(EA-*co*-**3**) (solid lines) and the degraded copolymers (dashed lines) by (A) methanolysis or reductive degradation using (B) P*n*Bu$_3$ or (C) DTT.

5. Simultaneous Polymerization of Styrene and 1. The simultaneous polymerization of styrene with **1** was attempted with CuCl/HMTETA in bulk at 80 °C, in which the initial charge ratios of two monomers were 50 to 1 (Figure 28). For the polymerization of styrene as a vinyl monomer, the highly selective chain-growth living polymerization completely proceeded first, and

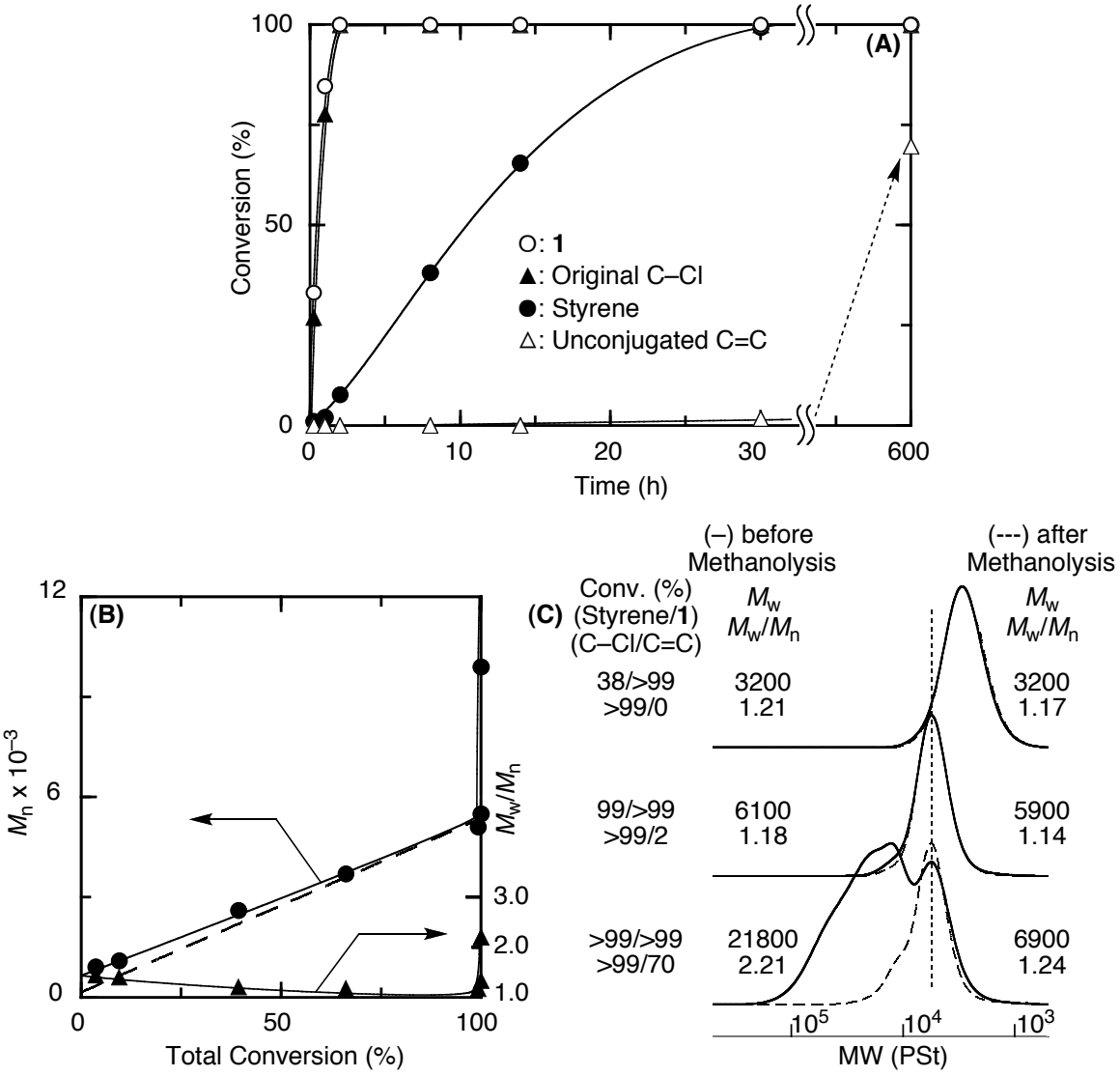

Figure 28. Simultaneous chain- and step-growth radical polymerization of styrene and **1** with CuCl/HMTETA in bulk at 80 °C: $[\text{styrene}]_0$ = 7.5 M; $[\mathbf{1}]_0$ = 0.15 M; $[\text{CuCl}]_0$ = 100 mM; $[\text{HMTETA}]_0$ = 100 mM. (A) Consumption of styrene, original C–Cl, and unconjugated C=C bonds measured by ^{1}H NMR and consumption of **1** measured by gas chromatography. (B) M_n and M_w/M_n values of the obtained copolymers vs total monomer conversion of styrene and **1**. The diagonal black dotted line indicates the calculated M_n assuming the formation of one living polymer of styrene per one **1** molecule. (C) Size-exclusion chromatograms of the obtained copolymers (solid lines) and the methanolyzed products (dashed lines).

then the much slow step-growth polymerization took place between the living polystyrene chains. Namely, the consumption rate of styrene was much greater than that of the unconjugated C=C double bond. This result is due to lower relative rate for addition of styryl radical than acrylic one to unconjugated C=C bond. The molecular weights of the products increased in direct proportion to the total monomer conversion in the initial stage and agreed well with the calculated values assuming that one living polymer chain is generated from one molecule of **1**. In addition, the SEC curves little changed by the methanolysis, which indicates that the chain-growth living radical polymerization of styrene quantitatively proceeded from the C–Cl bond in **1** to give polystyrene with narrow molecular weight distributions without significant step-growth propagation. After the complete consumption of styrene (>99%), the molecular weights values progressively increased and the SEC curves became multimodal as the unconjugated C=C bonds consumed. The methanolysis resulted in the unimodal SEC curve for the products in the later stage of the polymerization. This indicates that the step-growth polyaddition of the living polystyrenes obtained by the highly selective chain-growth polymerization proceeded between the C–Cl bond at the ω-end and the C=C bond at the α-end not via polymer–polymer coupling at the ω-ends.

Conclusions

The simultaneous chain- and step-growth radical polymerization proceeded for a series of conjugated vinyl monomers such as acrylate derivatives and styrene and ester- or amide-linked monomers possessing both an unconjugated C=C and active C–Cl bonds. This synthetic strategy could provide various novel random copolymers of vinyl polymer and polyester or polyamide. The functionalized copolymers were synthesized by the incorporation of functional groups in the pendant groups of the vinyl monomers as well as between the C=C and C–Cl groups in the

step-growth monomers. The simultaneous polymerization can thus widen the scope of material design based on the well-defined novel copolymer structures.

EXPERIMENTAL SECTION

Materials

MA (TCI, >99%), EA (TCI, >99%), *n*BA (TCI, >99%), *t*BA (TCI, >99%), DMAEA (TCI, >99%), HEA (TCI, >96%), and styrene (TCI, >99%) were distilled from calcium hydride under reduced pressure before use. 3-Butenyl 2-chloropropionate (**1**), 2-(allyloxy)ethyl 2-chloropropionate (**2**), and allyl 2-chloropropanamide (**4**) were synthesized according to the literature.[25,28] CuCl (Aldrich, 99.99%) was used as received. All metal compounds were handled in a glovebox (VAC Nexus) under a moisture- and oxygen-free argon atmosphere (O_2, < 1 ppm). Toluene was distilled over sodium benzophenone ketyl and bubbles with dry nitrogen for 15 min just before use. HMTETA (Aldrich, 97%) was distilled from calcium hydride before use.

Monomer Synthesis (3)

2-((2-(allyoxy)ethyl)disulfanyl)ethyl 2-chloropropionate (**3**) was synthesized by two steps reaction. Firstly, synthesis of the corresponding alcohol from allyl bromide (KANTO, >99%) and 2-hydroxyethyldisulfide (Aldrich), then synthesis of the monomer from the obtained alcohol and 2-chloropropionyl chloride (TCI, >95%). The details are as follows: the reaction was carried out by the use of a syringe technique under a dry argon atmosphere in an oven-dried glass tube equipped with three-way stopcocks. Allyl bromide (17.3 mL, 0.20 mol) was added dropwise with vigorous stirring to a solution of 2-hydroxyethyldisulfide (97.8 mL, 0.80 mol) and NaOH (8.8 g,

0.22 mol) in dry DMF (84.9 mL) at room temperature. The solution was heated to 70 °C for 24 h. After the dilution with diethyl ether, the mixture was washed with the aqueous solution of NaCl and was evaporated to remove the solvents. The crude product was purified by column chromatography on silica gel with diethyl ether as an eluent to give pure 2-((2-(allyoxy)ethyl)disulfanyl)ethanol (13.1 g, 0.067 mol; yield = 33.6%, purity >99%).

2-Chloropropionyl chloride (6.9 mL, 0.071 mol) was added dropwise with vigorous stirring to a solution of 2-((2-(allyoxy)ethyl)disulfanyl)ethanol (13.1 g, 0.067 mol) thus obtained and triethylamine (10.4 mL, 0.075 mol) in dry THF (37.6 mL) at 0 °C. The mixture kept stirred for 1 h at 0 °C, and then over 12 h at room temperature. After the dilution with diethyl ether, the mixture was washed with the aqueous solution of $NaHCO_3$ and then NaCl and was evaporated to remove the solvents. The crude product was purified by column chromatography on silica gel with toluene as an eluent to give pure 2-((2-(allyoxy)ethyl)disulfanyl)ethyl 2-chloropropionate (**3**) (7.7 mL, 0.034 mol; yield = 51.3%, purity >99%). ^{1}H NMR ($CDCl_3$) d/ppm: 1.70 (d, 3H, CH–C*H*$_3$, *J* = 6.9 Hz), 2.91, 2.95 (t, t, 2H, 2H, OCH$_2$C*H*$_2$S, SC*H*$_2$CH$_2$O, *J* = 6.6 Hz, *J* = 6.6 Hz), 3.68 (t, 2H, OC*H*$_2$CH$_2$S, *J* = 6.6 Hz), 4.01 (dt, 2H, CH$_2$=CHC*H*$_2$O, *J* = 1.3, 4.5 Hz), 4.40 (q, 1H, C*H*–CH$_3$, *J* = 6.9 Hz), 4.43 (t, 2H, SCH$_2$C*H*$_2$O, *J* = 6.6 Hz), 5.23 (m, 2H, C*H*$_2$=CH), 5.89 (m, 1H, CH$_2$=C*H*).

Polymerization

Polymerization was carried under dry nitrogen in baked glass tubes equipped with a three-way stopcock. A typical example for the polymerization procedure is given below. To a suspension of CuCl (39.6 mg, 0.40 mmol) in toluene (1.91 mL) was added HMTETA (0.11 mL, 0.40 mmol), and the mixture kept stirred for 12 h at 80 °C to give a heterogeneous solution of

CuCl/HMTETA complex. After the solution was cooled to the room temperature, MA (0.72 mL, 8.0 mmol) and 3-butenyl 2-chloropropionate (**1**) (1.26 mL, 8.0 mmol) were added. The solution was evenly charged in 7 glass tubes and the tubes were sealed by flame under nitrogen atmosphere. The tubes were immersed in thermostatic oil bath at 80 °C. In predetermined intervals, the polymerization was terminated by cooling the reaction mixtures to –78 °C. Monomer conversion was determined from the concentration of residual monomer measured by gas chromatography with toluene as an internal standard. The conversions of the functional groups (C=C and C–Cl) of **1** were determined from the concentration of C=C and C–Cl by ^{1}H NMR spectroscopy with toluene as an internal standard.

Methanolysis

Methanolysis of the copolymers was carried under dry nitrogen in baked glass tubes equipped with a three-way stopcock. A portion of the obtained poly(MA-*co*-**1**) (30 mg) was dispersed in CH_3OH (30 mL) containing Na_2CO_3 (3.2 g) and the solution was refluxed for 48 h. After the dilution with toluene, the product was washed with distilled water and evaporated to remove the solvents to result in the mehanolyzed products (13 mg).[33]

Reductive degradation

The poly(EA-*co*-**3**) (5.0 mg) was dissolved in DMF (0.5 mL) containing DTT (7.7 mg) or P*n*Bu$_3$ (0.025 ml) and the solution was kept at room temperature for 2 days. The sample was analyzed by SEC.[30]

Measurements

Monomer conversion was determined from the concentration of residual monomer measured by gas chromatography [Shimadzu GC-8A equipped with a thermal conductivity detector and a 3.0 mm i.d. × 2 m stainless-steel column packed with SBS-200 (Shinwa Chemical Industries Ltd.) supported on Shimalite W; injection and detector temperature = 200 °C, column temperature = 140 °C] with toluene as an internal standard under He gas flow. The conversions of the functional groups (C=C and C–Cl) of step-growth monomer were determined from the concentration of C=C and C–Cl by ^{1}H NMR spectroscopy with toluene as an internal standard. ^{1}H NMR spectra were recorded in $CDCl_3$ at 25 °C on a JEOL ECS–400 or a Varian Gemini 2000 spectrometer, operating at 400 MHz. The number-average molecular weight (M_n), weight-average molecular weight (M_w), and the molecular weight distribution (M_w/M_n) of the product polymers were determined by size-exclusion chromatography (SEC) in THF at 40 °C on two polystyrene gel columns [Shodex K-805L (pore size: 20–1000 Å; 8.0 mm i.d. × 30 cm); flow rate 1.0 mL/min] connected to Jasco PU-980 precision pump and a Jasco 930-RI refractive index detector. The columns were calibrated against 8 standard poly(MMA) samples (Shodex; M_p = 202–1950000; M_w/M_n = 1.02–1.09) or 8 standard polystyrene samples (Shodex; M_p = 520–900000; M_w/M_n = 1.01–1.14). MALDI-TOF-MS spectra were measured on a SHIMADZU AXIMA-CFR Plus mass spectrometer (reflector mode) with dithranol (1,8,9-anthracenetriol) as the ionizing matrix and sodium trifluoroacetate as the ion source.

NOTES AND REFERENCES

(1) Georges, M. K.; Veregin, R. P. N.; Kazmaier, P. M.; Hamer, G. K. *Macromolecules* **1993**, *26*, 2987–2988.

(2) (a) Hawker, C. J. *J. Am. Chem. Soc.* **1994**, *116*, 11185–11186. (b) Hawker, C. J.; Bosman, A. W.; Harth, E. *Chem. Rev.* **2001**, *101*, 3661–3688.

(3) (a) Kato, M.; Kamigaito, M.; Sawamoto, M.; Higashimura, T. *Macromolecules* **1995**, *28*, 1721–1723. (b) Kamigaito, M.; Ando, T.; Sawamoto, M. *Chem. Rev.* **2001**, *101*, 3689–3746. (c) Kamigaito, M.; Ando, T.; Sawamoto, M. *Chem. Rec.* **2004**, *4*, 159–175. (d) Ouchi, M.; Terashima, T.; Sawamoto, M. *Chem. Rev.* **2009**, *109*, 4963–5050.

(4) (a) Wang, J.-S.; Matyjaszewski, K. *J. Am. Chem. Soc.* **1995**, *117*, 5614–5615. (b) Patten, T. E.; Xia, J.; Abernathy, T.; Matyjaszewski, K. *Science* **1996**, *272*, 866–868. (c) Matyjaszewski, K.; Xia, J. *Chem. Rev.* **2001**, *101*, 2921–2990. (d) Tsarevsky, N. V. Matyjaszewski, K.; *Chem. Rev.* **2007**, *107*, 2270–2299. (e) Braunecker, W. A.; Matyjaszewski, K. *Prog. Polym. Sci.* **2007**, *32*, 93–146.

(5) (a) Chiefari, J.; Chong, Y. K.; Ercole, F.; Krstina, J.; Jeffery, K.; Tam, P. T. Le.; Mayadunne, R. T. A.; Meijs, G. F.; Moad, C. L.; Moad, G.; Rizzardo, E.; Thang, S. H. *Macromolecules* **1998**, *31*, 5559–5562. (b) Chong, Y. K.; Krstina, J.; Tam, P. T. Le.; Moad, G.; Postma, A.; Rizzardo, E.; Thang, S. H. *Macromolecules* **2003**, *36*, 2256–2272. (c) Chiefari, J.; Mayadunne, R. T. A.; Moad, C. L.; Moad, G.; Rizzardo, E.; Postma, A.; Skidmoe, M. A.; Thang, S. H. *Macromolecules* **2003**, *36*, 2273–2283. (d) Moad, G.; Rizzardo, E.; Thang, S. H. *Aust. J. Chem.* **2005**, *58*, 379–410.

(6) (a) Percec, V.; Barboiu, B. *Macromolecules* **1995**, *28*, 7970–7972. (b) Rosen, B, M.; Percec, V. *Chem. Rev.* **2009**, *109*, 5069–5119.

(7) Granel, C.; Dubois, Ph.; Jérôme, R.; Teyssié, Ph. *Macromolecules* **1996**, *29*, 8576.

(8) Haddleton, D. M.; Jasieczek, C. B.; Hannon, M. J.; Shooter, A. J. *Macromolecules* **1997**, *30*, 2190.

(9) (a) Kharasch, M. S.; Jensen, E. V.; Urry, W. H. *Science* **1945**, *102*, 128. (b) Kharasch, M. S.; Urry, W. H. *J. Am. Chem. Soc.* **1945**, *67*, 1626–1626. (c) Matsumoto, H.; Nakano, T.; Nagai, Y. *Tetrahedron Lett.* **1973**, 5147–5150. (d) Minisci, F, *Acc. Chem. Res.* **1975**, *8*, 165–171. (e) Iqbal, J.; Bhatia, B.; Nayyar, N. K. *Chem. Rev.* **1994**, *94*, 519–564. (f) Gossage, R. A.; van de Kuil, L. A.; van Koten, G. *Acc. Chem. Res.* **1998**, *31*, 423–431. (g) Nagashima, H. In *Ruthenium in Organic Synthesis*; Murahashi, S.-I. Ed.; Wiley-VCH, Weinheim, 2004; pp. 333–343. (h) Delaude, L.; Demonceau, A.; Noels, A. F. *Top. Organomet. Chem.* **2004**, *11*, 155–171. (i) Pintauer, T.; Matyjaszewski, K. *Chem. Soc. Rev.* **2008**, *37*, 1087–1097. (j) Fernández-Zúmel, M. A.; Thommes, K.; Kiefer, G.; Sienkiewicz, A.; Pierzchala, K.; Severin, K. *Chem. Eur. J.* **2009**, *15*, 11601–11607.

(10) Kotani, Y.; Kato, M.; Kamigaito, M.; Sawamoto, M. *Macromolecules* **1996**, *29*, 6979–6982.

(11) (a) Ueda, J.; Matsuyama, M.; Kamigaito, M.; Sawamoto, M. *Macromolecules* **1998**, *31*, 557–562. (b) Ueda, J.; Kamigaito, M.; Sawamoto, M. *Macromolecules* **1998**, *31*, 6762–6768. (c) Baek, K.-Y.; Kamigaito, M.; Sawamoto, M. *Macromolecules* **2001**, *34*, 215–221. (d) Terashima, T.; Kamigaito, M.; Baek, K.-Y.; Ando, T.; Sawamoto, M. *J. Am. Chem. Soc.* **2003**, *125*, 5288–5289.

(12) (a) Roos, S. G.; Müller, A. H. E.; Matyjaszewski, K. *Macromolecules* **1999**, *32*, 8331–8335. (b) Haddleton, D. M.; Perrier, S.; Bon, S. A. F. *Macromolecules* **2000**, *33*, 8246–8251. (c) Cheng, G.; Böker, A.; Zhang, M.; Krausch, G.; Müller, A. H. E.; *Macromolecules* **2001**, *34*, 6883–6888. (d) Li, C.; Gunari, N.; Fischer, K.; Janshoff, A.; Schmidt, M. *Angew. Chem. Int. Ed.* **2004**, *43*, 1101–1104. (e) Miura, Y.; Satoh, K.; Kamigaito, M.; Okamoto, Y. *Polym. J.* **2006**, *38*, 930–939.

(13) (a) Ando, T.; Kamigaito, M.; Sawamoto, M. *Macromolecules* **1998**, *31*, 6708–6711. (b)

Coessens, V.; Matyjaszewski, K. *Macromol. Rapid Commun.* **1999**, *20*, 127–134. (c) Coessens, V.; Pyun, J.; Miller, P. J.; Gaynor, S. G.; Matyjaszewski, K. *Macromol. Rapid Commun.* **2000**, *21*, 103–109. (d) Bon, S. A. F.; Steward, A. G.; Haddleton, D. M. *J. Polym. Sci. Part A: Polym. Chem* **2000**, *38*, 2678–2686. (e) Coessens, V.; Pintauer, T.; Matyjaszewski, K. *Prog. Polym. Sci.* **2001**, *26*, 337–377. (f) Baek, K.-Y.; Kamigaito, M.; Sawamoto, M. *J. Polym. Sci. Part A: Polym. Chem.* **2002**, *40*, 1937–1944. (g) Nakatani, K.; Terashima, T.; Ouchi, M.; Sawamoto, M. *Macromolecules* **2010**, *43*, 8910–8916.

(14) (a) Gaynor, S. G.; Edelman, S.; Matyjaszewski, K. *Macromolecules* **1996**, *29*, 1079–1081. (b) Matyjaszewski, K.; Gaynor, S. G.; Kulfan, A.; Podwika, M. *Macromolecules* **1997**, *30*, 5192–5194. (c) Matyjaszewski, K.; Gaynor, S. G.; Müller, A. H. E. *Macromolecules* **1997**, *30*, 7034–7041. (d) Matyjaszewski, K.; Gaynor, S. G. *Macromolecules* **1997**, *30*, 7042–7049. (e) Matyjaszewski, K.; Pyun, J.; Gaynor, S. G. *Macromol. Rapid Commun.* **1998**, *19*, 665–670.

(15) Weimer, M. W.; Fréchet, J. M. J.; Gitsov, I. *J. Polym. Sci. Part A: Polym. Chem.* **1998**, *36*, 955–970.

(16) (a) Mori, H.; Böker, A.; Krausch, G.; Müller, A. H. E. *Macromolecules* **2001**, *34*, 6871–6882. (b) Bibiao, J.; Yang, Y.; Jian, D.; Shiyang, F.; Rongqi, Z.; Jianjun, H.; Wenyun, W. *J. Appl. Polym. Sci.* **2002**, *83*, 2114–2123. (c) Mori, H.; Seng, D. C.; Zhang, M.; Müller, A. H. E. *Langmuir* **2002**, *18*, 3682–3693. (d) Powell, K. T.; Cheng, C.; Wooley, K. L. *Macromolecules* **2007**, *40*, 4509–4515.

(17) Sugiyama, F.; Satoh, K.; Kamigaito, M. *Macromolecules* **2008**, *41*, 3042–3048.

(18) (a) Matyjaszewski, K.; Ziegler, M. J.; Arehart, S. V.; Greszta, D.; Pakula, T. *J. Phys. Org. Chem.* **2000**, *13*, 775–786. (b) Borner, H. G.; Duran, D.; Matyjaszewski, K.; da Silva, M.; Sheiko, S. S. *Macromolecules* **2002**, *35*, 3387–3394. (c) Nakatani, K.; Terashima, T.;

Sawamoto, M. *J. Am. Chem. Soc.* **2009**, *131*, 13600–13601.

(19) Koumura, K.; Satoh, K.; Kamigaito, M. *J. Polym. Sci. Part A: Polym. Chem.* **2009**, *47*, 1343–1353.

(20) (a) Sugiyama, Y.; Satoh, K.; Kamigaito, M.; Okamoto, Y. *J. Polym. Sci. Part A: Polym. Chem.* **2006**, *44*, 2086–2098. (b) Shibata, T.; Satoh, K.; Kamigaito, M.; Okamoto, Y. *J. Polym. Sci. Part A: Polym. Chem.* **2006**, *44*, 3609–3615. (c) Kamigaito, M.; Satoh, K. *J. Polym. Sci. Part A: Polym. Chem.* **2006**, *44*, 6147–6158. (d) Iizuka, Y.; Li, Z.; Satoh, K.; Kamigaito, M.; Okamoto, Y.; Ito, J.; Nishiyama, H. *Eur. J. Org. Chem.* **2007**, 782–791. (e) Kamigaito, M.; Satoh, K. *Macromolecules* **2008**, *41*, 269–276. (f) Satoh, K.; Kamigaito, M. *Chem. Rev.* **2009**, *109*, 5120–5156.

(21) Miura, Y.; Shibata, T.; Satoh, K.; Kamigaito, M.; Okamoto, Y. *J. Am. Chem. Soc.* **2006**, *128*, 16026–16027.

(22) Percec, V.; Barboiu, B.; Grigoras, C.; Bera, T. K. *J. Am. Chem. Soc.* **2003**, *125*, 6503–6516.

(23) (a) Miura, Y.; Kaneko, T.; Satoh, K.; Kamigaito, M.; Jinnai, H. Okamoto, Y. *Chem. Asian J.* **2007**, *2*, 662–672. (b) Miura, Y.; Satoh, K.; Kamigaito, M.; Okamoto, Y.; Kaneko, T.; Jinnai, H.; Kobukata, S. *Macromolecules* **2007**, *40*, 465–473.

(24) Koumura, K.; Satoh, K.; Kamigaito, M. *Macromolecules* **2009**, *42*, 2497–2504.

(25) (a) Satoh, K.; Mizutani, M.; Kamigaito, M. *Chem. Commun.* **2007**, 1260–1262. (b) Mizutani, M.; Satoh, K.; Kamigaito, M. *Macromolecules* **2009**, *42*, 472–480.

(26) Satoh, K.; Ozawa, S.; Mizutani, M.; Nagai, K.; Kamigaito, M. *Nat. Commun.* **2010**, *1*, 6.

(27) Mizutani, M.; Satoh, K.; Kamigaito, M. *J. Am. Chem. Soc.* **2010**, *132*, 7498–7507.

(28) Mizutani, M.; Satoh, K.; Kamigaito, M. *Macromolecules*, **2011**, in press.

(29) Zeng, F.; Shen, Y.; Zhu, S. *Macromol. Rapid Commun*. **2002**, *23*, 1113–1117.

(30) (a) Cleland, W. W. *Biochemistry* **1964**, *3*, 480–482. (b) Butler, J.; Spielberg, S. P.; Schulman, J. D. *Anal. Biochem.* **1976**, *75*, 674–675. (c) Jocelyn, P. C. *Methods Enzymol* **1987**, *143*, 246–256.

(31) (a) Humphrey, R. E.; Hawkins, J. M. *Anal. Chem.* **1964**, *36*, 1812–1814. (b) Humphrey, R. E.; Potter, J. L. *Anal. Chem.* **1965**, *37*, 146–147.

(32) (a) Tsarevsky, N. V.; Matyjaszewski, K. *Macromolecules* **2002**, *35*, 9009–9014. (b) Tsarevsky, N. V.; Matyjaszewski, K. *Macromolecules* **2005**, *38*, 3087–3092. (c) Gao, H.; Tsarevsky, N. V.; Matyjaszewski, K. *Macromolecules* **2005**, *38*, 5995–6004. (d) Wang, L.; Li, C.; Ryan, A. J.; Armes, S. P. *Adv. Mater.* **2006**, *18*, 1566–1570. (e) Li, C.; Madsen, J.; Armes, S. P.; Lewis, A. L. *Angew. Chem. Int. Ed.* **2006**, *45*, 3510–3513. (f) Paulusse, J. M. J.; Amir, R. J.; Evans, R. A.; Hawker, C. J. *J. Am. Chem. Soc.* **2009**, *131*, 9805–9812.

(33) Corey, E. J.; Achiwa, K. J.; Katzenellenbogen, A. *J. Am. Chem. Soc.* **1969**, *91*, 4318–4320.

Chapter 5

Degradable Poly(*N*-Isopropylacrylamide) with Tunable Thermosensitivity by Simultaneous Chain- and Step-Growth Radical Polymerization

ABSTRACT

A very fast metal-catalyzed simultaneous chain- and step-growth radical polymerization of *N*-Isopropylacrylamide (NIPAM) and ester- or amide-linked monomers was achieved at room temperature to afford the segmented poly(NIPAM) with controlled segment lengths connected by those linkages. The thermosensitivity of the polymer can be tuned from 24 to 40 °C by the comonomer and feed ratios. Furthermore, upon hydrolysis of the ester linkages in the main chains, the phase-transition temperature of poly(NIPAM) dramatically increased to 38–81 °C.

Introduction

Poly(*N*-isopropylacrylamide) [poly(NIPAM)] is one of the most attractive polymeric materials, because it has a thermal stimuli-responsive character in aqueous solutions.[1] The aqueous solution of poly(NIPAM) is well-known to exhibit a reversible liquid–solid phase transition with a lower critical solution temperature (LCST) between 31–35 °C. This thermoresponsive property has allowed this material to be used in interdisciplinary applications, such as biosensors and membranes, in the fields of bioengineering and nanotechnology. Recent efforts in developing the well-controlled radical polymerization of NIPAM have provided an insight into the influence of the primary structure of poly(NIPAM), such as the molecular weight and its distribution,[2] end-groups,[3] tacticity,[4] and block copolymers,[5] on the thermoresponsive properties. Among them, the CuCl/tris[2-(dimethylamino)ethyl]amine (Me_6TREN) system effectively induced fast and well-controlled polymerizations of acrylamides, including NIPAM, in specific solvents, such as DMF, 2-propanol, water and DMF/water mixture, to produce polymers having a narrow molecular weight distribution (MWD) even at ambient temperature.[6,7] The system is referred to as the metal-catalyzed atom transfer or single-electron transfer (SET) living radical polymerization.

Meanwhile, the author found that the same metal catalysis as in the controlled radical polymerization can be evolved into the step-growth radical polyaddition of designed monomers possessing unconjugated carbon–carbon double (C=C) and an active carbon-chlorine (C–Cl) bonds in a molecule.[8] In this polymerization, the active or dormant C–X bond in the monomer is activated by the metal catalysts to form a radical species, which adds to the C=C double bond of another monomer molecule to generate a C–C bond as the main chain, along with an inactive C–X bond as the pendant. Furthermore, the author has successfully combined the step-growth radical polyaddition with the metal-catalyzed polymerization by the judicious choice of the catalyst, in

which the simultaneous step- and chain-growth polymerization proceeds via the radical intermediates by the single metal catalyst.[9] For example, the simultaneous living radical polymerization of methyl acrylate (MA) and radical polyaddition of an ester-linked 3-butenyl 2-chloropropionate (**1**) was achieved with CuCl/1,1,4,7,10,10-hexamethyltriethylenetetramine (HMTETA) to afford the controlled polymers, in which the homopolymer segments with the controlled chain length were connected by the ester linkage.

Herein, the author reports the simultaneous chain- and step-growth radical polymerization of NIPAM for the dual control in degradability and thermoresponsivity of the product (Scheme 1). The simultaneous polymerization of NIPAM and an amide- or ester-linked monomer proceeded

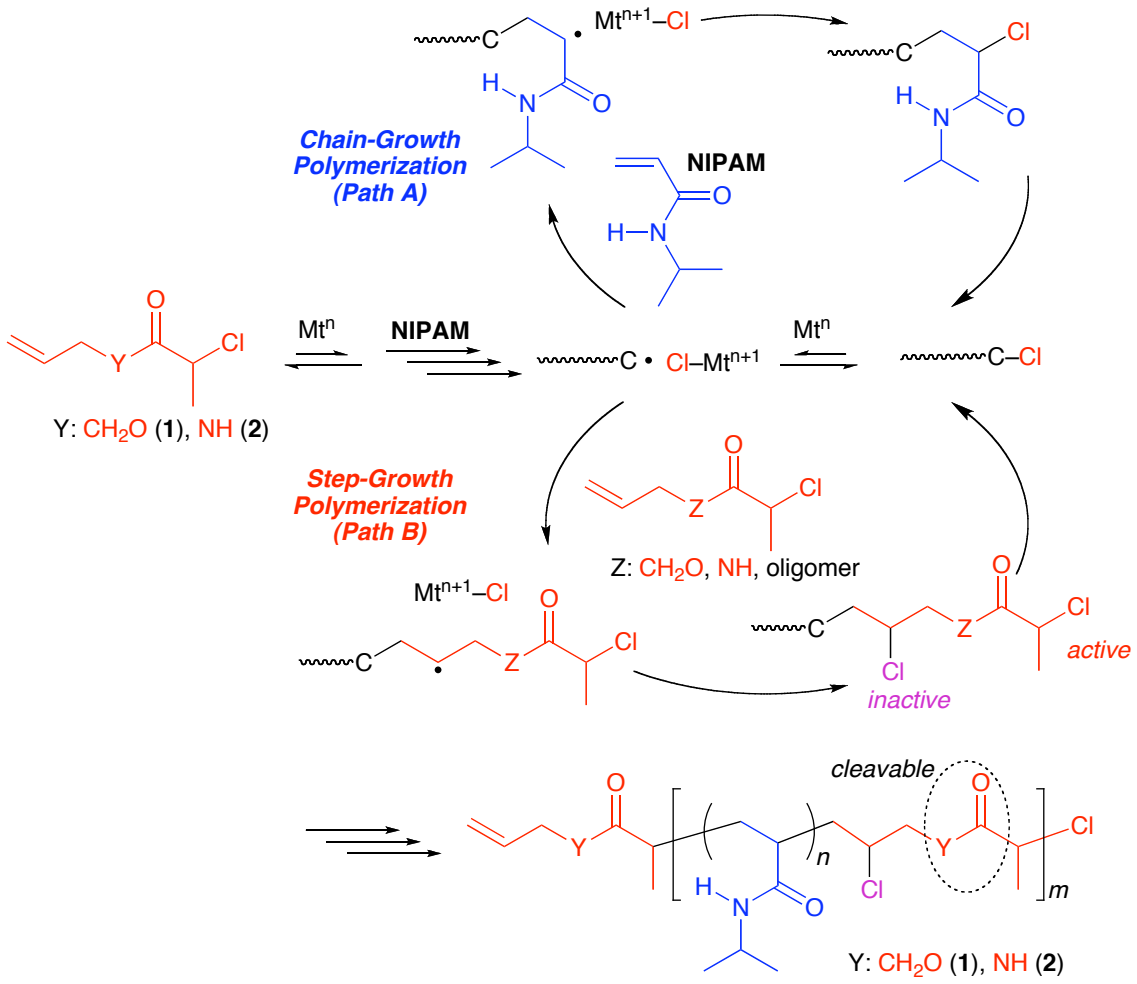

Scheme 1. Simultaneous chain- and step-growth radical polymerization of NIPAM with **1** and **2**.

very fast in aqueous media at ambient temperature. The degradability and thermoresponsivity of the produced poly(NIPAM) can be tuned by changing the monomer structure or initial feed ratios.

Results and Discussion

1. Simultaneous Polymerization of NIPAM. The simultaneous chain- and step-growth radical polymerization of NIPAM was examined in conjunction with *N*-allyl-2-chloropropanamide (**2**), in which the unconjugated C=C and reactive C–Cl bonds are linked via an amide linkage. The polymerization of NIPAM and **2** (50:1 molar ratio) was performed in a DMF and water mixture (1/1) at 20 °C using CuCl/Me_6TREN as the catalyst.[6,7] Both of the monomers were simultaneously consumed, of which the consumption rates were much faster than those of the ester counterparts, i.e., the polymerization of MA and **1**, and the reaction reached an almost quantitative monomer conversion in several minutes even at 20 °C as in the living polymerization of NIPAM with the CuCl/Me_6TREN system (Figure 1A). The consumption of the original C–Cl bonds in **2** (filled triangles) determined by ^{1}H NMR agreed well with that of **2** itself by gas chromatography, while the unconjugated C=C double bonds (open triangles) were consumed much slower than **2**. This suggests that **2** was mainly consumed via the reaction of the C–Cl bond to induce the NIPAM polymerization during the initial stage of the polymerization. Although the reaction of the unconjugated C=C double bonds was slower, the consumption of the C=C bonds proceeded even after the quantitative consumption of the monomers. The molecular weights (M_n) of the obtained products increased in almost direct proportion to the total monomer conversion with a relatively narrow molecular weight distribution at the initial stage (Figure 1B). After the complete consumption of the monomers, the M_n values progressively increased and the SEC curves became broader and somehow multimodal (Figure 1C). These results indicated that the NIPAM

polymerization first proceeded from the C–Cl bond in **2** mainly to give the living oligomers of NIPAM. The polymerization was then followed by a step-growth propagation between the active C–Cl bond at ω-end and the unconjugated C=C double bond at the a-end of the living oligo(NIPAM) or residual **2** to give the multiblock polymers consisting of living poly(NIPAM) segments connected by the amide linkages.

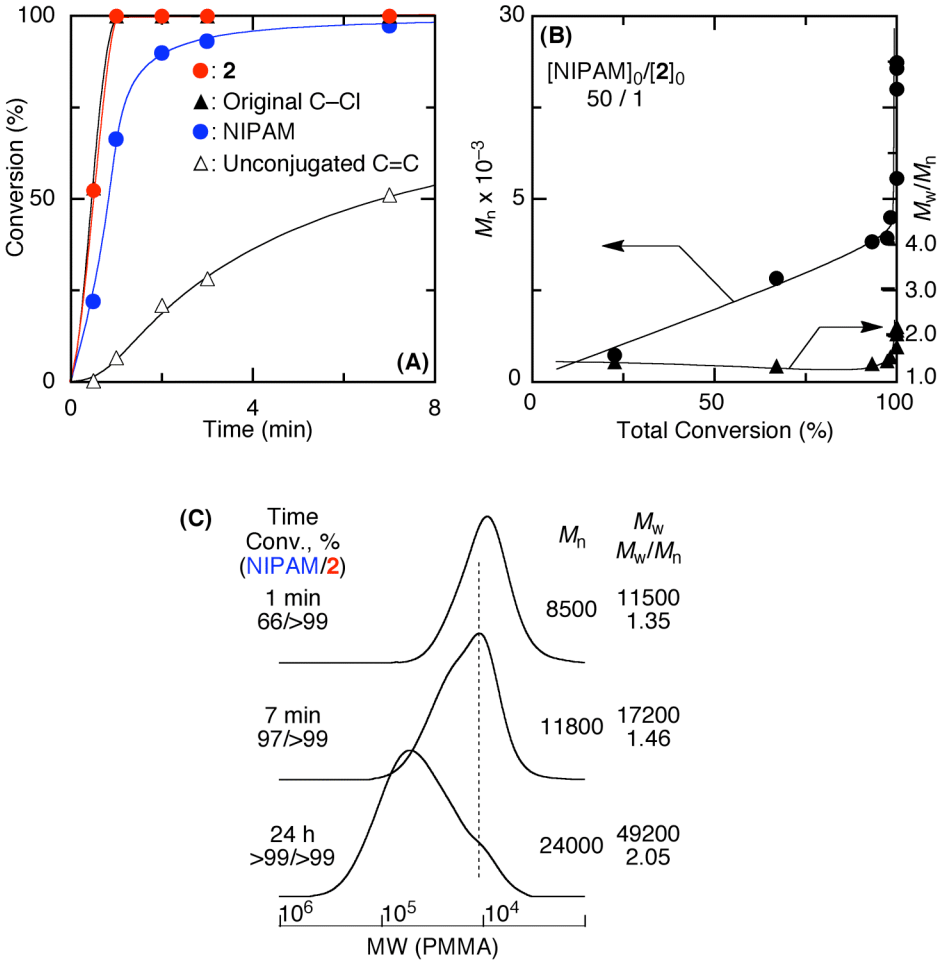

Figure 1. Simultaneous chain- and step-growth radical polymerization of NIPAM and **2** with CuCl/Me_6TREN in DMF/H_2O = 1/1 at 20 °C: $[NIPAM]_0$ = 4.0 M; $[\mathbf{2}]_0$ = 0.080 M; $[CuCl]_0$ = 40 mM; $[Me_6TREN]_0$ = 40 mM. (A) Consumption of NIPAM and original C–Cl and unconjugated C=C bonds measured by ^{1}H NMR and **2** measured by gas chromatography. (B) M_w and M_w/M_n values of the obtained copolymers vs total monomer conversion of NIPAM and **2**. (C) Size-exclusion chromatograms of the obtained copolymers.

A series of simultaneous polymerizations of NIPAM were then carried out in combination with **1** or **2** by the different feed ratios ($[NIPAM]_0/[\mathbf{1}$ or $\mathbf{2}]_0$ = 50/1, 20/1, 5/1, and 1/1) as summarized in Table 1 (entries 1–8). In all of the cases, both monomers were simultaneously and smoothly consumed (Figure 2). Especially, for the combination with **1**, the obtained copolymers could be easily degraded by the cleavage of the ester linkage in the main-chain originating from **1**

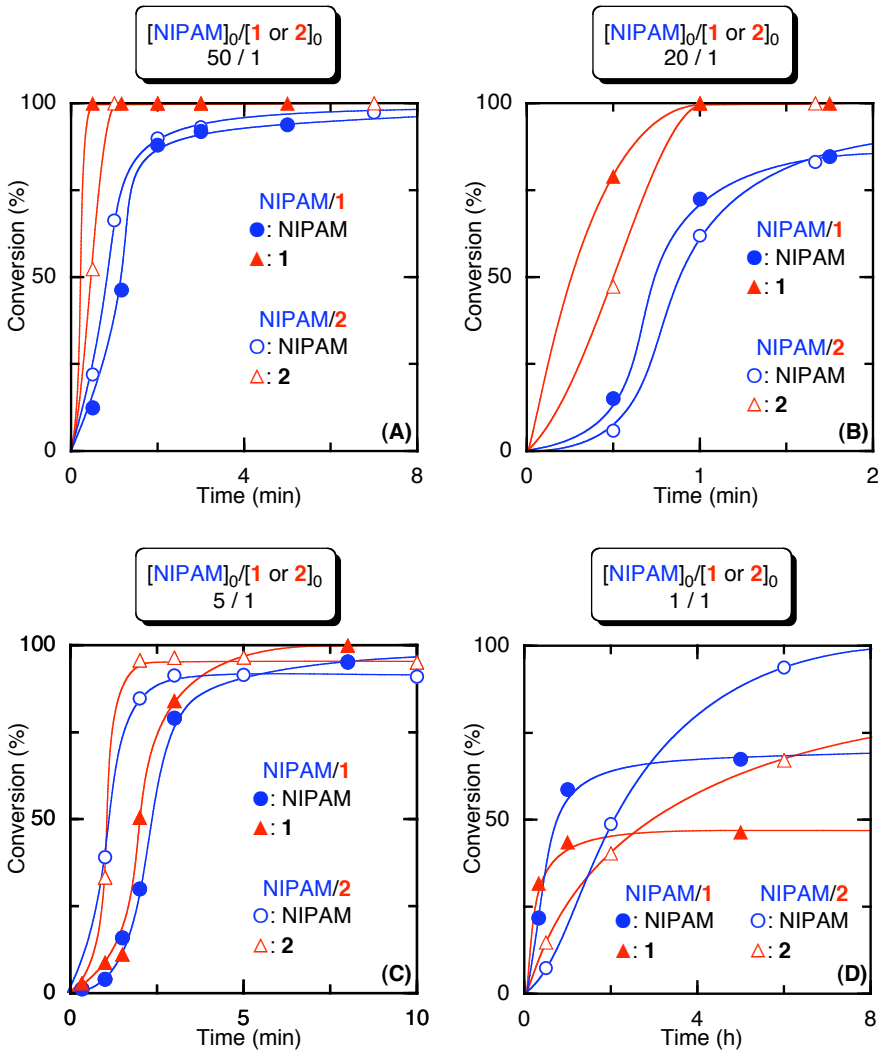

Figure 2. Time–conversion curves for simultaneous chain- and step-growth radical polymerization of NIPAM and **1** or **2** with CuCl/Me_6TREN in DMF/H_2O = 1/1 at 20 °C: $[NIPAM]_0$ = 4.0, 4.0, 4.0 or 2.0 M; $[\mathbf{1}$ or $\mathbf{2}]_0$ = 0.080, 0.20, 0.80 or 2.0 M; $[CuCl]_0$ = 40 or 100 mM; $[Me_6TREN]_0$ = 40 or 100 mM.

Table 1. Simultaneous Chain- and Step-Growth Radical Polymerization of NIPAM with 1 or 2 in DMF/H_2O (1/1 v/v) at 20 °C

Entry	Monomer	[Monomer]$_0$, mol/L		Time, h	Monomer Conv., %		M_w[f]	M_w/M_n[f]	NIPAM/ **1** or **2** in Polymer[d]	Cloud Point, °C[g]
		NIPAM	**1** or **2**		NIPAM[d]	**1** or **2**[e]				
1[a]	NIPAM/**2**	4.0	0.08	24	>99	>99	49200	2.05	98/2	34.1
2[a]		4.0	0.20	30	99	>99	13100	1.84	95/5	37.8
3[b]		4.0	0.80	20	94	97	3400	1.63	83/17	39.6
4[b]		2.0	2.0	190	>99	89	3000	2.11	53/47	soluble[h]
5[a]	NIPAM/**1**	4.0	0.08	330	>99	>99	35300 (9900)[c]	1.71 (1.26)[c]	98/2	33.2 (37.9)[c]
6[a]		4.0	0.20	200	>99	>99	9000 (3900)[c]	1.55 (1.47)[c]	95/5	30.5 (49.6)[c]
7[b]		4.0	0.80	340	>99	>99	5700 (1500)[c]	1.99 (1.48)[c]	83/17	24.5 (81.3)[c]
8[b]		2.0	2.0	220	80	59	1200	1.86	58/42	insoluble[i]

[a][CuCl]$_0$ = [tri s[2-(dimethylamino)ethyl]amine (Me_6TREN)]$_0$ = 40 mM. [b][CuCl]$_0$ = [M e_6TREN]$_0$ = 100 mM. [c]Values in parenthesis are for the methanolyzed product. [d]Determined by ^{1}H NMR. [e]Determined by gas chromatography. [f]The weight-average molecular weight (M_w) and distribution (M_w/M_n) were determined by size-exclusion chromatography. [g]Determined by turbidimetric analysis. Conditions: concentration = 10 mg/mL, heating rate = 1.0 °C/min, cloud point was determined by the temperature, at which the transmittance (l = 500 nm) of aqueous solution became 50%. [h]Soluble at temperatures below 100 °C. [i]Insoluble at temperatures above 0 °C.

(Figure 3). The methanolysis of the polymers obtained from NIPAM and **1** were investigated by Na_2CO_3 in CH_3OH for the cleavage of the main-chain ester linkage originating from **1** to generate the lower molecular weight polymers or oligomers of NIPAM as shown by the dashed SEC curves. Especially, with a lower amount loading of **1** ($[NIPAM]_0/[\mathbf{1}]_0$ = 50/1), the methanolysis resulted in poly(NIPAM) with unimodal SEC curves having narrow molecular weight distributions (M_w/M_n ~ 1.2) and the M_ns were close to the values based on the assumption that one molecule of **1** generates one polymer chain, suggesting that the successive oligo- or poly(NIPAM) units sandwiched between the **1** units were generated via the almost ideal living polymerization.

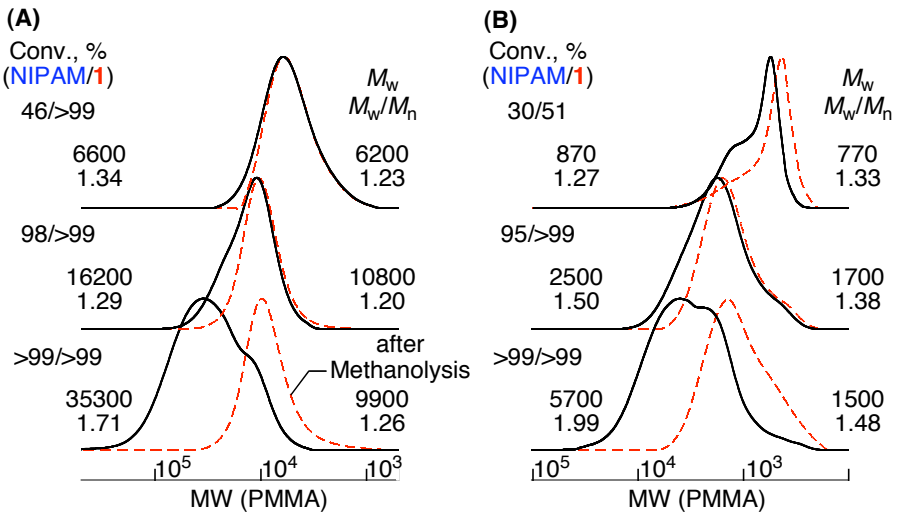

Figure 3. Size-exclusion chromatograms of the obtained copolymers (solid lines) and the methanolyzed products (dashed lines) in the simultaneous chain- and step-growth radical polymerization of NIPAM and **1** with CuCl/Me_6TREN in DMF/H_2O = 1/1 at 20 °C: $[NIPAM]_0$ = 4.0 M; $[\mathbf{1}]_0$ = 0.080 (A) or 0.80 M (B); $[CuCl]_0$ = 40 or 100 mM; $[Me_6TREN]_0$ = 40 or 100 mM.

2. Model Reaction of Simultaneous Polymerization. The copolymer obtained form NIPAM and **1** was then analyzed by MALDI-TOF-MS spectrometry (Figure 4). All of the peaks were assigned to the random copolymers consisting of NIPAM and **1**, though many series of peaks

other than the ideal structure were observed due to the loss of Cl atom at the NIPAM terminal during the ionization process.[2] To confirm the simultaneous polymerizations in more detail, the model reaction was performed using NIPAM, methyl 2-chloropropanamide (**3**), and allyl acetamide (**4**), which can be regarded as model compounds of the active C–Cl and unconjugated C=C bonds of **1**, respectively, in a 1:1:1 ratio ($[NIPAM]_0 = [\mathbf{3}]_0 = [\mathbf{4}]_0 = 2.0$ M) using CuCl/Me_6TREN similar to the polymerization (Figure 5). NIPAM, **3**, and **4** were smoothly consumed and the total conversion was over 90% (>99%, 90%, and 85%, respectively), and the molecular weights of the obtained products were low ($M_n \sim 600$) (Figure 6). The MALDI-TOF-MS spectrum of the products showed a series of peaks consisting of one unit of **3**, a small number of NIPAM units (*n* =

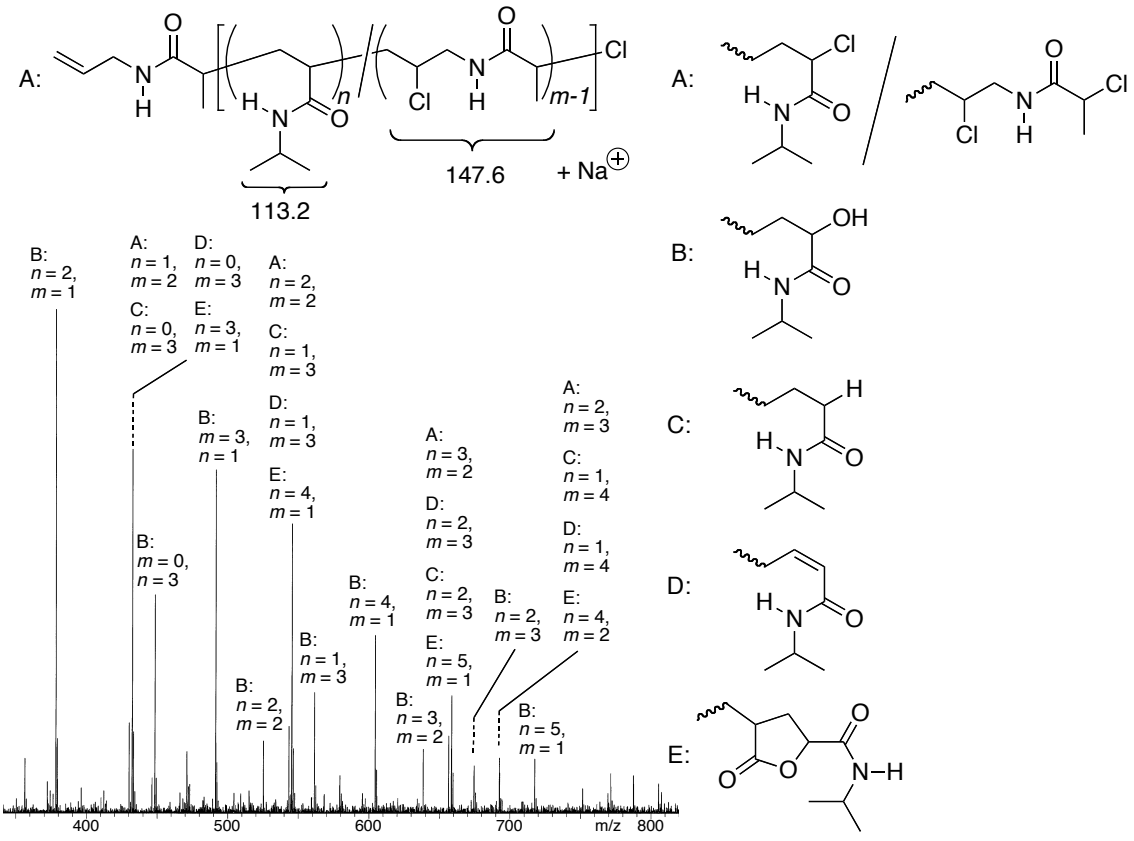

Figure 4. MALDI-TOF-MS spectrum of poly(NIPAM-*co*-**2**) obtained with CuCl/Me_6TREN in DMF/H_2O = 1/1 at 20 °C: $[NIPAM]_0 = 2.0$ M; $[\mathbf{2}]_0 = 2.0$ M; $[CuCl]_0 = 100$ mM; $[Me_6TREN]_0 = 100$ mM. (Conversion: >99 % for NIPAM, 79% for **2**, $M_n = 1100$, $M_w = 1800$, $M_w/M_n = 1.73$).

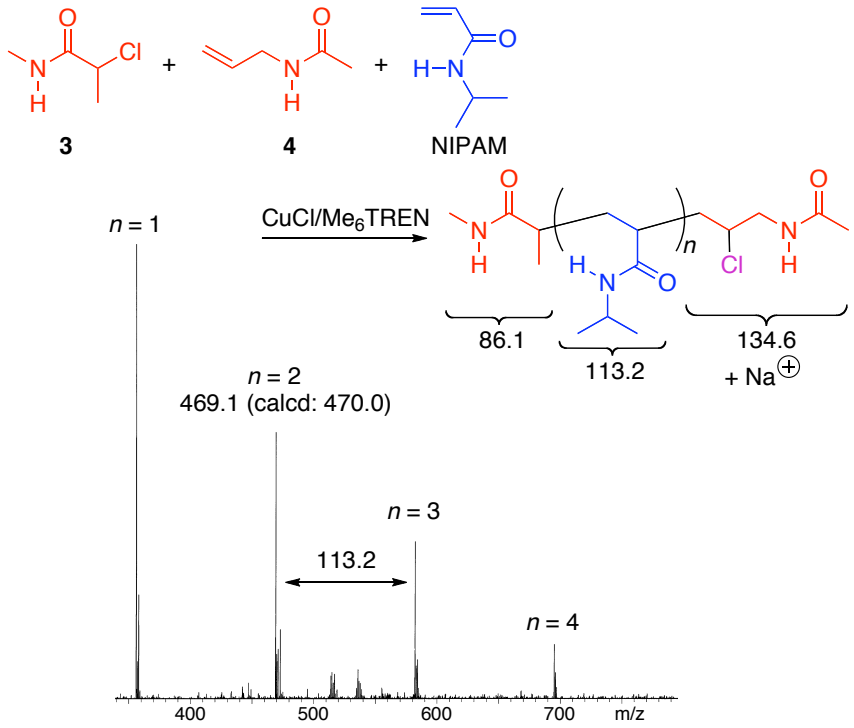

Figure 5. MALDI-TOF-MS spectrum of the obtained in the model reaction of NIPAM, **3**, and **4** with CuCl/Me_6TREN in DMF/H_2O = 1/1 at 20 °C: $[NIPAM]_0$ = 2.0 M; $[\mathbf{3}]_0$ = 2.0 M; $[\mathbf{4}]_0$ = 2.0 M; $[CuCl]_0$ = 100 mM; $[Me_6TREN]_0$ = 100 mM. (Conversion: >99 % for NIPAM, 90% for **3**, 85% for **4**, M_n = 570, M_w = 920, M_w/M_n = 1.62).

1–4), and one unit of **4**, which indicated NIPAM oligomers possessing the model compound units at both terminals (Figure 5). In contrast to the fact that the CuCl/Me_6TREN system induced the chain-growth copolymerization of MA and **1** as a side reaction in toluene at 80 °C,[9] another possible series of peaks for the polymerization of NIPAM with more than 2 units of **4** or bimolecular termination between the radical species were not observed in the present model reaction, probably due to the milder reaction condition at ambient temperature. These results support the fact that the ideal simultaneous polymerizations proceeded via the chain- and step-growth mechanism without a significant amount of side reactions. It is noteworthy that the model reaction studies provided facile methods for the synthesis of α,ω-hetero-functionalized

telechelic oligomers or polymers of NIPAM. According to the model reaction, the poly(NIPAM) with high functionalities at both ends can be produced using the halide initiator and olefin terminator bearing various functional groups in just one shot by the CuCl/Me_6TREN catalytic system, compared to the conventional multi-step functionalization by olefin terminators.

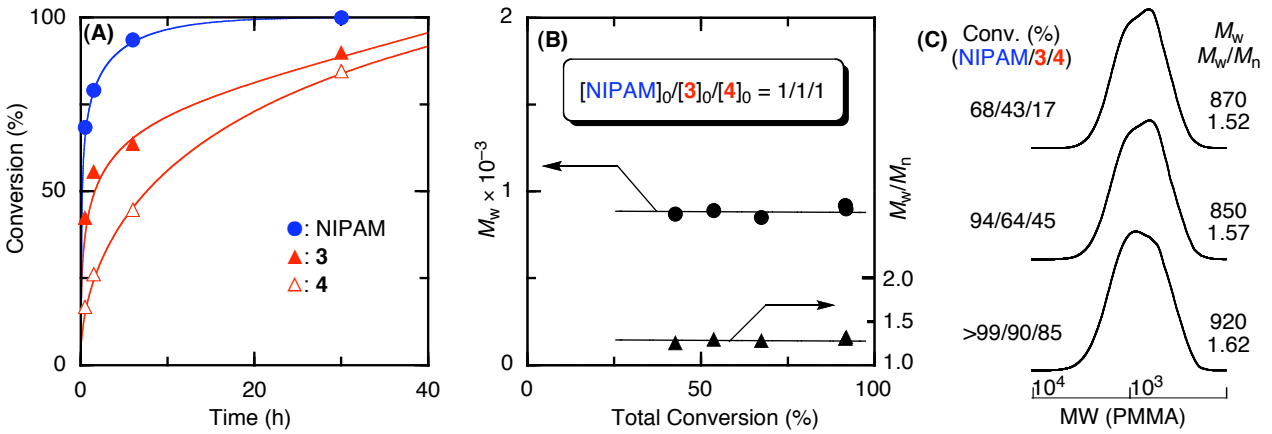

Figure 6. Model reaction of NIPAM, **3**, and **4** with CuCl/Me_6TREN in DMF/H_2O = 1/1 at 20 °C: $[NIPAM]_0$ = 2.0 M; $[\mathbf{3}]_0$ = 2.0 M; $[\mathbf{4}]_0$ = 2.0 M; $[CuCl]_0$ = 100 mM; $[Me_6TREN]_0$ = 100 mM. (A) Consumption of NIPAM, **3**, and **4** measured by ^{1}H NMR. (B) M_w and M_w/M_n values of the obtained oligomers in the model reaction vs total conversion of NIPAM, **3**, and **4**. (C) Size-exclusion chromatograms of the obtained oligomers in the model reaction.

3. Thermosensitivity of Poly(NIPAM). The thermoresponsive properties of the NIPAM polymers obtained in the simultaneous polymerization with various monomer feed ratios were analyzed. Figure 7 is plots of the transmittances as a function of temperature, namely cloud-point curves, for the aqueous solutions of the copolymers (Figure 8). As the hydrophilic amide-monomer contents increased, the cloud temperature became higher (Figure 7A), while as the hydrophobic ester-monomer contents increased, it decreased (filled squares, circles, and triangles in

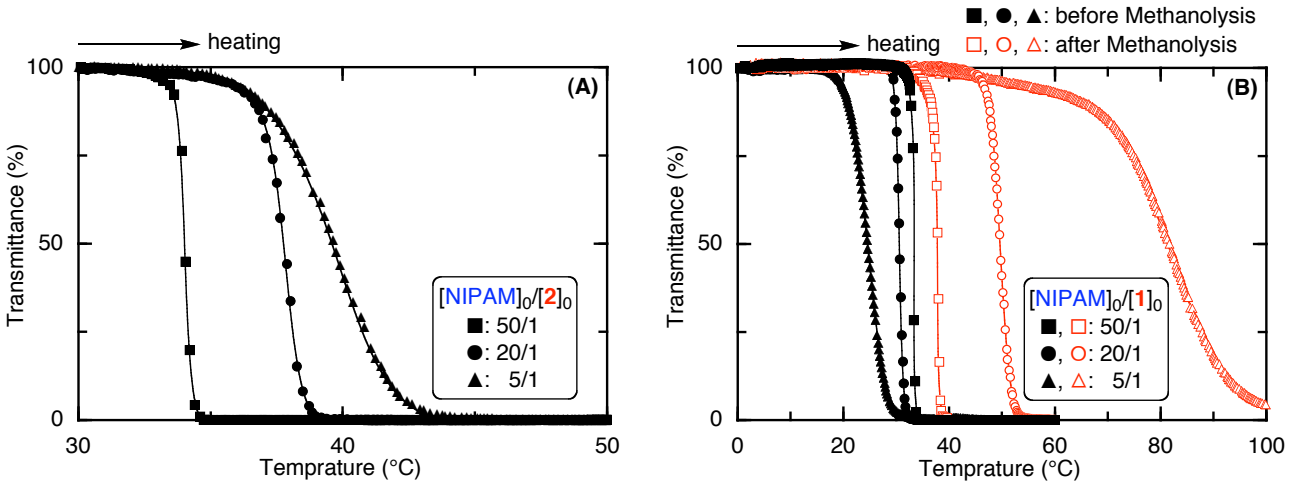

Figure 7. Cloud-point curves for the aqueous solutions of the obtained copolymers and the methanolyzed products in the simultaneous chain- and step-growth radical polymerization of (A) NIPAM and **2** or (B) NIPAM and **1** with various monomer feed ratios ([NIPAM]$_0$/[**1** or **2**]$_0$ = 50/1, 20/1, and 5/1). Conditions: concentration = 10 mg/mL, heating rate = 1.0 °C/min, cloud point was determined by the temperature at which the transmittance (λ = 500 nm) of aqueous solution reach 50%.

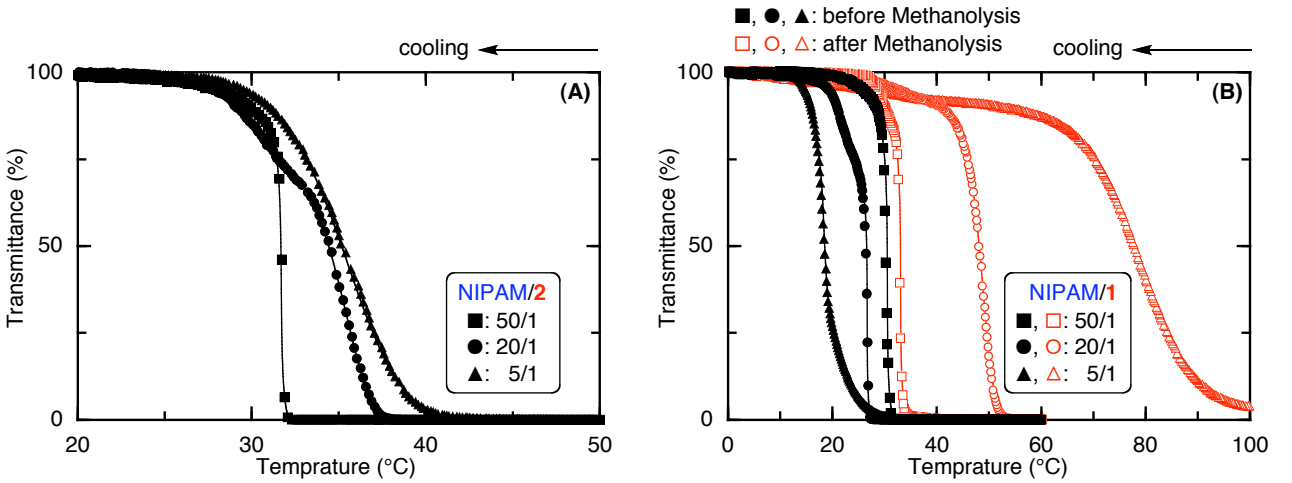

Figure 8. Cloud point curves for the aqueous solutions of the obtained copolymers and the methanolyzed products in the simultaneous chain- and step-growth radical polymerization of (A) NIPAM and **2** or (B) NIPAM and **1** with various monomer feed ratios ([NIPAM]$_0$/[**1** or **2**]$_0$ = 50/1, 20/1 and 5/1). Conditions: concentration = 10 mg/mL, cooling rate = 1.0 °C/min. Cloud point was determined by the temperature at which the transmittance (λ = 500 nm) of aqueous solution reached 50%.

Figure 7B). These results indicated that the structures of the step-growth monomer and the monomer feed ratios strongly influenced the thermoresponsivity of the NIPAM polymers.

Furthermore, in the case of the combination with **1**, the aqueous solutions of the methanolyzed products exhibit LCST phase transitions at a higher temperature than that of thepolymer before methanolysis (open squares, circles, and triangles in Figure 6B). As the initial charge ratios of the degradable monomer to NIPAM increased ($[\mathbf{1}]_0/[\text{NIPAM}]_0$ = 1/50, 1/20, and 1/5), the aqueous solutions of the methanolyzed products had a higher cloud point at 37.9, 49.6, and 81.3 °C, respectively, which are higher than those of the original polymers before the methanolysis with increases of 4.7, 19.1, and 56.8 °C. The cloud points of the methanolyzed products increased with the increasing **1** contents in the copolymers, which most probably suggests hydrophilic hydroxy groups being introduced at the hydrolyzed chain end. Thus, the thermoresponsivity of the NIPAM copolymers was significantly changed by the degradation of the copolymers, varying the comonomer structures, or the different monomer feed ratios.

Conclusions

In conclusion, the CuCl/Me_6TREN system enabled the very fast and quantitative simultaneous chain- and step-growth radical polymerization of NIPAM and ester- or amide-linked monomers (**1** and **2**) at ambient temperature in aqueous solvents. This provides a facile and practical approach to a tunable thermoresponsivity and degradability of the NIPAM polymers. More specifically, any change or increase in the phase-transition temperature upon degradation will lead to further application such as a more intelligent drug-delivery system.

EXPERIMENTAL SECTION

Materials

N-Isopropylacrylamide (NIPAM) (TCI, > 98%) was recrystallized from hexane and toluene. 3-Butenyl 2-chloropropionate (**1**) was synthesized according to the literature.[8] CuCl (Aldrich, 99.99%) was used as received. CuCl was handled in a glovebox (VAC Nexus) under a moisture- and oxygen-free argon atmosphere (O_2 < 1 ppm). DMF was distilled from calcium hydride under reduced pressure and bubbled with dry nitrogen for 15 min just before use. Distilled water was bubbled with dry nitrogen for 15 min just before use.

Synthesis of Allyl 2-chloropropanamide (2)

Allyl 2-chloropropanamide (**2**) was synthesized from 2-chloropropionyl chloride (TCI, > 95%) and allylamine (TCI, > 99%). The reaction was carried out by the use of a syringe technique under dry argon atmosphere in an oven-dried glass tube equipped with three-way stopcocks. 2-Chloropropionyl chloride (51.0 mL, 0.525 mol) was added dropwise with vigorous stirring to a solution of allylamine (37.5 mL, 0.500 mol) and triethylamine (76.7 mL, 0.550 mol) in dry THF (84.8 mL) at 0 °C. The mixture kept stirred for 1 h at 0 °C, and then over 12 h at room temperature. After the dilution with diethyl ether, the mixture was washed with aqueous solution of Na_2CO_3 and then NaCl and was evaporated to remove the solvents. The product was distilled over calcium hydride under reduced pressure to give pure allyl 2-chloropropanamide (**2**) (56.0 mL, 0.408 mol; yield = 81.6%, purity > 99%). ^{1}H NMR ($CDCl_3$) δ/ppm: 1.74 (d, 3H, CH–C*H*$_3$, *J* = 6.9 Hz), 3.91 (m, 2H, C*H*$_2$NHCO), 4.45 (q, 1H, C*H*–CH$_3$, *J* = 6.9 Hz), 5.19 (m, 2H, C*H*$_2$=CH), 5.85 (m, 1H, CH$_2$=C*H*), 6.70–7.10 (br, 1H, N*H*CO).

Synthesis of Model Compound (3 and 4)

Methyl 2-chloropropanamide (**3**) was synthesized from 2-chloropropionyl chloride (TCI, > 95%) and methylamine hydrochloride (TCI, > 98%). Allyl acetamide (**4**) was synthesized from allylamine (TCI, > 99%) and acetic anhydride (KANTO, > 99%). Methyl 2-chloropropanamide (**3**): ^{1}H NMR ($CDCl_3$) δ/ppm: 1.74 (d, 3H, CH–C*H*$_3$, *J* = 6.9 Hz), 2.87, 2.89 (s, 3H, C*H*$_3$NHCO), 4.43 (q, 1H, C*H*–CH$_3$, *J* = 6.9 Hz), 6.40–6.90 (br, 1H, N*H*CO). Allyl acetamide (**4**): ^{1}H NMR ($CDCl_3$) d/ppm: 2.01 (s, 3H, COC*H*$_3$), 3.88 (m, 2H, C*H*$_2$NHCO), 5.16 (m, 2H, C*H*$_2$=CH), 5.84 (m, 1H, CH$_2$=C*H*), 5.70–6.10 (br, 1H, N*H*CO).

Polymerization

Polymerization was carried under dry nitrogen in baked glass tubes equipped with a three-way stopcock. A typical example for the polymerization procedure is given below. The polymerization was initiated by adding solution of CuCl (28.9 mg, 0.291 mmol) and Me_6TREN (0.08 mL, 0.291 mmol) in water (1.91 mL) into monomer solution (1.99 mL), containing NIPAM (3.30 g, 29.1 mmol) and allyl 2-chloropropanamide (**2**) (0.08 mL, 0.582 mmol) in DMF (1.91 mL) at 20 °C. The total volume of the reaction mixture was thus 7.28 mL. In predetermined intervals, the polymerization was terminated by cooling the reaction mixtures to –78 °C. Monomer conversion of **2** was determined from the concentration of residual monomer measured by gas chromatography with DMF as an internal standard. The conversions of NIPAM and the functional groups (C=C and C–Cl) of **2** were determined from the concentration of NIPAM, C=C, and C–Cl by ^{1}H NMR spectroscopy with DMF as an internal standard. The samples were dissolved in THF and passed through a short plug of silica gel column to remove the catalyst.

Methanolysis

Methanolysis of the copolymers was carried under dry nitrogen in baked glass tubes equipped with a three-way stopcock. A portion of the obtained poly(NIPAM-*co*-**1**) (80 mg) was dispersed in CH_3OH (80 mL) containing Na_2CO_3 (8.5 g) and the solution was refluxed for 48 h. The products were dissolved in THF and passed through a short plug of silica gel column and evaporated to remove the solvents to result in the methanolyzed products (60 mg).[10]

Measurements

Monomer conversion was determined from the concentration of residual monomer measured by gas chromatography [Shimadzu GC-8A equipped with a thermal conductivity detector and a 3.0 mm i.d. × 2 m stainless-steel column packed with SBS-200 (Shinwa Chemical Industries Ltd.) supported on Shimalite W; injection and detector temperature = 200 °C, column temperature = 160 °C] with DMF as an internal standard under He gas flow. The conversions of NIPAM and the functional groups (C=C and C–Cl) of **2** were determined from the concentration of NIPAM, C=C, and C–Cl by ^{1}H NMR spectroscopy with toluene as an internal standard. ^{1}H NMR spectra were recorded in $CDCl_3$ at 25 °C on a JEOL ECS–400 or a Varian Gemini 2000 spectrometer, operating at 400 MHz. The number-average molecular weight (M_n), weight-average molecular weight (M_w), and the molecular weight distribution (M_w/M_n) of the product polymers were determined by size-exclusion chromatography (SEC) in DMF containing 100 mM LiCl at 40 °C on two polystyrene gel columns [Shodex K-805L (pore size: 20–1000 Å; 8.0 mm i.d. × 30 cm); flow rate 1.0 mL/min] connected to Jasco PU-980 precision pump and a Jasco 930-RI refractive index detector. The columns were calibrated against 7 standard poly(MMA) samples (Shodex; M_p = 1850–1950000; M_w/M_n = 1.02–1.09). MALDI-TOF-MS spectra were measured on a SHIMADZU

AXIMA-CFR Plus mass spectrometer (reflector mode) with dithranol (1,8,9-anthracenetriol) as the ionizing matrix and sodium trifluoroacetate as the ion source. The LCST was determined as the temperature at which the transmittance of a 500 nm light beam through the aqueous solution of the samples became lower than 50% (cloud point). The transmittance of a 10 mg/mL aqueous solution of the samples was measured by monitoring the transmittance through a 1 cm quarts sample cell during the heating and cooling process at the rate of 1.0 °C/min. The transmittance was recorded using a JASCO V-550 UV/vis spectrometer equipped with a Peltier-type ETC-505 thermostatic cell holder.

NOTES AND REFERENCES

(1) (a) Schild, H. G. *Prog. Polym. Sci*. **1992**, *17*, 163–249. (b) Hsu, S.-H.; Yu, T.-L. *Macromol. Rapid Commun*. **2000**, *21*, 476–480. (c) Bergbreiter, D. E. *Chem. Rev.* **2002**, *102*, 3345–3384. (d) Bergbreiter, D. E.; Tian, J.; Hngfa, C. *Chem. Rev.* **2009**, *109*, 530–582.

(2) (a) Tong, Z.; Zeng, F.; Zheng, X.; Sato, T. *Macromolecules* **1999**, *32*, 4488–4490. b) Xia, Y.; Yin, X.; Burke, N. A. D.; Stöver, H. D. H. *Macromolecules* **2005**, *38*, 5937–5943.

(3) (a) Ringdorf, H.; Venzmer, J.; Winnik, F. M. *Macromolecules* **1991**, *24*, 1678–1686. b) Xia, Y.; Burke, N. A. D.; Stöver, H. D. H. *Macromolecules* **2006**, *39*, 2275–2283. c) Duan, Q.; Narumi, A.; Miura, Y.; Shen, X.; Sato, S.-I.; Satoh, T.; Kakuchi, T. *Polym. J.* **2006**, *38*, 306–310. d) Narumi, A.; Fuchise, K.; Kakuchi, R.; Toda, A.; Satoh, T.; Kawaguchi, S.; Sugiyama, K.; Hirao, A.; Kakuchi, T. *Macromol. Rapid Commun.* **2008**, *29*, 1126–1133.

(4) (a) Ray, B.; Isobe, Y.; Morioka, K.; Habaue, S.; Okamoto, Y.; Kamigaito, M.; Sawamoto, M. *Macromolecules* **2003**, *36*, 543–545. (b) Hirano, T.; Okumura, Y.; Kitajima, H.; Seno, M.; Sato, T. *J. Polym. Sci., Part A: Polym. Chem.,* **2006**, *44*, 4450–4460.

(5) (a) Schilli, C. M.; Zhang, M.; Rizzardo, E.; Thang, S. H.; Chong, Y. K.; Edwards, K.; Karlsson, G.; Müller, A. H. E. *Macromolecules* **2004**, *37*, 7861–7866. (b) Convertine, A. J.; Lokitz, B. S.; Vasileva, Y.; Myrick, L. J.; Scales, C. W.; Lowe, A. B.; McCormick, C. L. *Macromolecules* **2006**, *39*, 1724–1730.

(6) (a) Teodorescu, M.; Matyjaszewski, K. *Macromol. Rapid Commun.* **2000**, *21*, 190–194. (b) Masci, G.; Giacomelli, L.; Crescenzi, V. *Macromol. Rapid Commun.* **2004**, *25*, 559–564. (c) Millard, P. E.; Mougin, N. C.; Böker, A.; Müller, A. H. E. *ACS Symp. Ser.* **2009**, *1023*, 127–137.

(7) Nguyen, N. A.; Rosen, B. M.; Percec, V. *J. Polym. Sci., Part A: Polym. Chem.,* **2010**, *48*, 1752–1763.

(8) (a) Satoh, K.; Mizutani, M.; Kamigaito, M. *Chem. Commun.* **2007**, 1260–1262. (b) Mizutani, M., Satoh, K.; Kamigaito, M. *Macromolecules* **2009**, *42*, 472–480. (c) Satoh, K.; Ozawa, S.; Mizutani, M.; Nagai, K.; Kamigaito, M. *Nat. Commun.* **2010**, *1*, 6.

(9) Mizutani, M.; Satoh, K.; Kamigaito, M. *J. Am. Chem. Soc.* **2010**, *132*, 7498–7507.

(10) Corey, E. J.; Achiwa, K.; Katzenellenbogen, J. A. *J. Am. Chem. Soc.* **1969**, *91*, 4318–4320.

Chapter 6

Design and Synthesis of Self-Degradable Antimicrobial Polymers Consisting of Vinyl Polymer and Polyester Units by Simultaneous Chain- and Step-Growth Radical Copolymerization

ABSTRACT

Self-degradable antimicrobial copolymers bearing cationic side chains and main-chain ester linkages were synthesized using the simultaneous chain- and step-growth radical polymerization of *t*-butyl acrylate and 3-butenyl 2-chloropropionate, followed by the transformation of *t*-butyl groups into primary ammonium salts. The acrylate copolymers displayed antimicrobial activity against *E. coli* and moderate activity against *S. aureus*, while the acrylamide copolymers showed activity against *S. aureus* and no activity against *E. coli*. The copolymers were degraded to lower molecular weight products by the nucleophilic attack of primary amine groups in the side chains for cleaving the main chain esters in aqueous solution. The degradation mechanism was studied in detail by the model reactions between amine compounds and precursor copolymers.

Introduction

In recent years, there has been considerable interest in synthetic and naturally occurring polymers that can degrade in physiological conditions to give non-toxic low molecular weight compounds because of their biomedical and medicinal applicaitons.[1] In this filed, polymers with ester groups in polymer main chains have been utilized as biodegradable sutures, fracture fixation, oral implant, and drug delivery microspheres, which include polylactate, polyglycolide, and polycaprolactone.[2–4] The degradation process of these polymers involves hydrolysis of main-chain ester linkage in water or enzymes,[3] resulting in session of polymer chains. Upon degradation, particles can release drugs.[5] Although these polymers have been utilized to produce something, particles, scaffold, it has been difficult to control the degradation rate, and the inherent low water-solubility of polyesters limits the applications of the materials in aqueous conditions. To that end, polyester platforms containing primary amine groups in the side chains have been synthesized previously based on polycondensation of hydroxyacids.[6–8] These cationic polyesters are water-soluble at neutral pH because of protonation of amine groups. In the degradation process, the ester linkages of the polymer main chains are cleaved by the nucleophilic attack of amine groups in the side chains; the following amide formation and release of the polymer segment with an alcohol group at the terminal end result in the scission of polymer main chains. This self-degradation mechanism facilitates the quick disintegration of polymer structures at neutral pH in an aqueous environment. In addition to the bio-degradability of polymers, the primary amine functionality has been useful for covalent linking of biologically active compounds for a variety of therapeutic purposes.[9] The biodegradable polymers containing ammonium salts have been used previously as some applications such as a nanoparticle DNA carrier[10] and a gene carrier.[8]

On the other hand, cationic polymers with ammonium groups in the side chains have long attracted scientific and commercial interest due to their ability to kill bacteria in solution and on surfaces by a mechanism involving disruption of bacterial cytoplasmic membranes.[11] Alkyl quaternary groups have been widely used as cationic groups. Recently, the design of antimicrobial polymers has been extended to use primary ammonium groups to mimic the amphiphilic property and cationic functionality of natural antimicrobial peptides.[12–15] In this new approach, the random copolymers based on methacrylates,[16–18] methacrylamides,[19] and b-lactams,[14] displayed potent antimicrobial activity and hemocompatibility, which can be controlled by tuning the balance between hydrophobic and cationic properties as well as the polymer length. These synthetic polymers are chemically stable in physiological conditions, which would be available as disinfectants due to the extended life-time at the infection sites; however, it would be of interest for biomedical applications to develop such polymers that can degrade with controlled time frame to inactive oligomers after the antimicrobial actions to avoid undesired long-term toxicity.

In this study, the author demonstrates the synthesis and biological activity of self-degradable antimicrobial copolymers, which contain main-chain ester linkages and primary amine side chains. The author hypothesized that polyester-based polymers with cationic functionality could display antimicrobial activity, and the primary amines in the side chains would cleave the main chains for self-degradation after the antimicrobial actions (Scheme 1: Schematic presentation of this scission of polymer main chain). To test the hypothesis, the author utilized a new polymerization method based on the metal-catalyzed simultaneous chain- and step-growth radical polymerization to prepare the cationic polymers. This polymerization method was quite recently developed to involve evolution of the conventional radical addition reaction[20–25] into simultaneous chain- and step-growth propagation, enabling incorporation of ester unit into the

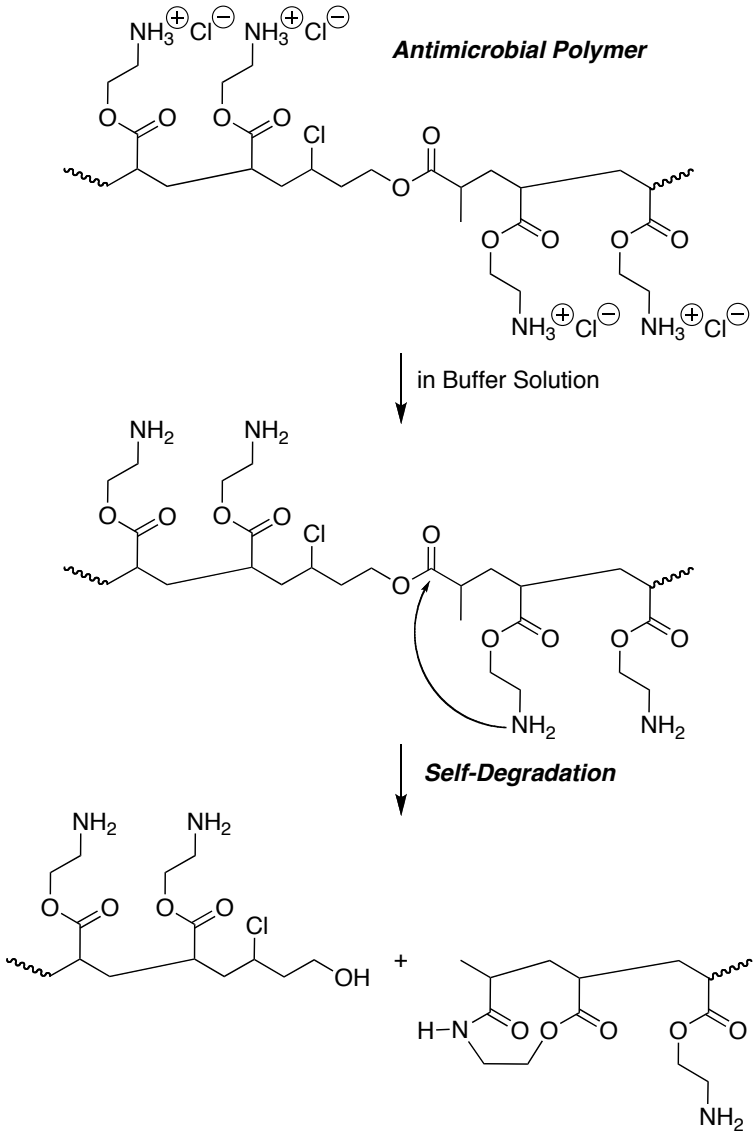

Scheme 1. Degradation Mechanism of Antimacrobial Polymer via Intramolecular Amidation.

polymer backbones as well as functional groups into the side chain in one polymerization procedure (Scheme 2: Sythesis).[26] Since the polyester units are relatively hydrophobic, the amphiphilic properties of polymers could be controlled by altering the chemical structures of ester units and ratios between amine and ester units. To that end, the author prepared and characterized the polymers with different amphiphilic properties and amine groups. The author evaluated their antimicrobial activity of these polymers as well as investigated the self-degradation mechanism of the polymers and model compounds in detail by matrix-assisted laser desorption/ionization

time-of-flight mass spectrometry (MALDI-TOF-MS). The experimental data indicated the proof of principle that these antimicrobial polymers are self-degraded into oligomeric or monomeric units at neutral pH in water.

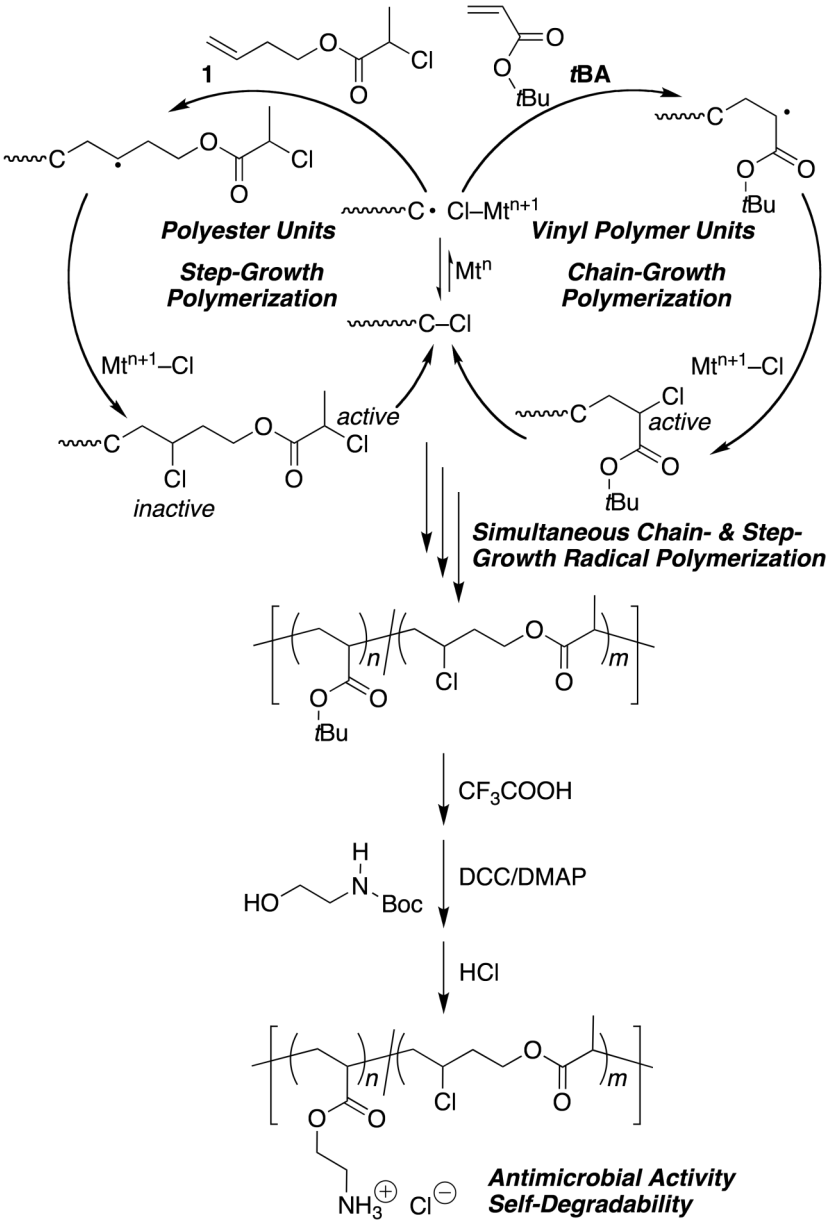

Scheme 2. Synthesis of Self-Degradable Antimicrobial Polymers.

Results and Discussion

1. Polymer Synthesis. For the synthesis of the copolymers bearing cationic side chains and main-chain ester linkages, the precursor copolymers were first prepared by simultaneous

polymerization of *t*BA and **1** (1:1 molar ratio) (Figure 1). The copolymerization was performed in toluene at 80 °C using CuCl/1,1,4,7,10,10-hexamethyltriethylenetetramine (HMTETA) as the catalyst, which is effective for the simultaneous polymerization of methyl acrylate (MA) and **1**.[26] Similar to the polymerization of MA and **1**, both of *t*BA and **1** were simultaneously and quantitatively consumed in 140 h. The molecular weights of the obtained products were relatively low during the initial stage of the polymerization. As the polymerization proceeded, however, the size-exclusion chromatograms (SEC) shifted to higher molecular weights, especially after the complete consumption of *t*BA (>99%). The ^{1}H NMR spectrum of the obtained product principally showed the combined signals of both the homopolymers of *t*BA and **1**, which suggests the polymerization via the chain- and step-growth mechanism, respectively (Figure 2). In addition, the MALDI-TOF-MS spectrum showed that each monomer unit was randomly distributed in the main chains (Figure 3). This result shows that the simultaneous polymerization of *t*BA with **1**

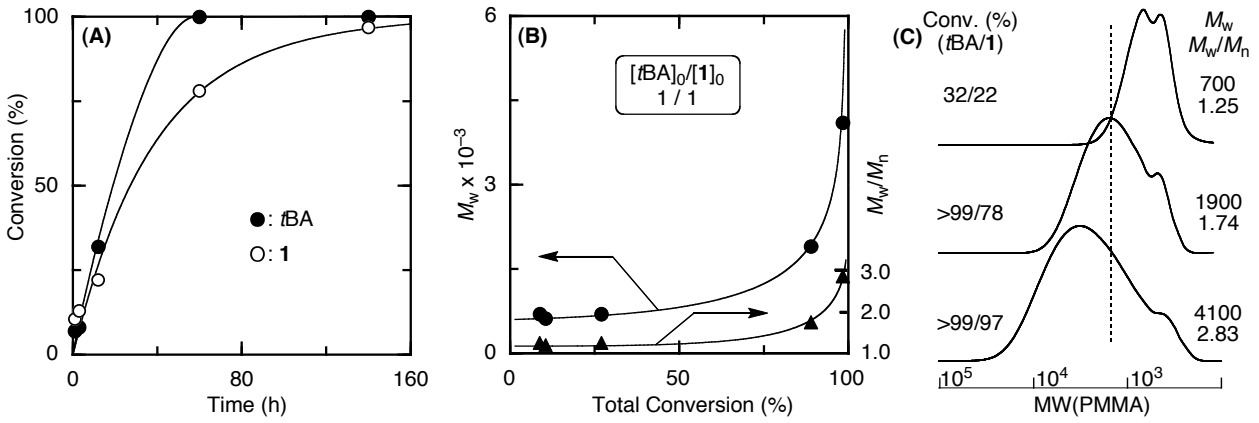

Figure 1. Simultaneous chain- and step-growth radical polymerization of *t*BA and **1** with CuCl/HMTETA in toluene at 80 °C: $[t\text{BA}]_0$ = 2.0 M; $[\mathbf{1}]_0$ = 2.0 M; $[\text{CuCl}]_0$ = 100 mM; $[\text{HMTETA}]_0$ = 100 mM. (A) Consumption of *t*BA measured by ^{1}H NMR and **1** measured by gas chromatography. (B) M_w and M_w/M_n values of the obtained copolymers vs total monomer conversion of *t*BA and **1**. (C) Size-exclusion chromatograms of the obtained copolymers.

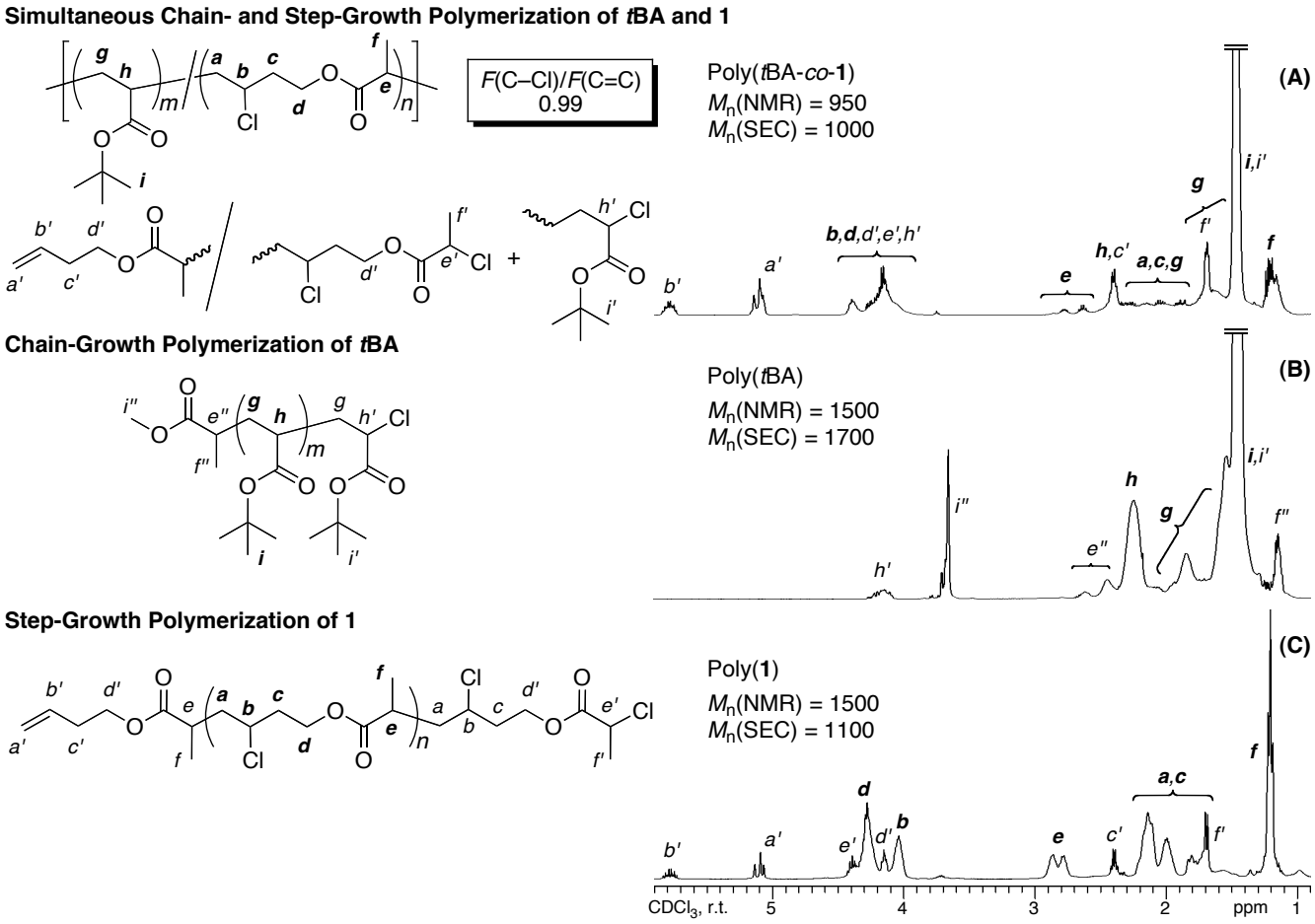

Figure 2. ^{1}H NMR spectra of (A) poly(*t*BA-*co*-**1**) (n = 3.67, m = 2.95), (B) poly(*t*BA), and (C) poly(**1**) ($CDCl_3$, r.t.).

successfully proceeded to afford the copolymers consisting of both vinyl polymer and polyester units as the main chain structure.

The copolymerization was also carried out with various monomer feed ratios of *t*BA and **1** ($[t\text{BA}]_0/[\mathbf{1}]_0$ = 3/1 and 1/3) (Table 1). In all cases, the copolymerization proceeded smoothly and the total monomer conversions reached >98%. The copolymers possessed the molecular weights in the range of 1200–2500 with similar molecular weight distributions ($M_w/M_n \sim 2.5$). Although the molecular weights were relatively low, they would be high enough to kill bacteria in solution, as observed with synthetic antimicrobial polymers.[16] The mole fractions of the main-chain ester

groups was thus from 0.25 to 0.74, which are expected to control the antimicrobial activity and degradability of copolymers.

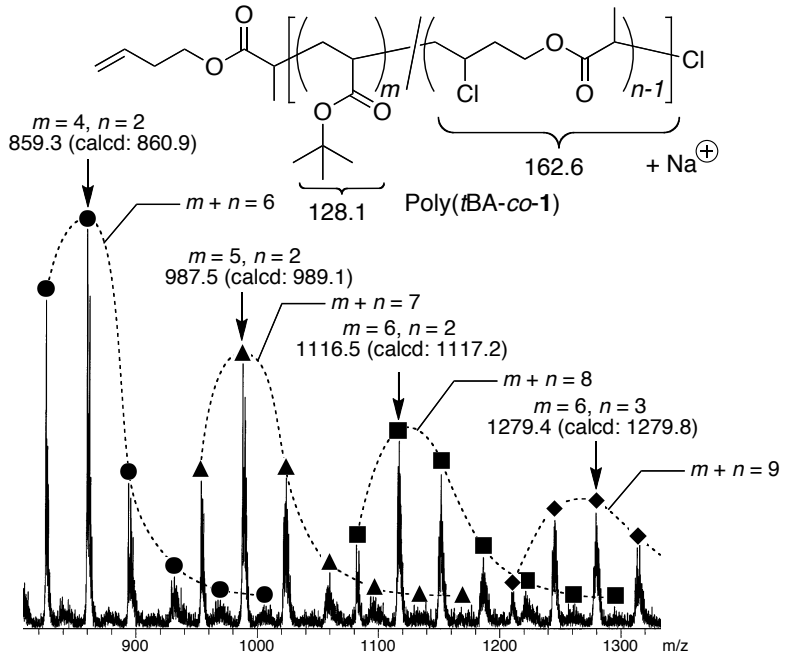

Figure 3. MALDI-TOF-MS spectrum of poly(*t*BA-*co*-**1**) (M_n = 950, n = 3.67, m = 2.95).

Table 1. Simultaneous Chain- and Step-Growth Radical Polymerization of *t*BA and **1**.[a]

entry	[*t*BA/**1**]$_0$, M	Time, h	Conversion (*t*BA/**1**), %[b]	M_n[c]	M_w[c]	M_w/M_n[c]	Yield, %	*t*BA/**1**[b]
P1	2.0/2.0	140	>99/97	1500	4100	2.83	84	51/49
P2	3.0/1.0	140	>99/99	2500	6700	2.64	83	75/25
P3	1.0/3.0	500	>99/97	1200	3200	2.72	78	26/74

[a][CuCl]$_0$ = 100 mM, [1,1,4,7,10,10-hexamethyltriethylenetetramine (HMTETA)]$_0$ = 100 mM, in toluene at 80 °C. [b]Determined by ^{1}H NMR. [c]The number-average molecular weight (M_n), the weight-average molecular weight (M_w), and distribution (M_w/M_n) were determined by size-exclusion chromatography.

The *t*-butyl groups of the copolymers were acidolyzed using trifluoroacetic acid (TFA) and then esterified using aminoethanol protected with *t*-butyloxycarbonyl (Boc) groups in the presence of *N*,*N*'-dicyclohexylcarbodiimide (DCC) and *N*,*N*'-dimethyl-4-aminopyridine (DMAP). The quantitative acidolysis of the *t*-butyl groups was confirmed by the ^{1}H NMR spectra, where the

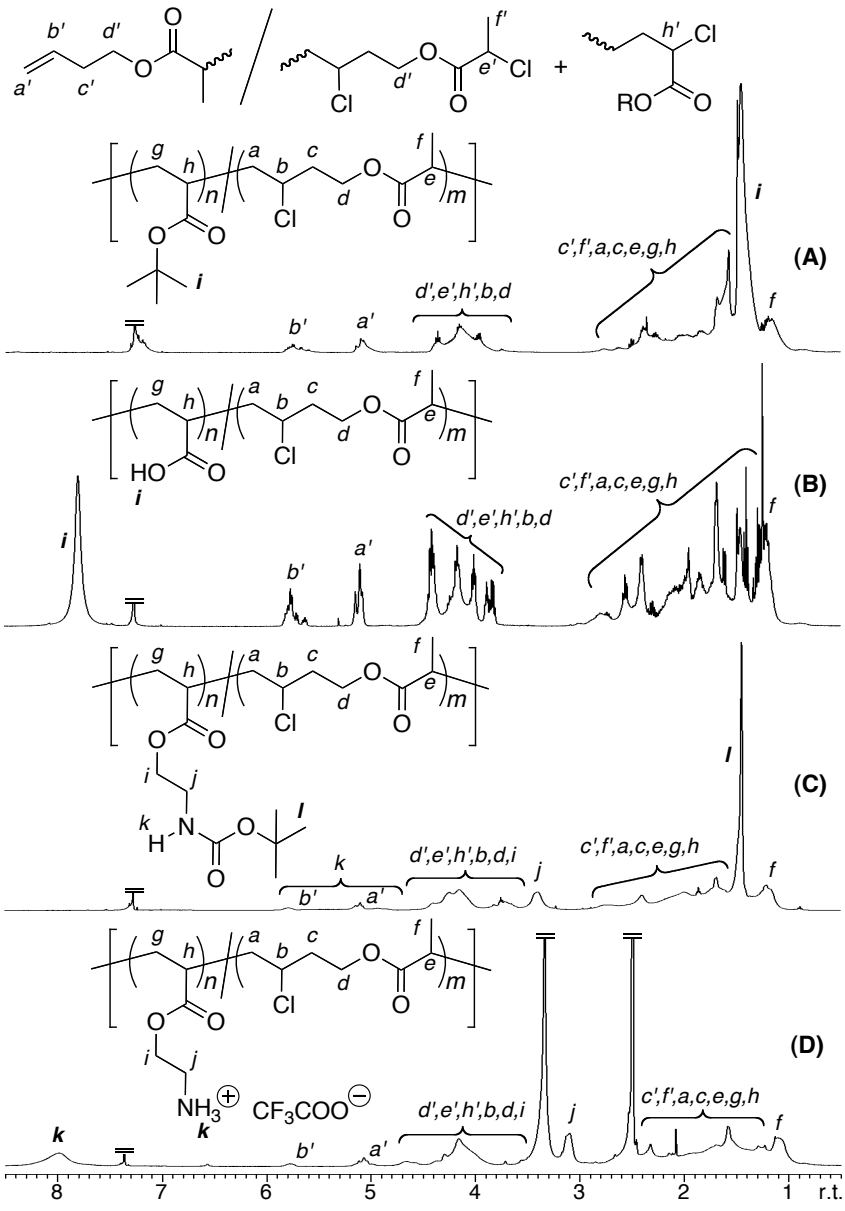

Figure 4. ^{1}H NMR spectra of (A) poly(*t*BA-*co*-**1**) (M_n = 1200, n = 4.9, m = 3.5), (B) poly(acrylic acid-*co*-**1**) (M_n = 890, n = 4.4, m = 3.5), (C) Boc-protected copolymer (M_n = 1500, n = 4.2, m = 3.4), and (D) cationic copolymer (M_n = 1400, n = 4.7, m = 3.6) (A–C: $CDCl_3$, r.t.; D: DMSO-d_6, r.t.).

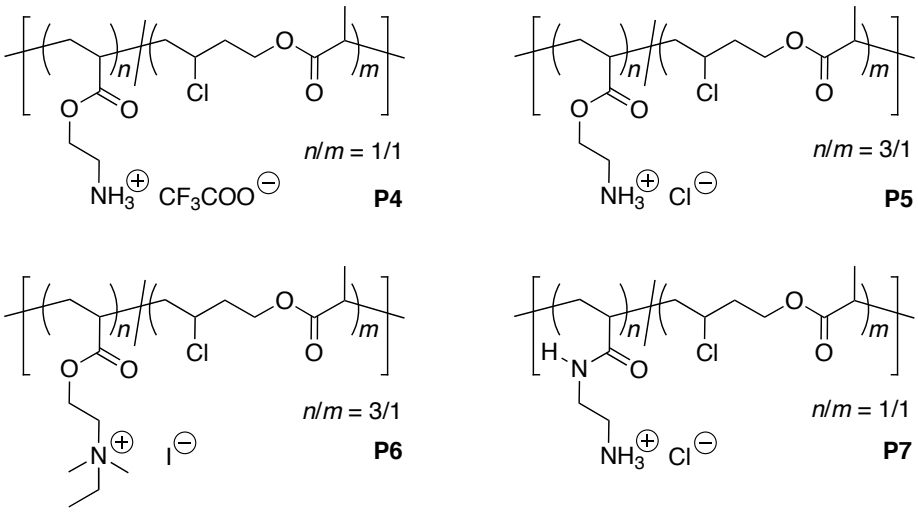

Figure 5. Copolymers possessing main-chain ester linkages and pendent ammonium salts.

broad peak of the carboxylic acid (7.6–8.0 ppm) appeared along with the disappearance of the *t*-butyl signal (1.4–1.5 ppm) (Figure 4A and 4B). The following successful introduction of the Boc-protected aminoethyl group was supported by the ^{1}H NMR spectrum, which that the peak of the carboxylic acid disappeared and that large sharp peak of Boc groups appeared (1.4–1.5 ppm) (Figure 4C). Finally, the Boc-protected amine groups were deprotected with TFA or HCl treatment to result in the desired cationic copolymers with primary amine groups as trifluoroacetic or hydrochloric salts, respectively (P4 and P5) (Figure 4D). With similar procedures, acrylate copolymers with quaternary ammonium salts (P6) and acrylamide copolymers bearing primary amine groups (P7) were also prepared as shown in Figure 5.

2. Antimicrobial Activity. Cationic, amphiphilic polymers with primary amines in the side chains have previously displayed antimicrobial effects against a broad spectrum of bacteria.[12–15] The author evaluated the antimicrobial activity of the polymers P4–P7 in a turbidity-based assay and determined the minimal inhibitory concentration of the polymers (MIC), in which the bacterial growth is completely inhibited (Table 2. Include precursor polymers in the

table.). The acrylate copolymers containing primary amines P4 displayed moderate activity against *E. coli* (MIC = 500μg/mL). The acrylate polymer P5, which has higher molecular weight and higher ratio of ammonium groups to the ester units than P4, displayed higher activity (MIC = 250mg/mL). On the other hand, the copolymer with quaternary ammonium groups P6 didn't show any activity against *E. coli* (MIC >500mg/mL) although P6 have higher molecular size, but similar ratios of cationic and ester groups compared to P5. This result is in agreement with the previous report on the antimicrobial activity of polymethacrylate derivatives with primary or quaternary ammonium groups.[18] The acrylamide copolymer P7 showed no activity against *E. coli*. It might be due to the hydrophilic nature of acrylamide, which discourages the binding to bacterial surfaces and insertion of polymers into the hydrophobic regions of cell membranes, resulting in low antimicrobial activity. It has been reported that polymethacrylamide derivatives are less active than the polymethacrylate counterparts and needs more hydrophobic groups to be effective in the membrane disruption.[19] This also supports our results on the difference in the activity of P4 and P7. Only P4 and P7 showed activity against *S. aureus*. Interestingly P7 is more potent against *S. aureus*, while P7 didn't show any activity against *E. coli.* A similar result was reported for polymethacrylamides with more active against *S. aureus* than *E. coli*.[18] The activity distinctions of the antimicrobial polymers may arise from the differences in membrane structures between the two tested bacteria. These results support the initial hypothesis that the copolymer with main chain ester linkage and amine side chains are antimicrobial, and the activity can be tuned by altering the contents of amine side chain groups and chemical structures of side chains (acrylate and acrylamide).

Table 2. Antimicrobial Activities of Copolymers.

Entry	Precursor	Vinyl Monomer	Ammonium	Ammonium (m)/Ester (n) Units in Polymer[a]	*DP*	M_n[b]	MIC, mg/mL	
							E. coli	*S. aureus*
P4	P1	acrylate	primary	5.4/5.4	10.8	2100	500	500
P5	P2	acrylate	primary	23.2/8.1	31.3	4800	250	>500
P6	P2	acrylate	quaternary	16.9/5.8	22.7	6000	>500	>500
P7	P1	acrylamide	primary	12.3/13.3	25.6	4000	>500	125

[a]Determined by ^{1}H NMR. [b]M_n was calculated based on the m and n values.

3. Polymer degradation. The degradation of the copolymer was performed in buffer solution in the range of pH 7.0–12.0 at 37 °C for 18 h (The structure of the polymer was confirmed by ^{1}H NMR in Figure 6.). The MALDI-TOF-MS spectra show that the copolymer was degraded faster as the pH of the solution was increased (Figure 7). This result is consistent with the fact that the copolymer must be degraded more quickly by free amine groups at a higher pH solution. This copolymer proved another example of a self-degradable polymer, of which the main chain cleaves by the amine groups of the copolymer itself.[6–8]

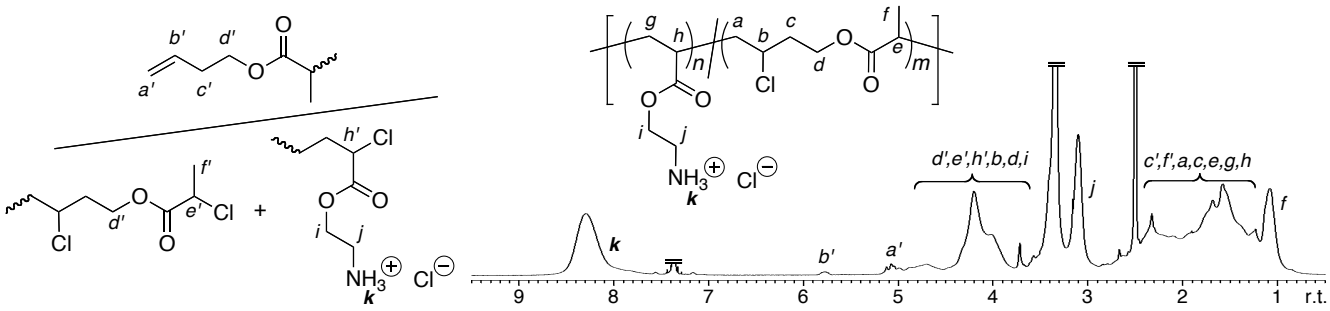

Figure 6. ^{1}H NMR spectrum of cationic copolymer (M_n = 2700, n = 12.7, m = 4.9) (DMSO-d_6, r.t.).

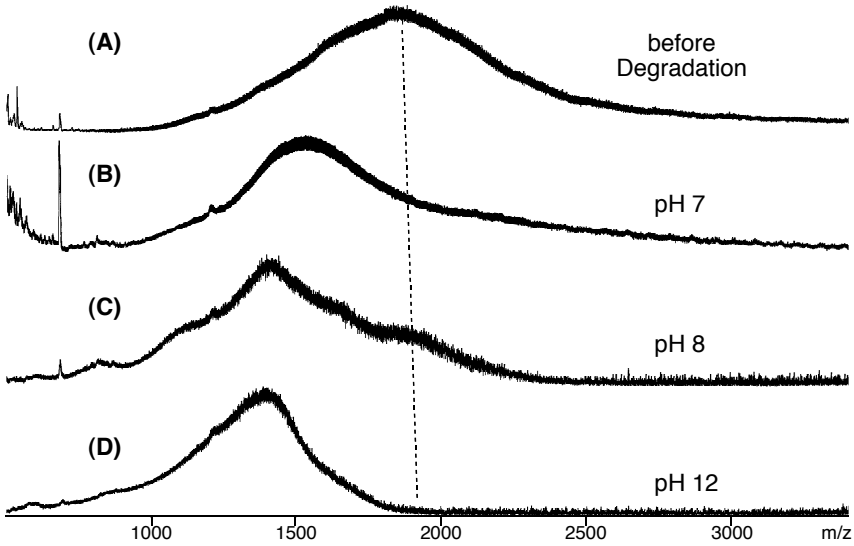

Figure 7. MALDI-TOF-MS spectra of (A) cationic copolymer (M_n = 2700, n = 12.7, m = 4.9) and the degraded products at pH (B) 7.0, (C) 8.0, and (D) 12.0 in buffer solution for 18 h at 37 °C: $[\text{cationic polymer}]_0$ = 500 mg/mL, $[\text{HEPES, Tris, or } K_2CO_3]_0$ = 10 mM, $[NaCl]_0$ = 150 mM.

4. Degradation mechanism. To understand the self-degradable mechanism of the cationic copolymers in more detail, the author investigated the degradation reaction of the precursor copolymers using a salt of primary amine in the buffer solution. The reaction was conducted between poly(acrylic acid-*co*-**1**) and 2-ethanolamine hydrochloride as a function of solution pH, which was monitored by electrospray ionization mass spectrometry (ESI-MS) (Figure 8). The products degraded at pH 7 consisted of two series of peaks, of which the major series was assignable to the products degraded by 2-ethanolamine hydrochloride (opened circles), while the minor series was similar to those of the corresponding control, poly(acrylic acid-*co*-**1**) (filled circles). The signals of the original copolymer apparently diminished and the spectra shifted to the lower molecular weight regions as the pH increased. Finally, at pH 12, the spectrum showed only the peaks of completely degraded products. The negligible amount of the products degraded by water indicates no significant hydrolysis of the copolymers (Figure 9). This also supports that the

cationic copolymers were degraded at the backbone ester linkages by pendant ammonium salts in the aqueous medium.

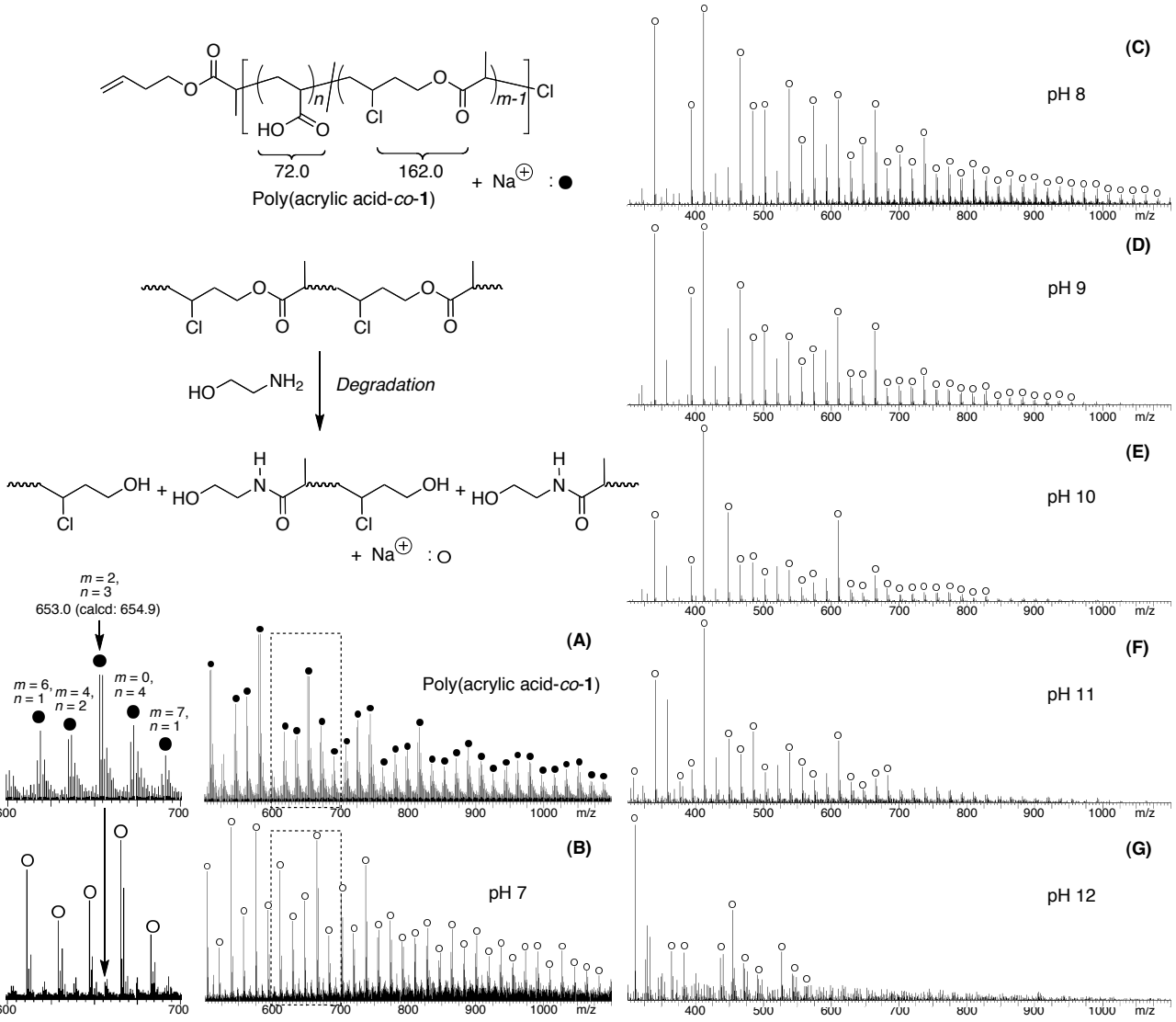

Figure 8. ESI-MS spectra of (A) poly(acrylic acid-*co*-**1**) (M_n = 1300, n = 5.5, m = 5.4), (B) the degraded products at pH 7.0, (C) 8.0, (D) 9.0, (E) 10.0, (F) 11.0, and (G) 12.0 in buffer solution for 18 h at 37 °C: [poly(acrylic acid-*co*-**1**)]$_0$ = 500 mg/mL, [2-(dimethylamino)ethanol]$_0$ = 2.2 mM, [HEPES, Tris, $NaHCO_3$, or K_2CO_3]$_0$ = 10 mM, [NaCl]$_0$ = 150 mM.

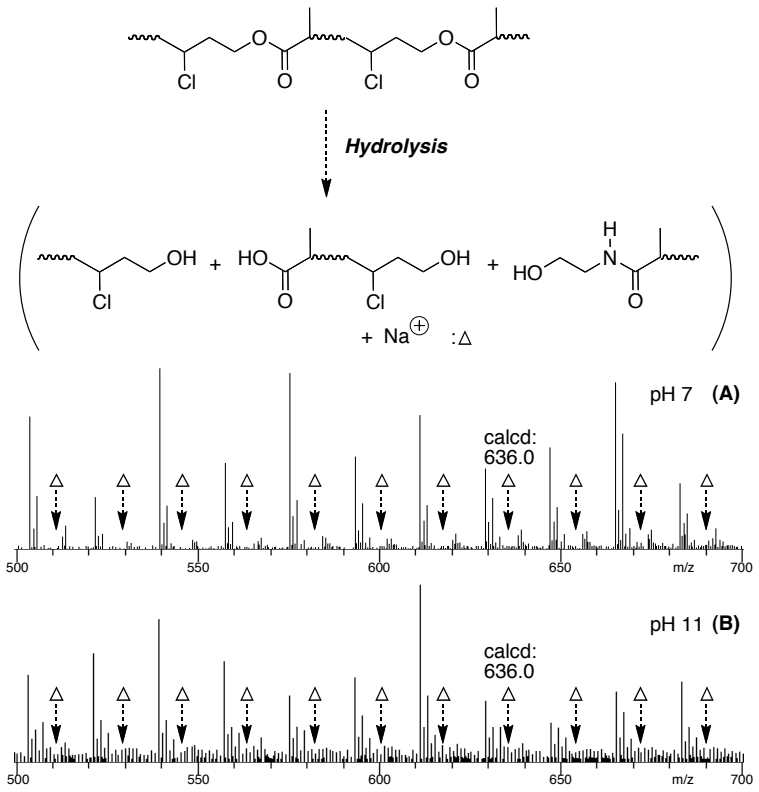

Figure 9. ESI-MS spectra of the degraded products (A) at pH 7.0, (B) 8.0, (C) 11.0, and (D) 12.0 in buffer solution for 18 h at 37 °C: [poly(acrylic acid-*co*-**1**)]$_0$ = 500 mg/mL, [2-(dimethylamino)ethanol]$_0$ = 2.2 mM, [HEPES, Tris, $NaHCO_3$, or K_2CO_3]$_0$ = 10 mM, [NaCl]$_0$ = 150 mM.

Conclusions

In conclusion, the author has developed self-degradable antimicrobial polymers bearing ammonium side chains and main-chain ester linkage by using the simultaneous chain- and step-growth radical polymerization. Although the antimicrobial activities of the copolymers are still relatively low, the activities can be changed by varying the polymer structures or the different monomer ratios.

EXPERIMENTAL SECTION

Materials

*t*BA (TCI, >98%) was distilled from calcium hydride under reduced pressure before use. 3-Butenyl 2-chloropropionate (**1**) was synthesized according to the literature.[27] CuCl (Aldrich, 99.99%) was used as received. CuCl was handled in a glovebox (VAC Nexus) under a moisture- and oxygen-free argon atmosphere (O_2, < 1 ppm). Toluene and CH_2Cl_2 were further dried and deoxygenized by passage through columns of Glasscontour solvent system before use. HMTETA (Aldrich, 97%) was distilled from calcium hydride before use. Trifluoroacetic acid (TFA) (TCI, >99%), 2-Boc-ethanolamine (TCI, >96%), *N*,*N*'-dicyclohexylcarbodiimide (DCC) (TCI, >98%), *N*,*N*'-dimethyl-4-aminopyridine (DMAP) (TCI, >99%), hydrogen chloride in 1,4-dioxane (4 M, TCI), *N*-Boc-ethylenediamine (TCI, >97%), 2-(dimethylamino)ethanol (TCI, >99%), and iodoethane (TCI, >99%) were used as received.

Polymerization

Polymerization was carried under dry nitrogen in baked glass tubes equipped with a three-way stopcock. A typical example for the polymerization procedure is given below. To a suspension of CuCl (99.0 mg, 1.0 mmol) in toluene (3.64 mL) was added HMTETA (0.27 mL, 1.0 mmol), and the mixture kept stirred for 12 h at 80 °C to give a heterogeneous solution of CuCl/HMTETA complex. After the solution was cooled to the room temperature, *t*BA (2.93 mL, 20.0 mmol) and 3-butenyl 2-chloropropionate (**1**) (3.16 mL, 20.0 mmol) were added. The tube was immersed in thermostatic oil bath at 80 °C. The polymerization was terminated by cooling the reaction mixtures to room temperature. Monomer conversions were determined from the concentration of residual monomers by ^{1}H NMR spectroscopy with toluene as an internal standard.

Deprotection of *tert*-Butyl Group

The poly(*t*BA-*co*-**1**) (2.77 g) in CH_2Cl_2 (9.0 mL) was treated with TFA (9.0 mL) at room temperature. Within 30 min ^{1}H NMR indicated disappearance of the *tert*-butyl group. The product was evaporated to remove the solvents to result in the poly(acrylic acid-*co*-**1**).[28]

Esterification of Poly(acrylic Acid-*co*-1)

The 2-Boc-ethanolamine (9.6 g) was added with vigorous stirring to a solution of poly(acrylic acid-*co*-**1**) (1.5 g), DCC (4.5 g), and DMAP (3.3 g) in CH_2Cl_2 (22.6 mL) at 0 °C. The mixture was stirred for 5 min at 0 °C and then for 3 h at room temperature. After the dilution with $CHCl_3$, the mixture was washed with distilled water and was evaporated to remove the solvents. The products were purified by repeated precipitation from $CHCl_3$ into hexane and dried under vacuum.

Deprotection of Boc-Protected Copolymer

The Boc-protected copolymer (6.7 mg) was treated with TFA (2.0 mL) or hydrochloric acid in 1,4-dioxane (4.0 M; 0.2 mL) at room temperature. Within 1 h ^{1}H NMR indicated disappearance of the Boc group. The product was evaporated to remove the solvents to result in the deprotected products.[16]

Synthesis of Copolymers Containing Quaternary Ammonium Salts

The 2-(dimethylamino)ethanol (0.45 mL) was added with vigorous stirring to a solution of poly(acrylic acid-*co*-**1**) (35.1 mg), DCC (0.34 g), and DMAP (0.15 g) in CH_2Cl_2 (2.06 mL) at 0 °C. The mixture was stirred for 5 min at 0 °C and then for 3 h at room temperature. After the

dilution with $CHCl_3$, the mixture was washed with distilled water and was evaporated to remove the solvents. The products were purified by repeated precipitation from $CHCl_3$ into hexane and dried under vacuum. The obtained product (2.0 mg) was dissolved in methanol (0.05 mL). Ethyl iodide (0.01 mL) was added to the solution. After 2 h, the product was evaporated to remove the solvents to result in the products containing quaternary ammonium salts.[18]

Amidation of Poly(acrylic Acid-*co*-1)

The *N*-Boc-ethylenediamine (0.27 mL) was added with vigorous stirring to a solution of poly(acrylic acid-*co*-**1**) (50.0 mg), DCC (0.13 g), and DMAP (0.06 g) in CH_2Cl_2 (0.69 mL) at 0 °C. The mixture was stirred for 5 min at 0 °C, then for 3 h at room temperature, and was evaporated to remove the solvents. The products were purified by repeated precipitation from $CHCl_3$ into hexane and dried under vacuum.

Antimicrobial Activity

The lowest polymer concentration required to completely inhibit growth of bacteria, defined as the minimum inhibitory concentration (MIC), was determined by a turbidity-based microdilution assay in Muller Hinton (MH) broth according to the procedure approved by The National Committee for Clinical Laboratory Standard (NCCLS), with the modifications proposed by Wiegand et al.[29] and Giacometti et al.[30] Each polymer was dissolved in dimethyl sulfoxide (DMSO), and eight 2-fold serial dilutions of the stock were prepared in 0.01% acetic acid. *Escherichia coli* ATCC 25922 or *Staphylococcus aureus* ATCC 25923 in the midlogarithmic growth phase were diluted to OD_{600} = 0.001 in MH broth. This stock suspension of bacteria (90 mL) was mixed with serial dilutions of a polymer stock solution (10 mL) in each well of a 96-well

polypropylene microplate, which was not treated for the tissue culture (Coming #3359). After incubating at 37 °C for 18 h, the OD_{600} in each well was recorded using a microplate reader (Perkin-Elmer Lambda Reader). The MIC was defined as the lowest polymer concentration at which no turbidity was observed relative to the negative growth control, sterile MH broth. As an additional negative control, 2-fold serial dilutions of the DMSO in 0.01% acetic acid, without polymer, were tested in the same conditions and showed no inhibitory effects, even at the highest DMSO concentration (5%). All experiments were performed three times in triplicate and MIC values reported are the average of the three trials. The MIC values were determined below the solubility limit of the polymers in MH broth in every case.

Degradation of Cationic Copolymer in Buffer Solution

A portion of the polymer (5 mg) was dissolved in ethanol (0.5 mL) and diluted into phosphate buffered saline of pH varying from 7.0 to 12.0 (10 mL; 10 mM 4-(2-hydroxyethyl)piperazine 1-ethanesulfonic acid, tris(hydroxymethyl)aminomethane, $NaHCO_3$, or K_2CO_3, 150 mM NaCl) in a vial. The solution was reacted for 18 h at 37 °C. The products were evaporated to remove the solvents to result in the degraded products.

Degradation of Poly(acrylic acid-*co*-1) in Buffer Solution

A portion of the polymer (5 mg) and 2-(dimethylamino)ethanol (2.1 mg) was dissolved in ethanol (0.5 mL) and diluted into buffered saline (10 mL; 10 mM 4-(2-hydroxyethyl)piperazine 1-ethanesulfonic acid, tris(hydroxymethyl)aminomethane, $NaHCO_3$, or K_2CO_3, 150 mM NaCl) in a vial. The solution was reacted for 18 h at 37 °C. The products were evaporated to remove the

solvents to result in the degraded products.

Measurements

Monomer conversions were determined from the residual monomers by ^{1}H NMR spectroscopy with toluene as an internal standard. ^{1}H NMR spectra were recorded in $CDCl_3$ at 25 °C on a JEOL ECS–400 or a Varian Gemini 2000 spectrometer, operating at 400 MHz. The number-average molecular weight (M_n), the weight-average molecular weight (M_w), and the molecular weight distribution (M_w/M_n) of the product polymers were determined by size-exclusion chromatography (SEC) in THF at 40 °C on two polystyrene gel columns [Shodex K-805L (pore size: 20–1000 Å; 8.0 mm i.d. × 30 cm); flow rate 1.0 mL/min] connected to Jasco PU-980 precision pump and a Jasco 930-RI refractive index detector. The columns were calibrated against 8 standard poly(MMA) samples (Shodex; M_p = 202–1950000; M_w/M_n = 1.02–1.09). MALDI-TOF-MS spectra were measured on a SHIMADZU AXIMA-CFR Plus mass spectrometer (linear mode) with dithranol (1,8,9-anthracenetriol) as the ionizing matrix and sodium trifluoroacetate as the ion source. ESI-MS spectra were recorded on a JEOL JMS-T100CS spectrometer.

NOTES AND REFERENCES

(1) Langer, R.; Vacanti, J. P. *Science* **1993**, *260*, 920–926.

(2) *Okada, M. Prog. Polym. Sci.* **2002**, *27*, 87–133.

(3) Coulembiera, O.; Degéea, P.; Hedrickb, J. L.; Dubois, P. *Prog. Polym. Sci.* **2006**, *31*, 723–747.

(4) Nair, L. S.; Laurencin, C. T. *Prog. Polym. Sci.* **2007**, *32*, 762–798.

(5) Nivasu, M. V.; Tammishetti, S. *J. Appl. Polym. Sci.* **2006**, *102*, 4058–4065.

(6) Lim, Y.; Choi, Y. H.; Park, J. *J. Am. Chem. Soc.* **1999**, *121,* 5633–5639.

(7) Lim, Y.; Kim, C.; Kim, K.; Kim, S. W.; Park, J. *J. Am. Chem. Soc.* **2000**, *122,* 6524–6525.

(8) Lim, Y.; Han, S.; Kong, H.; Lee, Y.; Park, J.; Jeong, B.; Kim, S. W. *Pharmaceutical Research* **2000**, *17,* 811–816.

(9) Won, C.; Chu, C. *Macromol. Rapid Commun*. **1996**, *17*, 653–659.

(10) Maruyama, A.; Ishihara, T.; Kim, J.; Kim, S. W.; Akaike, T. *Bioconjugate Chem.* **1997**, *8*, 735–742.

(11) Kenawy, E. R.; Worley, S. D.; Broughton, R. *Biomacromolecules* **2007**, *8*, 1359–1384.

(12) Palermo, E. F.; Kuroda, K. *Appl. Microbiol. Biotechnol.* **2010**, *87*, 1605–1615.

(13) Gabriel, G. J.; Som, A.; Madkour, A. E.; Eren, T.; Tew, G. N. *Mater. Sci. Eng., R* **2007**, *57*, 28–64.

(14) Mowery, B. P.; Lee, S. E.; Kissounko, D. A.; Epand, R. F.; Epand, R. M.; Weisblum, B.; Stahl, S. S.; Gellman, S. H. *J. Am. Chem. Soc.* **2007**, *129*, 15474–15476.

(15) Tew, G. N.; Scott, R. W.; Klein, M. L.; Degrado, W. F. *Acc. Chem. Res.* **2010**, *43*, 30–39.

(16) Kuroda, K.; DeGrado, W. F. *J. Am. Chem. Soc.* **2005**, *127*, 4128–4129.

(17) Kuroda, K.; Caputo, G. A.; DeGrado, W. F. *Chem. –Eur. J.* **2009**, *15*, 1123–1133.

(18) Palermo, E. F.; Kuroda, K. *Biomacromolecules* **2009**, *10*, 1416–1428.

(19) Palermo, E. F.; Sovadinova, I.; Kuroda, K. *Biomacromolecules* **2009**, *10*, 3098–3107.

(20) Kharasch, M. S.; Jensen, E. V.; Urry, W. H. *Science* **1945**, *102*, 128.

(21) Kharasch, M. S.; Urry, W. H. *J. Am. Chem. Soc.* **1945**, *67*, 1626.

(22) Minisci, F. *Acc. Chem. Res.* **1975**, *8*, 165–171.

(23) Iqbal, J.; Bhatia, B.; Nayyar, N. K. *Chem. Rev.* **1994**, *94*, 519–564.

(24) Pintauer, T.; Matyjaszewski, K. *Chem. Soc. Rev.* **2008**, *37*, 1087–1097.

(25) Fernández-Zúmel, M. A.; Thommes, K.; Kiefer, G.; Sienkiewicz, A.; Pierzchala, K.; Severin, K. *Chem. –Eur. J.* **2009**, *15*, 11601–11607.

(26) Recently, the simultaneous chain- and step-growth radical polymerization via the metal-catalyzed radical copolymerization of conjugated vinyl monomers and designed monomers possessing unconjugated C=C and active C–Cl bonds to produce a series of novel linear copolymers consisting of vinyl polymer and polyester units; Mizutani, M.; Satoh, K.; Kamigaito, M. *J. Am. Chem. Soc.* **2010**, *132*, 7498–7507.

(27) Mizutani, M.; Satoh, K.; Kamigaito, M. *Macromolecules* **2009**, *42*, 472–480.

(28) Nicolaou, K. C.; He, Y.; Vourloumis, D.; Vallberg, H.; Roschangar, F.; Sarabia, F.; Ninkovic, S.; Yang, Z.; Trujillo, J. I. *J. Am. Chem. Soc.* **1997**, *119*, 7960–7973.

(29) Wiegand, I.; Hilpert, K.; Hancock, R. E. W. *Nat. Protoc.* **2008**, *3*, 163–175.

(30) Giacometti, A.; Cirioni, O.; Barchiesi, F.; Del Prete, M. S.; Fortuna, M.; Caselli, F.; Scalise, G. *Antimicrob. Agents Chemother.* **2000**, *44*, 1694–1696.

LIST OF PUBLICATIONS

Papers

Chapter 1

"Metal-Catalyzed Radical Polyaddition as a Novel Polymer Synthetic Route"
Kotaro Satoh, Masato Mizutani, and Masami Kamigaito
Chem. Commun. **2007**, 1260–1262.

Chapter 2

"Metal-Catalyzed Radical Polyaddition for Aliphatic Polyesters via Evolution of Atom Transfer Radical Addition into Step-Growth Polymerization"
Masato Mizutani, Kotaro Satoh, and Masami Kamigaito
Macromolecules **2009**, *42*, 472–480.

Chapter 3

"Metal-Catalyzed Living Radical Polymerization and Radical Polyaddition for Precision Polymer Synthesis"
Masato Mizutani, Kotaro Satoh, and Masami Kamigaito
J. Phys. Conf. Ser. **2009**, *184*, 012025.

"Metal-Catalyzed Simultaneous Chain- and Step-Growth Radical Polymerization: Marriage of Vinyl Polymers and Polyesters"
Masato Mizutani, Kotaro Satoh, and Masami Kamigaito
J. Am. Chem. Soc. **2010**, *132*, 7498–7507.

Chapter 4

"Novel Copolymers by Metal-Catalyzed Simultaneous Chain- and Step-Growth Radical Polymerization of Various Monomers"
Masato Mizutani, Kotaro Satoh, and Masami Kamigaito
in preparation.

Chapter 5

"Degradable Poly(*N*-Isopropylacrylamide) with Tunable Thermosensitivity by Simultaneous Chain- and Step-Growth Radical Polymerization"

Masato Mizutani, Kotaro Satoh, and Masami Kamigaito

Macromolecules **2011**, in press.

Chapter 6

"Design and Synthesis of Self-Degradable Antimicrobial Polymers Consisting of Vinyl Polymer and Polyester Units by Simultaneous Chain- and Step-Growth Radical Copolymerization"

Masato Mizutani, Kenichi Kuroda, Kotaro Satoh and Masami Kamigaito

in preparation.

Other Related Papers

"Sequence-regulated vinyl copolymers by metal-catalysed step-growth radical polymerization"

Kotaro Satoh, Satoshi Ozawa, Masato Mizutani, Kanji Nagai and Masami Kamigaito

Nat. Commun. **2010**, *1*, 6.

"Immobilization of Amphiphilic Polycations by Catechol Functionality for Antimicrobial Coatings"

Hua Han, Jianfeng Wu, Christpher W. Avery, Masato Mizutani, Xiaoming Jiang, Masami Kamigaito, Zhan Chen, Chuanwu Xi and Kenichi Kuroda

Langmuir, **2011**, in press.

ACKNOWLEDGEMENT

This thesis presents the studies which the author carried out from 2005 to 2011 at the Department of Applied Chemistry of Nagoya University under the direction of Professor Masami Kamigaito.

The author would like to express his deep gratitude to Professor Masami Kamigaito for their continuous guidance and encouragement throughout the course of his work. He is also grateful to Associate Professor Kotaro Satoh for his helpful and convincing suggestions, stimulating discussions, and his kind guidance in experimental techniques. Very sincere thanks to Drs. Chiyo Yamamoto and Kanji Nagai for their help and advice. It is pleasure to express his appreciation to Drs. Yu Miura, A. K. M. Fakhrul Azam, Tomoyuki Ikai, Kazuhiko Koumura, Messrs. Edmund F. Palermo, Tomohiro Abe, Kenji Ishitake, Satoshi Ozawa, Hiroshi Aoshima, Masaru Matsuda, Daisuke Ito, Tsuyoshi Hamada, Kenta Ishiduka, Takamasa Soejima, Masato Handa, and all colleagues for useful suggestion and sharing his pleasant student life.

He wishes to thank for all "ORION" members, especially to Professors Yoshio Okamoto (Nagoya University; Harbin Engineering University), Mitsuo Sawamoto (Kyoto University), Sadahito Aoshima (Osaka University), Eiji Yashima (Nagoya University), and Associate Prof. Tsuyoshi Ando (Nara Institute of Science and Technology) for their meaningful discussion and kind encouragement. He also appreciates Assistant Professor Kenichi Kuroda (University of Michigan) for taking care of him for study abroad.

He is very grateful to the Fellowship of the Grobal COE program "Elucidation and Design of Materials and Moleculer Functions" during 2008–2010 and the Research Fellowship of the Japan Society for the Promotion of Science for Young Scientists during 2010–2011.

He would like to give his special thanks to Professors Eiji Yashima and Shigehiro Yamaguchi for serving on his dissertation committee.

Finally, he wishes to express his deep appreciation to his parents, Mr. Miyoshi Mizutani and Mrs. Shinobu Mizutani and his all family for their constant care and affectionate encouragement.

January, 2011

水谷将人

Masato MIZUTANI